APPLICATIONS OF ORGANIC PHOTOREDOX CATALYSIS IN THE DEVELOPMENT OF ALKENE FUNCTIONALIZATION METHODS TOWARD THE SYNTHESIS OF α–BENZYLOXYAMINO- AND HALO-LACTONES

Cortney L. Cavanaugh

A dissertation submitted to the faculty at the University of North Carolina at Chapel Hill in partial fulfillment of the requirements for the degree of Doctor of Philosophy in Department of Chemistry.

Chapel Hill
2018

Approved by:

David Nicewicz

Simon Meek

Jeffrey Aubé

Michel Gagné

Frank Leibfarth

ABSTRACT

Cortney L. Cavanaugh: APPLICATIONS OF ORGANIC PHOTOREDOX CATALYSIS IN THE DEVELOPMENT OF ALKENE FUNCTIONALIZATION METHODS TOWARD THE SYNTHESIS OF α–BENZYLOXYAMINO- AND HALO-LACTONES
(Under the direction of David A. Nicewicz)

I. Introduction To Organic Photoredox Catalysis

An overview of the photophysical and electrochemical components of organic photoredox catalysis and its applications in alkene functionalization reactions is addressed.

II. Synthesis of α-Benzyloxyamino-γ-Butyrolactones Via a Polar Radical Crossover Cycloaddition Reaction

The development of a direct catalytic synthesis of substituted α-benzyloxyamino-γ-butyrolactones, beginning from simple oxime acids and alkenes, is discussed. The substituted *O*-benzyloxime acid starting materials undergo cyclization with oxidizable alkenes, via Polar Radical Crossover Cycloaddition (PRCC) reactions. The catalytic reaction is carried out using an acridinium photooxidant and substoichiometric amounts of a redox-active cocatalyst. The utility of this methodology is demonstrated through the cyclization of 3 oxime acids and 19 oxidizable olefins to generate 21 highly substituted α-amino lactone products.

III. Reversing The Regioselectivity Of Halofunctionalization Reactions Through Cooperative Photoredox And Copper Catalysis

A novel method for reversing the regioselectivity of classic alkene halofunctionalization reactions is presented. This transformation relies on the implementation of a dual-catalytic system, incorporating the use of an acridinium photoredox catalyst in conjunction with a coppercocatalyst. The utility of the method is demonstrated through the application of chloro-

and bromo-functionalization conditions in both an intra- and intermolecular fashion. Over 15 synthetically and biologically relevant halo-lactones are accessed in a highly regioselective fashion.

To my mom and dad, thank you for making all of this possible.

ACKNOWLEDGEMENTS

There is no way I can thank my parents enough for their encouragement and support throughout life, but especially through my graduate school career. I can genuinely say that none of this would have been possible without them. I would also like to thank my twin brother Michael for never letting me take myself too seriously and keeping me laughing through our shared trudge through graduate school. Leaving my family to pursue my degree was a painful decision but they have been there all along the way to keep me motivated and pushing forward. I would like to thank you with all of my heart for that.

Thank you to my friends, at UNC and beyond, for making the tough times easier. Despite all of its challenges, graduate school wasn't without fun times and laughter. I am especially appreciative to Jake Green. I couldn't have been luckier to meet my best friend who was there through every struggle and accomplishment I encountered. Additionally, graduate school would have been unimaginable without my roommate Lilo who always kept me smiling.

I am grateful to my PI, David Nicewicz, for supporting me through this entire process and giving me the opportunity to learn so much throughout my time at UNC. I owe an additional thank you to the Nicewicz lab, past and present, for their help and camaraderie. Thank you to Jeremy Griffin for his support on the halofunctionalization project and to Cole Cruz for helping me survive this process.

Finally, I would like to thank those who have served as members of my defense committee for their time and commitment.

TABLE OF CONTENTS

LIST OF TABLES

LIST OF FIGURES

LIST OF SCHEMES

LIST OF ABBREVIATIONS AND SYMBOLS

α	Alpha
β	Beta
γ	Delta
δ	Gamma
λ_{max}	Lambda Max
τ_F	Lifetime Of Fluorescence
τ_{S1}	Lifetime Of First Singlet Excited State
ϕ_F	Quantum Yield Of Fluorescence
1D-NOESY	One-Dimensional Nuclear Overhauser Effect Spectroscopy
A	Acceptor
Ac	Acetyl
AIBN	Azobisisobutyronitrile
Alpha	Alpha
Ar	Aryl
ATRP	Atom Transfer Radical Polymerization
BDE	Bond Dissociation Evergy
BET	Back Electron Transfer
Bn	Benzyl
Boc	*tert*-Butyloxycarbonyl
bpy	2,2′-Bipyridine
Bz	Benzoyl
CSCS	C_3-Symmetric Cinchonine-Squaramide

CV	Cyclic Voltammogram
D	Donor
DCB	1,4-Dicyanobenzene
DCC	N, N'-Dicyclohexylcarbodiimide
DCDMH	1,3-Dichloro-5,5-Dimethylhydantoin
DCDPH	1,3-Dichloro-5,5-Diphenylhydantoin
DCE	1,2-Dichloroethane
DCM	Dichloromethane
DDQ	2,3-Dichloro-5,6-Dicyanobenzoquinone
DEBM	Diethyl Bromomalonate
DEM	Diethyl Malonate
$(DHQD)_2PHAL$	Hydroquinidine 1,4-Phthalazinediyl Diether
DIBALH	Diisobutylaluminum Hydride
DMAP	4-Dimethylaminopyridine
DNA	Deoxyribonucleic Acid
dr	Diastereomeric Ratio
e^-	Electron
$E_{0,0}$	Excited State Energy
EDG	Electron Donating Group
ee	Enantiomeric Excess
equiv	Equivalent
$E_{1/2}^{red}$	Half-Wave Potential
Et	Ethyl

EWG	Electron Withdrawing Group
F	Faraday Constant
GC-MS	Gas Chromatography–Mass Spectrometry
H^+	Proton
HAD	Hydrogen Atom Donor
HAT	Hydrogen Atom Transfer
HIV	Human Immunodeficiency Virus
HOMO	Highest Energy Occupied Molecular Orbital
Hz	Hertz
hv	Photon Or Energy Of A Photon
IC	Internal Conversion
*i*Pr	Isopropyl
ISC	Intersystem Crossing
k	General Symbol For Rate Constant
kcal	Kilocalorie
LEDs	Light-Emitting Diode
LUMO	Lowest Energy Occupied Molecular Orbital
Lut+	Lutidinium
M	Molarity
m-	Meta
Me	Methyl
MeCN	Acetonitrile
MRSA	Methicillin-Resistant *Staphylococcus Aureus*

NAAN	Nucleophile-Assisted Alkene Activation
NBP	*N*-Bromophthalimide
NBS	*N*-Bromosuccinimide
NCP	*N*-Chlorophthalimide
NCS	*N*-Chlorosuccinimide
NIS	*N*-Iodosuccinimide
nm	Nanometre
NMA	9-Mesityl-10-Methylacridinium
NMR	Nuclear Magnetic Resonance
NNRTI	Non-Nucleoside Reverse-Transcriptase Inhibitor
NOE	Nuclear Overhauser Effect
NPhA	9-Mesityl-10-Phenylacridinium
NPhDMA	9-Mesityl-2,7-Dimethyl-10-Phenylacridinium
ns	Nanosecond
Ns	4-Nitrobenzenesulfonyl
Nuc	Nucleophile
o-	*ortho*
p-	*para*
PET	Photoinduced Electron Transfer
Ph	Pehnyl
phen	Phenanthroline
Phth	Phthalamide
pKa	Logarithmic Acid Dissociation Constant

PMN	2-Phenylmalononitrile
PMP	*p*-Methoxyphenyl
ppm	Parts Per Million
PRCC	Polar Radical Crossover Cycloaddition
psi	Pounds Per Square Inch
RNA	Ribonucleic Acid
rr	Regiomeric Ratio
rt	Room Temperature
s	Seconds
S0	Ground State Singlet
S1	First Singlet Excited State
SCE	Saturated Calomel Electrode
SET	Single Electron Transfer
SOMO	Singly Occupied Molecular Orbital
Suc	Succinimide
T1	First Triplet Excited State
TBS	*tert*-Butyldimethylsilyl Ether
*t*Bu	*tert*-Butyl
TFA	Trifluoroacetic Acid
TFAA	Trifluoroacetic Anhydride
TFE	2,2,2-Trifluoroethanol
THF	Tetrahydrofuran
TPT	Triphenylpyrylium

Tr	Trityl
Ts	Toluenesulfonyl (Tosyl)
UV/Vis	Ultraviolet–Visible Spectroscopy
V	Volts
VREF	Vncomycin-Resistant *Enterococcus Faecium*
•	Radical
*	Excited State

CHAPTER ONE: INTRODUCTION TO ORGANIC PHOTOREDOX CATALYSIS

1.1 Introduction

Modern advances in photoredox catalysis stemmed from work out of the late 1970s and have continued to greatly impact recent synthetic methods.[1–3] Over the past 40 years, the number of papers published annually in the field of organic photoredox catalysis has increased substantially approaching nearly 200 in 2015.[4] These data are a direct reflection of the groundbreaking and exciting advancements being made in the field, garnering significant attention in both academia and industry. A major asset to using photon-absorbing catalysts (i.e. photoredox catalysts) is the ability to accesses unique substrate reactivity, which has been considered difficult, or even impossible, under classic organic reaction conditions. While significant advances have been made in the field of visible light photoredox catalysis using transition metal complexes,[5] it is worth focusing directly on the rapidly advancing, distinctive field of organic photoredox catalysis, in which the Nicewicz laboratory and this thesis are grounded.

1.2 The Photophysical and Electrochemical Components of Photoredox Catalysis

At their foundation, organic photoredox catalysts are highly prized as participants in a process known as photoinduced electron transfer or PET. This term refers, overall, to an electron transfer event that occurs between an excited state and ground state molecule.[6] In the case of visible light organic photoredox catalysis, the excited state refers to that of an organic chromophore. When the chromophore absorbs visible light ($h\upsilon$), an electronically excited molecule is formed as an electron is promoted to a higher energy state from its original ground state (S_0). The direct excitation from the ground singlet state to the first singlet excited state (S_1)

can be represented with a Jablonski diagram (Figure 1-1).[7] Though many singlet excited states, of varying vibrational energy exist and may be accessed, non-radiative relaxation to the lowest energy S_1 state occurs in a matter of picoseconds. The fate of S_1 is dependent on both radiative and non-radiative photophysical pathways. A radiative pathway, for S_1 to return to S_0, involves the dissipation of energy in the form of a photon and is termed fluorescence. Two potential non-radiative pathways may also dictate the fate of S_1. Similar to fluorescence, S_1 may also return to S_0 through internal conversion (IC), however, in this case, the loss of energy is thermal. The final process is intersystem crossing (ISC) and involves the transition of S_1 to T_1, the first triplet excited state. This process is spin forbidden and is therefore slow. Upon entering T_1, an additional radiative pathway, known as phosphorescence, may occur, allowing T_1 to return to S_0. This transition may also involve non-radiative pathways.

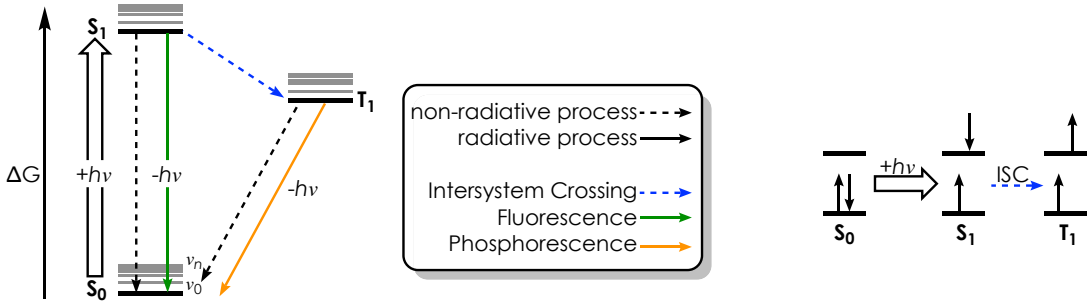

Figure 1-1. Jablonski Diagram and a Simplistic View of Excitation/ISC

As a result of entering S_1 or T_1, organic chromophores become capable of participating in an electron transfer process. In principle, the excited state catalyst can act as an oxidant or reductant. This interaction may involve electron transfer in two directions; the excited state of the photoredox catalyst may donate an electron to the substrate, through an oxidative quenching process, or it may accept an electron through a reductive quenching cycle. To gain a thorough

understanding of the transformations to be discussed herein, an emphasis will be placed on exploring electron transfer through the reductive quenching cycle of photoredox catalysts.

In this relationship, the photon-absorbing catalyst acts as an acceptor molecule (A), while the substrate functions as the donor molecule (D) (Figure 1-2). This simplified model demonstrates the interactions between the corresponding molecular orbitals of the catalyst and substrate in their ground and excited states. In the ground state, the acceptor molecule possesses a highest occupied molecular orbital (HOMO) and a lowest unoccupied molecular orbital (LUMO) that are each lower in energy than that of the corresponding HOMO and LUMO for the donor. As a result of these relative energy levels, electron transfer in either direction (A → D or D → A) is endergonic and therefore unfavorable. However, upon excitation by visible light, A is capable of accessing its excited state (A*), transferring an electron from its HOMO to its LUMO. The newly formed vacancy in the former HOMO of A* makes it an excellent excited state oxidant as it is more easily reduced than its ground state counterpart. As a result, single electron transfer (SET) from the HOMO of D to the lower energy SOMO (singularly occupied molecular orbital) of A* allows for the oxidation of D to an electron-deficient $D^{+\bullet}$ species and the concurrent reduction of A* to the electron-rich $A^{-\bullet}$ species.

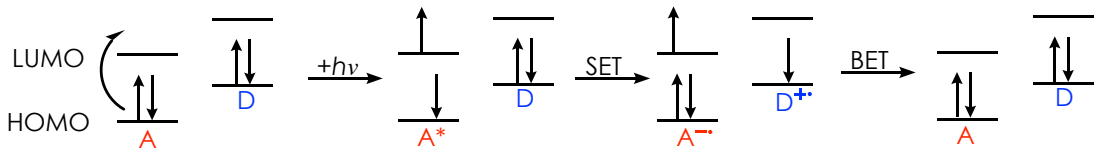

Figure 1-2. Single Electron Transfer Model

While this PET process is highly desirable for the single electron oxidation of organic substrates by a photoredox catalyst, its efficiency can be limited by an unproductive back

electron transfer (BET) pathway. BET is a general term associated with any event in which $A^{-\bullet}$ transfers an electron back to $D^{+\bullet}$. This process may occur as a result of a close physical relationship between the radical ion pairs and is also a highly exergonic, competitive pathway.[8] To help promote forward electron transfer and limit BET, more polar solvents can be utilized as they stabilize polar intermediates and promote the separation of the radical ion pairs.[9] The excited state from which PET occurs can either be the singlet or triplet state, though reaction efficiency is higher for those occurring from the latter.[10] Though an acceptor in S_1 possesses a higher oxidizing ability, PET from this state is less efficient than that from T_1. This is a direct result of the long-lived nature of T_1, which provides sufficient time for the species to diffuse, collide, and undergo electron transfer. The slower rate of BET associated with the triplet state allows for the radical ion pair to separate sufficiently before the unproductive event can occur. In order to achieve successful PET and limit BET, an appropriate acceptor/donor system must be identified.

To aid in this determination, a general equation can be applied to identify the likelihood of a PET event occurring.[6] Before considering the photoinduced transfer event, it is worth considering the equation that describes the Gibbs free energy of a single electron transfer event occurring in the ground state (Equation 1-1). This equation relates the redox potentials for A and D, undergoing reduction (E_{red}) and oxidation (E_{ox}) events, respectively. It is worth clarifying the nomenclature and noting that that E_{red} specifically refers to the single electron reduction of A to $A^{-\bullet}$ ($A \rightarrow A^{-\bullet}$, $E_{1/2}(A/A^{-\bullet})$) and this value, measured in volts (V), is usually negative for most acceptors in the ground state. This value is associated with the fact noted previously, that single electron reduction of the acceptor molecule, in its ground state, is generally thermodynamically unfavorable. The oxidation potential of D, or E_{ox}, is technically defined as the reduction half

potential and is associated with the $D^{+\bullet}$ to D reaction ($D^{+\bullet} \rightarrow D$, $E_{1/2}(D^{+\bullet}/D)$). Unlike the reduction of A, the single electron reduction of $D^{+\bullet}$ is generally an energetically favorable process and results in a positive voltage value.

Equation 1-1. Gibbs Free Energy of Single Electron Transfer

$$\Delta G_{ET} = -F(E_{red} - E_{ox}) = -F(E_{1/2}(A/A^{\cdot -}) - E_{1/2}(D^{\cdot +}/D))$$

F = Faraday's constant (23.061 kcal V^{-1} mol^{-1})

Having considered single electron transfer in the ground state, the equation for PET can now be explored. The free energy of PET occurring between the excited state photoredox catalyst acceptor (where A = cat*) and a ground state substrate (D = sub) can be modeled by Equation 1-2, where Coulombic interactions are disregarded. Here, E^*_{red} refers to the excited state reduction potential for the photoredox catalyst under consideration and can be calculated according to Equation 1-3. The excited state energy ($E_{0,0}$) refers to the transition between the lowest vibrational state of S_1 or T_1 to that of S_0. This value can be estimated at the midpoint between the absorption and emission maxima from the overlaid spectra.

Equation 1-2. Gibbs Free Energy of PET

$$\Delta G_{PET} = -F(E^*_{red}(cat^*/cat^{\cdot -}) - E_{ox}(sub^{\cdot +}/sub))$$

Equation 1-3. Excited State Reduction Potential of Photoredox Catalyst

$$E^*_{red}(cat^*/cat^{\cdot -}) = E_{red}(cat/cat^{\cdot -}) + E_{0,0}$$

While a significant amount of information is contained within these equations, a valuable tool can be simplified from the mathematical relationship to determine the likelihood of a proposed PET between a photoredox catalyst and a substrate. A successful photoinduced electron transfer event is possible when E^*_{red} in more positive than E_{ox} of the substrate. Determining the feasibility of an electron transfer event can aid in the selection of a photoredox catalyst depending on substrate that is to be oxidized.[6]

Cyclic voltammetry is commonly employed to measure the redox potential for a given substrate. From the cyclic voltammogram (CV), one can identify the oxidation potential for an organic compound by estimating the potential at half the maximum current, also known as the half-peak potential. A series of potentials, for a variety of organic functional groups, was reported by Roth et al.[11] in 2016, to aid in the selection of an effective catalyst-substrate pairing. An abbreviated collection of these substrates, and the range for their corresponding potentials, are represented in Figure 1-3 with the values reported against a saturated calomel electrode (SCE). These potentials can be compared to the excited state reduction potential of some commonly used organic photoredox catalysts.[6,12] Often, these catalysts are combined with sufficiently oxidizable substrates to carry out single electron oxidation of the organic donor molecule to generate reactive cation radical intermediates.

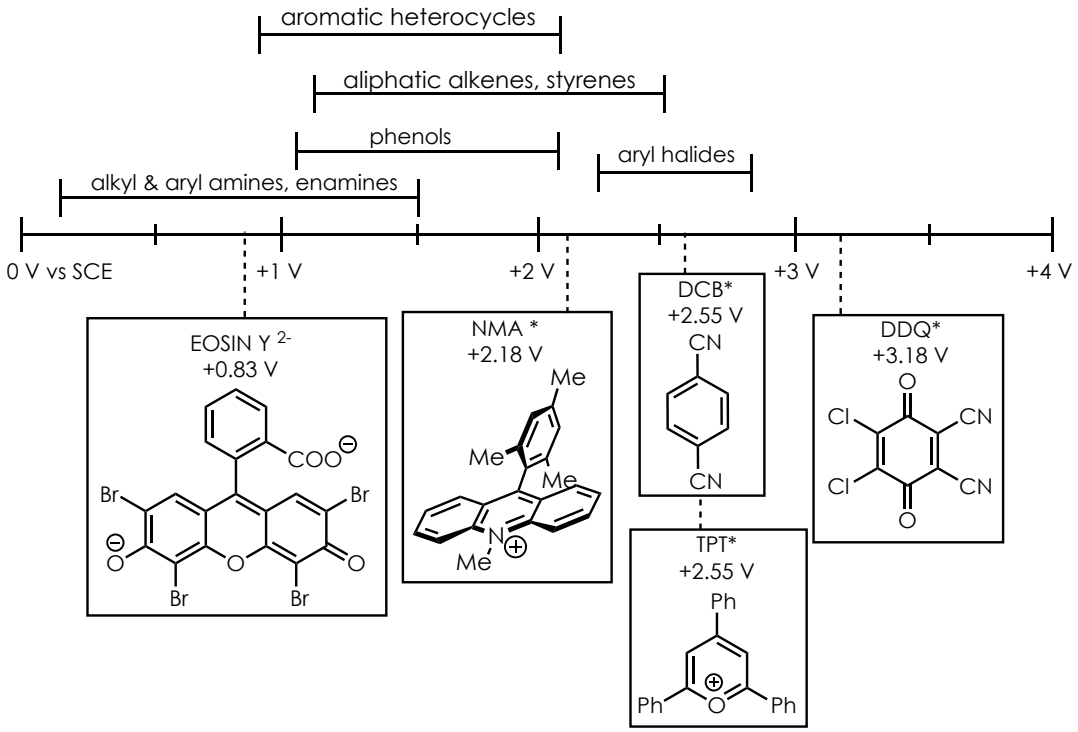

Figure 1-3. Series of Potentials for Various Organic Functional Groups and Catalysts

Early evidence for gaining access to these valuable cation radical intermediates through PET was first provided in groundbreaking work by the Arnold lab.[13] While studying photocycloadditions, it was observed that when 1,1-diphenylethylene was reacted with methyl 4-cyanobenzoate in acetonitrile an unexpected product had formed (Scheme 1-1). Ultimately, it was determined that the product corresponded to tetrahydronaphthalene product 1.2 and formed as a result of single electron oxidation of the olefin by 4-cyanobenzoate to generate the corresponding cation radical 1.1. Upon reacting with another equivalent of 1,1-diphenylethylene and ring closure, the observed product was formed. Arnold expanded this transformation to include an intermolecular variant in which alcohols, such as methanol and isopropanol were used as solvents to generate the corresponding ether products in an anti-Markovnikov fashion.

Scheme 1-1. Cyclization of 1,1-Diphenylethylene via Cation Radical Intermediate Formation

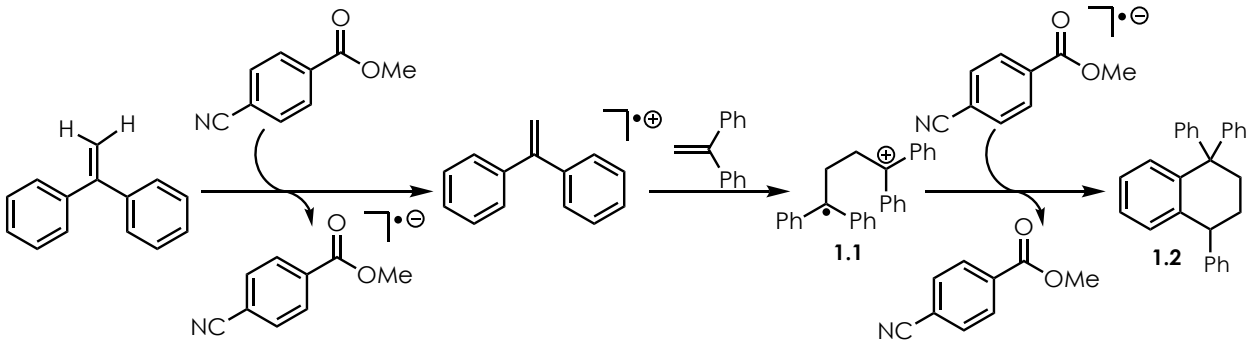

From these results, it was concluded that, upon nucleophilic trapping of the cation radical, two potential carbon-centered radicals might form. However, the more populated form was that of the more stabilized radical, resulting in formation of the observed alkene functionalization product (Scheme 1-2). This pioneering work, towards the development of cation radical-mediated anti-Markovnikov functionalization, was expanded upon by both Arnold[14] and Gassman.[15,16] While impressive, initial results in the fields were limited by nearly stoichiometric use of the photooxidant and undesirable reactivity and byproduct formation.

Scheme 1-2. Anti-Markovnikov Functionalization of Alkenes via Cation Radical Intermediate

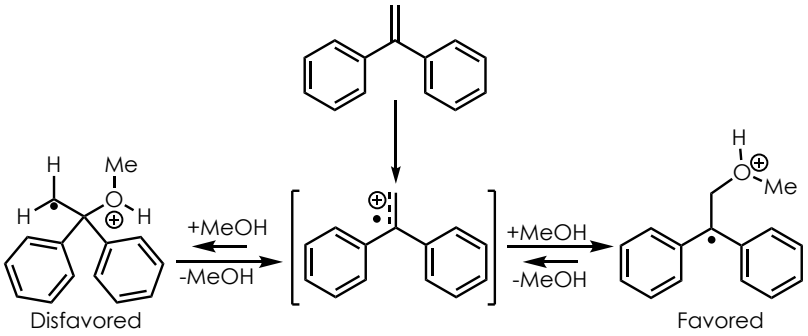

1.3 Organic Photoredox Catalysis and its Applications in Anti-Markovnikov Alkene Hydrofunctionalization

The functionalization of alkenes through the addition of a proton and heteroatom across the double bond is one of the oldest and most applied transformations in organic chemistry. Typically, this reaction leads to the corresponding Markovnikov product. While this reactivity is often desirable, a significant amount of attention has been directed towards reversing the regioselectivity of olefin hydrofunctionalization reactions to favor the more elusive anti-Markovnikov adduct.

In response to this interest in developing anti-Markovnikov alkene functionalization methods, and based on precedent from within the field, the Nicewicz lab has turned its attention towards the development of an organic photoredox-mediated method, with a specific focus on identifying an effective catalytic variant. We have developed and applied methods for accessing anti-Markovnikov hydrofunctionalization products through PET between organic photoredox catalysts and olefin substrates. This method relies on the formation of a uniquely reactive cation radical intermediate and has proven to be a general approach towards alkene functionalization. In order to achieve the desired catalytic reactivity, we have applied a dual organic catalyst system in the transformation, utilizing an acridinium photoredox catalyst and a redox active, organic, hydrogen atom donor.

Since our seminal publication in 2012, this methodology has been applied to the anti-Markovnikov addition of alcohols,[17] carboxylic acids,[18] amines,[19] trifluoromethyl groups,[20] and mineral acids[21] in the presence of a hydrogen atom source (Scheme 1-3). A variety of electron-rich olefins were successfully functionalized, regioselectivly, using this novel method. This photoredox-meditated transformation was also expanded upon to include the synthesis of a variety of heterocycles through a related Polar Radical Crossover Cycloaddition (PRCC) reaction

approach.[22–24] Though this approach has proven to be a highly successful method of functionalizing alkenes in a regioselective fashion, a substantial amount of attention has been placed on understanding the general transformation. Specifically, the identity of the organic photoredox catalyst (Figure 1-3) and hydrogen atom donor cocatalyst has required a thorough analysis to develop an optimal and effective dual catalytic process.

Scheme 1-3. Previous Anti-Markovnikov Hydrofunctionalization Methods Developed by Nicewicz et al.

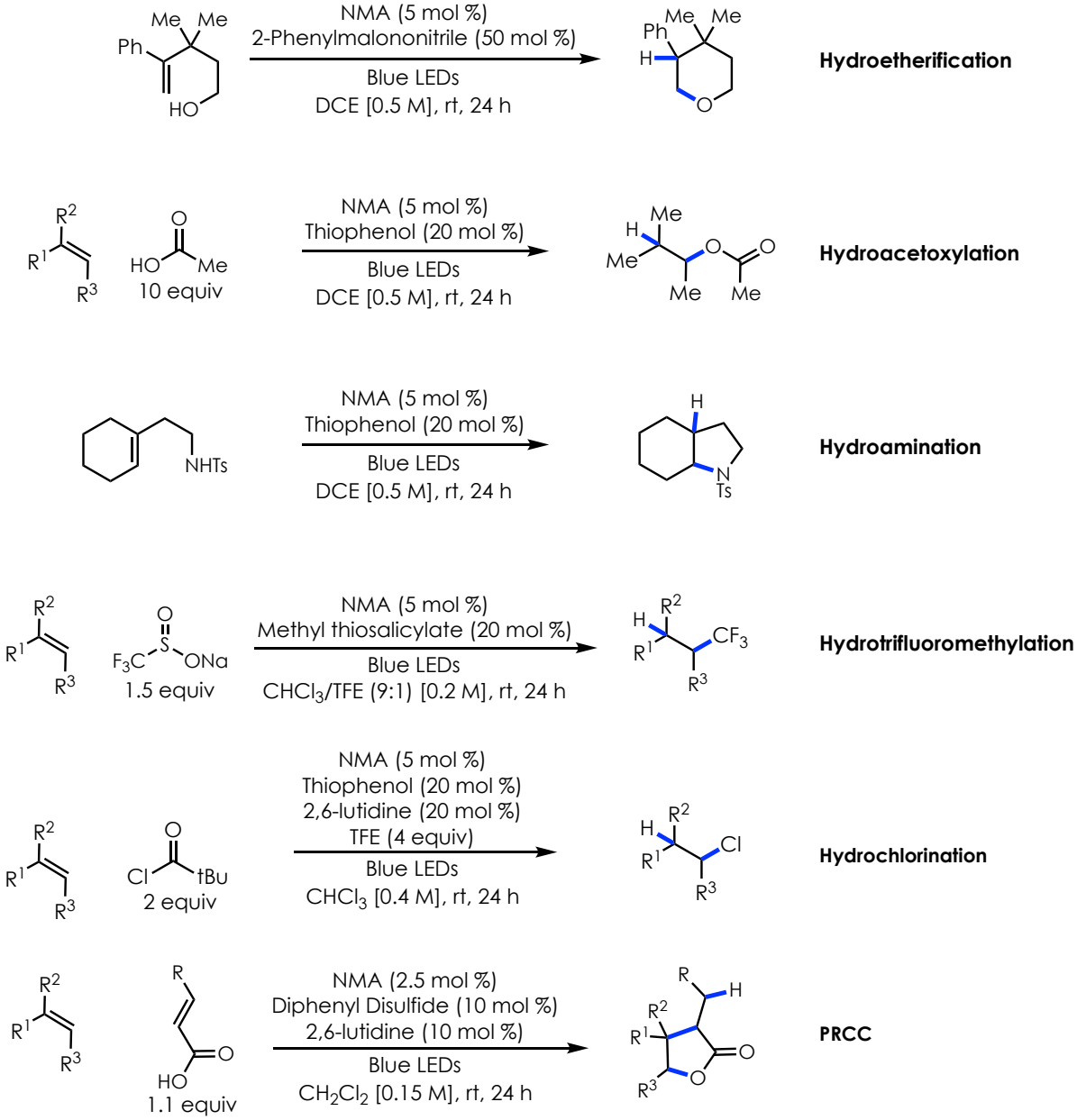

1.3.1 Selecting an Effective Organic Photoredox Catalyst

With the goal of creating a generally applicable, catalytic method in mind, we sought to identify an organic photoredox catalyst that met necessary criteria. Since the reaction was

expected to proceed through the single electron oxidation of olefins, the organic dye of choice would need to be capable of oxidizing a variety of alkenes, with a wide range of oxidation potentials, to ensure a thorough and diverse substrate scope. In order to ensure optimal reactivity, the photocatalyst would also need to exhibit key characteristics including the ability to undergo excitation upon irradiation with visible light, a sufficient fluorescence lifetime and quantum yield, and it must undergo limited, unproductive BET. Lastly, to access catalytic reactivity, the chromophore of choice would need to exhibit redox reversibility, ensuring that the catalyst would remain intact and could be turned over in the presence of a suitable oxidant. Upon an exploration of the literature, it was determined that 9-mesityl-10-methylacridinium (NMA), as disclosed by Fukuzumi, would best embody these characteristics and could be successfully applied as a photoredox catalyst in the hydrofunctionalization of alkenes.[25]

The photophysical characteristics of the acridinium catalyst lend itself well towards its incorporation into our hydrofunctionalization methodology (Figure 1-4).[6] Firstly, the excited state reduction potential of NMA is +2.18 V vs SCE. With such a highly positive potential, NMA gives access to a variety of olefin substrates that are capable of being oxidized to their corresponding cation radical intermediate. Additionally, the excited state of the acridinium can be achieved through irradiation by visible light. While the absorbance maximum is reported to be 425 nm for NMA, it is best to irradiate at the highest possible wavelength to prevent potentially competing photochemical pathways. Light emitting diodes (LEDs) have proven to be an asset in the development of photoredox mediated methods, as they are efficient, high-intensity light sources that are selective due to their narrow emission band. As a result, commercially available blue LEDs can be applied when NMA is used as a photoredox catalyst.

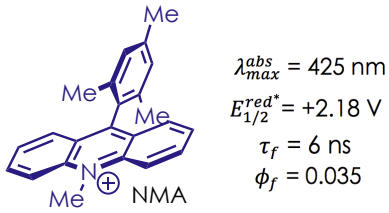

Figure 1-4. Photophysical Properties of 9-Mesityl-10-Methylacridinium Photoredox Catalyst

Before it can be applied in synthesis, it is necessary to determine whether a photoredox catalyst can efficiently undergo PET with a given substrate. This determination is based on the fluorescence lifetime (τ_f). Longer lifetimes are indicative of photooxidants that are more likely to undergo PET with a substrate. Those exhibiting a lifetime of less than 1 ns will be unlikely to undergo efficient PET. The fluorescence lifetime of NMA is 6 ns, and while not impressively long, the value indicates that the acridinium is capable of undergoing PET. The likelihood of PET can also be gathered from the fluorescence quantum yield (ϕ_f) for a given catalyst. A value close to one indicates that PET from S_1 could be more efficient as deactivation pathways are limited. That is, nearly all molecules in S_1 undergo fluorescence rather than relaxing through a nonradiative pathway. With a ϕ_f of 0.035, nonradiative pathways are considered competitive but the value has proven to be sufficiently high to make NMA an effective photoredox catalyst.[6] Not all of these nonradiative processes are deleterious however. For example, ISC would allow for PET to still occur efficiently from T_1 despite the fact that it is lower in energy. Evidence has shown that NMA has a variety of singlet and triplet states that are capable of oxidizing organic substrates. Lastly, the acridinium cationic structure lends itself well to preventing back electron transfer as its overall positive charge, prior to electron transfer, makes it less likely to transfer the electron back to the oxidized substrate. A critical characteristic of NMA is its ability to be

efficiently turned over by a co-oxidant. The delicate balance between the photoredox catalyst and cocatalyst system has been explored closely through a series of mechanistic studies.

1.4 Mechanistic Insight

Ultimately, a suitable photoredox catalyst must successfully interact with all of the hydrofunctionalization reaction components as a cohesive, redox neutral system. As discussed previously, in order to achieve a net redox-neutral transformation, the photocatalyst's reductive quenching cycle must be coupled with an additional oxidative quenching cycle. Through a series of reports, it was determined that NMA functions effectively in a system with a redox active hydrogen atom donor such as phenylmalononitrile (PMN).[17,22] However, it was discovered that higher yields and shorter reaction times could be achieved using thiophenol (PhSH) and diphenyl disulfide ($(PhS)_2$) as alternative hydrogen atom donors. An exploration of a general reaction mechanism is necessary to illustrate how the photoredox catalyst and cocatalyst function together to afford the generation of an anti-Markovnikov, alkene hydrofunctionalization product (Scheme 1-4). Initially, olefin substrate 1.3 undergoes single electron transfer to an excited state acridinium NMA* to afford the characteristic cation radical intermediate (1.4). This intermediate can be detected through laser flash photolysis.[26] Nucleophilic trapping of the cationic component affords the more stable (1.5) of the two potential carbon-centered radicals. The hydrofunctionalized product (1.7) is generated upon deprotonation and trapping of the radical intermediate (1.6) through efficient hydrogen atom transfer (HAT) by the thiophenol cocatalyst.

Scheme 1-4. General Mechanism for Anti-Markovnikov Alkene Hydrofunctionalization

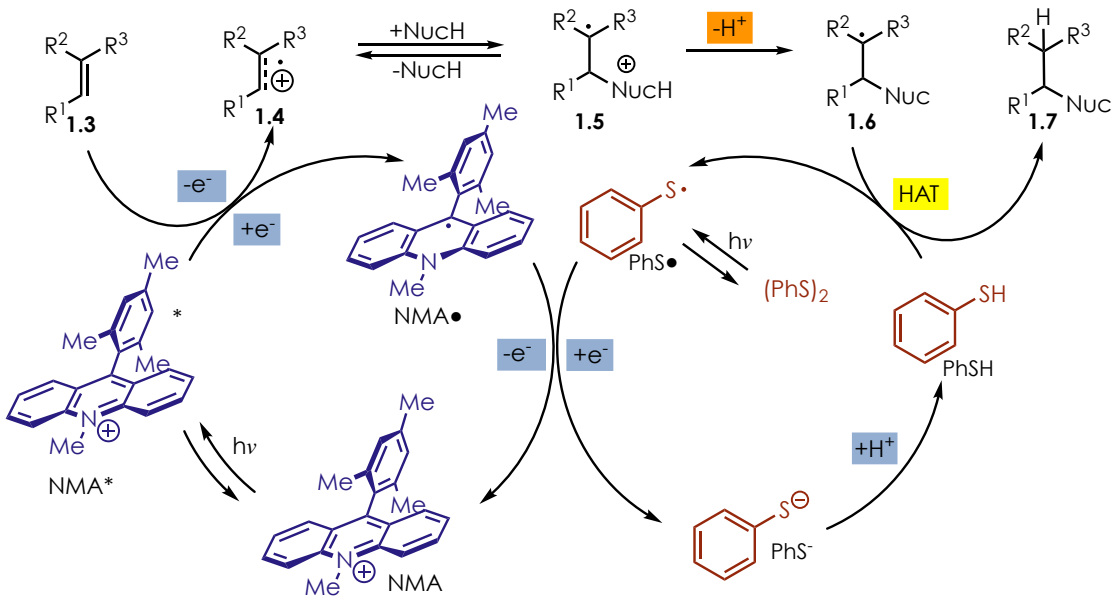

A critical point in the transformation is where the two catalytic cycles intersect. As a result of HAT, a phenylthiyl radical (PhS•) is generated which can function as a one-electron oxidant to turn over the acridine radical (NMA•). The reduction potential of the thiyl radical ($E_{1/2}^{red}$ = +0.16 V vs. SCE) indicates that it is sufficiently oxidizing to undergo an exergonic electron transfer with NMA• ($E_{1/2}^{red}$ = -0.55 V vs. SCE).[26] The thiophenol catalyst can be regenerated upon protonation of the resulting thiolate (PhS^-) by an equivalent of substrate. Interestingly, the hydrogen atom donor cocatalyst serves multiple purposes in the production of product by functioning as an electron, hydrogen atom, and proton transfer agent throughout the reaction.

An interesting observation was made when it was determined that diphenyl disulfide also functioned effectively as a HAT agent. The concept of using diphenyl disulfide was initially proposed after observing its formation as a byproduct during reactions that used thiophenol as a cocatalyst. The inverse observation was also noted when diphenyl disulfide was applied as a

HAT catalyst. It was hypothesized that the disulfide undergoes homolytic cleavage upon irradiation by visible light, ultimately generating thiophenol in situ. To support this proposed pathway, a crossover experiment was conducted in which diphenyl disulfide (1.8) was irradiated in the presence of 4-methyl diphenyl disulfide (1.9) and NMA (Scheme 1-5).[26] The mixed-disulfide product (1.10) was obtained along with the symmetric disulfides (1.8 and 1.9) as a 2:1:1 mixture. These results were also observed when NMA was left out of the reaction conditions but no exchange was noted when the reaction was conducted in the dark, even when heated. In combination, these results strongly supported the visible light induced homolytic cleavage of diphenyl disulfide.

Scheme 1-5. Diaryl Disulfide Crossover Experiment

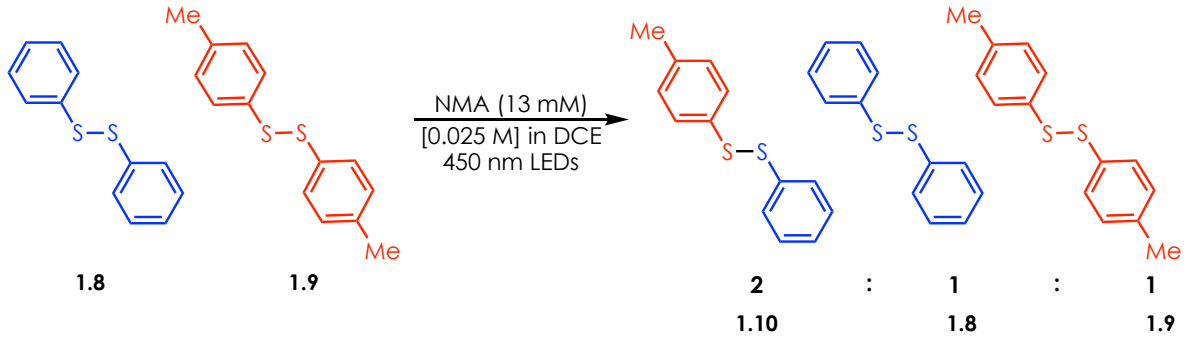

While it has been noted that the rate-limiting step may change throughout the span of the reaction, evidence suggests that the deprotonation of intermediate 1.3 (Scheme 1-4) may have a rate determining influence.[26] Reaction rates are higher when the thiol cocatalyst is employed as the disulfide, likely due to the buildup of thiolate, which leads to a higher rate of deprotonation. When thiophenol is used, it must first undergo HAT and oxidation of NMA• to generate the

thiolate necessary to carry out the deprotonation event. These observations, in addition to being easier to handle, make diphenyl disulfide an ideal cocatalyst in this novel organic photoredox-mediated hydrofunctionalization of alkenes.

1.5 Conclusion

A rudimentary understanding of the photophysical and electrochemical factors that influence the activity of an organic photoredox catalyst is fundamental to the successful employment of such a species in a transformation. By understanding the oxidizing ability and photophysical properties of 9-mesityl-10-methylacridinium, we were able utilize this photoredox catalyst in the synthesis of a diverse set of hydrofunctionalized alkenes. The general, dual-catalytic process utilizes a redox active hydrogen atom donor cocatalyst in a concurrent cycle to access an overall, net redox neutral transformation. Photoredox catalysis has enabled access to unique reactivity, that is often difficult or impossible to achieve, including the anti-Markovnikov addition of nucleophiles to olefin substrates. An exploration of two novel transformations, based on this concept, is discussed herein.

REFERENCES

(1) Hedstrand, D. M.; Kruizinga, W. H.; Kellogg, R. M. *Tetrahedron Lett.* **1978**, *19*, 1255–1258.

(2) Hironaka, K.; Fukuzumi, S.; Tanaka, T. *J. Chem. Soc. Perkin Trans. 2* **1984**, *0*, 1705–1709.

(3) Pac, C.; Ihama, M.; Yasuda, M.; Miyauchi, Y.; Sakurai, H. *J. Am. Chem. Soc.* **1981**, *103*, 6495–6497.

(4) Shaw, M. H.; Twilton, J.; MacMillan, D. W. C. *J. Org. Chem.* **2016**, *81*, 6898–6926.

(5) Prier, C. K.; Rankic, D. A.; MacMillan, D. W. C. *Chem. Rev.* **2013**, *113*, 5322–5363.

(6) Romero, N. A.; Nicewicz, D. A. *Chem. Rev.* **2016**, *116*, 10075–10166.

(7) Anslyn, E. V.; Dougherty, D. A. *Modern Physical Organic Chemistry*; University Science: Sausalito, CA, 2006.

(8) Narra, S.; Nishimura, Y.; Witek, H. A.; Shigeto, S. *ChemPhysChem* **2014**, *15*, 2945–2950.

(9) Mattay, J. *Synthesis* **1989**, *1989*, 233–252.

(10) Miranda, M. A.; Izquierdo, M. A.; Pérez-Ruiz, R. *J. Phys. Chem. A* **2003**, *107*, 2478–2482.

(11) Roth, H. G.; Romero, N. A.; Nicewicz, D. A. *Synlett* **2016**, *27*, 714–723.

(12) Majek, M.; Jacobi von Wangelin, A. *Acc. Chem. Res.* **2016**, *49*, 2316–2327.

(13) Neunteufel, R. A.; Arnold, D. R. *J. Am. Chem. Soc.* **1973**, *95*, 4080–4081.

(14) Mangion, D.; Arnold, D. R. *Acc. Chem. Res.* **2002**, *35*, 297–304.

(15) Gassman, P. G.; Bottorff, K. J. *Tetrahedron Lett.* **1987**, *28*, 5449–5452.

(16) Gassman, P. G.; Bottorff, K. J. Photoinduced Lactonization. *J. Am. Chem. Soc.* **1987**, *109*, 7547–7548.

(17) Hamilton, D. S.; Nicewicz, D. A. *J. Am. Chem. Soc.* **2012**, *134*, 18577–18580.

(18) Perkowski, A. J.; Nicewicz, D. A. *J. Am. Chem. Soc.* **2013**, *135*, 10334–10337.

(19) Nguyen, T. M.; Nicewicz, D. A. *J. Am. Chem. Soc.* **2013**, *135*, 9588–9591.

(20) Wilger, D. J.; Gesmundo, N. J.; Nicewicz, D. A. *Chem. Sci.* **2013**, *4*, 3160–3165.

(21) Wilger, D. J.; Grandjean, J.-M. M.; Lammert, T. R.; Nicewicz, D. A. *Nat. Chem.* **2014**, *6*, 720–726.

(22) Grandjean, J.-M. M.; Nicewicz, D. A. *Angew. Chem. Int. Ed.* **2013**, *52*, 3967–3971.

(23) Zeller, M. A.; Riener, M.; Nicewicz, D. A. *Org. Lett.* **2014**, *16*, 4810–4813.

(24) Cavanaugh, C. L.; Nicewicz, D. A. *Org. Lett.* **2015**, *17*, 6082−6085.

(25) Fukuzumi, S.; Kotani, H.; Ohkubo, K.; Ogo, S.; Tkachenko, N. V.; Lemmetyinen, H. *J. Am. Chem. Soc.* **2004**, *126*, 1600–1601.

(26) Romero, N. A.; Nicewicz, D. A. *J. Am. Chem. Soc.* **2014**, *136*, 17024–17035.

CHAPTER TWO: SYNTHESIS OF α-BENZYLOXYAMINO-γ-BUTYROLACTONES VIA A POLAR RADICAL CROSSOVER CYCLOADDITION REACTION

2.1 Introduction

Cyclic esters, known as lactones, are structural motifs that have garnered significant attention for their presence in natural products and medicinal chemistry targets.[1] In addition to being used as simple synthetic building blocks and monomers of polyesters, lactones possess significant economic value, especially in the fragrance industry.[2] A subset of lactones that are especially valuable, due to their prevalence in synthesis, stability, and diverse bioactivity, are γ-butyrolactones.

The significance of γ-butyrolactones can be enhanced by the addition of heteroatom substituents at the α-position, with nitrogen functionality being particularly valuable. These α-amino-γ-butyrolactones are a class of bioactive heterocycles that show especially great utility in synthesis and are highly prevalent in nature. Existing as the lactone form of the amino acid homoserine, α-amino lactones can be easily converted to the straight-chain, γ-hydroxyamino acid equivalent through hydrolysis or can be used in the preparation of several amino acids that are expensive and difficult to access, such as methionine[3] and canaline.[4]

α-Amino-γ-butyrolactones, also known as homoserine lactones, have been used as scaffolds in anti-allergy, immunosuppressant, and anti-asthma agents[5] and in the synthesis of antibiotics, antifungal peptides, and serine protease inhibitors.[6] This class of γ-butyrolactones have displayed anti-tumor and anti-cancer activity towards human colorectal and breast cancer

cell lines.[7] The most significant biological activity exhibited by α-amino-γ-butyrolactones makes them desirable targets as antibiotics. In their *N*-acylated/sulfonylated form, these lactones act as signaling molecules for a population-density based, bacterial communication mechanism known as quorum sensing (Figure 2-1).[7–9] This cell-to-cell communication, between individual microorganisms, controls several factors including the growth of biofilms, as well as enzyme and virulence factor production. Consequently, these small molecules can be targeted to intercept quorum sensing for the treatment of bacterial infections. The inherent biological activity of α-amino-γ-butyrolactones makes them highly desirable as synthetic targets.

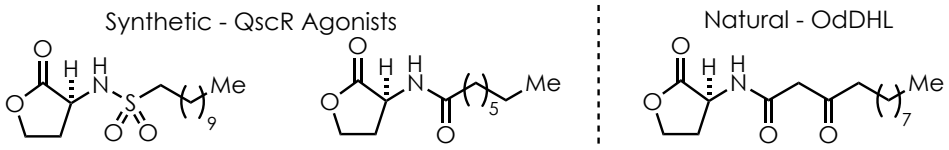

Figure 2-1. Natural and Synthetic *N*-Acylated/Sulfonylated α-Amino-γ-Butyrolactones

2.2 Synthesis of α-Amino-γ-Butyrolactones

Given their apparent importance, several methods have been reported for the synthesis of α-amino-γ-butyrolactones. Amino lactones are most commonly accessed via the cyclization of amino acids including homoserine, methionine, and aspartic acid. The most direct route to generate α-amino lactones is through the cyclization of homoserine (Scheme 2-1).[10] A protected α-amino-γ-butyrolactone can be achieved in two steps in an overall yield of 50%. While an achievable route, this method can be prohibitively expensive given the $316/g value of the amino acid starting material.[11]

Scheme 2-1. Cyclization of Homoserine to Generate a Protected α-Amino-γ-Butyrolactone

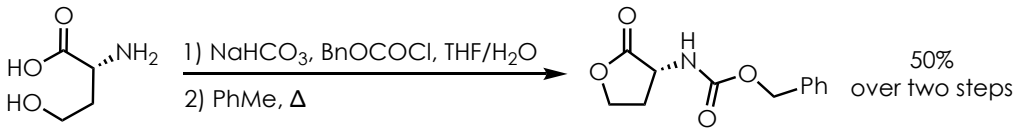

Starting from methionine, upon acid protection and methylation, the resulting sulfonium intermediate is then cyclized under basic conditions to generate the Boc-protected α-amino-γ-butyrolactone in 70% yield (Scheme 2-2).[12]

Scheme 2-2. Cyclization of Methionine to Generate a Protected α-Amino-γ-Butyrolactone

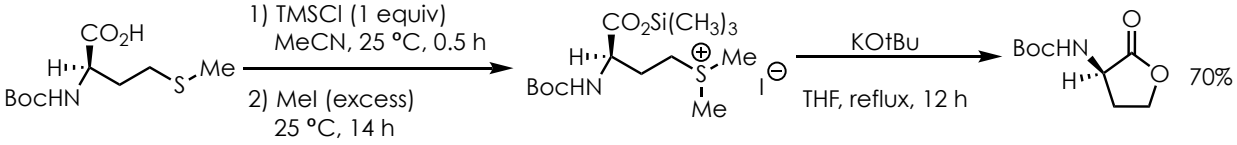

In 1978, Baldwin demonstrated the cyclization of protected, tritylated aspartic acid under reductive conditions (Scheme 2-3).[13] The α-amino-γ-butyrolactone product was isolated as the HCl salt in excellent yield. A major shortcoming associated with the cyclization of amino acid is the limited substitution pattern and functionality achievable around the resulting lactone ring, due to the lack of substation on the carbon backbone of the starting material.

Scheme 2-3. Cyclization of Aspartic Acid to Generate a Protected α-Amino-γ-Butyrolactone

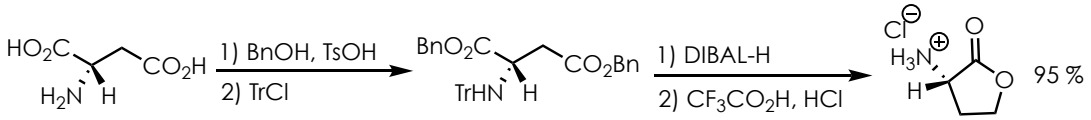

In 2014, Babu and coworkers demonstrated a stereoselective, acid-mediated, lactonization method beginning from α-amino γ,δ-unsaturated carboxylic acid esters (Scheme 2-4).[14] This method was applied to the synthesis of over 30, functionalized α-amino-γ-butyrolactones with varying substitution on the amine. Despite its diverse product scope, this route is limited to non-commercially available, terminal alkene substrates, which are not always trivial to prepare.

Scheme 2-4. Acid-Mediated Lactonization of α-Amino γ,δ-Unsaturated Carboxylic Acid Esters

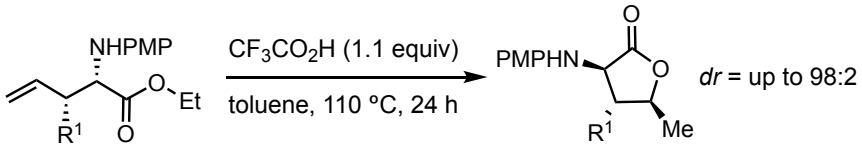

An impressive enantioselective method for generating homoserine lactones has also been achieved through the use of dual organo- and biocatalysis (Scheme 2-5).[15] Both enantiomer of an amino ketoesters can be converted to either possible diastereomers with high selectivity, in two steps, by altering the identity of the biocatalyst. The lactone product was obtained in high yield as well as enantio-, and diastereoselectivity. Despite the fact that only a single lactone product was obtained, this work demonstrates an excellent proof of concept for the selective generation of these valuable lactones.

Scheme 2-5. Accessing Homoserine Lactones via Dual Organo- and Biocatalytic System

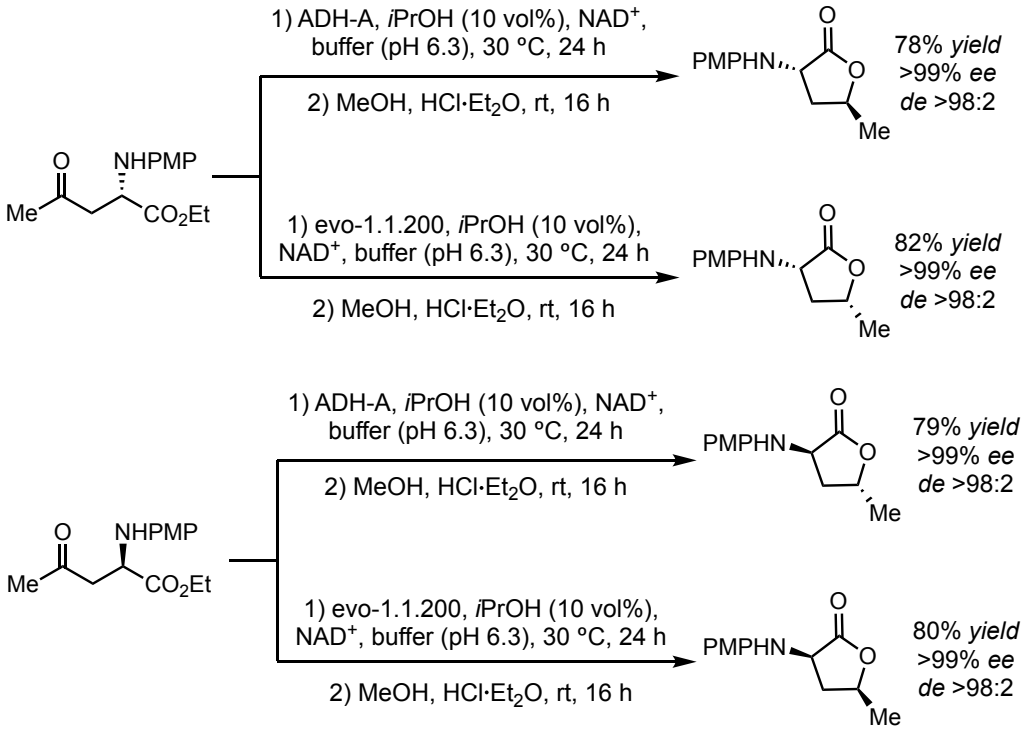

While intramolecular cyclizations have often been favored for the synthesis of α-amino lactones, several multicomponent methods have also been developed, including an interesting aza-Prins cyclization (Scheme 2-6).[16] Beginning with isobutylene and α-hydroxyhippuric acid, it has been demonstrated that a γ-butyrolactone can be obtained under acidic conditions, albeit, in a 7% yield.

Scheme 2-6. Synthesis of an α-Amino-γ-Butyrolactone via an Aza-Prins Cyclization

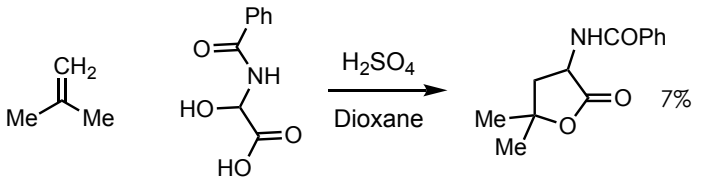

Additional methods have been reported for the production of α-amino lactones including the ring opening of aziridines (Scheme 2-7). The Loreto group successfully converted γ-ylidene-lactones to their corresponding aziridines, which were then opened to reveal the α-amino-γ-butyrolactones products.[17]

Scheme 2-7. Aziridines Opening to Reveal α-Amino-γ-Butyrolactones Products

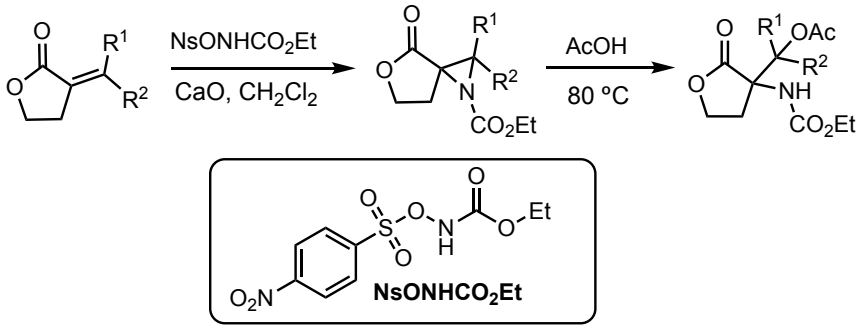

In the early 1990s, it was also demonstrated that the HCl salt of homoserine lactone could be accessed through the acidic hydrolysis of a substituted morpholinone derivative (Scheme 2-8).[18] While there is value to all of the routes discussed, current methods for synthesizing valuable α-amino-γ-butyrolactones are limited by their multistep nature, need for activated and

prefunctionalized starting materials, use of harsh conditions and exotic reagents, and the underwhelming diversity in substitution on the lactone product core.

Scheme 2-8. Acidic Hydrolysis of Morpholinone Derivative Toward the Synthesis of α-Amino-γ-Butyrolactones

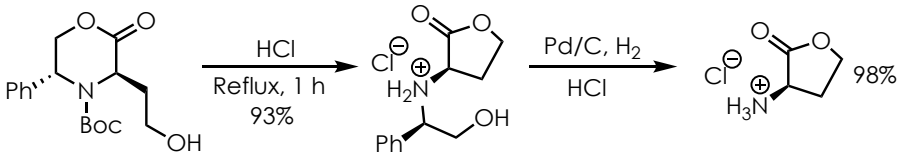

2.3 Synthesis of α-Benzyloxyamino-γ-Butyrolactones via Photoredox Catalysis

2.3.1 Background and Precedent

To overcome the limitations exhibited by current synthetic methods, we envisioned applying photoredox catalysis to the synthesis of α-amino-γ-butyrolactones, beginning from simple alkene starting materials, based on precedent from within our group. In 2013, Grandjean and Nicewicz reported the first example in our series of polar radical crossover cycloaddition (PRCC) reactions. The PRCC method involves the formation of multiple bonds through both a polar and radical reaction vector. Here, an intermolecular cycloaddition, between alkenes and alkenol coupling partners, was employed to generate highly substituted tetrahydrofurans (Scheme 2-9).[19]

Scheme 2-9. Tetrahydrofuran Synthesis Through PRCC Between Alkenes and Alkenols

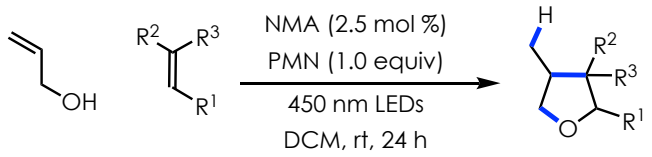

Typically, alkene functionalization reactions occur through standard substrate reactivity in which an olefin interacts in a nucleophilic fashion with an electrophilic coupling partner. In order to expand the scope of reactivity for alkenes, our lab has sought to apply organophotoredox catalysis to achieve umpolung reactivity. As a result of this polarity reversal, alkene substrates can be rendered electrophilic and can then react with nucleophiles to obtain unique products in a regioselective fashion.

To achieve this desired reactivity, 9-mesityl-10-methylacridinium (NMA) tetrafluoroborate, was employed as an excited state, single electron, photo-oxidant. When irradiated with blue LEDs, the ground state NMA enters its excited state (NMA*), allowing it to carry out single electron oxidation of an alkene substrate, such as β-methylstyrene (2.1) (Scheme 2-10). The resulting cation-radical species (2.2) then proceeds to react in both a polar and radical fashion. Initial trapping of the cation by allyl alcohol (2.3) occurs at the β-position to produce the stabilized benzylic radical (2.4). Upon deprotonation, the radical intermediate is poised to undergo a favorable 5-*exo* cyclization, with the tethered olefin, to generate a new reactive, radical species (2.5), which is then trapped with a hydrogen atom to give the final tetrahydrofuran product (2.6). In this system, terminal hydrogen atom transfer (HAT) was achieved using redox-active phenylmalononitrile (2.7) as a hydrogen atom donor. The resulting phenylmalononitrile radical (2.8) is capable of acting as a single electron oxidant, turning over the acridine radical (NMA•). Phenylmalononitrile serves an additional purpose as its anionic

form (2.9) can neutralize acid that is generated during the course of the reaction to regenerate the H-atom donor.

Scheme 2-10. Mechanism for Tetrahydrofuran Synthesis via PRCC

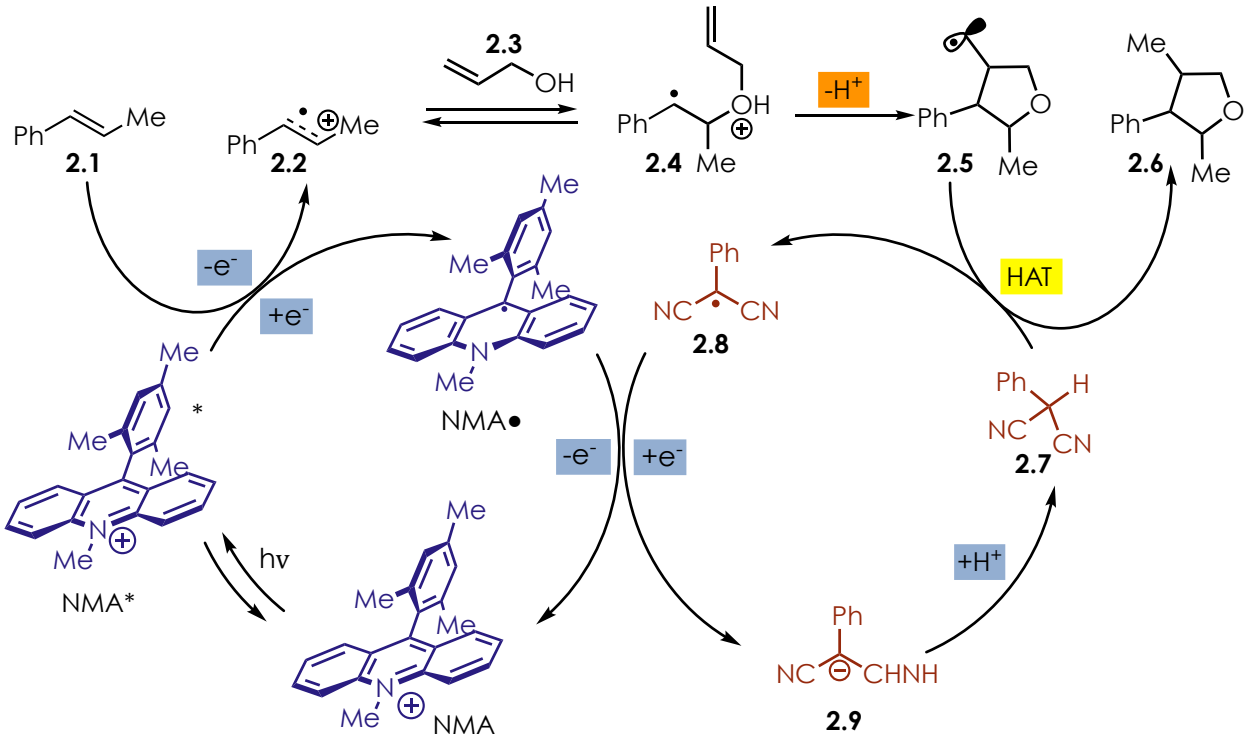

Ultimately, this photoredox system was applied to the synthesis of 18 highly substituted, tetrahydrofuran products beginning from a variety of alkenol and oxidizable alkene coupling partners (Figure 2-2).

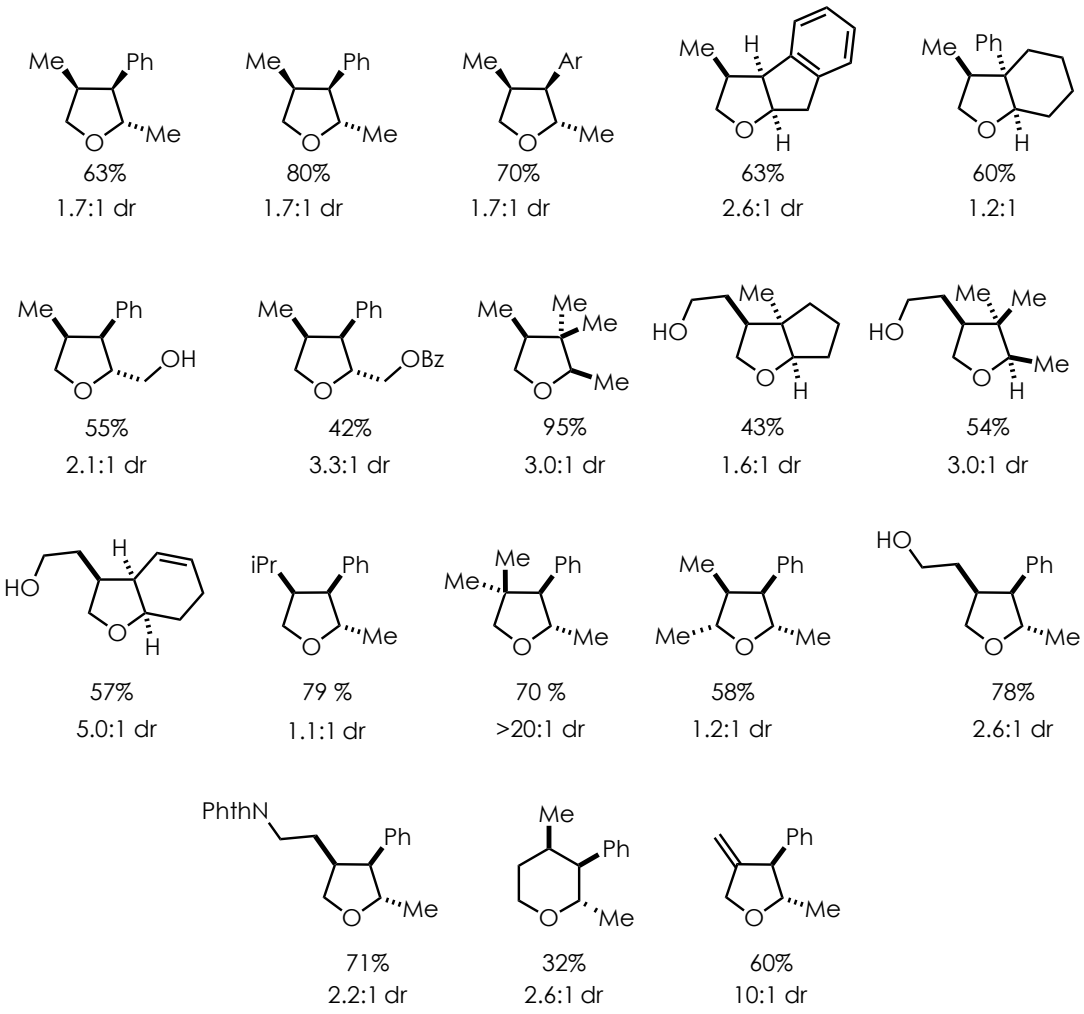

Figure 2-2. Tetrahydrofuran Synthesis Substrate Scope

In the following year, Zeller, Riener, and Nicewicz applied a similar photoredox-mediated PRCC to the synthesis of γ-butyrolactones (Scheme 2-11).[20] These valuable products could be accessed from a variety of oxidizable olefins and α,β-unsaturated acids. In this example, thiophenol (PhSH) ultimately acted as the redox-active H-atom donor, which was also capable of turning over the acridinium photoredox catalyst.

Scheme 2-11. γ-Butyrolactones Accessed Through a Photoredox Mediated PRCC

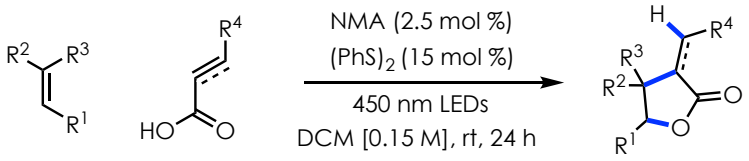

Through the development of multiple photoredox-mediated transformations, our lab has been able to draw critical conclusions regarding the reactivity of the hydrogen atom donor co-catalyst as utilized in the PRCC systems. In order to achieve successful HAT, it is necessary that the redox-active donor meet key requirements including the following:

1) The hydrogen atom donor must possess a bond dissociation energy (BDE) that falls within the range of 70-80 kcal/mol for the X-H bond for the HAT event to occur
2) The resulting radical that forms, upon HAT to the substrate, must be capable of undergoing single electron reduction to successfully turn over the photoredox catalyst and complete the catalytic cycle
3) The pKa of the hydrogen atom transfer agent must be sufficiently high enough so that it is reformed upon reduction, allowing the donor to be utilized catalytically

Multiple H-atom donors meeting these requirements have been utilized in our PRCC transformations (Figure 2-3). Thiophenol and its derivatives are often relied on as efficient H-atom donors given their sufficient BDE and pKa values. However, diphenyl disulfide[21] is commonly employed as an alternative thiophenol source due to its ease of use, lack of odor, and weak sulfur-sulfur bond (BDE ~50 kcal/mol[22]).[23]

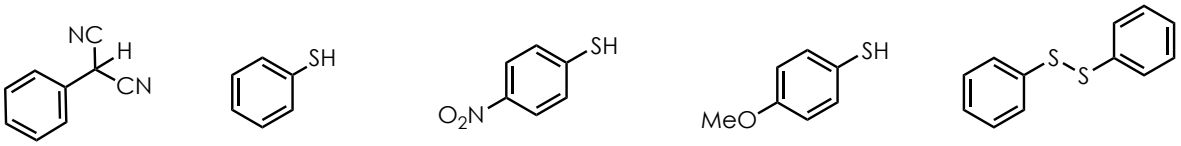

Phenylmalononitrile	thiophenol	4-nitro thiophenol	4-methoxy thiophenol	diphenyl disulfide
BDE = 77 kcal/mol	BDE = 79 kcal/mol	BDE = 81 kcal/mol	BDE = 77 kcal/mol	BDE ~ 50 kcal/mol
pKa = 4.2	pKa = 6.6	pKa = 4.5	pKa = 11.2	

Figure 2-3. Hydrogen Atom Donors and Their Corresponding BDE/pKa Values

Using catalytic quantities of diphenyl disulfide as a hydrogen atom donor, Zeller et al. successfully synthesized over 20 γ-butyrolactones varying both the olefin and α,β-unsaturated acid coupling partners (Scheme 2-12). In addition to trisubstituted alkenes (2.7), the oxidizable alkene scope included β-methylstyrene (2.8-2.10), as well as its derivatives substituted with both electron-withdrawing (2.11) and moderately electron-donating substituents (2.12-2.13). α-Methylstyrene also proved to be a competent substrate providing the lactone product, containing an all carbon quaternary center, in an 81% yield (2.14). Impressively, it was shown that substituted alkynoic acids could be utilized as coupling partners to provide the corresponding unsaturated lactones in good yield (2.15). This abbreviated exploration of the substrate scope merely touches on the impressive diversity of the transformation, though several reaction conditions were necessary to achieve this variety.

Scheme 2-12. Abbreviated γ-Butyrolactones Substrate Scope

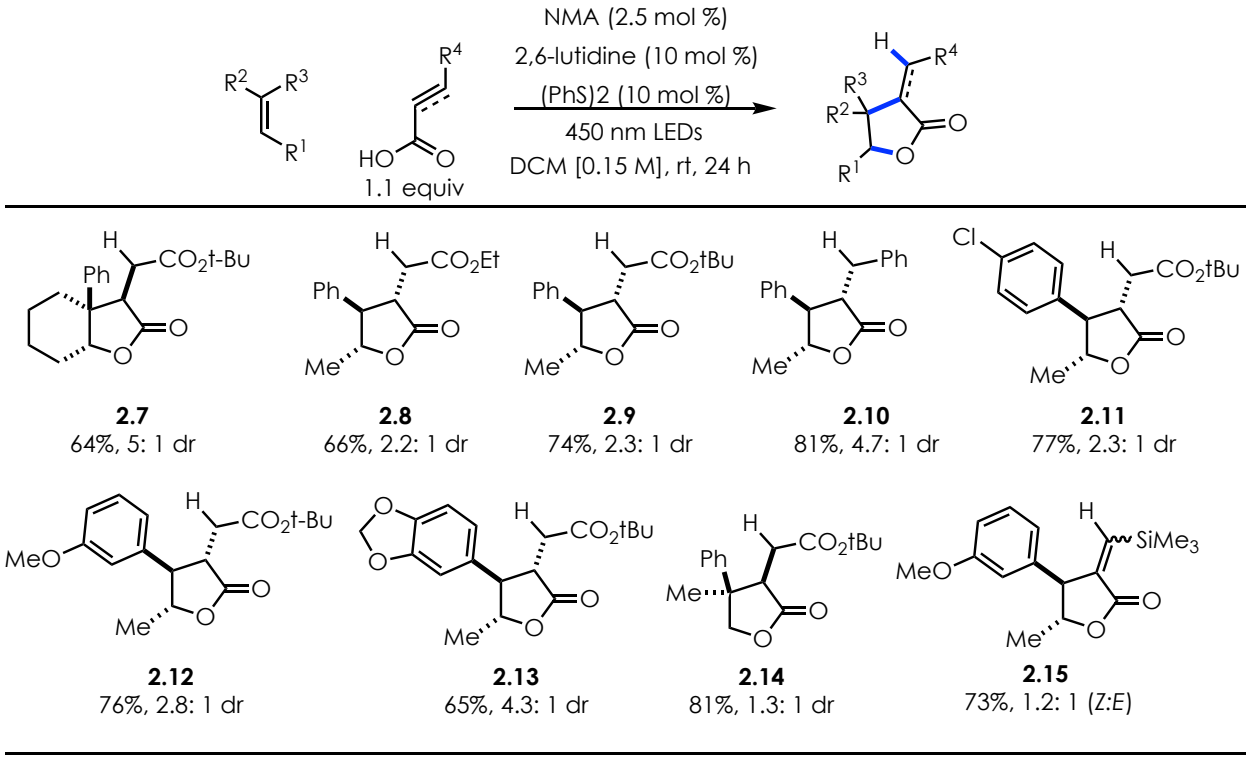

In addition, the value of this system was further demonstrated with the synthesis of two bioactive, α-methylene paraconic acids (Scheme 2-13) known as methylenolactocin (2.16) and protolichesterinic acid (2.17).

Scheme 2-13. Synthesis of Methylenolactocin and Protolichesterinic Acid via PRCC

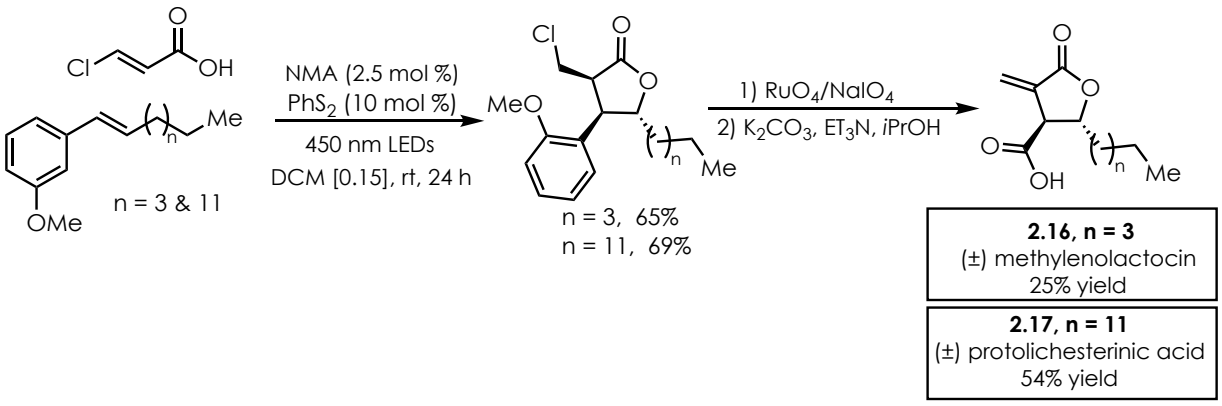

Gesmundo, Grandjean, and Nicewicz accomplished a logical and valuable expansion of this PRCC method to the formation of γ-lactams and pyrrolidines.[24] Using a system similar to those discussed previously, oxidizable olefins were found to couple successfully with unsaturated amides and protected amines to catalytically generate a variety of highly substituted, nitrogen heterocycles in a regioselective manner (Scheme 2-14). In a similar fashion to the previous PRCCs, this system was optimized using β-methylstyrene as the substrate of choice. Beginning with a protected cinnamamide coupling partner (2.18), the authors sought to overcome the major challenge of identifying reaction conditions that favored nucleophilic attack, at the cation radical intermediate, by the nitrogen, rather than the oxygen functionality, to favor lactam (2.19) over imidate (2.20) formation. Upon a closer analysis of amide protecting group identity, it was determined that a lack of protecting group or a labile group, such as a Boc group, led to substrate decomposition and a lack of product formation. However, sulfonyl-protected substrates were found to work efficiently, with more electron deficient groups leading to higher yields and a higher N:O addition ratio, favoring N-addition.

Scheme 2-14. Regioselective Synthesis of γ-Lactams Through a PRCC

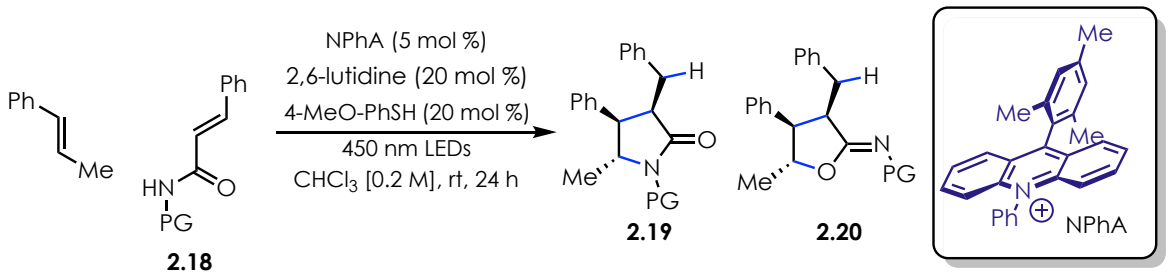

The alkene scope explored in this system is reflective of those studied in previous PRCC work (Scheme 2-15). A variety of styrenyl (2.21-2.32) and non-styrenyl (2.33-2.35) oxidizable alkenes were demonstrated to work well in the formation of lactam products, displaying good to great regioselectivity and functional group tolerance.

Scheme 2-15. γ-Lactam Scope

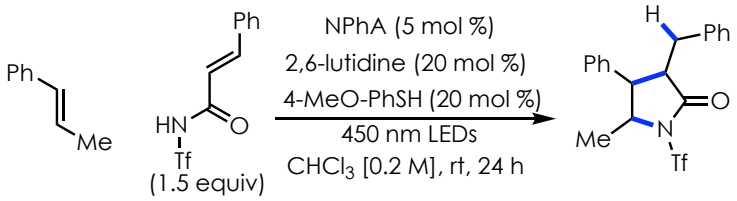

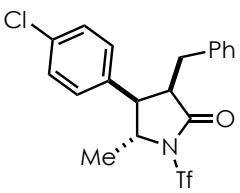

2.21
60%, 3.3:1 dr
N/O addition: 4:1

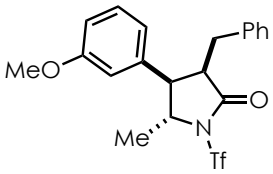

2.22
54%, 3.8:1 dr
N/O addition: 4.8:1

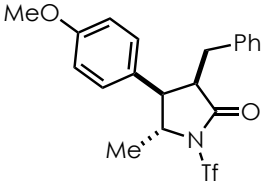

2.23
65%, 3.6:1 dr
N/O addition: 17:1

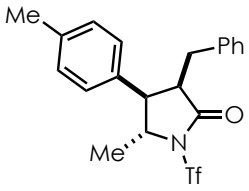

2.24
66%, 4:1 dr
N/O addition: 5.8:1

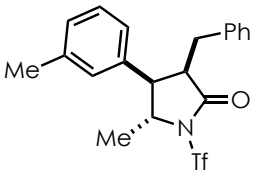

2.25
65%, 3.5:1 dr
N/O addition: 5:1

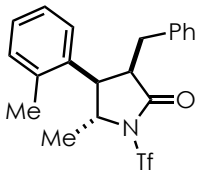

2.26
62%, 2:1 dr
N/O addition: 5.2:1

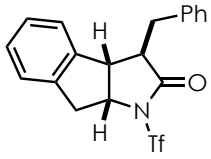

2.27
60%, 10:1 dr
N/O addition: 10:1

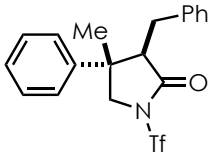

2.28
40%, 7:1 dr
N/O addition: 9:1

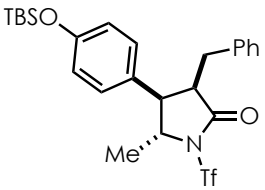

2.29
62%, 3.4:1 dr
N/O addition: 16:1

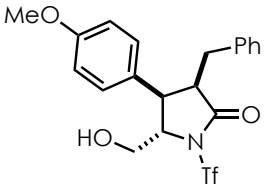

2.30
35%, 6.3:1dr
N/O addition: >20:1

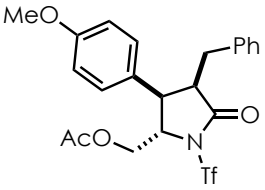

2.31
52%, 5:1 dr
N/O addition: 3:1

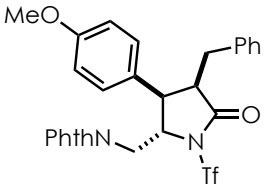

2.32
42% 5.7:1 dr
N/O addition: 2.9:1

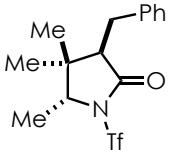

2.33
35%, 1.7:1 dr
N/O addition: 10:1

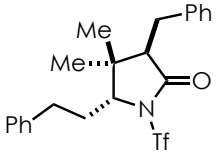

2.34
37%, 2.4:1 dr
N/O addition: 7:1

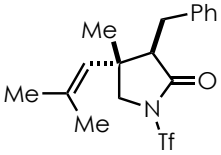

2.35
35%, 6.8:1 dr
N/O addition: 11.2:1

While protected cinnamamide derivatives worked well as an amide substrate (Scheme 2-16, 2.35-2.40), it was determined that β-aryl functionality was not required for the cyclization to occur successfully (2.41-2.44).

Scheme 2-16. Amide Scope for the Synthesis of Highly Substituted Lactams

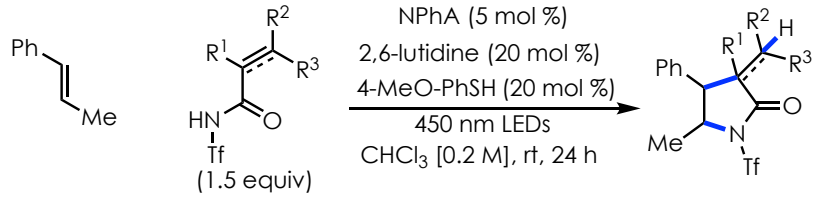

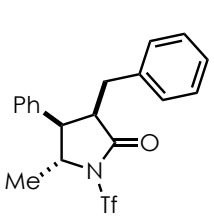

2.36
64%, 3.6:1 dr
N/O addition: 5.2:1

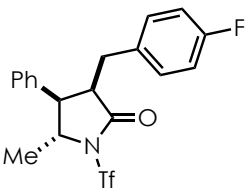

2.37
65%, 1.4:1 dr
N/O addition: 5.2:1

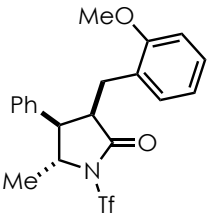

2.38
55%, 3.1:1 dr
N/O addition: 4.5:1

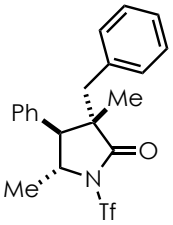

2.39
59%, 1.7:1 dr
N/O addition: 12:1

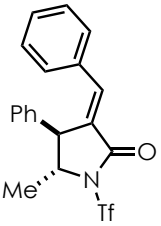

2.40
70%, 6.4:1 E/Z
N/O addition: 8.1:1

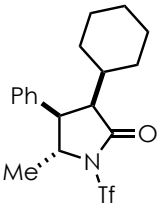

2.41
70%, 4.9:1 dr
N/O addition: 9.2:1

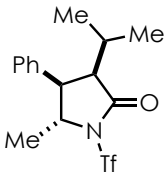

2.42
74%, 5.8:1 dr
N/O addition: >20:1

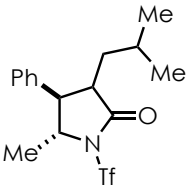

2.43
52%, 1:1 dr
N/O addition: >20:1

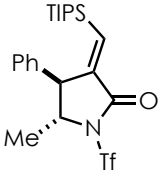

2.44
73%, 8.1:1 E/Z
N/O addition: 8.3:1

The disclosed scope for pyrrolidine product formation was limited compared to that of the γ-lactams (Scheme 2-17). Valuable however, was the discovery that the cyclization could be achieved using Boc-protected, unsaturated amines, which could then be easily deprotected upon treatment with TFA to afford the final, highly substituted, heterocycles.

Scheme 2-17. Pyrrolidine Product Scope

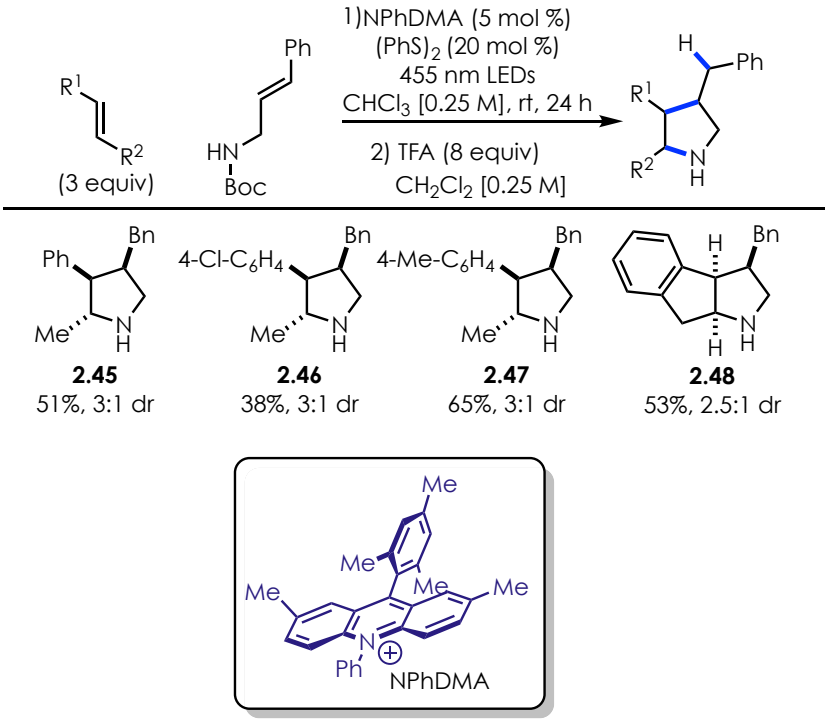

Our lab has demonstrated great success in applying PRCC systems to the preparation of highly functionalized tetrahydrofurans, γ-butyrolactones, γ-lactams, and pyrrolidine. Given this substantial amount of precedent, we believed that it would be possible to develop a similar, mild, and efficient catalytic method, toward the synthesis of valuable and potentially bioactive, α-amino-γ-butyrolactones. Work out of Derrick Clive's lab in 1997 provided further evidence that

it would be possible to use *O*-benzyloxime acids as substrates, along with oxidizable olefins, to generate these products.[25,26] In this work, Clive presented the generation of a radical precursor (2.49) derived from glyoxylic acid *O*-benzyloxime with β-bromo alcohol, which is poised to undergo a radical cyclization to generate α-benzyloxyamino-γ-butyrolactone 2.50 (Scheme 2-18). Upon esterification, the radical precursor was treated with Bu_3SnH to generate the radical intermediate, which undergoes a 5-*exo*-trig cyclization to form the final lactone product in two steps and a 51% yield. Precedent for this ring closure and formation of the nitrogen-centered radical are strong evidence that a similar intermediate, achieved through a photoredox-mediated PRCC, could undergo successful conversion to a lactone product. This method, in combination with the PRCC reactions developed within the Nicewicz lab, inspired us to develop a system for the formation of highly substituted, α-benzyloxyamino-γ-butyrolactones, in a single synthetic step, via photoredox catalysis.[27]

Scheme 2-18. Clive's Radical Cyclization of an *O*-Benzyloxime Derivative to Access an α-Benzyloxyamino-γ-Butyrolactones

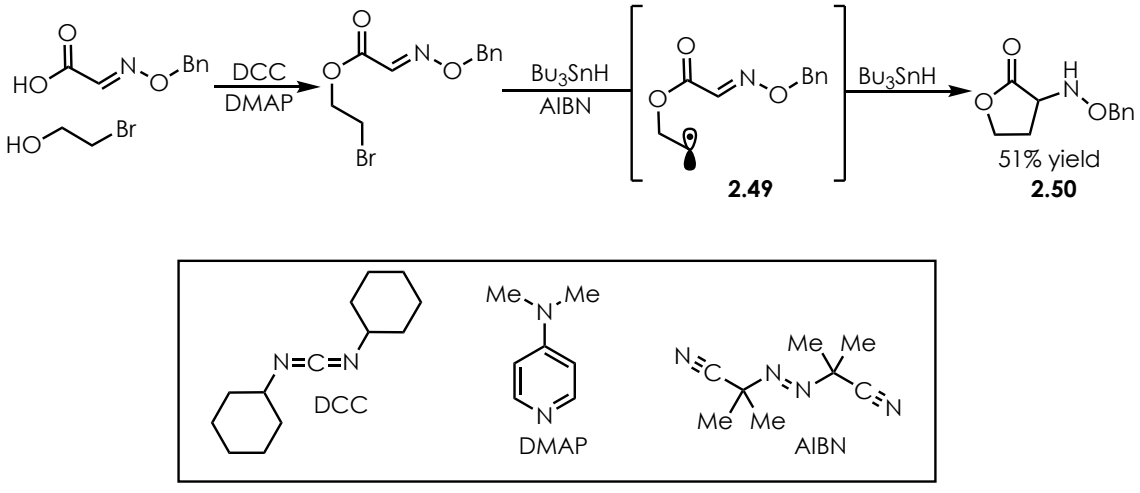

2.3.2 Results and Discussion

The investigation into the synthesis of α-benzyloxyamino-γ-butyrolactones began with conditions based on those optimized for the synthesis of γ-butyrolactones (Table 2-1). Initially, we tested *β*–methylstyrene and *O*-benzyloxime acid as the two potential reaction partners. The *O*-benzyloxime acid substrate was prepared through the efficient condensation of benzyloxyamine hydrochloride onto glyoxylic acid in a 96% yield (Scheme 2-19).

Scheme 2-19. Preparation of *O*-Benzyloxime Coupling Partner

A promising initial hit was realized using catalytic quantities of NMA and diphenyl disulfide, in DCM, which resulted in the formation of the desired lactone product in a moderate yield (57%) (Table 2-1, entry 1). A solvent screen revealed that solvents of varying polarity, including DCE, chloroform, and acetone, led to suppressed yields or complete inhibition of the reaction (Table 2-1, entries 2-4). Given the diversity of hydrogen atom donors that had been considered previously in similar systems, we believed it would be valuable to consider the identity of the cocatalyst in this transformation (Table 2-1, entries 5-7). Despite screening thiophenol derivatives of varying electronics, it was determined that diphenyl disulfide was the most efficient hydrogen atom donor cocatalyst. As was the case in the synthesis of γ-butyrolactones and γ-lactams, it was found that the addition of catalytic quantities of 2,6-lutidine could help to enhance the reactivity, likely via deprotonation of the carboxylic acid nucleophile

in situ (Table 2-1, entries 8-11). An optimal loading of 15 mol% was observed, resulting in a yield of 69% (Table 2-1, entry 10). Higher (Table 2-1, entry 11) and lower (Table 2-1, entry 9) loadings of base led to diminished yields.

Table 2-1. Optimization of PRCC Conditions for the Synthesis of α-Benzyloxyamino-γ-Butyrolactones

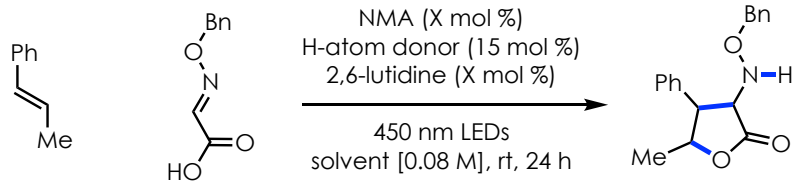

Entry	H-atom donor	NMA (mol %)	2,6-Lutidine (mol %)	Solvent	Yield[a] (%)
1[b]	$(PhS)_2$	2.5	0	CH_2Cl_2	57
2	$(PhS)_2$	2.5	0	$CHCl_3$	35
3	$(PhS)_2$	2.5	0	acetone	0
4	$(PhS)_2$	2.5	0	$(CH_2Cl)_2$	39
5[b]	4-(MeO)PhSH	2.5	0	CH_2Cl_2	40
6[b]	4-(NH_2)PhSH	2.5	0	CH_2Cl_2	40
7	4-$(NO_2PhS)_2$	2.5	0	CH_2Cl_2	29
8	$(PhS)_2$	2.5	0	CH_2Cl_2	38
9	$(PhS)_2$	2.5	5	CH_2Cl_2	53
10	$(PhS)_2$	2.5	15	CH_2Cl_2	69
11	$(PhS)_2$	2.5	20	CH_2Cl_2	51
12[c,d]	$(PhS)_2$	0	15	CH_2Cl_2	0
13	$(PhS)_2$	5.0	0	CH_2Cl_2	42
14	$(PhS)_2$	7.5	0	CH_2Cl_2	39
15[d]	None	2.5	15	CH_2Cl_2	40
16[c,d]	$(PhS)_2$	2.5	15	CH_2Cl_2	88

Reactions were carried out on a 0.33 mmol scale in N_2-sparged solvent [0.08 M] under 2 LED lamps (λ_{max} = 450 *nm*) for 24 h. [a]Yields were obtained relative to $(Me_3Si)_2O$ ^{1}H NMR internal standard of crude reaction mixtures. [b]Reaction was run at [0.15 M] [c]10 mol % disulfide. [d]alkene/acid = 1.5:1.

Having achieved an increase in product yield, a series of control experiments were carried out to confirm the catalytic activity in our proposed transformation. Omitting NMA resulted in no product formation thereby demonstrating the necessity of the photocatalyst in the

system (Table 2-1, entry 12). It should be noted however, that an increase in the loading of NMA resulted in lower yields of the lactone product (Table 2-1, entries 13-14). A curious observation was made upon exclusion of the hydrogen atom donor cocatalyst as the product was still observed, though in a limited yield of 40% (Table 2-1, entry 15). This product formation is accounted for in the succeeding discussion of the reaction mechanism. It was demonstrated that a change in the alkene/oxime ratio from 1:1.1 to 1.5:1, along with lowering the disulfide loading to just 10 mol%, improved the yield of the lactone product to 88% (Table 2-1, entry 16).

Having developed optimal reaction conditions for the PRCC between oxidizable olefins and an oxime acid coupling partner, we then set out to study the scope of the transformation in relation to the *O*-benzyloxime acid (Scheme 2-20). *O*-Benzyloxime 2.51 was successfully reacted with *β*–methylstyrene to provide the α-benzyloxyamino-γ-butyrolactone (2.54) in a 71% yield. We were pleased to discover that the synthesis of oxime acids could be expanded to include substitution at the α-position. As a result, lactone products bearing α-quaternary carbons (2.55 and 2.56) could be accessed from pyruvic acid (2.52) and phenylglyoxylic acid (2.53) derived oximes without diminishing the yield of the reaction.

Scheme 2-20. Exploration of *O*-Benzyloxime Acid Scope

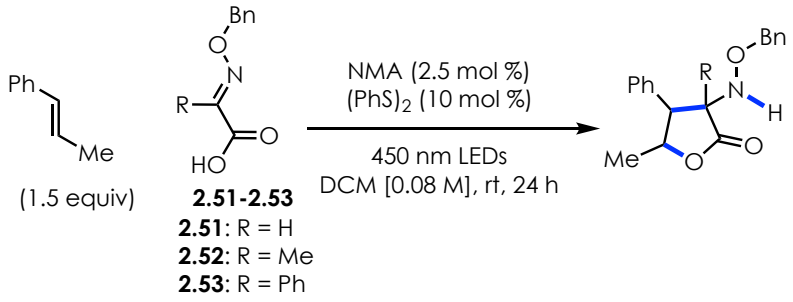

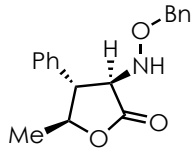

2.54
71%, 2.0:1 dr[a]

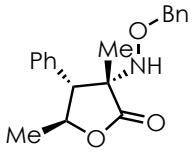

2.55
73%, 5.0:1 dr

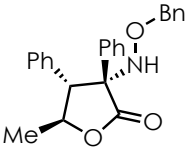

2.56
64%, 1.2:1 dr[b]

Reactions were carried out in N_2-sparged CH_2Cl_2 [0.08 M] on a 0.33 mmol scale under 2 LED lamps (450 nm λ_{max}) for 24 h. Yields represent an average of two isolated yields on a 0.33 mmol scale. [a]Reaction ran with 15 mol % 2,6-lutidine. [b]Reaction ran on a 0.17 mmol scale, [0.02 M].

Following the exploration of the oxime acid scope, a variety of alkene partners were then screened against benzyloxime acid 2.51 (Scheme 2-21). The initial investigation began with the consideration of various *β*–methylstyrene derivatives of varying substitution (2.57-2.68). Several halogenated derivatives were considered and produced the corresponding, desired lactones (2.57-2.62) in good to excellent yields regardless of the substitution pattern. Anethole, along with its *o*- and *m*-regioisomers, models the tolerance of the system for varying electronic and steric effects, furnishing each of the corresponding lactones in fair to good yields (2.63-2.65). Alkyl-substituted aryl rings verified that moderately electron-rich *β*–methylstyrene derivatives were also plausible coupling partners (2.66-2.68). Methyl-substituted products 2.66 and 2.67 were obtained in 64% and 62% yield, respectively. *tert*-Butyl-*β*–methylstyrene gave 2.68 in 60% yield. Changing from *β*–methyl to α-methylstyrene as the alkene component produced a *β*–

quaternary substituted lactone (2.69) in 58% yield. We also considered trisubstituted alkenes as coupling partners (2.70-2.71), which provided the lactone products in varying yields. Lactone 2.70 was obtained in an excellent yield of 88% from 1-phenylcyclohexene. Cyclization was more problematic when 2-methyl-2-butene was used as the coupling partner, furnishing the lactone product in a yield of 42% (2.71). We were pleased to observe that this method could be successfully applied to the formation of lactone products, possessing desirable all-carbon quaternary centers. Tricyclic lactone 2.72 was obtained in good yield (53%) from indene. Lastly, an alkene bearing a phthalimide-protected nitrogen and a *β*–methylstyrene derived *tert*-butyldimethylsilyl (TBS) ether resulted in derivatives 2.73 and 2.74 in 41% and 71% yields, respectively. Overall, these results demonstrate that this photoredox-mediated PRCC system can be used to efficiently generate the desired, substituted α-amino lactone products in fair to excellent yields.

Scheme 2-21. Alkene Scope for the Synthesis of α-Benzyloxyamino-γ-Butyrolactone

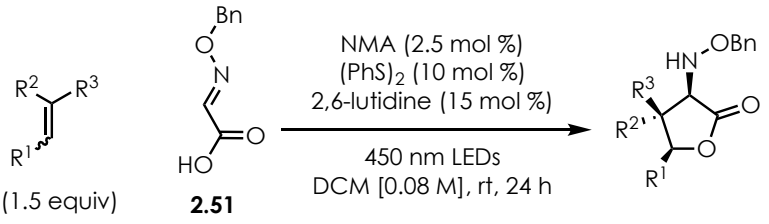

(1.5 equiv) **2.51**

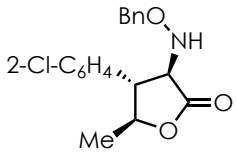
2.57 77%, 1.0:1 dr

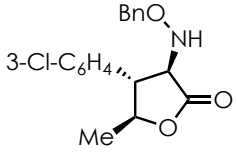
2.58 73%, 1.8:1 dr

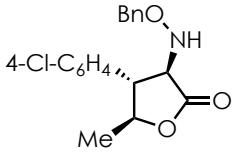
2.59 62%, 2.4:1 dr

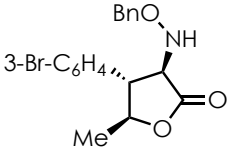
2.60 72%, 1.8:1 dr

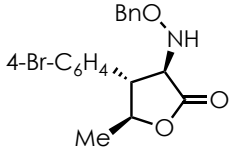
2.61 73%, 1.8:1 dr

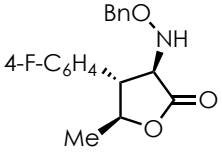
2.62 66%, 2.0:1 dr

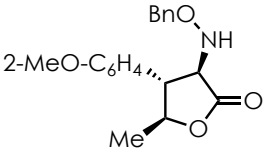
2.63 58%, 1.2:1 dr

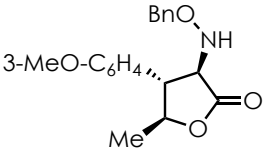
2.64 65%, 2.0:1 dr

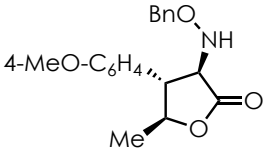
2.65 46%, 2.1:1 dr

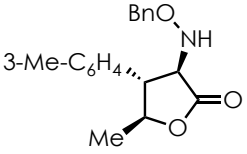
2.66 64%, 2.4:1 dr

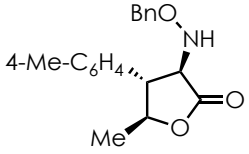
2.67 62%, 2.1:1 dr

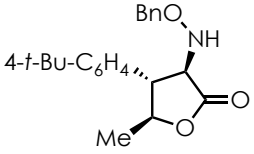
2.68 60%, 2.4:1 dr

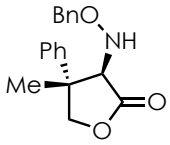
2.69 58%, 2.9:1 dr[a]

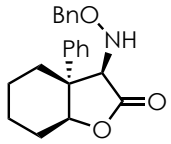
2.70 88%, 1.5:1 dr

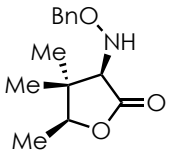
2.71 42%, 1.7:1 dr[a,b]

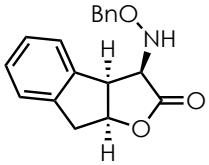
2.72 53%, 1.0:1 dr

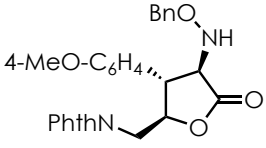
2.73 41%, 3.2:1 dr

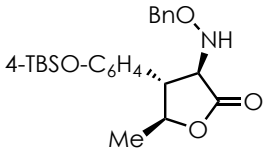
2.74 71%, 1.9:1 dr

Reactions were carried out in N_2-sparged CH_2Cl_2 [0.08 M] on a 0.33 mmol scale under 2 LED lamps (450 nm λ_{max}) for 24 h. Yields represent an average of two isolated yields on a 0.33 mmol scale. [a]Reaction ran with Mes-Acr-Ph. [b]Reaction ran with 3 equiv 2-methyl-2-butene.

The dual-catalytic mechanism, proposed for this transformation, is reflective of the previous PRCC systems explored within our lab (Scheme 2-22). Beginning in its ground state, the acridinium (NMA) enters its excited state (NMA*) upon absorption of visible light. The excited state photoredox catalyst is now capable of undergoing single electron transfer with the alkene substrate (2.75), generating a cation radical intermediate (2.76), which simultaneously leads to the formation of the acridine radical (NMA•). The cation radical is poised to undergo nucleophilic trapping by the oxime acid (2.77), resulting in the formation of carbon-centered radical 2.78. Following deprotonation of the intermediate, this radical undergoes an irreversible 5-*exo*-trig cyclization.

Scheme 2-22. Proposed Mechanism for the Production of α-Benzyloxyamino-γ-Butyrolactones via a PRCC

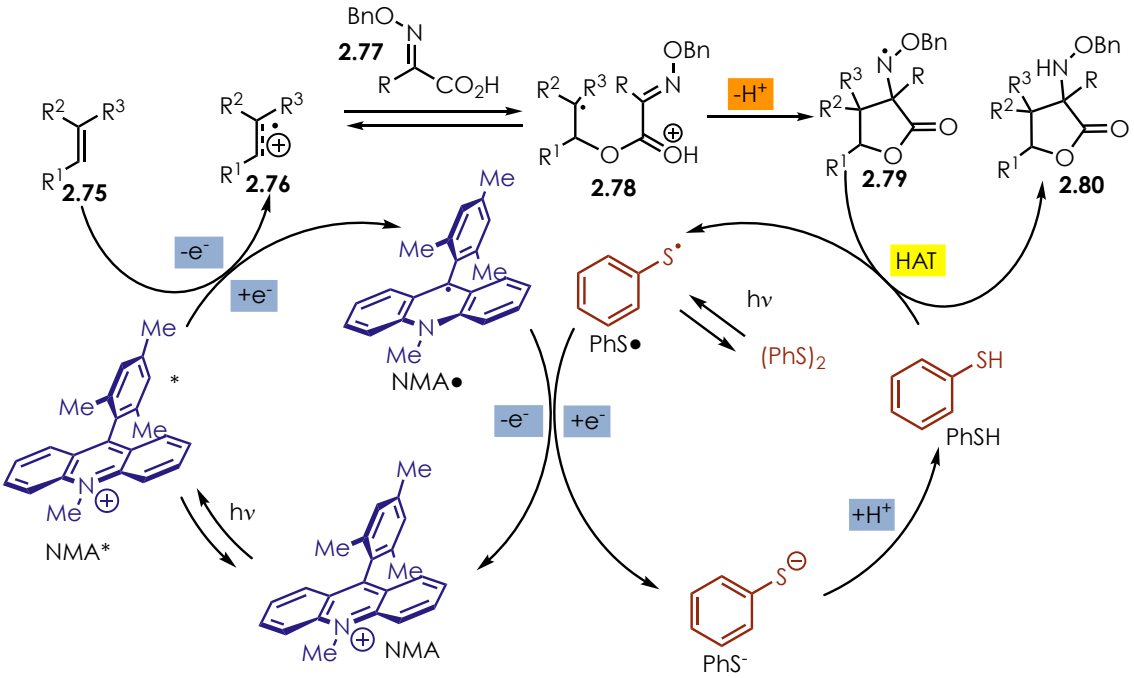

Zeller et al. conducted an additional test reaction to determine the potential reversibility of this cyclization step (Scheme 2-23). Classical radical hydrodehalogenation conditions were applied to *β*–bromo substrate 2.81 resulting in the formation of product 2.82 only. The lack of uncyclized product (2.83) formation is suggestive of an irreversible trapping step, as this product would have formed if the radical cyclization were reversible.

Scheme 2-23. Hydrodehalogenation of a *β*–Bromo Substrate to Test the Reversibility of the Radical Cyclization Step

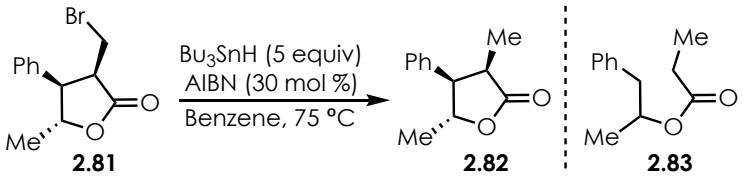

The unique component of this PRCC system resides in the formation of nitrogen-centered radical. While previous PRCC reactions have proceeded through the formation of a carbon-centered radical upon cyclization, this synthetic route requires irreversible radical trapping through the carbon-nitrogen double bond of the oxime, resulting in a stable nitrogen-centered radical 2.79.

A parallel, redox cycle exists for the hydrogen atom donor cocatalyst in conjugation with the photoredox catalyst cycle. This system was highly tolerant of diphenyl disulfide (PhS_2) as a cocatalyst, relying on photolytic homolysis to generate a phenylthiyl radical (PhS•) in situ. With a reduction potential of +0.16 V vs SCE,[23] this sulfur-centered radical functions efficiently as a single-electron oxidant to regenerate the acridinium ground state (NMA•, $E_{red}^{1/2}$ = -0.55 V vs SCE) and form the thiolate anion (PhS^-), which is converted to thiophenol (PhSH) upon proton

transfer. This HAT step has been identified as exhibiting a significant rate-limiting influence on the system. The thiophenol then acts as the terminal hydrogen atom donor, which converts 2.79 to the desired α-benzyloxyamino-γ-butyrolactone product (2.80). Ultimately, the resulting thiophenol can then reenter the catalytic cycle.

Based on the observation that a moderate amount of lactone product is generated in the absence of diphenyl disulfide (Table 2-1, entry 15), we proposed that an additional pathway likely operates without the involvement of a hydrogen atom donor cocatalyst (Scheme 2-24). To account for this observation in the mechanism, we propose that the nitrogen-centered radical 2.79 can be reduced by the acridine radical to simultaneously generate a nitrogen anion and regenerate the ground state acridinium (NMA). Protonation of the anion, likely via lutidinium or an equivalent of acid would lead to formation of the product.

Scheme 2-24. Explanation of Product Formation When Hydrogen Atom Donor is Omitted

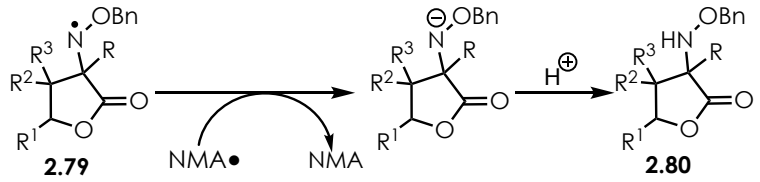

The final undertaking for this project was to determine the relative stereochemistry of the major and minor diastereomers. Though the transformation proved to not be especially selective for one stereoisomer over the other, we believed it was necessary to identify the major conformer. It is worth noting that no conclusions could be drawn directly from previously reported PRCC systems as the favored diastereomer alternates between a 3,4-*cis*/4,5-*trans* and 3,4-*trans*/4,5-*trans* substituent relationship depending on the system. The all-*trans* diastereomer

was favored for the synthesis of γ-butyrolactones. Conversely, tetrahydrofuran, lactam, and pyrrolidine products were isolated as the 3,4-*cis*/4,5-*trans* conformer. Initially, we attempted to use similar epimerization conditions, as those used previously, to identify the major adduct.

Based on previous evidence,[20] it was assumed that the product was the thermodynamically favored 3,4-*trans* isomer. As demonstrated in the synthesis of γ-butyrolactones, epimerization conditions can be used to determine the major/minor diastereomer (Scheme 2-25). Enrichment of the major diastereomer under epimerization conditions would suggest that the thermodynamically favored, all-*trans* conformation is the major diastereomer and the minor product exhibits a 3,4-*cis*/4,5-*trans* relationship. Epimerization, via deprotonation of the α-proton, leading to the enrichment of the minor diastereomer, would indicate that the *cis*-*trans* conformation is the major product.

Scheme 2-25. Determination of Major Diastereomer Conformation Under Epimerization Conditions

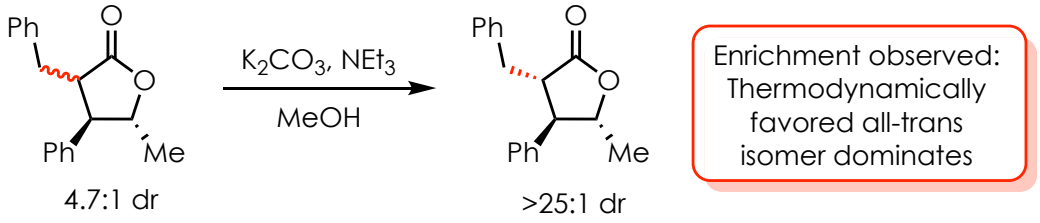

To our dismay, deprotonation at the α-carbon of the α-benzyloxyamino-γ-butyrolactone product resulted in a loss of the *O*-benzyl group (2.81) and subsequent enamine formation (2.82), as observed by GC-MS (Scheme 2-26).

Scheme 2-26. Enamine Formation Observed Under Epimerization Conditions

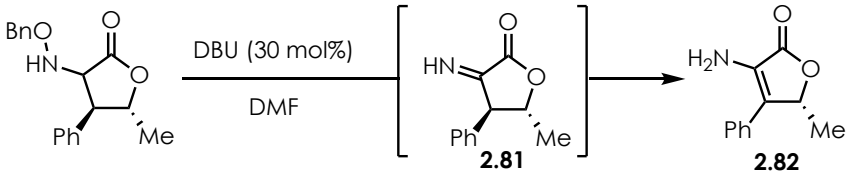

In an effort to circumvent the formation of the undesired elimination product, we directed our efforts towards the initial hydrogenation of the benzyloxyamino, followed by the application of the epimerization conditions to the free amine. Unfortunately, none of the reduced product was generated after screening several reduction methods (Table 2-2). We then attempted initial nitrogen acylation to facilitate benzyloxyamine reduction prior to applying the epimerization conditions.

Table 2-2. Exploration Of Reduction Conditions to Access the Free Amine Product

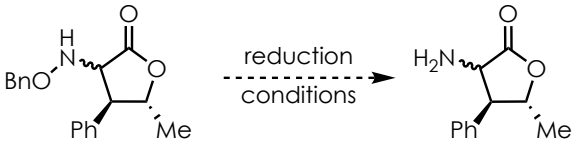

Catalyst	H_2	Solvent	Temp (°C)	Time (h)	Yield (%)	Observation
Zn(0)	---	AcOH	120	24	0	returned starting material
Pd/C	Balloon	MeOH	23	4	0	returned starting material
PtO_2	Balloon	EtOH	23	48	0	returned starting material

Acylation proved fruitless after many attempts using several methods and acylating agents (Table 2-3).

Table 2-3. Exploration Of Acylation Conditions to Access the *N*-Acyl Amine

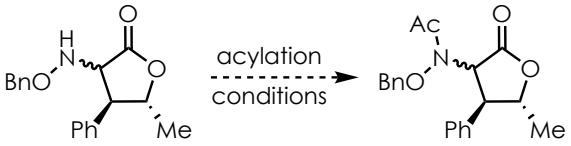

Acylating Reagent	Base	Additive	Solvent	Temp (°C)	Time (h)	Yield (%)
AcCl	TEA	---	THF	23	0.5	0
AcCl	TEA	DMAP	THF	23	24	0
AcCl	TEA	DMAP	THF	40	24	0
BzCl	K_2CO_3	---	H_2O:EtOAc	23	7	0
*p*Cl-BzCl	TEA	DMAP	THF	40	24	0
TFAA	TEA	---	TFAA	23	4	0
TFAA	TEA	---	TFAA	23	20	0

Ultimately, we determined that the most suitable method for identifying the preferred conformation of the benzyloxyamino lactones was through the use of selective 1D-NOESY NMR experiments (Figure 2-4) (see Experimental Section). Product 2.63 was used as a model to define the stereochemistry for the *β*–methylstyrene derived products. Due to challenges associated with separating diastereomers, this substrate was selected, as it possessed ^{1}H NMR peaks that were distinguishable between the inseparable diastereomers. Upon individual irradiation of each proton, a stronger NOE was observed between the protons at the 3 and 5 positions than between those at the 3/4 or 4/5 positions, indicating that the two were likely

located on the same face of the 5-membered ring in the major diastereomer. The minor diastereomer exhibited no NOE between the protons located at the 4 and 5 positions and a strong signal for protons in the 3 and 4. Based on these observations, we concluded that the major diastereomer was the all-*trans* product and the minor diastereomer exhibited a *cis-trans* relationship. So not to draw general conclusions from *β*–methylstyrene substrates, the stereochemistry of lactones 2.55 and 2.69-2.72 were assigned separately, using 1D-NOESY NMR experiments, from their respective spectra. In general, the product diastereoselectivity (dr) was consistently around 2.0:1 or less, with a few exceptions.

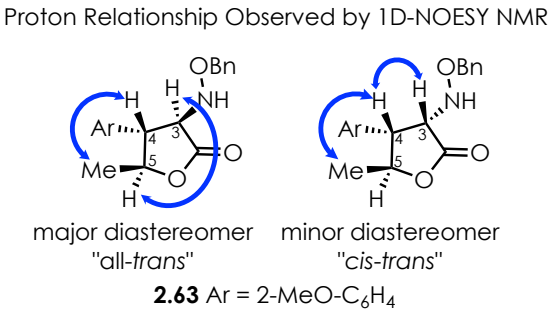

Figure 2-4. Major Diastereomer Identification Based on 1-D NOESY NMR Analysis

Lastly, we sought to demonstrate that our α-benzyloxyamino-γ-butyrolactones could be converted to the corresponding free amine. Since previous attempts to demonstrate the benzyloxyamine reduction failed, we turned our attention towards a report in the literature of the reduction of a similar substrate.[28] Ultimately, the reduction was found to require more forcing conditions, using a super-stoichiometric loading of Pearlman's catalyst, $Pd(OH)_2/C$, and high H_2 pressure (40 psi) to achieve the reduction of substrate 2.55 in a 72% yield without a deleterious

effect on the diastereoselectivity (Scheme 2-27). Obtaining the reduced, free amine product could allow for further functionalization of the lactones.

Scheme 2-27. *O*-Benzyl Amine Reduction to Generate Free α-Amino-γ-Butyrolactone

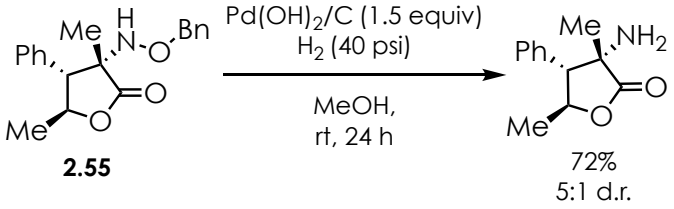

2.4 Conclusion

Ultimately, we have developed a useful method for the synthesis of substituted, α-benzyloxyamino-γ-butyrolactones from easily accessible oxime acid starting materials and simple, commercially available, alkenes. In addition to generating two α-disubstituted γ-butyrolactones, 19 highly substituted lactone products were also prepared in fair to excellent yield. The scope of the transformation exhibited wide steric and electronic tolerance as well as functional group compatibility. We are confident that the use of this photoredox-mediated PRCC, for the generation of α-benzyloxyamino-γ-butyrolactones, will be useful in synthesis of small molecules and that these highly substituted lactones could be studied further for biological activity.

In addition to these valuable features, this methodology provides a significant number of advantages over previously published methods for generating α-amino lactones. Unlike the work presented by Clive and others, this reaction is effective at forming three new σ bonds in a single step, beginning from easily made and/or commercially available starting materials. The

transformation also proceeds efficiently under mild reaction conditions, generating highly substituted, novel α-benzyloxyamino-γ-butyrolactone products, without the use of harsh and hazardous reagents.

To further develop this project, we have made initial attempts toward employing alkynes, in place of alkenes, in the PRCC reaction manifold. It has been observed that alkynes, such as diphenylacetylene and 4-ethynylanisole, would be oxidizable using acridinium photoredox catalysts given their redox potentials of $E_{p/2}$ = +1.84 V and +1.65 V vs SCE, respectively.[29] Using alkynes as potential coupling partners in PRCC reactions would allow us to build complexity into heterocyclic compounds (Figure 2-5). The addition of unsaturation into the previously prepared lactone and lactam cores will allow for additional functionalization of the β–γ-unsaturated ring. By incorporating unsaturation into the system, we are pursuing the generation of several highly substituted and valuable heterocycles including imidazoles, pyrroles, and thiophenes.

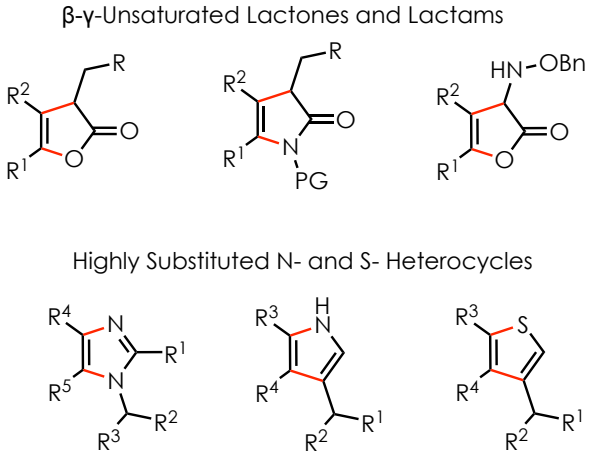

Figure 2-5. Potential Heterocycles Accessible Through PRCC With Alkyne Substrates

2.5 Experimental

General Information: Materials and Methods

Commercially available reagents were purchased from Sigma Aldrich, Acros, Alfa Aesar, or TCI, and used as received unless otherwise noted. Dichloromethane (DCM) was dried by passing through activated alumina columns under nitrogen prior to use. Irradiation of photochemical reactions was carried out using two 15W PAR38 blue LED floodlamp purchased from EagleLight (Carlsbad, CA) and one 21W PAR38 blue aquarium LED lamp (Model #6851) purchased from Ecoxotic (www.ecoxotic.com), with borosilicate glass vials purchased from Fisher Scientific. Thin layer chromatography (TLC) was performed on SiliaPlate 250 μm thick silica gel plates provided by Silicycle. Visualization was accomplished with short wave UV light (254 nm), aqueous basic potassium permanganate solution, or cerium ammonium molybdate solution followed by heating. Flash chromatography was performed using SiliaFlash P60 silica gel (40-63 μm) purchased from Silicycle. Yield refers to isolated yield of analytically pure material unless otherwise noted. Proton and carbon magnetic resonance spectra (^{1}H NMR and ^{13}C NMR) were recorded on a Bruker model DRX 400 or a Bruker AVANCE III 600 CryoProbe (^{1}H NMR at 400 MHz or 600 MHz and ^{13}C NMR at 101 or 151 MHz) spectrometer with solvent resonance as the internal standard (^{1}H NMR: $CDCl_3$ at 7.26 ppm, ^{13}C NMR: $CDCl_3$ at 77.0 ppm). ^{1}H NMR data are reported as follows: chemical shift, multiplicity (s = singlet, d = doublet, t = triplet, dd = doublet of doublets, ddt = doublet of doublet of triplets, ddd = doublet of doublet of doublets, dddd = doublet of doublet of doublet of doublets m = multiplet, brs = broad singlet), coupling constants (Hz), and integration. NMR yields were determined using hexamethyldisiloxane, $(Me_3Si)_2O$, as an internal standard. Infrared (IR) spectra were obtained using a Jasco 260 Plus Fourier transform infrared spectrometer. Dichloromethane (DCM) was

used as the solvent for FT-IR spectroscopy. High resolution mass spec (HRMS) was obtained on the Thermo LTqFT mass spectrometer with electro spray ionization in positive mode.

Lamp Setup:

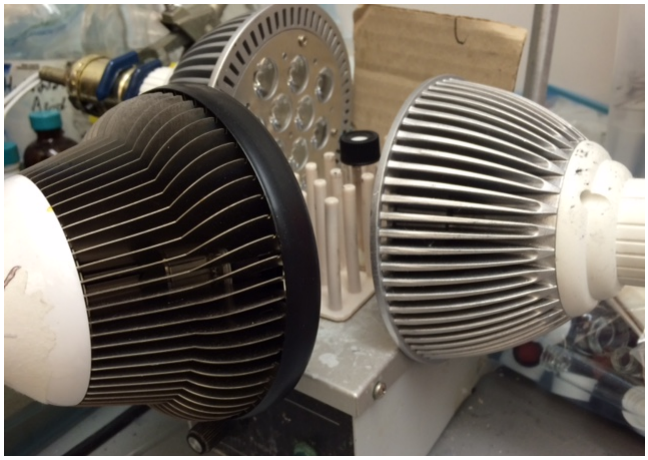

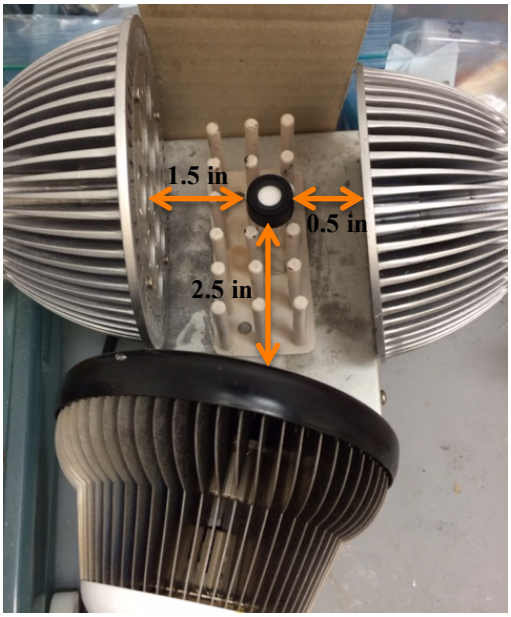

Preparation of Photoredox Catalyst

The acridinium photoredox catalyst (NMA) was prepared according to published literature procedures. Spectral data were in agreement with literature values.[30]

Preparation of Alkene Substrates

Purchased Alkenes: β-methylstyrene (**1a**), anethole (**1b**), indene (**1c**), α-methylstyrene (**1d**), 1-phenyl-1-cyclohexene (**1e**), and 2-methyl-2-butene (**1f**) were purchased from a commercial source.

Synthesized Styrenes: The following alkenes were prepared according to a published Wittig olefination procedure.[24]

β-Methyl-3-bromostyrene (1g): Spectral data were in agreement with literature values.[31]

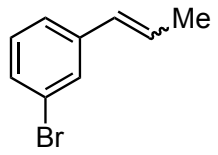

β-Methyl-4-bromostyrene (1h): Spectral data were in agreement with literature values.[32]

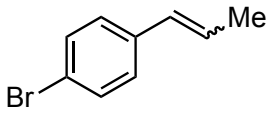

β-Methyl-2-chlorostyrene (1i): Spectral data were in agreement with literature values.[33]

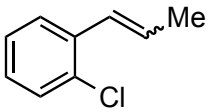

β-Methyl-3-chlorostyrene (1j): Spectral data were in agreement with literature values.[31]

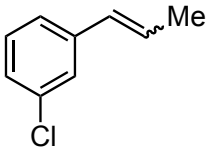

β-Methyl-4-chlorostyrene (1k): Spectral data were in agreement with literature values.[31]

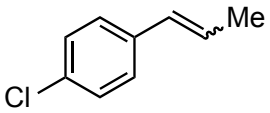

β-Methyl-4-fluorostyrene (1l): Spectral data were in agreement with literature values.[34]

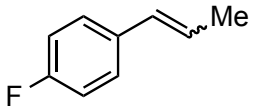

β-Methyl-3-methylstyrene (**1m**)**:** Spectral data were in agreement with literature values.[35]

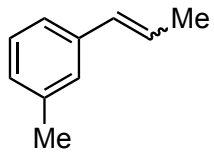

β-Methyl-4-methylstyrene (**1n**)**:** Spectral data were in agreement with literature values.[36]

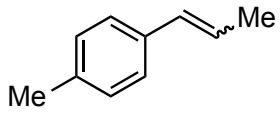

β-Methyl-4-*tert*-butylstyrene (**1o**)**:** Spectral data were in agreement with literature values.[37]

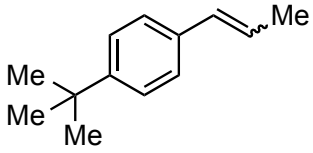

β-Methyl-2-methoxystyrene (**1p**): Spectral data were in agreement with literature values.[38]

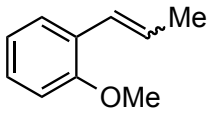

β-Methyl-3-methoxystyrene (**1q**): Spectral data were in agreement with literature values.[39]

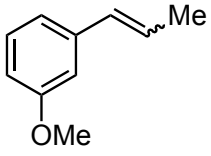

(*E*)-2-(3-(4-Methoxyphenyl)allyl)isoindoline-1,3-dione (1r): Prepared according to a published procedure. Spectral data were in agreement with literature values.[34]

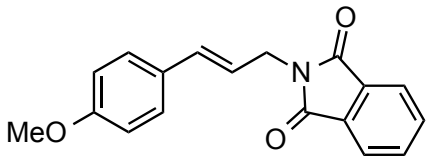

***tert*-Butyldimethyl(4-(prop-1-en-1-yl)phenyl)silane (1s):** Spectral data were in agreement with literature values.[40]

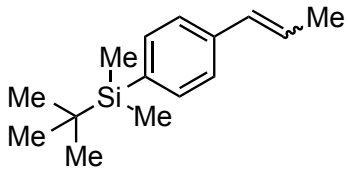

Preparation of *O*-Benzyl Oxime Acids

(*E*)-2-((Benzyloxy)imino)acetic acid (2.51): Prepared according to a published procedure. Spectral data were in agreement with literature values.[41]

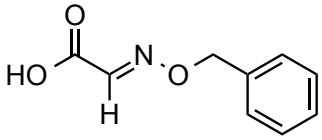

(*E*)-2-((Benzyloxy)imino)propanoic acid (2.52): Prepared according to a published procedure. Spectral data were in agreement with literature values.[41]

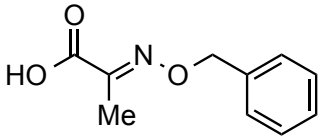

2-((Benzyloxy)imino)-2-phenylacetic acid (2.53): Prepared according to an adapted procedure.[41]

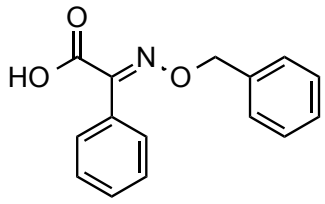

^{1}H NMR for major/minor diastereomers (600 MHz, $CDCl_3$) δ 9.11 (s, 1H), 7.69 – 7.62 (m, 1H), 7.57 – 7.51 (m, 1H), 7.50 – 7.32 (m, 8H), 5.35 (d, J = 3.1 Hz, 2H).

^{13}C NMR for major/minor diastereomers (151 MHz, $CDCl_3$) δ 167.55, 164.26, 150.21, 147.96, 130.72, 137.03, 136.03, 130.37, 129.86, 129.68, 128.91, 128.80, 128.68, 128.60, 128.39, 128.21, 128.18, 128.15, 126.66, 78.74, 77.50.

IR (thin film, cm^{-1}) 3450, 1722, 1496, 1454, 1366, 1213, 1082, 1059

HRMS: m/z calculated for $C_{15}H_{13}NO_3[Na]^+$: 278.07876; found: 278.07889

General Procedure A for Lactone Polar Radical Crossover Cyclization

A flame dried 2-dram vial, equipped with a Teflon-coated septum cap, was charged with a stir bar, the Fukuzumi acridinium photoredox catalyst (**Mes-Acr-Me**, 2.5 mol%), diphenyl disulfide (10 mol%) and the appropriate *O*-benzyl oxime (0.33 mmol, 1.0 equiv). The vial and its contents were transferred to an inert atmosphere (glove box, N_2). The alkene substrate (1.5 equiv) and 2,6-lutidine (15 mol%) were added by microsyringe to the vial, followed by the addition of solvent (CH_2Cl_2, 0.08 M) by syringe. The vial was capped and removed from the glove box and placed in front of a light setup where it was irradiated (3x450 nm blue LED lamps) and stirred for 24 hours. The crude reaction was concentrated under reduced pressure and purified via

column chromatography on silica gel.

Notes:

-Some substrates required deviations from standard conditions and are noted below.

-Integration of peaks in ^{1}H NMR spectra for inseparable diastereomers were determined based on the ratio between the methyl peaks of the major and minor diastereomers. The signals were assigned to the major and minor diastereomers where possible.

3-((Benzyloxy)amino)-5-methyl-4-phenyldihydrofuran-2(3*H*)-one (2.54)

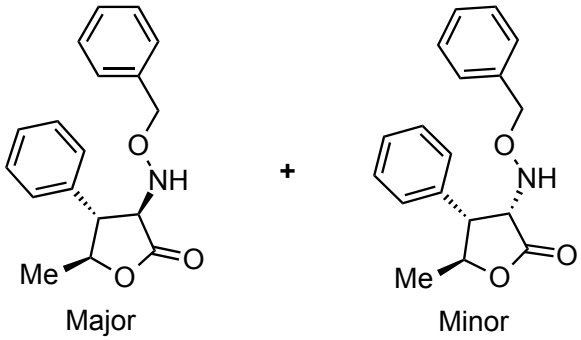

The average isolated yield for **2.54** was 70 mg, 71% (2 trials), synthesized using General Procedure A with β-methylstyrene **1a**, oxime **2.51**, and an irradiation time of 24 hours. The title compound was obtained as a 2.0:1 mixture of inseparable diastereomers based on an average of two trials. The product was isolated by column chromatography on silica gel (10% Et_2O/hexanes then 30% Et_2O/hexanes) as a yellow oil.

Analytical data for **2.54**:

^{1}H NMR for major/minor diastereomers (600 MHz, $CDCl_3$) δ 7.39 (t, *J* = 7.4 Hz, 3H), 7.37 – 7.27 (m, 7H), 7.24 – 7.20 (m, 5H), 6.11 (s, 1H-major), 5.67 (s, 1H-minor), 5.03 (dd, *J* = 7.4, 6.1 Hz, 1H-minor), 4.69 (q, *J* = 11.6 Hz, 2H-major), 4.55 – 4.43 (m, 3H-2 minor, 1 major), 4.08 –

4.02 (m, 2H-1 minor, 1 major), 3.45 – 3.39 (m, 2H-1 minor, 1 major), 1.46 (d, J = 6.3 Hz, 3H-minor), 1.42 (d, J = 6.1 Hz, 3H-major).

^{13}C NMR for major/minor diastereomer (151 MHz, $CDCl_3$) δ 174.02, 174.01, 173.46, 173.44, 137.18, 136.85, 136.51, 134.59, 129.25, 128.98, 128.89, 128.71, 128.49, 128.45, 128.06, 128.04, 127.97, 127.90, 80.73, 79.60, 77.24, 76.49, 67.89, 63.64, 52.92, 52.68, 20.12, 19.00.

IR (thin film, cm^{-1}) 3477, 3255, 3062, 3030, 2977, 2930, 1955, 1775, 1642, 1602, 1497, 1454, 1387, 1365, 1333, 1283, 1190, 1061

HRMS: m/z calculated for $C_{18}H_{19}NO_3$ $[Na]^+$: 320.12571; found: 320.12556

3-((Benzyloxy)amino)-3,5-dimethyl-4-phenyldihydrofuran-2(3*H*)-one (2.55)

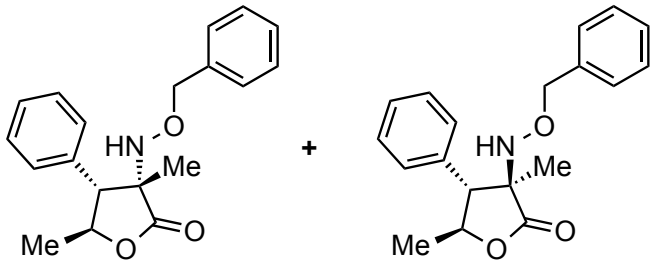

Major Minor

The average isolated yield for **2.55** was 75 mg, 73% (2 trials), synthesized using General Procedure A with β-methylstyrene **1a**, oxime **2.53**, (2,6-lutidine was omitted) and an irradiation time of 24 hours. The title compound was obtained as a 5.0:1 mixture of inseparable diastereomers based on an average of two trials. The product was isolated by column chromatography on silica gel (10% Et_2O/hexanes then 30% Et_2O/hexanes) as a yellow oil.

Analytical data for **3.55**:

^{1}H NMR for major/minor diastereomers (600 MHz, $CDCl_3$) δ7.44 – 7.38 (m, 2H), 7.38 – 7.35 (m, 2H), 7.35 – 7.32 (m, 4H), 7.30 (q, *J* = 3.9, 3.3 Hz, 3H), 7.14 (d, *J* = 7.5 Hz, 1H), 5.70 (s, 1H-minor), 5.28 (s, 1H-major), 5.16 – 5.06 (m, 1H-major), 4.93 – 4.80 (m, 3H-minor), 4.61 (d, *J* = 3.7 Hz, 2H-major), 3.78 (d, *J* = 10.6 Hz, 1H-minor), 3.05 – 2.95 (m, 1H-major), 1.48 (d, *J* = 6.0 Hz, 3H-minor), 1.37 (d, *J* = 6.2 Hz, 3H-major), 1.30 (d, *J* = 1.1 Hz, 3H-major), 0.84 (s, 3H-minor).

^{13}C NMR for major/minor diastereomer (151 MHz, $CDCl_3$) (some peaks of the minor/major diastereomers are overlapping) δ 177.25, 176.76, 137.35, 136.83, 134.16, 132.98, 129.42, 129.01, 128.83, 128.62, 128.57, 128.51, 128.30, 128.12, 128.06, 127.81, 78.48, 76.85, 76.65, 75.41, 67.86, 66.66, 60.61, 51.66, 20.35, 19.73, 19.48, 16.10.

IR (thin film, cm^{-1}) 3437, 3063, 3031, 2977, 2931, 2359, 1977, 1693, 1498, 1454, 1374, 1334, 1283, 1247, 1203, 1178, 1160, 1116

HRMS: m/z calculated for $C_{19}H_{21}NO_3$ $[Na]^+$: 334.14136; found: 334.14120

3-((Benzyloxy)amino)-5-methyl-3,4-diphenyldihydrofuran-2(3*H*)-one (2.56)

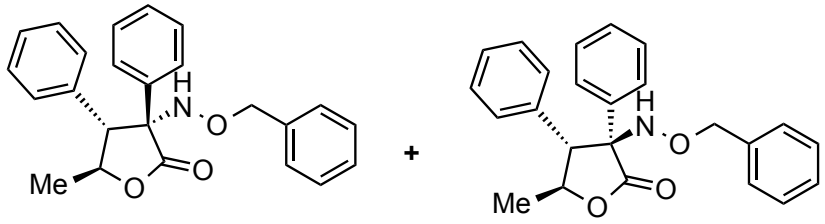

Major Minor

The average isolated yield for **2.56** was 41 mg, 64% (2 trials), synthesized using General

Procedure A with β-methylstyrene **1a**, oxime **2.53** (0.17 mmol), 0.024M, (2,6-lutidine was omitted) and an irradiation time of 24 hours. The title compound was obtained as a 1.2:1 mixture of inseparable diastereomers based on an average of two trials. The product was isolated by column chromatography on silica gel (10% Et_2O/hexanes then 30% Et_2O/hexanes) as a yellow oil.

Analytical data for **2.56**:

^{1}H NMR for major/minor diastereomers (600 MHz, $CDCl_3$) δ7.48 (d, *J* = 7.9 Hz, 2H), 7.40 (dd, *J* = 8.3, 6.8 Hz, 3H), 7.37 – 7.28 (m, 11H), 7.22 (ddd, *J* = 8.5, 5.3, 1.6 Hz, 3H), 7.20 – 7.15 (m, 1H), 7.15 – 7.08 (m, 6H), 6.84 (dt, *J* = 8.8, 1.6 Hz, 2H), 6.60 – 6.48 (m, 2H), 6.15 (s, 1H-major), 5.87 (s, 1H-minor), 5.32 – 5.17 (m, 1H-major), 5.05 – 4.92 (m, 2H-major), 4.76 – 4.61 (m, 3H-minor), 3.96 (dd, *J* = 10.8, 2.2 Hz, 1H-major), 3.42 (dd, *J* = 10.3, 2.1 Hz, 1H-minor), 1.43 (d, *J* = 6.1 Hz, 6H-3H minor, 3H major).

^{13}C NMR for major/minor diastereomer (151 MHz, $CDCl_3$) (some peaks of the minor/major diastereomers are overlapping) δ 176.41, 175.76, 138.15, 137.30, 136.69, 134.08, 133.17, 132.60, 129.58, 129.34, 128.93, 128.76, 128.74, 128.68, 128.66, 128.61, 128.53, 128.29, 128.22, 128.19, 128.16, 128.12, 127.63, 127.47, 126.48, 78.52, 76.86, 76.54, 76.35, 73.11, 62.40, 54.74, 19.89, 18.88.

IR (thin film, cm^{-1}) 3433, 3063, 3031, 2978, 2929, 2360, 1778, 1639, 1497, 1453, 1385, 1332, 1277, 1194, 1060

HRMS: m/z calculated for $C_{24}H_{23}NO_3$ $[Na]^+$: 396.15701; found: 396.15677

3-((Benzyloxy)amino)-4-(2-chlorophenyl)-5-methyldihydrofuran-2(3*H*)-one (2.57)

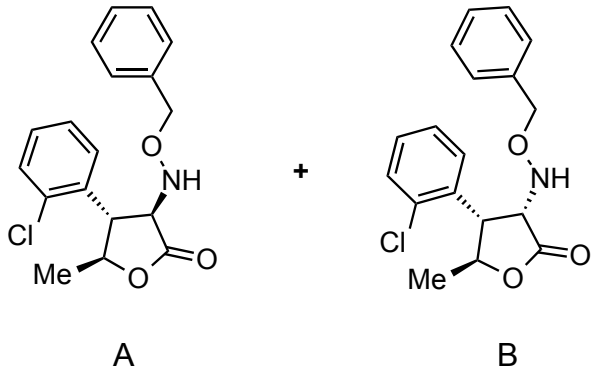

A B

The average isolated yield for **2.57** was 84 mg, 77% (2 trials), synthesized using General Procedure A with β-methyl-2-chlorostyrene **1i**, oxime **2.51**, and an irradiation time of 24 hours. The title compound was obtained as a 1:1 mixture of separable diastereomers based on an average of two trials. The products were isolated by column chromatography on silica gel (10% EtOAc/hexanes then 30% EtOAc/hexanes) as yellow oils.

Analytical data for **2.57**:

^{1}H NMR for major diastereomer (600 MHz, $CDCl_3$) δ 7.46 (dd, *J* = 7.8, 1.4 Hz, 1H), 7.33 – 7.27 (m, 5H), 7.23 (t, *J* = 7.7 Hz, 3H), 6.13 (s, 1H), 4.77 – 4.63 (m, 2H), 4.55 (dq, *J* = 9.4, 6.1 Hz, 1H), 4.22 (d, *J* = 10.8 Hz, 1H), 4.13 (dd, *J* = 10.9, 9.4 Hz, 1H), 1.45 (d, *J* = 6.1 Hz, 3H).

^{13}C NMR for major diastereomer (151 MHz, $CDCl_3$) δ 173.41, 137.15, 134.79, 134.57, 130.63, 129.20, 129.00, 128.60, 128.49, 128.08, 127.75, 79.80, 77.19, 67.25, 49.25, 19.53.

IR (thin film, cm^{-1}) 3054, 2360, 1778, 1421, 1265, 1189

HRMS: m/z calculated for $C_{18}H_{18}ClNO_3$ $[Na]^+$ 354.08674; found: 354.08655

^{1}H NMR for minor diastereomer (600 MHz, $CDCl_3$) δ 7.49 – 7.45 (m, 1H), 7.33 – 7.31 (m, 2H), 7.31 – 7.28 (m, 2H), 7.28 – 7.26 (m, 2H), 7.17 – 7.13 (m, 2H), 5.71 (s, 1H), 5.13 (dq, *J* = 8.9, 6.3 Hz, 1H), 4.38 – 4.28 (m, 2H), 4.22 (d, *J* = 8.7 Hz, 1H), 3.82 (t, *J* = 8.8 Hz, 1H), 1.48 (d, *J* = 6.3 Hz, 3H).

^{13}C NMR for minor diastereomer (151 MHz, $CDCl_3$) δ 174.39, 136.74, 135.30, 132.67, 130.08, 129.05, 128.89, 128.52, 128.39, 128.10, 127.17, 79.74, 76.33, 62.50, 49.51, 20.02.

IR (thin film, cm^{-1}) 3231, 3063, 3031, 2978, 2931, 1779, 1477, 1209, 1063

HRMS: m/z calculated for $C_{18}H_{18}ClNO_3$ $[Na]^+$: 354.08674; found: 354.08661

3-((Benzyloxy)amino)-4-(3-chlorophenyl)-5-methyldihydrofuran-2(3*H*)-one (2.58)

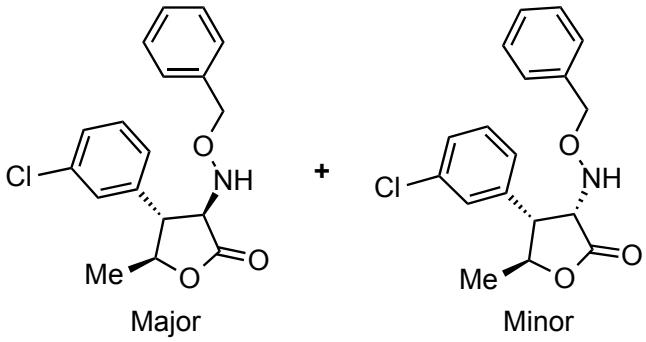

The average isolated yield for **2.58** was 80 mg, 73% (2 trials), synthesized using General Procedure A with β-methyl-3-chlorostyrene **1j**, oxime **2.51**, and an irradiation time of 24 hours. The title compound was obtained as a 1.8:1 mixture of inseparable diastereomers based on an average of two trials. The product was isolated by column chromatography on silica gel (10% EtOAc/hexanes then 30% EtOAc/hexanes) as a yellow oil.

Analytical data for **2.58**:

^{1}H NMR for major/minor diastereomers (600 MHz, $CDCl_3$) δ 7.32 (dt, *J* = 4.2, 1.8 Hz, 5H), 7.30

(dt, *J* = 5.0, 1.3 Hz, 3H), 7.26 – 7.21 (m, 3H), 7.16 (dd, *J* = 5.0, 2.6 Hz, 1H), 7.13 (d, *J* = 1.7 Hz, 1H), 7.06 (s, 1H), 6.10 (s, 1H -major), 5.68 (s, 1H-minor), 4.96 (dq, *J* = 7.6, 6.3 Hz, 1H-minor), 4.67 (s, 2H-major), 4.50 – 4.42 (m, 3H-2 minor, 1 major), 4.03 (d, *J* = 8.5 Hz, 1H -minor), 3.97 (d, *J* = 11.3 Hz, 1H-major), 3.38 (t, *J* = 8.0 Hz, 1H-minor), 3.34 (dd, *J* = 11.2, 9.9 Hz, 1H-major), 1.45 (d, *J* = 6.3 Hz, 3H-minor), 1.41 (d, *J* = 6.1 Hz, 3H-major).

^{13}C NMR for major/minor diastereomers (151 MHz, $CDCl_3$) δ 173.73, 173.08, 138.76, 137.12, 136.88, 136.52, 135.14, 134.89, 130.55, 130.23, 129.21, 128.89, 128.62, 128.60, 128.58, 128.35, 128.29, 128.24, 128.23, 128.19, 127.23, 125.99, 80.69, 79.30, 77.25, 76.51, 67.80, 63.61, 52.69, 52.26, 20.21, 19.13.

IR (thin film, cm^{-1}) 3063, 2981, 2931, 1772, 1455, 1266, 1191, 1065

HRMS: m/z calculated for $C_{18}H_{18}ClNO_3$ $[Na]^+$: 354.08674; found: 354.08664

3-((Benzyloxy)amino)-4-(4-chlorophenyl)-5-methyldihydrofuran-2(3*H*)-one (2.59)

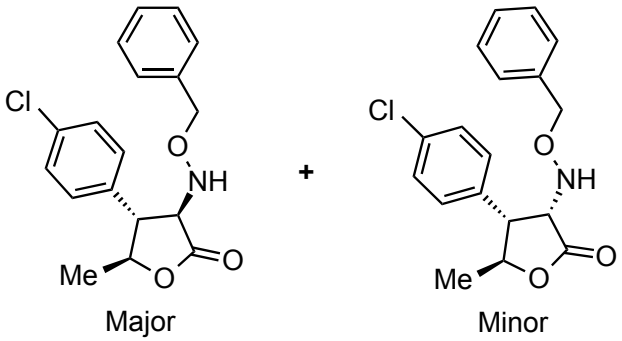

The average isolated yield for **2.59** was 67 mg, 62% (2 trials), synthesized using General Procedure A with β-methyl-4-chlorostyrene **1k**, oxime **2.51**, and an irradiation time of 24 hours. The title compound was obtained as a 2.4:1 mixture of inseparable diastereomers. The product

was isolated by column chromatography on silica gel (10% EtOAc/hexanes then 30% EtOAc/hexanes) as a yellow oil.

Analytical data for **2.59**:

^{1}H NMR for major/minor diastereomers (600 MHz, $CDCl_3$) δ 7.38 – 7.27 (m, 7H), 7.21 (ddd, *J* = 9.8, 7.3, 1.8 Hz, 3H), 7.13 – 7.08 (m, 2H), 6.12 (s, 1H-major), 5.67 (s, 1H-minor), 4.99 – 4.89 (m, 1H-minor), 4.69 – 4.61 (m, 2H-major), 4.50 – 4.38 (m, 3H-2 minor, 1 major), 4.03 (d, *J* = 8.5 Hz, 1H-minor), 3.97 (d, *J* = 11.3 Hz, 1H-major), 3.45 – 3.29 (m, 2H-1 minor, 1 major), 1.44 (d, *J* = 6.3 Hz, 3H-minor), 1.40 (d, *J* = 6.1 Hz, 3H-major).

^{13}C NMR for major/minor diastereomers (151 MHz, $CDCl_3$) δ 173.81, 173.15, 137.11, 136.63, 135.08, 133.95, 133.87, 133.28, 130.30, 130.02, 129.42, 129.24, 129.11, 128.79, 128.55, 128.52, 128.20, 128.17, 80.76, 79.34, 77.20, 76.47, 67.77, 63.49, 52.31, 52.12, 20.14, 18.98.

IR (thin film, cm^{-1}) 2980, 2931, 1777, 1592, 1494, 1455, 1386, 1266, 1191, 1091, 1014

HRMS: m/z calculated for $C_{18}H_{18}ClNO_3$ $[Na]^+$: 354.08674; found: 354.08657

3-((Benzyloxy)amino)-4-(3-bromophenyl)-5-methyldihydrofuran-2(3*H*)-one (2.60)

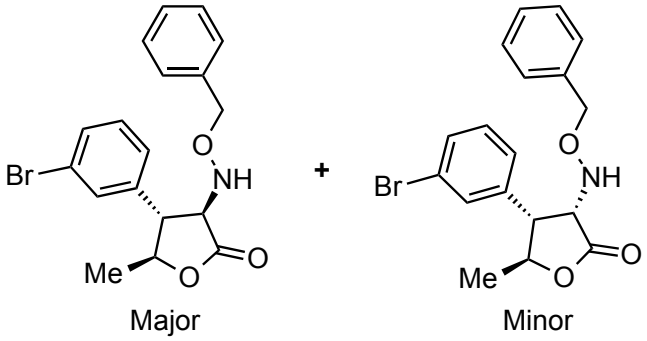

The average isolated yield for **2.60** was 89 mg, 72% (2 trials), synthesized using General

Procedure A with β-methyl-3-bromostyrene **1g**, oxime **2.51**, and an irradiation time of 24 hours. The title compound was obtained as a 1.8:1 mixture of inseparable diastereomers based on an average of two trials. The product was isolated by column chromatography on silica gel (10% EtOAc/hexanes then 30% EtOAc/hexanes) as a yellow oil.

Analytical data for **2.60**:

^{1}H NMR for major/minor diastereomers (600 MHz, $CDCl_3$) δ 7.53 – 7.46 (m, 2H), 7.38 – 7.33 (m, 4H), 7.33 – 7.29 (m, 2H), 7.29 – 7.22 (m, 5H), 7.13 (dt, *J* = 7.8, 1.2 Hz, 1H), 6.15 (s, 1H-major), 5.71 (s, 1H-minor), 5.02 – 4.95 (m, 1H-minor), 4.69 (s, 2H-major), 4.53 – 4.43 (m, 3H-2 minor, 1 major), 4.05 (d, *J* = 8.5 Hz, 1H-minor), 4.00 (d, *J* = 11.3 Hz, 1H-major), 3.40 (t, *J* = 8.1 Hz, 1H-minor), 3.34 (dd, *J* = 11.2, 9.9 Hz, 1H-major), 1.47 (dd, *J* = 6.3, 1.3 Hz, 3H-minor), 1.43 (dd, *J* = 6.1, 1.5 Hz, 3H-major).

^{113}C NMR for major/minor diastereomers (151 MHz, $CDCl_3$) δ 173.72, 173.06, 139.02, 137.12, 137.09, 136.59, 132.07, 131.22, 131.09, 131.03, 130.77, 130.46, 128.84, 128.56, 128.54, 128.24, 128.18, 127.68, 126.48, 126.45, 123.25, 123.00, 80.64, 79.25, 77.18, 76.42, 67.74, 63.57, 52.59, 52.15, 20.14, 19.07.

IR (thin film, cm^{-1}) 3251, 3062, 3030, 2977, 2929, 1777, 1714, 1595, 1567, 1476, 1192, 1064

HRMS: m/z calculated for $C_{18}H_{18}BrNO_3$ $[Na]^+$: 398.03623; found: 398.03612

3-((Benzyloxy)amino)-4-(4-bromophenyl)-5-methyldihydrofuran-2(3*H*)-one (2.61)

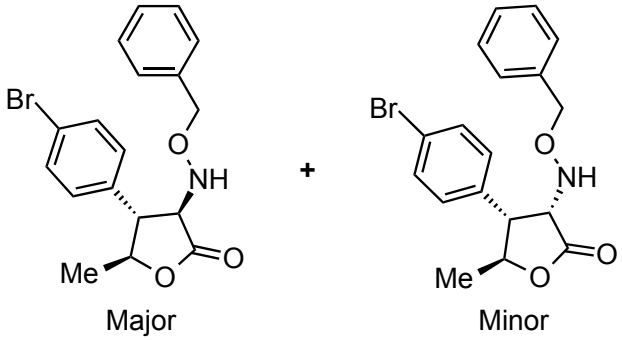

The average isolated yield for **2.61** was 91 mg, 73% (2 trials), synthesized using General Procedure A with β-methyl-4-bromostyrene **1h**, oxime **2.51**, and an irradiation time of 24 hours. The title compound was obtained as a 1.8:1 mixture of inseparable diastereomers based on an average of two trials. The product was isolated by column chromatography on silica gel (10% EtOAc/hexanes then 30% EtOAc/hexanes) as a yellow oil.

Analytical data for **2.61**:

^{1}H NMR for major/minor diastereomers (600 MHz, $CDCl_3$) δ 7.50 (dd, *J* = 10.5, 8.2 Hz, 3H), 7.35 – 7.28 (m, 5H), 7.24 – 7.18 (m, 3H), 7.15 (d, *J* = 8.4 Hz, 1H), 7.07 – 7.01 (m, 2H), 6.11 (s, 1H-major), 5.66 (s, 1H-minor), 5.00 – 4.88 (m, 1H-minor), 4.69 – 4.61 (m, 2H-major), 4.45 (q, *J* = 5.6, 5.1 Hz, 3H-2 minor, 2 major), 4.03 (d, *J* = 8.5 Hz, 1H-minor), 3.97 (d, *J* = 11.3 Hz, 1H-major), 3.41 – 3.29 (m, 2H-1 minor, 1 major), 1.44 (d, *J* = 6.3 Hz, 3H-minor), 1.40 (dd, *J* = 6.1, 1.2 Hz, 3H-major).

^{13}C NMR for major/minor diastereomers (151 MHz, $CDCl_3$) δ 173.76, 173.09, 137.10, 135.63, 135.62, 133.84, 132.41, 132.10, 130.65, 130. 09, 129.58, 128.82, 128.58, 128.55, 128.23, 128.21, 122.04, 122.01, 80.71, 79.29, 77.23, 76.51, 67.75, 63.47, 52.42, 52.26, 20.18, 19.02.

IR (thin film, cm^{-1}) 3470, 3257, 3063, 3031, 2978, 2930, 2871, 1779, 1715, 1587, 1491, 1455,

1386, 1192

HRMS: m/z calculated for $C_{18}H_{18}BrNO_3$ $[Na]^+$: 398.03623; found: 398.03617

3-((Benzyloxy)amino)-4-(4-fluorophenyl)-5-methyldihydrofuran-2(3*H*)-one (2.62)

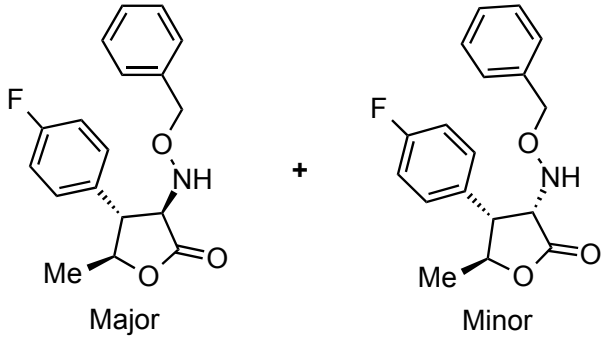

The average isolated yield for **2.62** was 69 mg, 66% (2 trials), synthesized using General Procedure A with β-methyl-4-fluorostyrene **1l**, oxime **2.51**, and an irradiation time of 24 hours. The title compound was obtained as a 2.0:1 mixture of inseparable diastereomers based on an average of two trials. The product was isolated by column chromatography on silica gel (10% EtOAc/hexanes then 30% EtOAc/hexanes) as a yellow oil.

Analytical data for **2.62**:

^{1}H NMR for major/minor diastereomers (600 MHz, $CDCl_3$) δ 7.31 (td, *J* = 6.9, 6.2, 3.3 Hz, 4H), 7.27 – 7.20 (m, 3H), 7.15 (dd, *J* = 8.5, 5.4 Hz, 2H), 7.07 (dt, *J* = 10.5, 8.6 Hz, 3H), 6.11 (s, 1H-major), 5.66 (s, 1H-minor), 5.00 – 4.91 (m, 1H-minor), 4.71 – 4.63 (m, 2H-major), 4.51 – 4.41 (m, 3H-2 minor, 1 major), 4.02 (d, *J* = 8.4 Hz, 1H-minor), 3.97 (dd, *J* = 11.5, 1.6 Hz, 1H-major), 3.46 – 3.32 (m, 2H-1 minor, 1 major), 1.44 (d, *J* = 6.3 Hz, 3H-minor), 1.41 (d, *J* = 6.1 Hz, 3H-major).

^{13}C NMR for major/minor diastereomers (151 MHz, $CDCl_3$) δ 173.88, 173.27, 163.28, 163.21, 161.65, 161.58, 137.17, 136.71, 132.28, 132.26, 130.61, 130.55, 130.46, 130.44, 129.49, 129.44, 128.78, 128.55, 128.52, 128.16, 116.27, 116.13, 115.98, 115.83, 80.96, 79.52, 77.22, 76.51, 67.88, 63.52, 52.27, 51.94, 20.11, 18.95.

IR (thin film, cm^{-1}) 3475, 2978, 2930, 1778, 1603, 1512, 1455, 1387, 1330, 1227, 1096

HRMS: m/z calculated for $C_{18}H_{18}FNO_3$ $[Na]^+$: 338.11629; found: 338.11612

3-((Benzyloxy)amino)-4-(2-methoxyphenyl)-5-methyldihydrofuran-2(3*H*)-one (2.63)

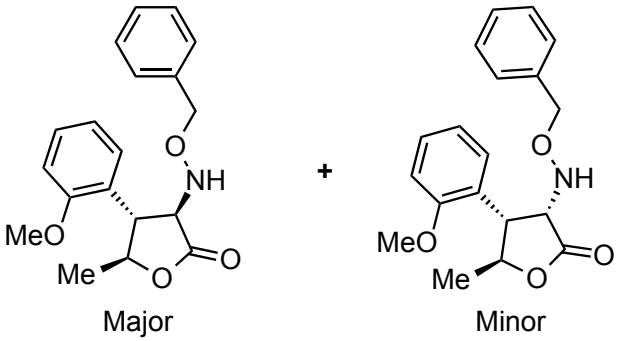

Major Minor

The average isolated yield for **2.63** was 63 mg, 58% (2 trials), synthesized using General Procedure A with β-methyl-2-methoxystyrene **1p**, oxime **2.51**, and an irradiation time of 24 hours. The title compound was obtained as a 1.2:1 mixture of inseparable diastereomers based on an average of two trials. The product was isolated by column chromatography on silica gel (10% EtOAc/hexanes then 30% EtOAc/hexanes) as a yellow oil.

Analytical data for **2.63**:

^{1}H NMR for major/minor diastereomers (600 MHz, $CDCl_3$) δ 7.36 – 7.28 (m, 5H), 7.26 (td, *J* = 6.9, 3.3 Hz, 4H), 7.19 (dd, *J* = 7.6, 1.6 Hz, 1H), 7.15 – 7.09 (m, 2H), 7.03 (dd, *J* = 7.4, 1.7 Hz,

1H), 7.00 (td, *J* = 7.5, 1.1 Hz, 1H), 6.97 – 6.89 (m, 3H), 6.11 (s, 1H-major), 5.67 (s, 1H-minor), 5.09 – 4.99 (m, 1H-minor), 4.76 – 4.64 (m, 3H-2 minor, 1 major), 4.43 (d, *J* = 10.4 Hz, 1H-major), 4.30 (s, 2H-minor), 4.15 (d, *J* = 8.8 Hz, 1H-minor), 3.82 (s, 3H-major), 3.79 (s, 3H-minor), 3.65 (t, *J* = 8.5 Hz, 1H-minor), 3.51 (dd, *J* = 10.3, 9.2 Hz, 1H-major), 1.47 (d, *J* = 6.3 Hz, 3H-minor), 1.37 (d, *J* = 6.2 Hz, 3H-major).

^{13}C NMR for major/minor diastereomers (151 MHz, $CDCl_3$) δ 174.97, 174.87, 157.86, 157.64, 137.40, 137.14, 130.92, 129.30, 128.92, 128.76, 128.57, 128.47, 128.38, 128.35, 128.03, 127.89, 124.63, 123.56, 121.14, 120.77, 111.28, 110.67, 79.79, 78.00, 77.20, 76.32, 65.58, 62.46, 55.44, 55.32, 50.16, 47.48, 20.46, 19.91.

IR (thin film, cm^{-1}) 3436, 3063, 3013, 2976, 2932, 2839, 1777, 1601, 1587, 1495, 1463, 1455, 1384, 1247

HRMS: m/z calculated for $C_{19}H_{21}NO_4$ $[Na]^+$: 350.13628; found: 350.13606

3-((Benzyloxy)amino)-4-(3-methoxyphenyl)-5-methyldihydrofuran-2(3*H*)-one (2.64)

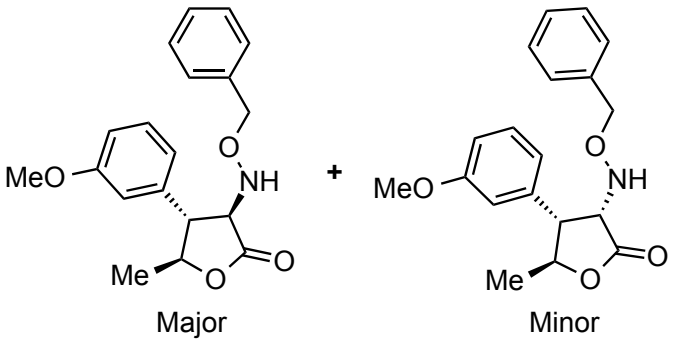

The average isolated yield for **2.64** was 70 mg, 65% (2 trials), synthesized using General Procedure A with β-methyl-3-methoxystyrene **1q**, oxime **2.51**, and an irradiation time of 24

hours. The title compound was obtained as a 2.0:1 mixture of inseparable diastereomers based on an average of two trials. The product was isolated by column chromatography on silica gel (10% EtOAc/hexanes then 30% EtOAc/hexanes) as a yellow oil.

Analytical data for **2.64**:

^{1}H NMR for major/minor diastereomers (600 MHz, $CDCl_3$) δ 7.33 – 7.27 (m, 6H), 7.25 – 7.22 (m, 3H), 6.89 – 6.83 (m, 3H), 6.81 (dt, *J* = 7.7, 1.2 Hz, 1H), 6.77 (t, *J* = 2.1 Hz, 1H), 6.09 (s, 1H-major), 5.68 (s, 1H-minor), 5.00 (dq, *J* = 7.8, 6.3 Hz, 1H-minor), 4.70 (q, *J* = 11.6 Hz, 2H-major), 4.55 – 4.46 (m, 3H-2 minor, 1 major), 4.07 – 3.99 (m, 2H-1 minor, 1 major), 3.81 (s, 3H-major), 3.79 (s, 3H-minor), 3.45 – 3.32 (m, 2H-1 minor, 1 major), 1.44 (d, *J* = 6.3 Hz, 3H-minor), 1.42 (d, *J* = 6.1 Hz, 3H-major).

^{13}C NMR for major/minor diastereomers (151 MHz, $CDCl_3$) δ 173.94, 173.45, 160.23, 160.07, 138.17, 137.21, 136.89, 135.98, 130.36, 130.06, 128.71, 128.59, 128.48, 128.42, 128.11, 128.09, 121.18, 120.07, 114.96, 114.18, 113.12, 112.93, 80.71, 79.53, 77.32, 76.67, 67.96, 63.73, 55.41, 55.35, 53.15, 52.61, 20.12, 19.12.

IR (thin film, cm^{-1}) 3434, 2348, 1777, 1643, 1602, 1491, 1455, 1291, 1265, 119, 1063

HRMS: m/z calculated for $C_{19}H_{21}NO_4$ $[Na]^+$: 350.13628; found: 350.13612

3-((Benzyloxy)amino)-4-(4-methoxyphenyl)-5-methyldihydrofuran-2(3*H*)-one (2.65)

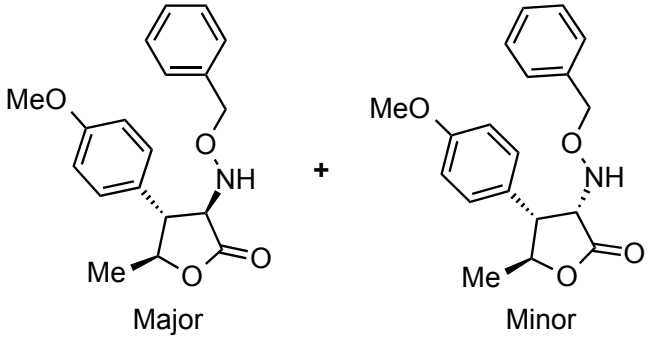

The average isolated yield for **2.65** was 50 mg, 46% (2 trials), synthesized using General Procedure A with anethole **1b**, oxime **2.51**, and an irradiation time of 24 hours. The title compound was obtained as a 2.1:1 mixture of inseparable diastereomers based on an average of two trials. The product was isolated by column chromatography on silica gel (10% EtOAc/hexanes then 30% EtOAc/hexanes) as a yellow oil.

Analytical data for **2.65**:

^{1}H NMR for major/minor diastereomers (600 MHz, $CDCl_3$) δ 7.34 – 7.27 (m, 5H), 7.25 – 7.19 (m, 4H), 7.14 – 7.10 (m, 2H), 6.93 – 6.88 (m, 3H), 6.09 (d, *J* = 1.9 Hz, 1H-major), 5.66 (d, *J* = 3.1 Hz, 1H-minor), 4.96 (dq, *J* = 7.8, 6.3 Hz, 1H-minor), 4.73 – 4.64 (m, 2H-major), 4.52 (d, *J* = 2.9 Hz, 2H-2 minor), 4.46 (dq, *J* = 10.0, 6.1 Hz, 1H-major), 4.02 – 3.94 (m, 2H-1 minor, 1 major), 3.82 (d, *J* = 4.2 Hz, 6H-3 minor, 3 major), 3.40 – 3.31 (m, 2H-1 minor, 1 major), 1.43 (d, *J* = 6.3 Hz, 3H-minor), 1.40 (d, *J* = 6.1 Hz, 3H-major).

^{13}C NMR for major/minor diastereomers (151 MHz, $CDCl_3$) δ ^{13}C NMR (151 MHz, $CDCl_3$) δ 174.18, 173.61, 159.37, 159.27, 137.20, 136.83, 130.04, 128.95, 128.76, 128.56, 128.51, 128.49, 128.21, 128.11, 126.14, 114.63, 114.38, 81.08, 79.76, 77.28, 76.60, 67.93, 63.68, 55.46, 55.43, 52.45, 51.85, 20.06, 18.93.

IR (thin film, cm^{-1}) 3465, 2975, 2932, 2837, 2348, 2282, 1778, 1613, 1515, 1455, 1386, 1250

HRMS: m/z calculated for $C_{19}H_{21}NO_4$ $[Na]^+$: 350.13628; found: 350.13607

3-((Benzyloxy)amino)-5-methyl-4-(*m*-tolyl)dihydrofuran-2(3*H*)-one (2.66)

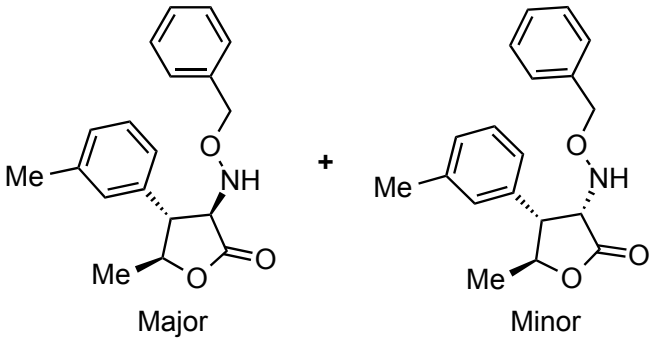

The average isolated yield for **2.66** was 66 mg, 64% (2 trials), synthesized using General Procedure A with β-methyl-3-methylstyrene **1m,** oxime **2.51**, and an irradiation time of 24 hours. The title compound was obtained as a 2.4:1 mixture of inseparable diastereomers based on an average of two trials. The product was isolated by column chromatography on silica gel (10% EtOAc/hexanes then 30% EtOAc/hexanes) as a yellow oil.

Analytical data for **2.66**:

^{1}H NMR for major/minor diastereomers (600 MHz, $CDCl_3$) δ 7.32 – 7.27 (m, 4H), 7.25 – 7.23 (m, 1H), 7.21 (td, *J* = 7.5, 1.7 Hz, 3H), 7.15 – 7.10 (m, 1H), 7.06 (d, *J* = 8.2 Hz, 1H), 6.99 (d, *J* = 8.4 Hz, 2H), 6.07 (s, 1H-major), 5.64 (s, 1H-minor), 5.04 – 4.96 (m, 1H-minor), 4.72 – 4.63 (m, 2H-major), 4.53 – 4.43 (m, 3H-2 minor, 1 major), 4.06 – 3.96 (m, 2H-1 major, 1 minor), 3.40 – 3.30 (m, 2H-1 major, 1 minor), 2.35 (d, *J* = 3.4 Hz, 6H-3 major, 3 minor), 1.43 (d, *J* = 6.3 Hz, 3H-minor), 1.40 (d, *J* = 6.1 Hz, 3H-major).

^{13}C NMR for major/minor diastereomers (151 MHz, $CDCl_3$) δ 174.07, 173.57, 139.00, 138.72, 137.25, 136.96, 136.49, 134.41, 129.64, 129.17, 128.92, 128.88, 128.80, 128.77, 128.61, 128.51, 128.49, 128.11, 128.07, 125.95, 124.99, 80.77, 79.72, 77.29, 76.57, 68.00, 63.72, 53.04, 52.61, 21.60, 21.58, 20.15, 19.09.

IR (thin film, cm^{-1}) 3446, 3030, 2977, 2928, 1777, 1716, 1654, 1608, 1493, 1454, 1386, 1328, 1190

HRMS: m/z calculated for $C_{19}H_{21}NO_3$ $[Na]^+$: 334.14136; found: 334.14120

3-((Benzyloxy)amino)-5-methyl-4-(*p*-tolyl)dihydrofuran-2(3*H*)-one (2.67)

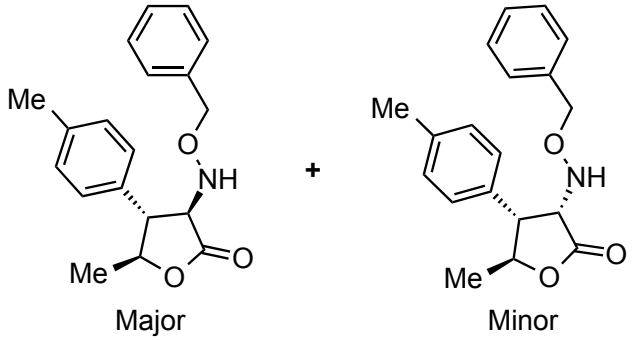

The average isolated yield for **2.67** was 64 mg, 62% (2 trials), synthesized using General Procedure A with β-methyl-4-methylstyrene **1n**, oxime **2.51**, and an irradiation time of 24 hours. The title compound was obtained as a 2.1:1 mixture of inseparable diastereomers based on an average of two trials. The product was isolated by column chromatography on silica gel (10% EtOAc/hexanes then 30% EtOAc/hexanes) as a yellow oil.

Analytical data for **2.67**:

^{1}H NMR for major/minor diastereomers (600 MHz, $CDCl_3$) δ 7.33 – 7.27 (m, 5H), 7.22 (ddt, *J* = 5.1, 3.6, 1.6 Hz, 3H), 7.21 – 7.15 (m, 5H), 7.11 (d, *J* = 7.9 Hz, 2H), 6.08 (s, 1H-major), 5.66 (s, 1H-minor), 5.04 – 4.97 (m, 1H-minor), 4.68 (q, *J* = 11.6 Hz, 2H-major), 4.54 – 4.44 (m, 3H-2 minor, 1 major), 4.05 – 3.97 (m, 2H-1 minor, 1 major), 3.43 – 3.33 (m, 2H-1 minor, 1 major), 2.37 (d, *J* = 2.4 Hz, 6H-3 minor, 3 major), 1.44 (d, *J* = 6.3 Hz, 3H-minor), 1.41 (d, *J* = 6.1 Hz, 3H-major).

^{13}C NMR for major/minor diastereomers (151 MHz, $CDCl_3$) δ 174.11, 173.56, 137.92, 137.81, 137.25, 136.93, 133.43, 131.33, 129.97, 129.74, 128.80, 128.74, 128.56, 128.49, 128.47, 128.09, 127.80, 80.86, 79.72, 77.30, 76.59, 67.99, 63.73, 52.79, 52.37, 21.22, 21.20, 20.10, 19.01.

IR (thin film, cm^{-1}) 3444, 1778, 1644, 1516, 1454, 1385, 1188, 1063

HRMS: m/z calculated for $C_{19}H_{21}NO_3$ $[Na]^+$: 334.14136; found: 334.14118

3-((Benzyloxy)amino)-4-(4-(*tert*-butyl)phenyl)-5-methyldihydrofuran-2(3*H*)-one (2.68)

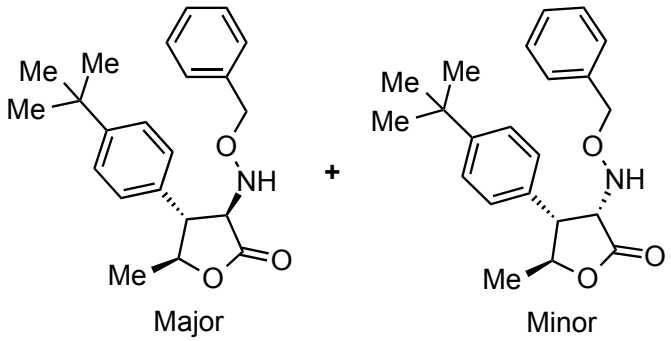

Major Minor

The average isolated yield for **2.68** was 70 mg, 60% (2 trials), synthesized using General

Procedure A with β-methyl-4-*tert*-butylstyrene **1o**, oxime **2.51**, and an irradiation time of 24 hours. The title compound was obtained as a 2.4:1 mixture of inseparable diastereomers based on an average of two trials. The product was isolated by column chromatography on silica gel (10% EtOAc/hexanes then 30% EtOAc/hexanes) as a yellow oil.

Analytical data for **2.68**:

^{1}H NMR for major/mnor diastereomers (600 MHz, $CDCl_3$) δ 7.43 – 7.38 (m, 3H), 7.33 – 7.27 (m, 4H), 7.24 – 7.19 (m, 4H), 7.18 – 7.14 (m, 2H), 6.11 (s, 1H-major), 5.66 (s, 1H-minor), 5.05 – 4.99 (m, 1H-minor), 4.74 – 4.64 (m, 2H-major), 4.54 – 4.46 (m, 3H-2 minor, 1 major), 4.08 – 3.99 (m, 2H-1 minor, 1 major), 3.40 (t, J = 10.5 Hz, 2H-1 minor, 1 major), 1.45 (d, J = 6.3 Hz, 3H-minor), 1.42 (d, J = 6.1 Hz, 3H-major), 1.36 – 1.33 (m, 18H-9 minor, 9 major).

^{13}C NMR for major/minor diastereomers (151 MHz, $CDCl_3$) δ 174.11, 173.58, 151.06, 151.00, 137.16, 136.95, 133.36, 131.27, 128.75, 128.61, 128.54, 128.45, 128.08, 128.04, 127.56, 126.18, 125.92, 80.81, 79.71, 77.32, 76.55, 67.94, 63.72, 52.67, 52.33, 34.66, 31.42, 20.10, 19.07.

IR (thin film, cm^{-1}) 3458, 3063, 3031, 2963, 2868, 2359, 1777, 2644, 1516, 1455, 1386, 1363, 1330, 1268, 1189, 1064

HRMS: m/z calculated for $C_{19}H_{21}NO_3$ $[Na]^+$: 376.18831; found: 376.18822

3-((Benzyloxy)amino)-4-methyl-4-phenyldihydrofuran-2(3*H*)-one (2.69)

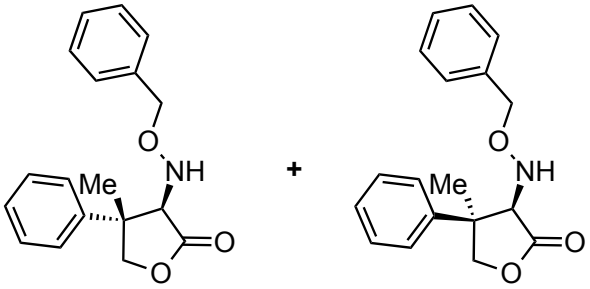

Major Minor

The average isolated yield for **2.69** was 57 mg, 58% (2 trials), synthesized using General Procedure A with α-methylstyrene **1d**, oxime **2.51**, **Mes-Acr-Ph**, 2.5 mol%, and an irradiation time of 24 hours. The title compound was obtained as a 2.9:1 mixture of separable diastereomers based on an average of two trials. The products were isolated by column chromatography on silica gel (15% EtOAc /hexanes then 20% EtOAc/hexanes) as yellow oils.

Analytical data for **2.69**:

^{1}H NMR for major diastereomer (600 MHz, $CDCl_3$) δ 7.47 – 7.43 (m, 2H), 7.39 (dd, *J* = 8.4, 6.8 Hz, 2H), 7.34 – 7.28 (m, 4H), 7.22 – 7.16 (m, 2H), 6.20 – 6.07 (m, 1H), 4.71 – 4.58 (m, 2H), 4.35 (d, *J* = 3.0 Hz, 1H), 4.31 (d, *J* = 1.2 Hz, 2H), 1.50 (s, 3H).

^{13}C NMR for major diastereomer (151 MHz, $CDCl_3$) δ 174.57, 142.57, 136.94, 129.04, 128.75, 128.51, 128.18, 127.46, 125.93, 76.90, 76.72, 68.07, 47.43, 21.23.

IR (thin film, cm^{-1}) 3447, 3062, 3036, 2969, 2915, 2360, 1778, 1639, 1497, 1454, 1366, 1292, 1188, 1141, 1062

HRMS: m/z calculated for $C_{18}H_{19}NO_3$ $[Na]^+$: 320.12571; found: 320.12557

^{1}H NMR for minor diastereomer (600 MHz, $CDCl_3$) δ 7.40 (ddd, *J* = 8.0, 6.6, 1.2 Hz, 2H), 7.34 – 7.27 (m, 4H), 7.26 – 7.22 (m, 2H), 7.15 (dd, *J* = 7.7, 1.8 Hz, 2H), 5.70 (d, *J* = 4.4 Hz, 1H), 4.83

(d, J = 8.5 Hz, 1H), 4.39 – 4.25 (m, 3H), 3.77 (d, J = 4.2 Hz, 1H), 1.57 (s, 3H).

^{13}C NMR for minor diastereomer (151 MHz, $CDCl_3$) δ 175.16, 140.14, 136.97, 128.97, 128.63, 128.46, 128.09, 127.55, 126.79, 77.04, 76.48, 68.79, 46.90, 27.42.

IR (thin film, cm^{-1}) 3433, 3061, 3030, 2965, 2923, 2871, 2359, 1779, 1634, 1602, 1497, 1454, 1387, 1364, 1291, 1213, 1176, 1118

HRMS: m/z calculated for $C_{18}H_{19}NO_3$ $[Na]^+$: 320.12571; found: 320.12551

3-((Benzyloxy)amino)-3a-phenylhexahydrobenzofuran-2(3*H*)-one (2.70)

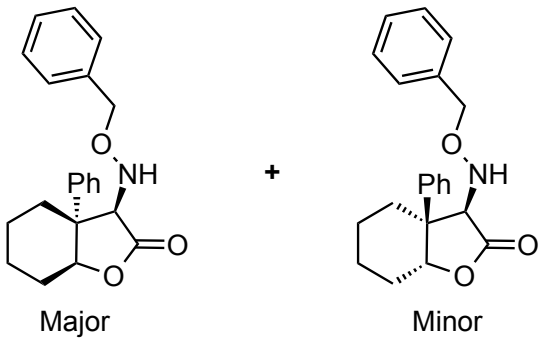

Major Minor

The average isolated yield for **2.70** was 98 mg, 88% (2 trials), synthesized using General Procedure A with 1-phenyl-1-cyclohexene **1e**, oxime **2.51**, and an irradiation time of 24 hours. The title compound was obtained as a 1.5:1 mixture of separable diastereomers based on an average of two trials. The products were isolated by column chromatography on silica gel (20% EtOAc /hexanes then 30% EtOAc/hexanes). The minor product was obtained as a coconut-scented, yellow oil and the major product as a cream-colored solid.

Analytical data for **2.70**:

^{1}H NMR for major diastereomer (600 MHz, $CDCl_3$) δ 7.52 (dd, *J* = 8.3, 1.3 Hz, 2H), 7.43 (t, *J* = 7.8 Hz, 2H), 7.37 – 7.30 (m, 1H), 7.23 (dd, *J* = 4.9, 1.9 Hz, 3H), 6.96 (dd, *J* = 6.7, 2.9 Hz, 2H), 6.04 – 5.92 (m, 1H), 4.90 (t, *J* = 2.4 Hz, 1H), 4.50 – 4.36 (m, 2H), 4.26 (d, *J* = 2.3 Hz, 1H), 2.44 (dt, *J* = 15.0, 3.2 Hz, 1H), 2.20 – 2.07 (m, 1H), 1.71 (dt, *J* = 13.2, 3.2 Hz, 1H), 1.59 – 1.45 (m, 4H), 1.39 (dd, *J* = 11.2, 2.6 Hz, 1H).

^{13}C NMR for major diastereomer (151 MHz, $CDCl_3$) δ 173.96, 139.33, 136.87, 128.96, 128.61, 128.31, 127.98, 127.24, 126.89, 80.65, 76.66, 74.72, 48.61, 26.61, 24.91, 20.98, 19.56.

IR (thin film, cm^{-1}) 3436, 3258, 3054, 2934, 2867, 1779, 1601, 1496, 1449, 1364, 1297, 1264, 1190, 1140, 1094, 1055, 1018

HRMS: m/z calculated for $C_{21}H_{23}NO_3$ $[Na]^+$: 360.15701; found: 360.15690

^{1}H NMR for minor diastereomer (some major diastereomer peaks are present in the major diastereomers spectrum) (600 MHz, $CDCl_3$) δ 7.43 (t, *J* = 7.7 Hz, 3H), 7.37 – 7.30 (m, 2H), 7.28 (dd, *J* = 7.6, 2.0 Hz, 3H), 7.09 (dd, *J* = 7.4, 2.1 Hz, 2H), 5.60 (s, 1H), 5.35 (t, *J* = 3.4 Hz, 1H), 4.24 (dd, *J* = 66.5, 11.4 Hz, 2H), 3.56 (s, 1H), 2.31 – 2.22 (m, 1H), 2.04 (d, *J* = 13.9 Hz, 1H), 2.00 – 1.93 (m, 1H), 1.72 (td, *J* = 13.3, 3.2 Hz, 1H), 1.59 (ddt, *J* = 11.2, 7.6, 3.3 Hz, 2H), 1.53 – 1.48 (m, 1H), 1.18 – 1.07 (m, 1H).

^{13}C NMR for minor diastereomer (151 MHz, $CDCl_3$) δ 173.97, 139.35, 136.88, 128.98, 128.62, 128.32, 127.99, 127.25, 126.91, 80.66, 76.68, 74.73, 48.62, 26.63, 24.92, 20.99, 19.57.

IR (thin film, cm^{-1}) 3446, 3060, 3030, 2938, 2861, 2360, 2341, 1771, 1669, 1601, 1496, 1366, 1290, 1267, 1248, 1204

HRMS: m/z calculated for $C_{21}H_{23}NO_3$ $[Na]^+$: 360.15701; found:360.15691

3-((Benzyloxy)amino)-4,4,5-trimethyldihydrofuran-2(3*H*)-one (2.71)

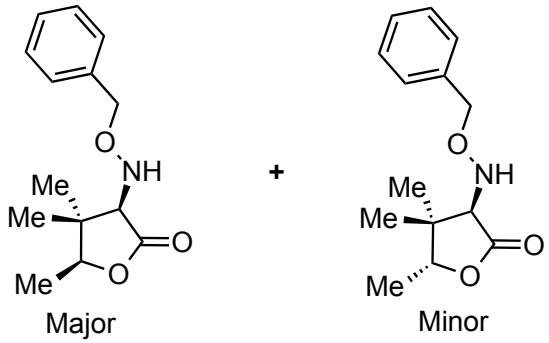

The average isolated yield for **2.71** was 34 mg, 42% (2 trials), synthesized using General Procedure A with 2-methyl-2-butene **1f** (3.0 equiv), oxime **2.51**, **Mes-Acr-Ph**, 2.5 mol%, and an irradiation time of 24 hours in a 1-dram vial. The title compound was obtained as a 1.7:1 mixture of inseparable diastereomers based on an average of two trials. The product was isolated by column chromatography on silica gel (20% EtOAc /hexanes then 30% EtOAc/hexanes) as a yellow oil.

Analytical data for **2.71**:

^{1}H NMR for major/minor diastereomers (600 MHz, $CDCl_3$) δ 7.35 (t, *J* = 4.9 Hz, 6H), 7.34 – 7.29 (m, 2H), 5.94 (s, 2H-1 minor, 1 major), 4.79 – 4.69 (m, 4H-2 minor, 2-major), 4.36 (q, *J* = 6.7 Hz, 1H-minor), 4.15 (q, *J* = 6.5 Hz, 1H-major), 3.74 (s, 1H-major), 3.54 (s, 1H-minor), 1.28(dd, *J* = 6.6, 3.5 Hz, 6H-3-minor, 3-major), 1.17 (s, 3H-major), 1.11 (s, 3H-minor), 1.09 (s, 3H-minor), 0.89 (s, 3H-major).

^{13}C NMR for major/minor diastereomer (151 MHz, $CDCl_3$) δ 174.80, 174.05, 137.23 ,137.01, 128.76, 128.67, 128.60, 128.56, 128.21, 128.19, 84.39, 82.18, 76.71, 76.46, 70.07, 68.27, 43.80, 41.51, 23.37, 22.02, 21.27, 15.45, 15.22, 13.07.

IR (thin film, cm^{-1}) 3516, 3257, 3088, 5063, 3031, 2976, 2932, 2873, 1772, 1639, 1536, 1469, 1469, 1455, 1389, 1572, 1284, 1212, 1186, 1064

HRMS: m/z calculated for $C_{14}H_{19}NO_3$ $[Na]^+$: 272.12571; found: 272.12557

3-((Benzyloxy)amino)-3,3a,8,8a-tetrahydro-2*H*-indeno[2,1-*b*]furan-2-one (2.72)

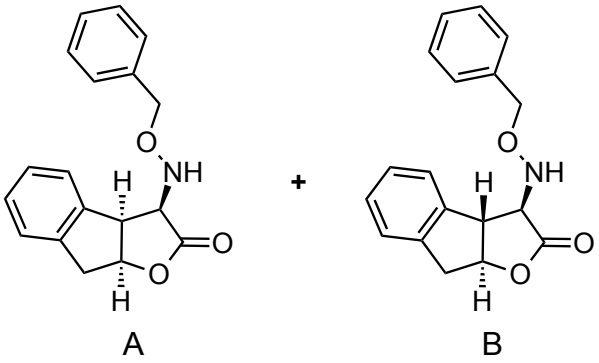

The average isolated yield for **2.72** was 51 mg, 53% (2 trials), synthesized using General Procedure A with indene **1c**, oxime **2.51**, and an irradiation time of 24 hours. The title compound was obtained as a 1.0:1 mixture of separable diastereomers based on an average of two trials. The products were isolated by column chromatography on silica gel (10% EtOAc /hexanes then 30% EtOAc/hexanes). The minor product was obtained as a brown solid and the major product as a purple oil.

Analytical data for **2.72**:

^{1}H NMR for major diastereomer (600 MHz, $CDCl_3$) δ 7.54 – 7.26 (m, 7H), 7.25 (s, 2H), 6.23 (s, 1H), 5.33 (s, 1H), 4.82 (d, *J* = 6.5 Hz, 2H), 3.91 (dd, *J* = 6.0, 1.8 Hz, 1H), 3.79 (d, *J* = 1.9 Hz, 1H), 3.31 – 3.27 (m, 2H).

^{13}C NMR for major diastereomer (151 MHz, $CDCl_3$) δ 175.89, 140.59, 140.35, 137.07, 128.78, 128.70, 128.60, 128.42, 127.91, 125.51, 125.09, 84.52, 77.22, 66.91, 51.12, 38.88.

IR (thin film, cm^{-1}) 3505, 3241, 3030, 2921, 1772, 1481, 1455, 1425, 1354, 1294, 1269, 1205, 1176, 1114

HRMS: m/z calculated for $C_{18}H_{17}NO_3$ $[Na]^+$: 318.11006; found: 318.10989

^{1}H NMR for minor diastereomer (600 MHz, $CDCl_3$) δ 7.50 (d, *J* = 7.5 Hz, 1H), 7.42 – 7.35 (m, 4H), 7.35 – 7.30 (m, 1H), 7.30 – 7.26 (m, 2H), 7.23 (td, *J* = 6.7, 5.9, 2.7 Hz, 1H), 5.97 (d, *J* = 5.2 Hz, 1H), 5.23 (dt, *J* = 5.4, 3.4 Hz, 1H), 4.78 – 4.70 (m, 2H), 4.40 (d, *J* = 8.8 Hz, 1H), 4.20 (ddd, *J* = 8.8, 5.5, 1.0 Hz, 1H), 3.29 (d, *J* = 3.4 Hz, 2H).

^{13}C NMR for minor diastereomer (151 MHz, $CDCl_3$) δ 173.40, 141.26, 137.22, 136.87, 128.78, 128.67, 128.65, 128.29, 127.55, 127.33, 125.50, 81.82, 76.38, 62.89, 48.91, 39.18.

IR (thin film, cm^{-1}) 3428, 3055, 3030, 2922, 1770, 1699, 1496, 1478, 1455, 1425, 1362, 1296, 1266, 1173

HRMS: m/z calculated for $C_{18}H_{17}NO_3$ $[Na]^+$: 318.11006; found: 318.10991

2-((4-((Benzyloxy)amino)-3-(4-methoxyphenyl)-5-oxotetrahydrofuran-2-yl)methyl)isoindoline-1,3-dione (2.73)

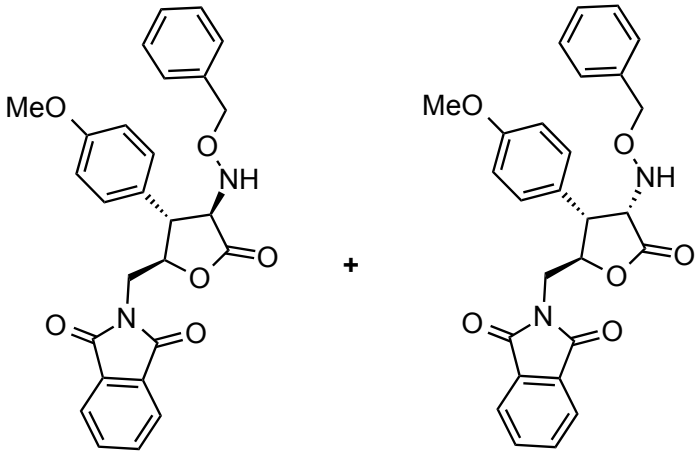

Major Minor

The average isolated yield for **2.73** was 64 mg, 41% (2 trials), synthesized using General Procedure A with (E)-2-(3-(4-methoxyphenyl)allyl)isoindoline-1,3-dione **1r**, oxime **2.51**, and an irradiation time of 24 hours. The title compound was obtained as a 3.2:1 mixture of inseparable diastereomers based on an average of two trials. The product was isolated by column chromatography on silica gel (30% EtOAc /hexanes then 50% EtOAc/hexanes) as a cream solid.

Analytical data for **2.73**:

^{1}H NMR for major/minor diastereomers (600 MHz, $CDCl_3$) δ 7.74 (dd, *J* = 5.4, 3.1 Hz, 3H), 7.67 (dd, *J* = 5.5, 3.0 Hz, 3H), 7.34 – 7.24 (m, 6H), 7.19 (ddd, *J* = 14.2, 7.4, 1.9 Hz, 1H), 7.12 – 7.07 (m, 2H), 6.73 (t, *J* = 8.5 Hz, 3H), 6.00 (s, 1H-major), 5.60 (s, 1H-minor), 5.25 (dt, *J* = 8.8, 6.7 Hz, 1H-minor), 4.90 (dt, *J* = 10.1, 6.2 Hz, 1H-major), 4.74 – 4.64 (m, 2H-major), 4.51 (q, *J* = 11.7 Hz, 2H-minor), 4.07 (dd, *J* = 14.1, 6.6 Hz, 2H-1 minor, 1 major), 3.99 – 3.94 (m, 2H-1 minor, 1 major), 3.84 (d, *J* = 11.1 Hz, 2H-1 minor, 1 major), 3.68 (d, *J* = 1.6 Hz, 6H-3 minor, 3 major), 3.61 (t, *J* = 10.6 Hz, 1H-major), 3.55 (t, *J* = 8.6 Hz, 1H-minor).

^{13}C NMR for major/minor diastereomers (151 MHz, $CDCl_3$) δ 173.24, 172.57, 167.96, 167.94, 159.27, 159.24 137.17, 134.12, 134.11, 131.77, 130.08, 128.80, 128.78, 128.53, 128.11, 127.93, 124.89, 123.41, 79.77, 78.06, 77.31, 76.64, 68.39, 63.38, 55.35, 55.31, 49.13, 47.72, 40.64, 40.10.

IR (thin film, cm^{-1}) 3470, 3560, 3061, 2937, 2838, 1774, 1716, 1694, 1515, 1467, 1455, 1422, 1395, 1369, 1307, 1254, 1181, 1087

HRMS: m/z calculated for $C_{27}H_{24}N_2O_6$ $[H]^+$: 473.17071; found: 473.17079

3-((Benzyloxy)amino)-4-(4-(*tert*-butyldimethylsilyl)phenyl)-5-methyldihydrofuran-2(3*H*)-one (2.74)

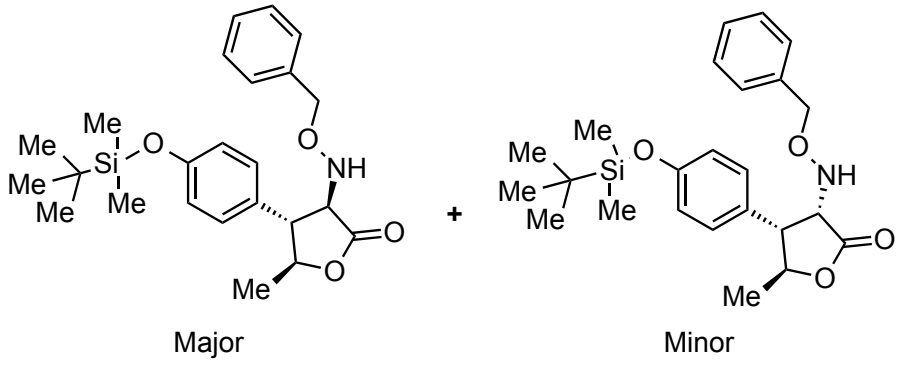

Major Minor

The average isolated yield for **2.74** was 100 mg, 71% (2 trials), synthesized using General Procedure A with *tert*-butyldimethyl(4-(prop-1-en-1-yl)phenyl)silane **1s**, oxime **2.51**, and an irradiation time of 24 hours. The title compound was obtained as a 1.9:1 mixture of inseparable diastereomers based on an average of two trials. The product was isolated by column chromatography on silica gel (15% EtOAc /hexanes then 20% EtOAc/hexanes) as a yellow oil.

Analytical data for **2.74**:

^{1}H NMR for major/minor diastereomers (600 MHz, $CDCl_3$) δ 7.34 – 7.27 (m, 5H), 7.27 – 7.21 (m, 4H), 7.14 (d, *J* = 8.5 Hz, 1H), 7.09 – 7.04 (m, 2H), 6.84 (t, *J* = 8.4 Hz, 3H), 6.08 (s, 1H-major), 5.65 (d, *J* = 3.1 Hz, 1H-minor), 4.95 (dq, *J* = 7.7, 6.3 Hz, 1H-minor), 4.68 (q, *J* = 11.6 Hz, 2H-major), 4.50 (d, *J* = 2.9 Hz, 2H-minor), 4.44 (dq, *J* = 10.0, 6.1 Hz, 1H-major), 3.98 (dd, *J* = 9.9, 6.1 Hz, 2H-1 minor, 1 major), 3.38 – 3.30 (m, 2H-1 minor, 1 major), 1.43 (d, *J* = 6.3 Hz, 3H-minor), 1.40 (d, *J* = 6.1 Hz, 3H-major), 1.00 (s, 18H= 9 minor, 9 major), 0.21 (s, 12H-6 minor, 6 major).

^{13}C NMR for major/minor diastereomer (151 MHz, $CDCl_3$) δ 174.11, 173.60, 155.56, 155.49, 137.30, 136.99, 129.99, 128.91, 128.88, 128.75, 128.55, 128.49, 128.08, 126.95, 120.73, 120.55, 81.00, 79.77, 77.30, 76.63, 67.93, 63.63, 52.46, 52.01, 25.79, 25.77, 20.10, 18.97, 18.33, 18.30, -4.25, -4.27.

IR (thin film, cm^{-1}) 3251, 3062, 3032, 2955, 2930, 2895, 2895, 2857, 2302, 1779, 1692, 1609, 1511, 1472, 1455, 1421, 1387, 1362, 1329, 1266, 1199, 1174

HRMS: m/z calculated for $C_{24}H_{33}NO_4Si$ $[H]^+$: 428.22516; found: 428.2254

Benzyloxyamine Reduction

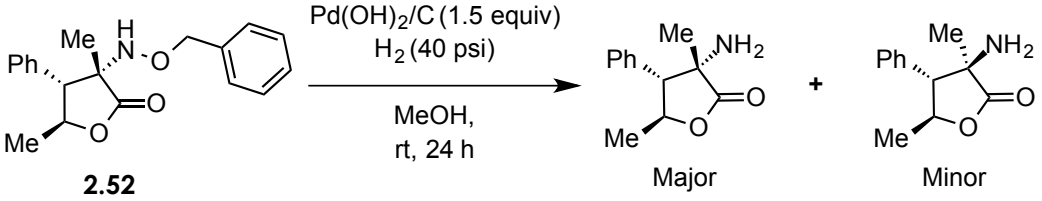

Reduction of product **2.52** was achieved using a procedure adapted from a previously reported method.[28] A flame dried high-pressure vessel was charged with a stir bar, lactone **2.52** (79 mg, 0.25 mmol), and Pearlman's catalyst $Pd(OH)_2/C$ (54 mg, 0.38 mmol). The mixture was stirred in MeOH (8.5 mL) under hydrogen (40 psi) for 24 hours followed by filtration over celite and a MeOH wash. After the solvent was evaporated, the product was dissolved in 5 mL DCM and acidified to pH 5 with 1N HCl. The aqueous layer was washed once with 10 mL Et_2O and then basified to pH 8 with saturated $NaHCO_3$. The product was extracted three times (3x) with 10 mL DCM. The combined organic layers we dried over $MgSO_4$ before the solvent was evaporated to afford the free amine product as a clear oil (37 mg, 72%). The product was obtained as a 5:1 mixture of inseparable diastereomers.

Analytical data:

^{1}H NMR for major/minor diastereomers (600 MHz, $CDCl_3$) δ 7.42 – 7.33 (m, 6H-3 minor, 3 major), 7.31 – 7.27 (m, 2H-major), 7.26 – 7.22 (m, 2H-minor), 5.04 (dq, *J* = 10.1, 6.2 Hz, 1H-major), 4.84 (dq, *J* = 12.0, 6.1 Hz, 1H-minor), 3.07 (d, *J* = 10.7 Hz, 1H-minor), 2.92 (d, *J* = 10.1 Hz, 1H-major), 1.45 (d, *J* = 6.1 Hz, 3H-minor), 1.39 (d, J = 6.2 Hz, 3H-major), 1.37 (s, 3H-major), 1.01 (s, 3H-minor).

13C NMR for major diastereomer (151 MHz, CDCl3) δ 179.64, 177.36, 132.76, 132.18, 128.31, 127.97, 127.88, 127.52, 127.37, 127.08, 76.37, 74.59, 59.79, 59.49, 59.00, 57.67, 24.83, 19.86, 18.25, 17.82.

IR (thin film, cm^{-1}) 3853, 3696, 3061, 3032, 2975, 2870, 2389, 1958, 1769, 1690, 1601, 1584, 1500, 1454, 1376, 1287, 1168,, 1061

HRMS: m/z calculated for CHNO $[H]^+$: 206.11756 ; found: 206.11761

Stereochemical Assignment- Selective 1D-NOESY

The stereochemistry for β-methylstyrene-derived products was determined based on 3-((benzyloxy)amino)-4-(2-methoxyphenyl)-5-methyldihydrofuran-2(3*H*)-one (**2.63**) using selective 1D-NOESY experiments. Four proton environments were selectively irradiated for the major and minor diastereomers. The relative peak amplifications, resulting from a NOE, were used to assign the relative stereochemistry of the product. The same procedure was used to identify the stereochemistry of 3-((benzyloxy)amino)-4-methyl-4-phenyldihydrofuran-2(3*H*)-one (**2.69**), 3-((benzyloxy)amino)-3a-phenylhexahydrobenzofuran-2(3*H*)-one (**2.70**), 3-((benzyloxy)amino)-4,4,5-trimethyldihydrofuran-2(3*H*)-one (**2.71**), and 3-((benzyloxy)amino)-3,3a,8,8a-tetrahydro-2*H*-indeno[2,1-*b*]furan-2-one (**2.72**) and 3-((benzyloxy)amino)-3,5-dimethyl-4-phenyldihydrofuran-2(3*H*)-one (**2.55**) (extrapolated to **2.56**). See below for spectra.

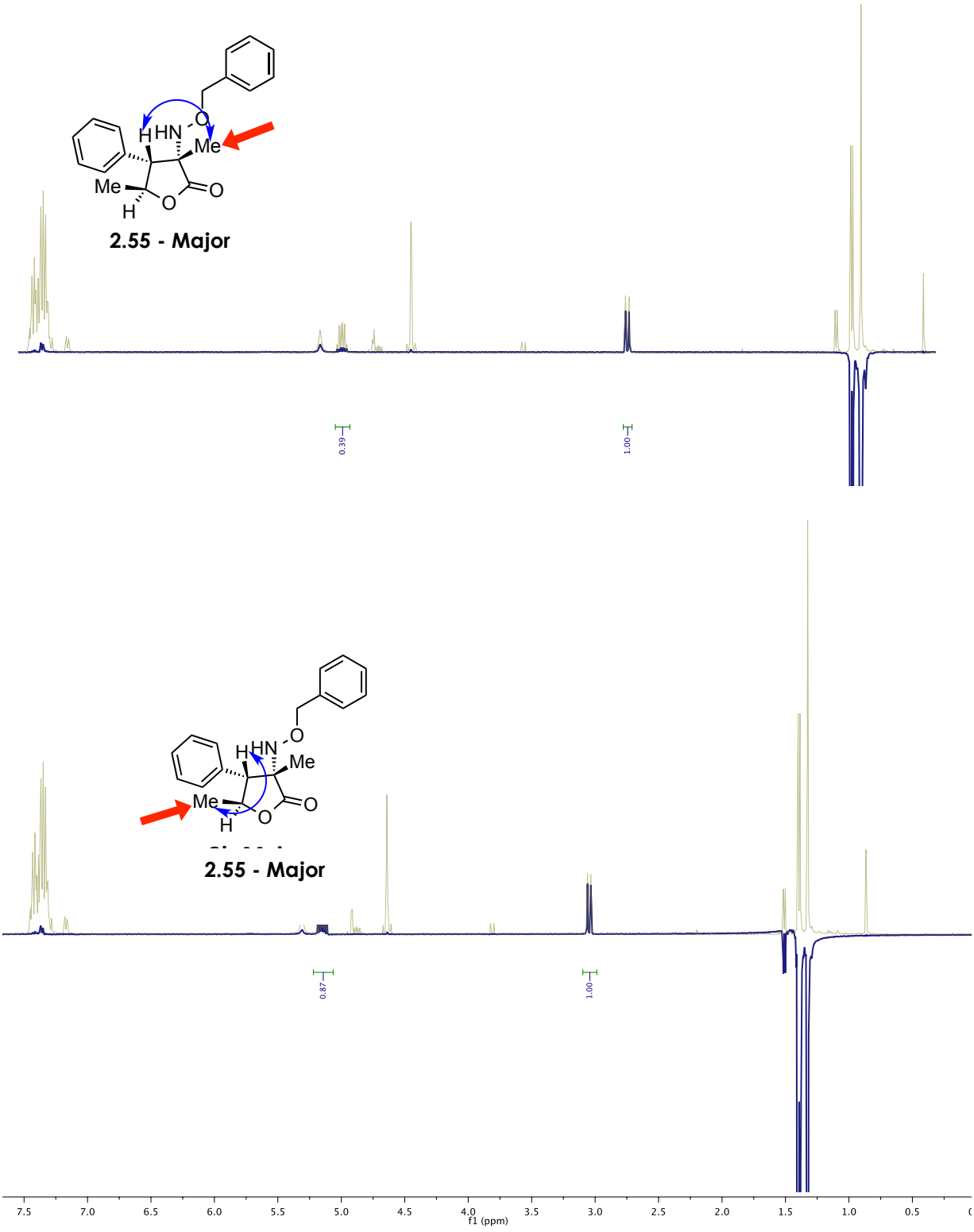
H
HN
O
Me
Me
O
O
H
2.55 - Major
0.39
1.00
H
HN
O
Me
Me
O
O
H
2.55 - Major
0.87
1.00
7.5
7.0
6.5
6.0
5.5
5.0
4.5
4.0
3.5
3.0
2.5
2.0
1.5
1.0
0.5
f1 (ppm)

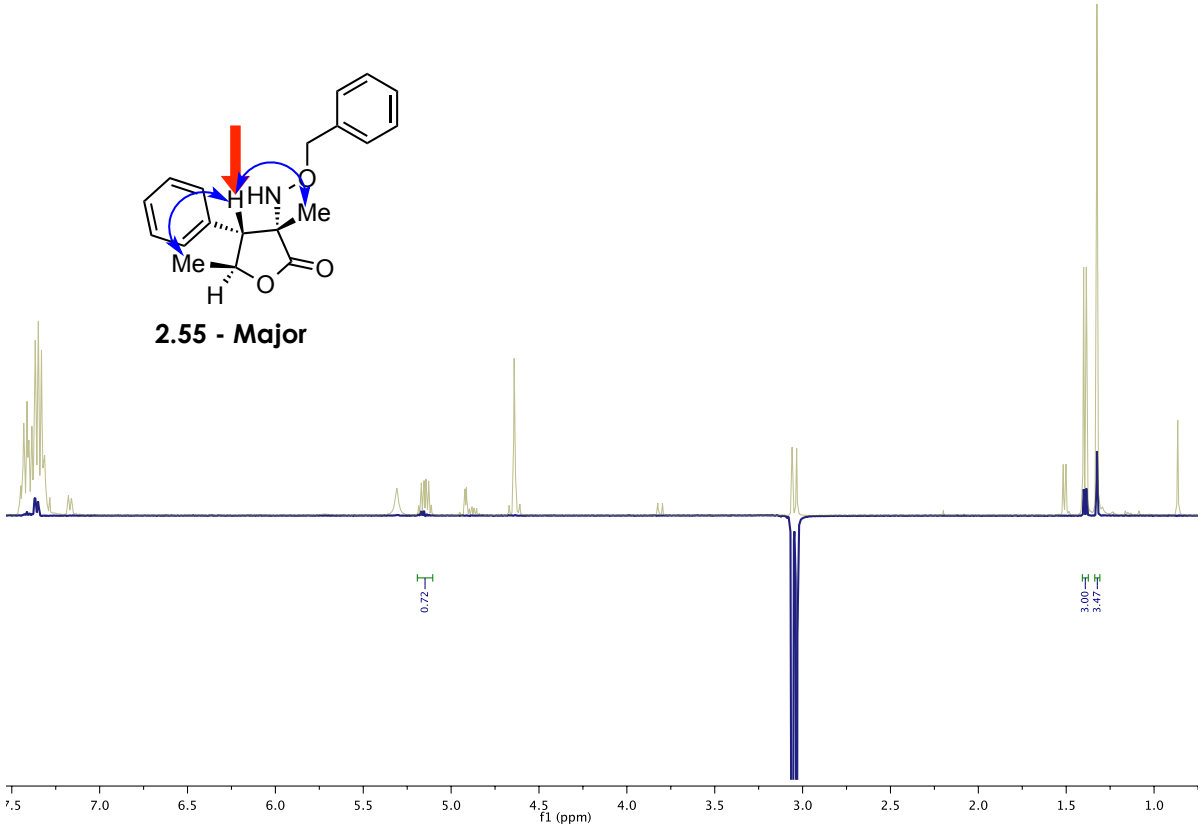

2.55 - Major

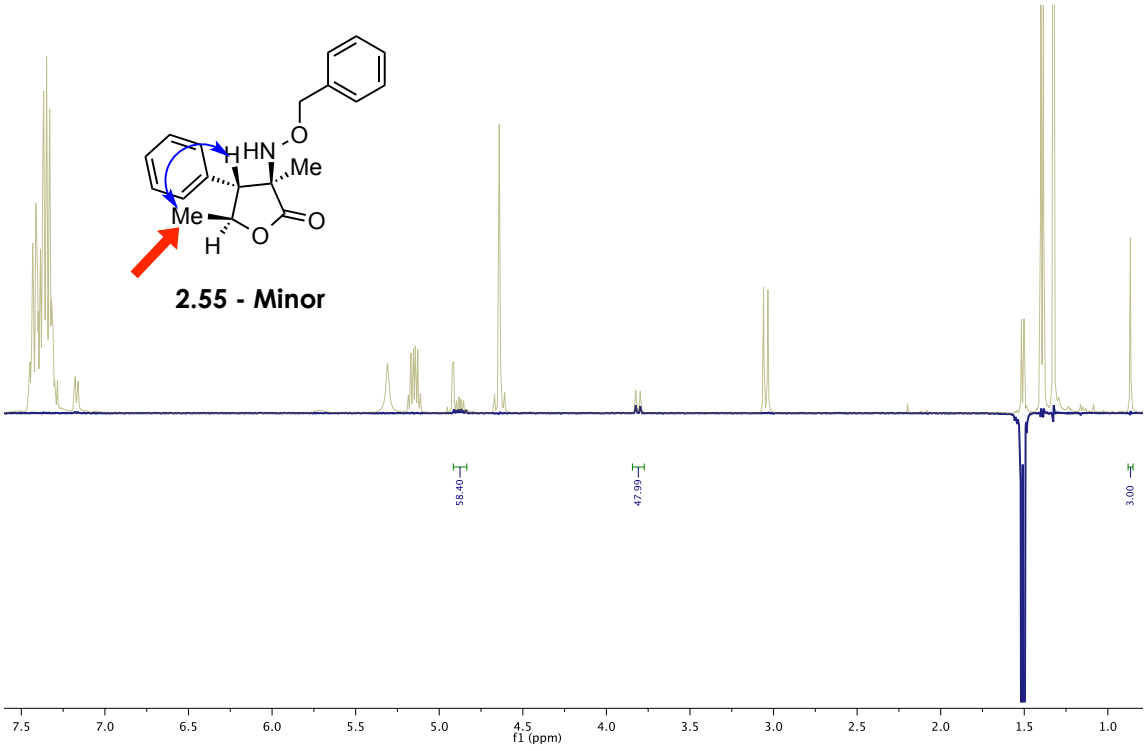

2.55 - Minor

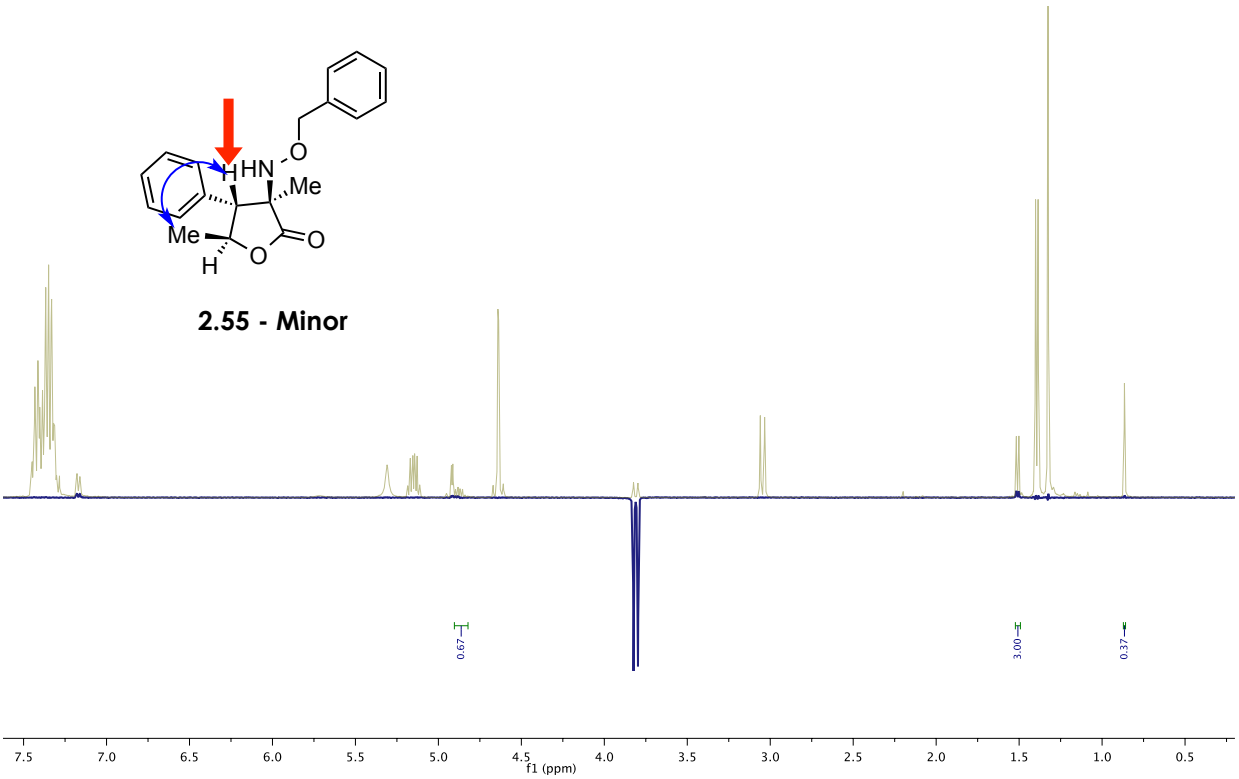

2.55 - Minor

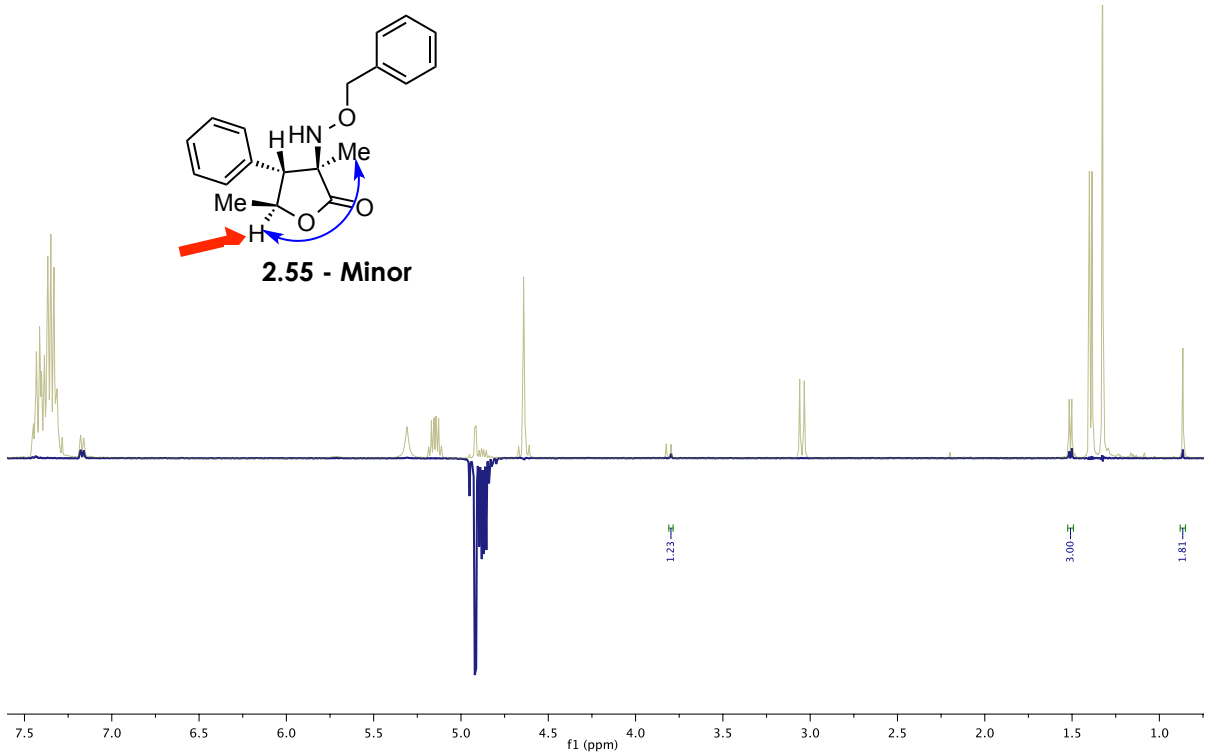

2.55 - Minor

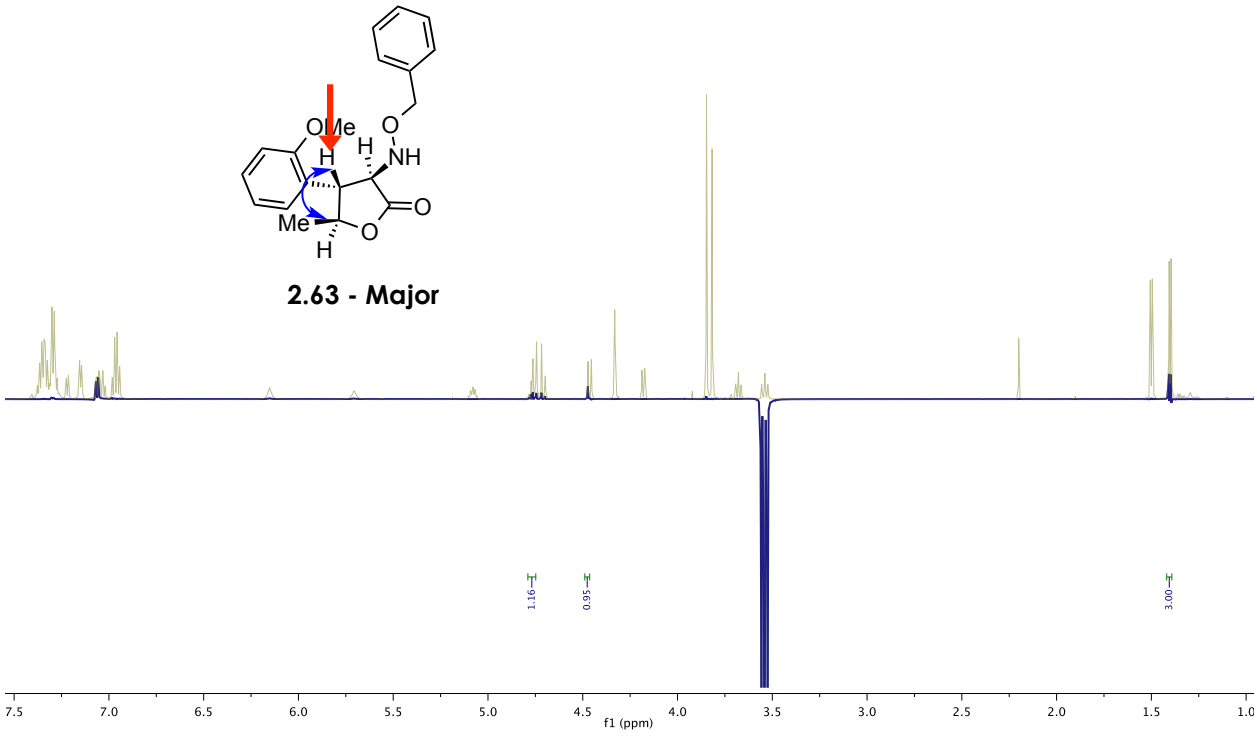

2.63 - Major

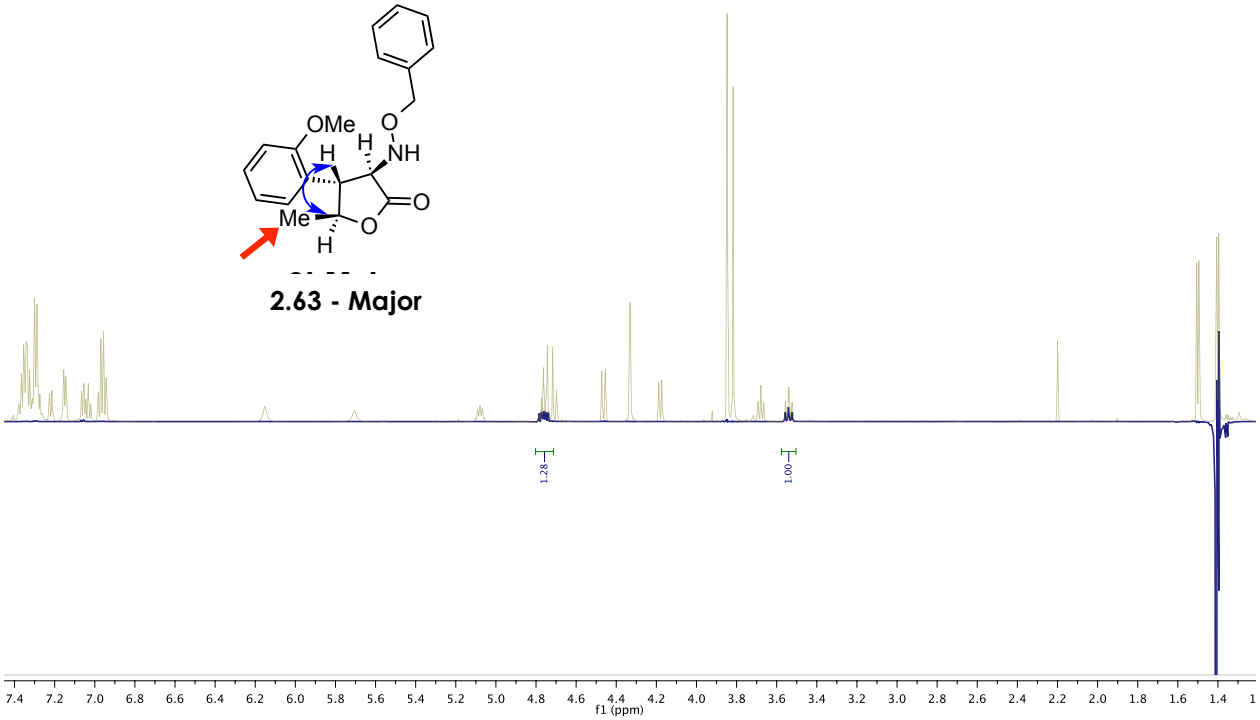

2.63 - Major

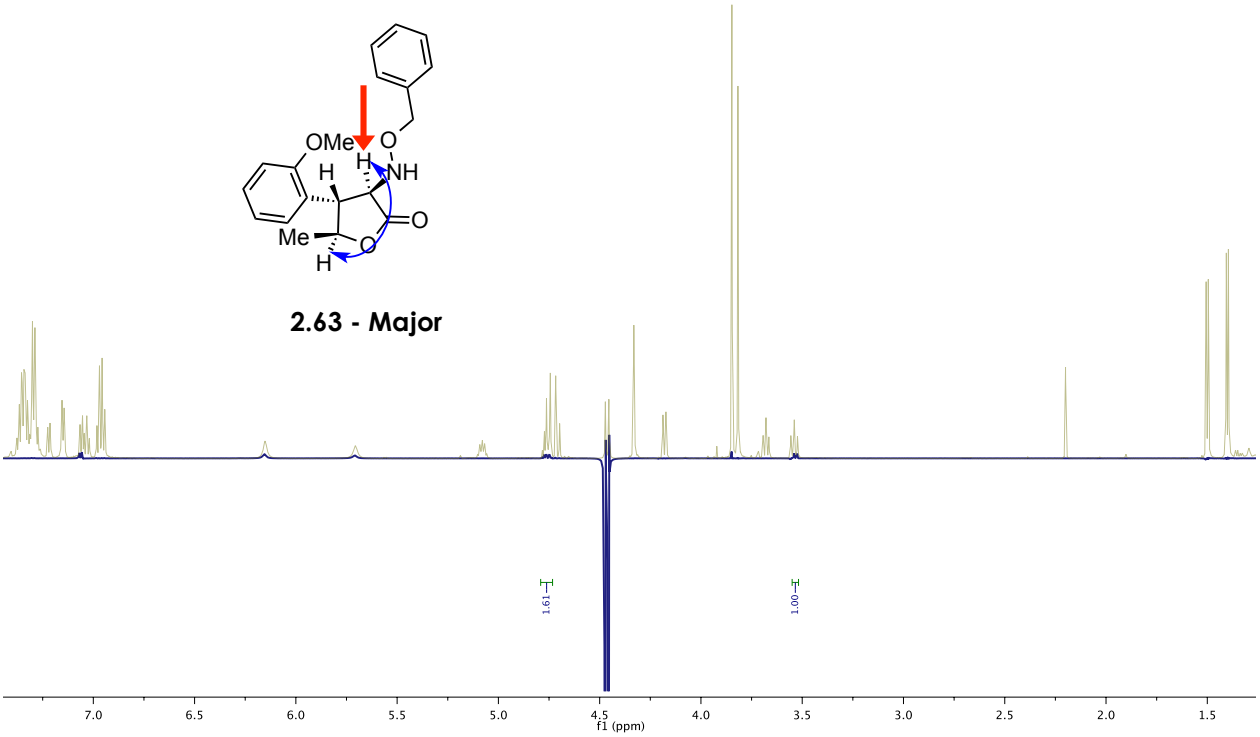
OMe
O
H
H
NH
O
Me
O
H
2.63 - Major
1.61
1.00
7.0
6.5
6.0
5.5
5.0
4.5
4.0
3.5
3.0
2.5
2.0
1.5
f1 (ppm)

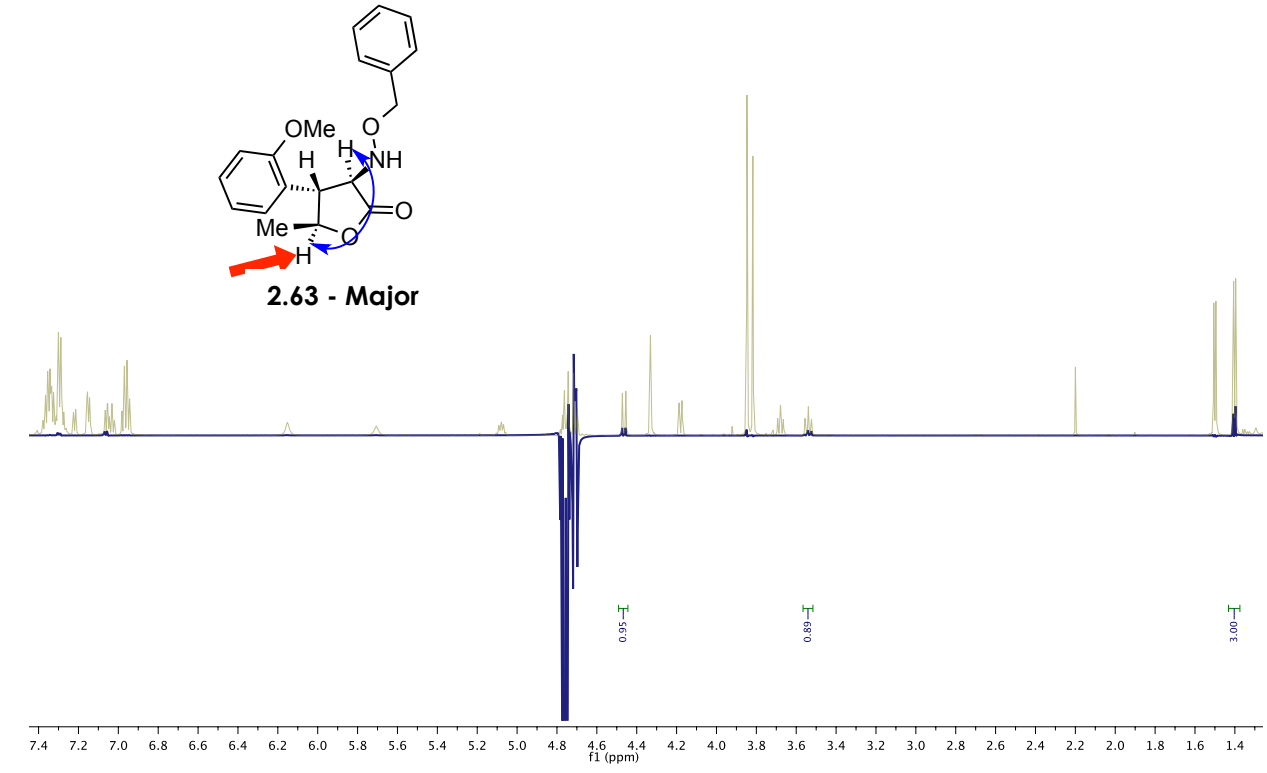
OMe
O
H
H
NH
O
Me
O
H
2.63 - Major
0.95
0.89
3.00
7.4
7.2
7.0
6.8
6.6
6.4
6.2
6.0
5.8
5.6
5.4
5.2
5.0
4.8
4.6
4.4
4.2
4.0
3.8
3.6
3.4
3.2
3.0
2.8
2.6
2.4
2.2
2.0
1.8
1.6
1.4
f1 (ppm)

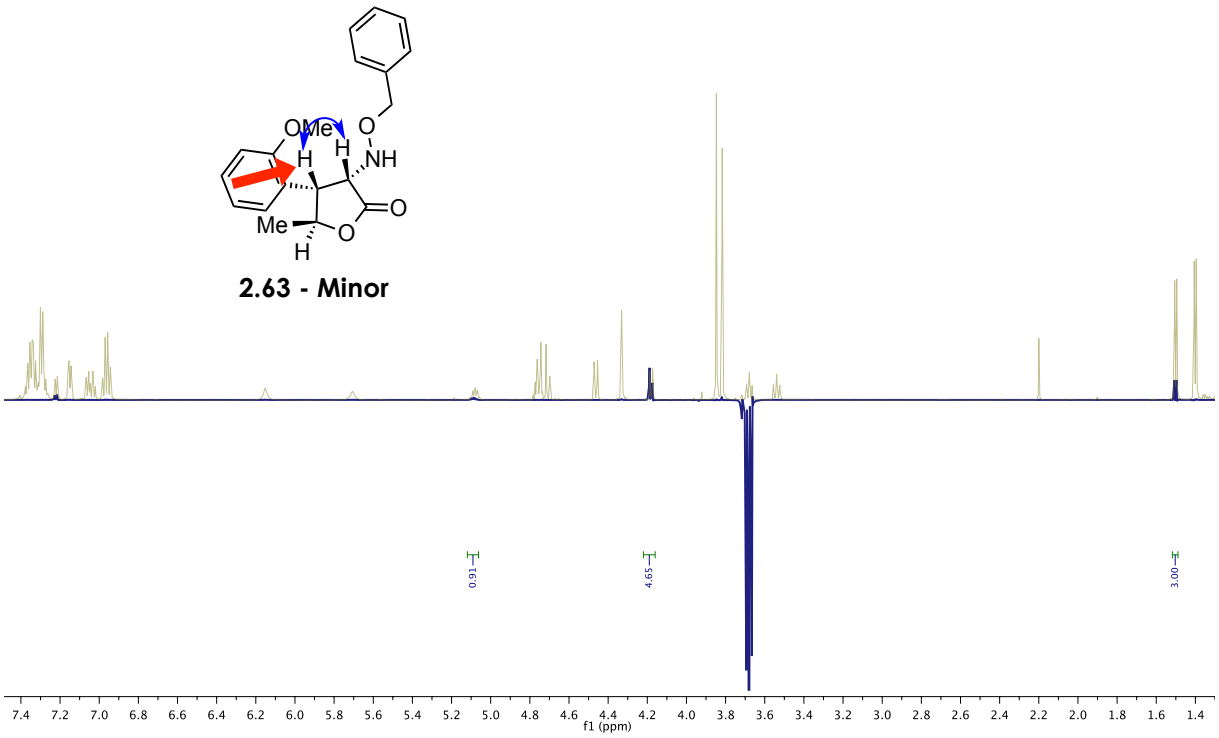
OMe
H
H
O
NH
O
Me
O
H
2.63 - Minor
0.91
4.65
3.00
7.4 7.2 7.0 6.8 6.6 6.4 6.2 6.0 5.8 5.6 5.4 5.2 5.0 4.8 4.6 4.4 4.2 4.0 3.8 3.6 3.4 3.2 3.0 2.8 2.6 2.4 2.2 2.0 1.8 1.6 1.4
f1 (ppm)

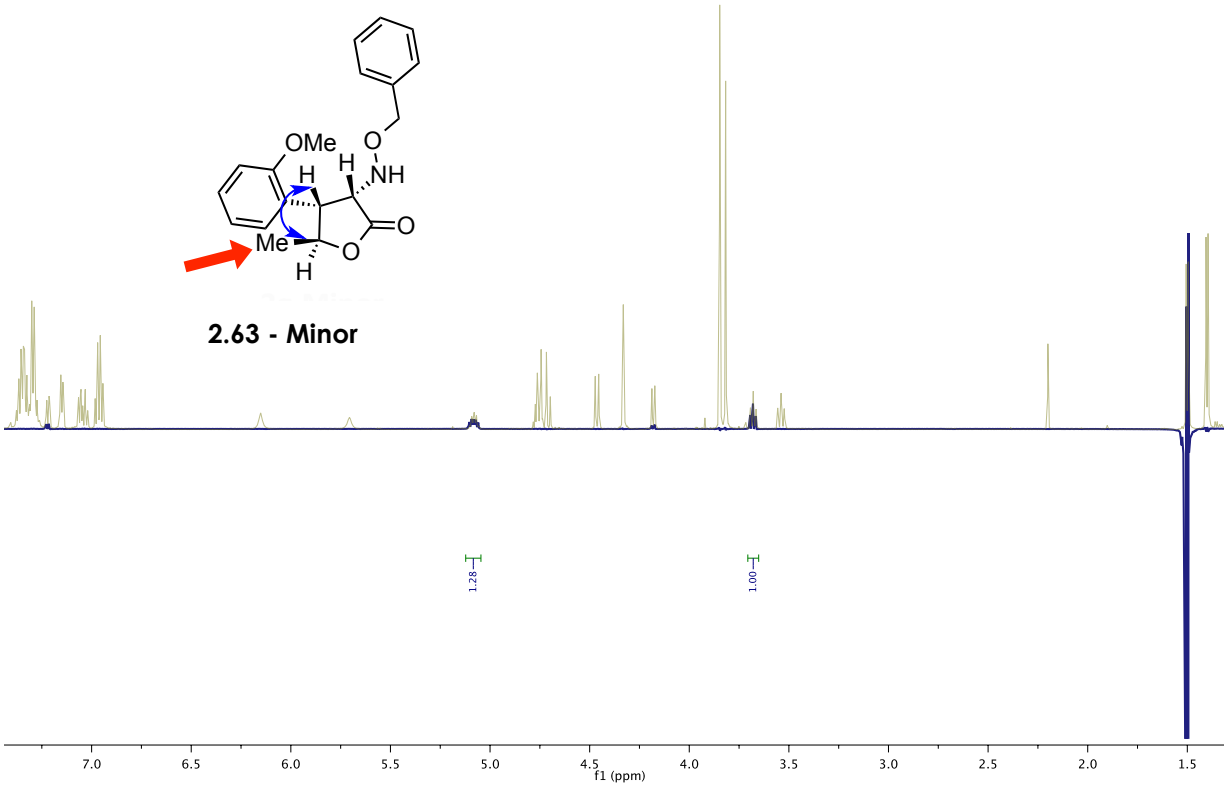
OMe
H
H
O
NH
O
Me
O
H
2.63 - Minor
1.28
1.00
7.0 6.5 6.0 5.5 5.0 4.5 4.0 3.5 3.0 2.5 2.0 1.5
f1 (ppm)

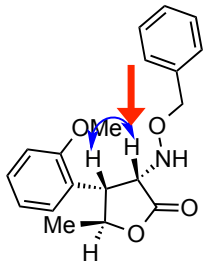

2.63 - Minor

No strong NOE observed

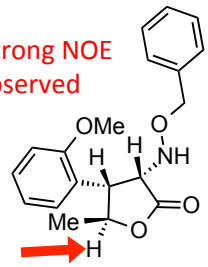

2.63 - Minor

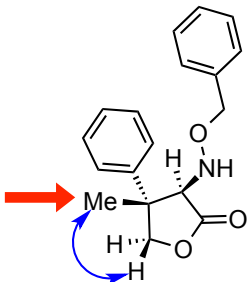

2.69 - Major

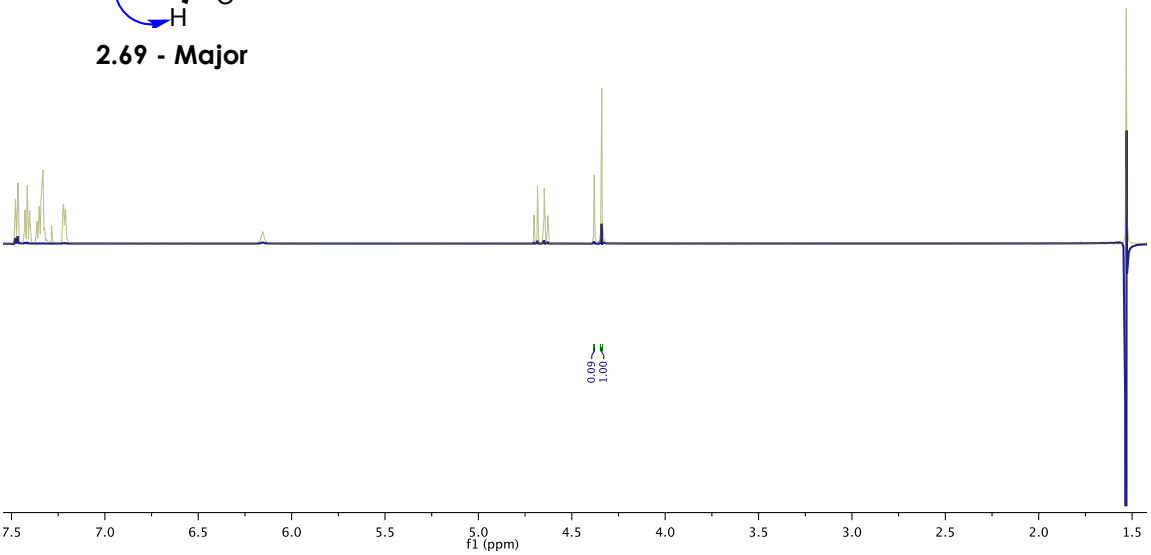

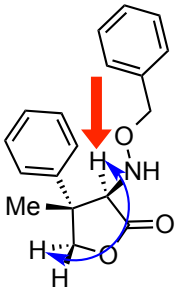

2.69 - Major

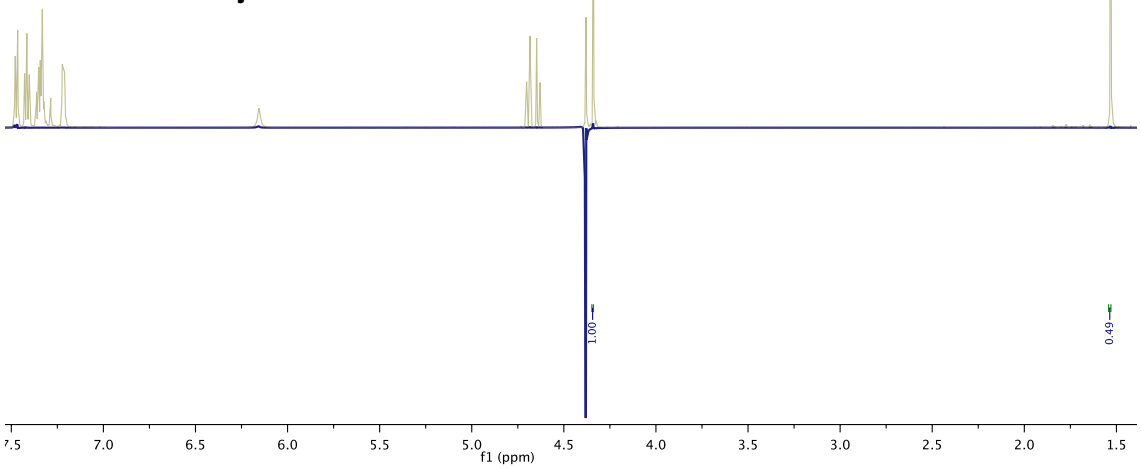

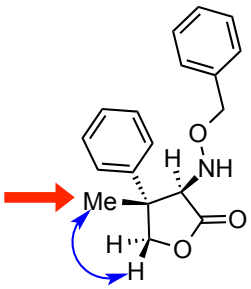

2.69 - Major

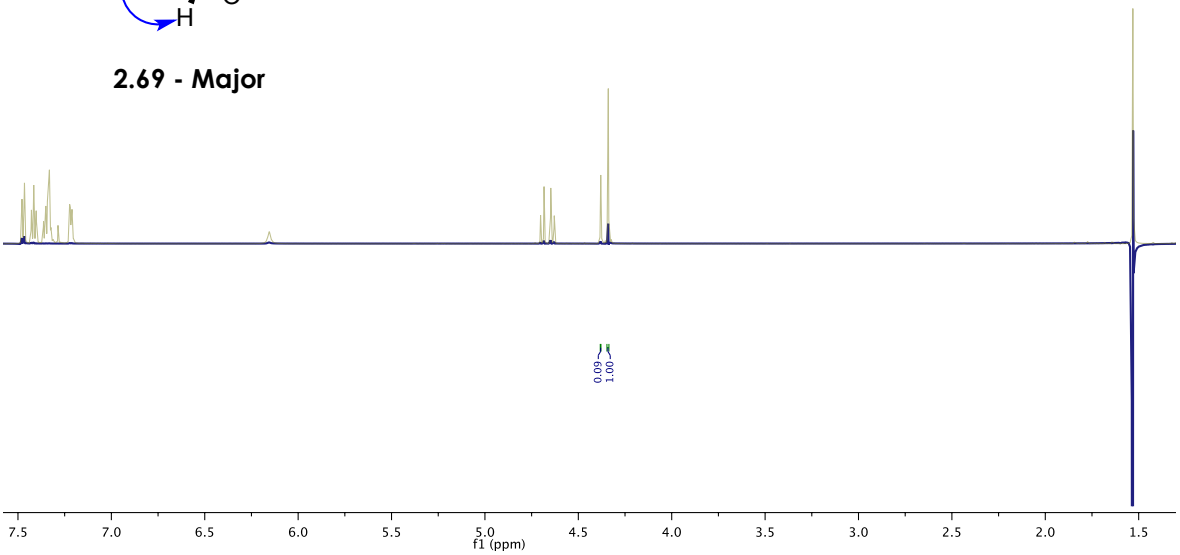

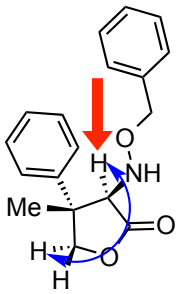

2.69 - Major

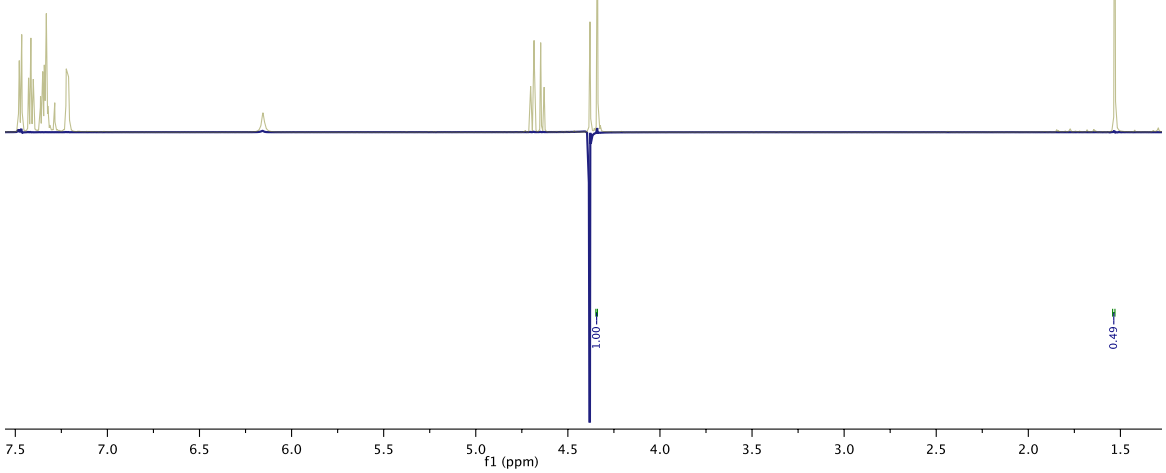

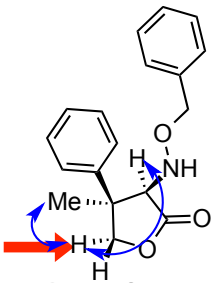

2.69 - Minor

No strong NOE observed

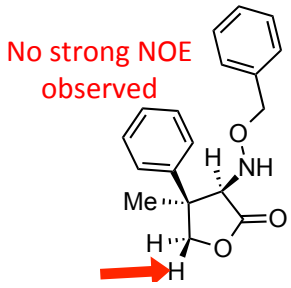

2.69 - Minor

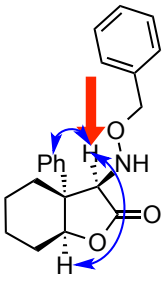

2.70- Major

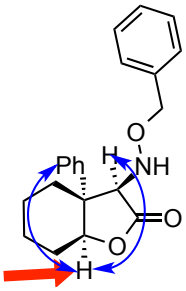

2.70- Major

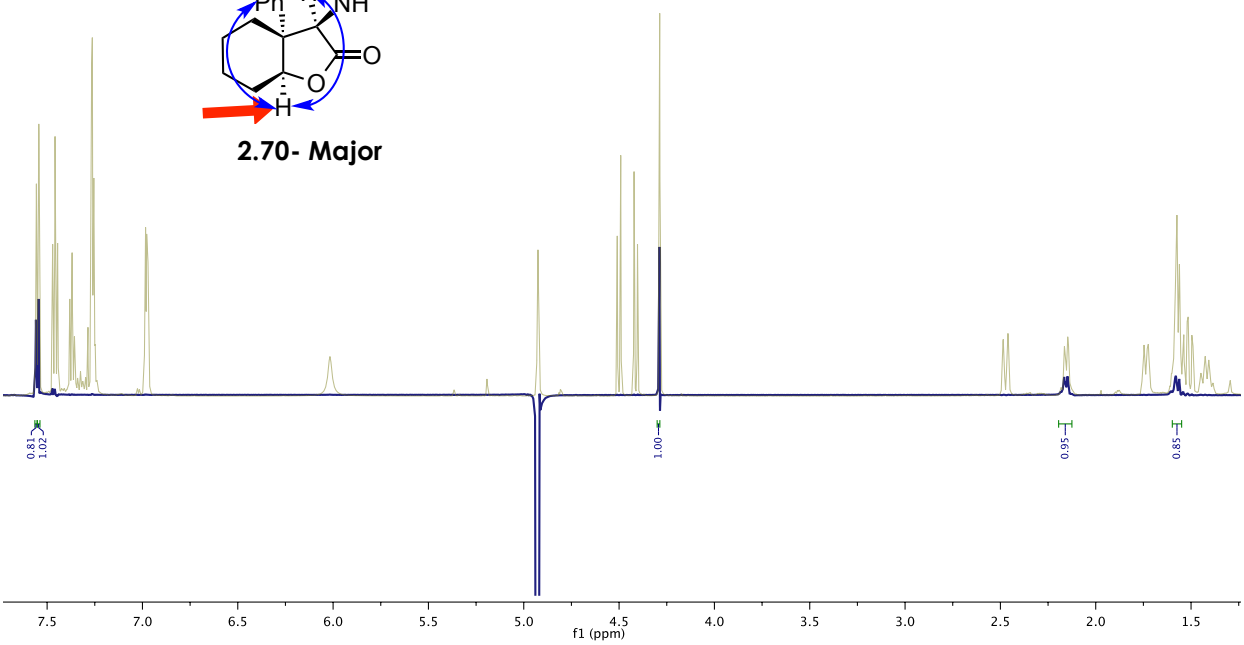

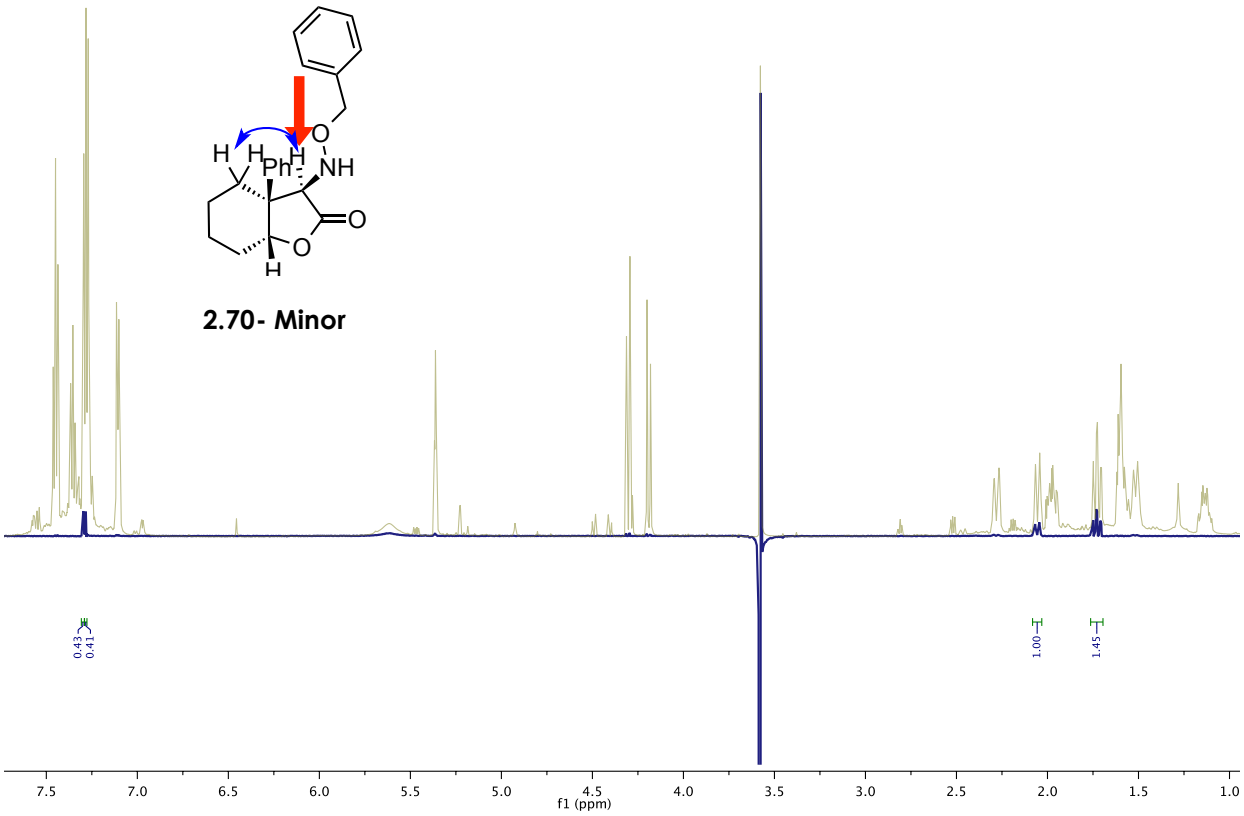
H
H
H
Ph
O
NH
O
O
H
2.70- Minor
0.43
0.41
1.00
1.45
7.5
7.0
6.5
6.0
5.5
5.0
4.5
4.0
3.5
3.0
2.5
2.0
1.5
1.0
f1 (ppm)

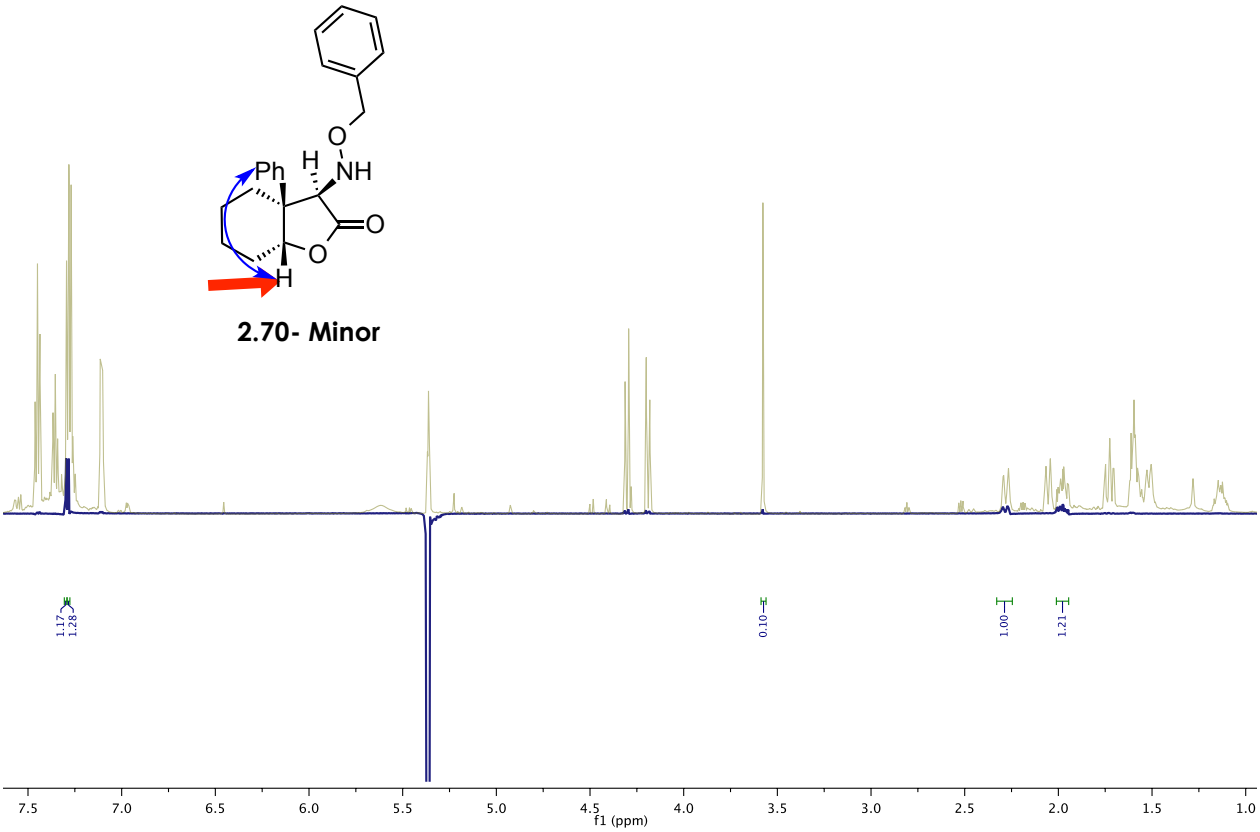
O
H
NH
Ph
O
O
H
2.70- Minor
1.17
1.28
0.10
1.00
1.21
7.5
7.0
6.5
6.0
5.5
5.0
4.5
4.0
3.5
3.0
2.5
2.0
1.5
1.0
f1 (ppm)

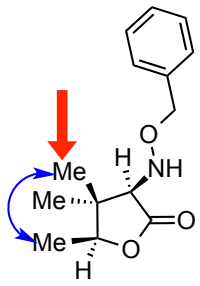

2.71- Major

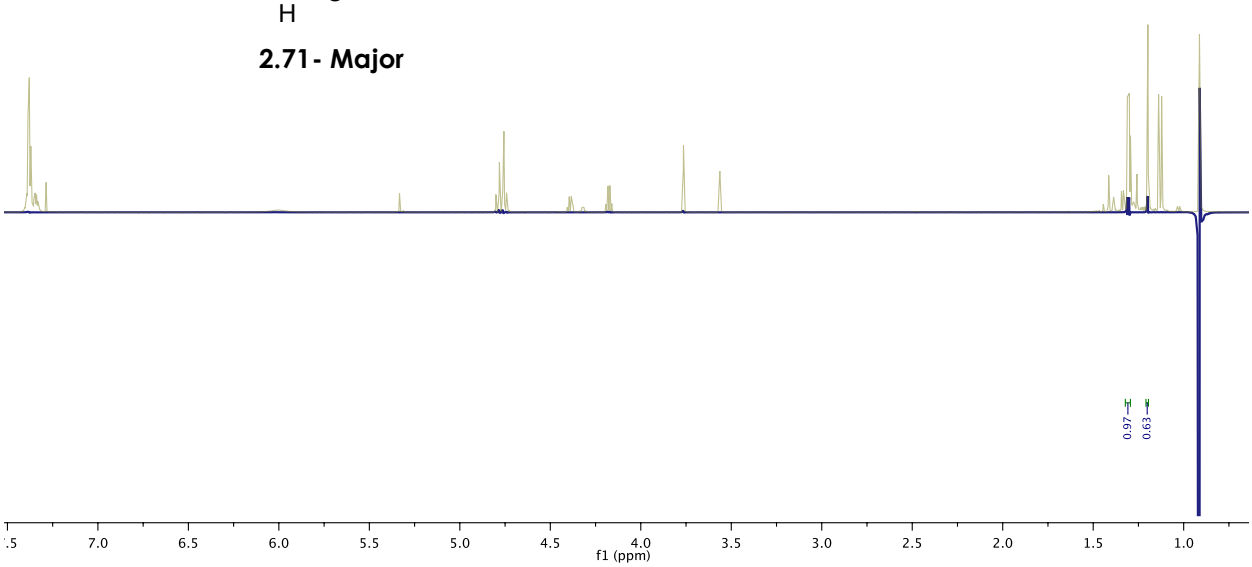

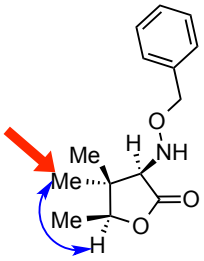

2.71- Major

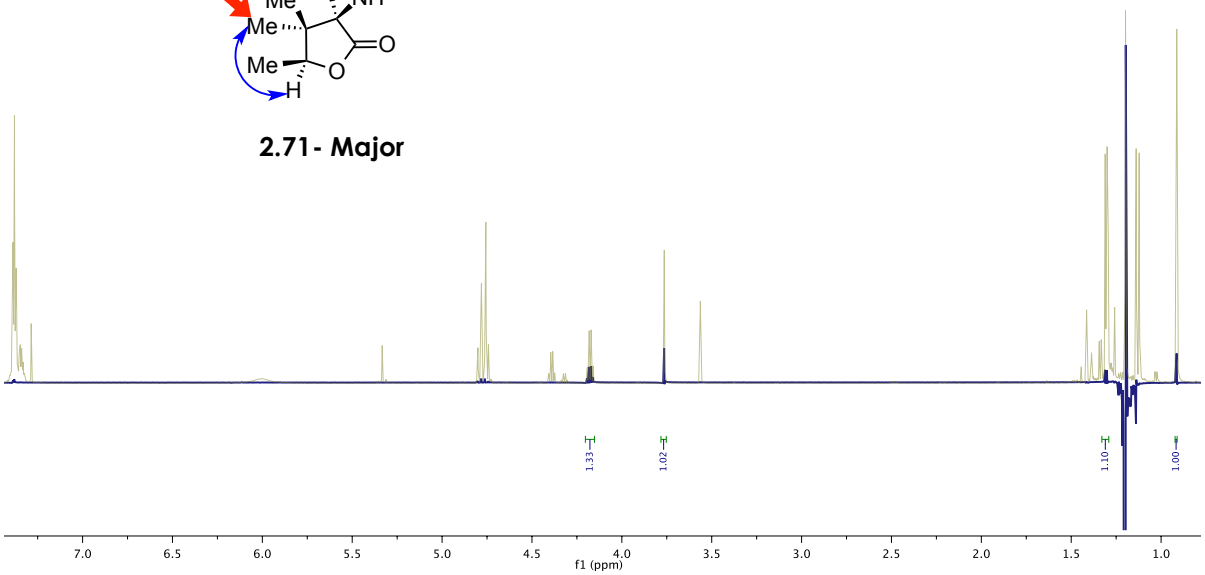

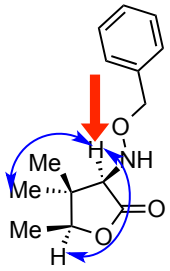

2.71 - Minor

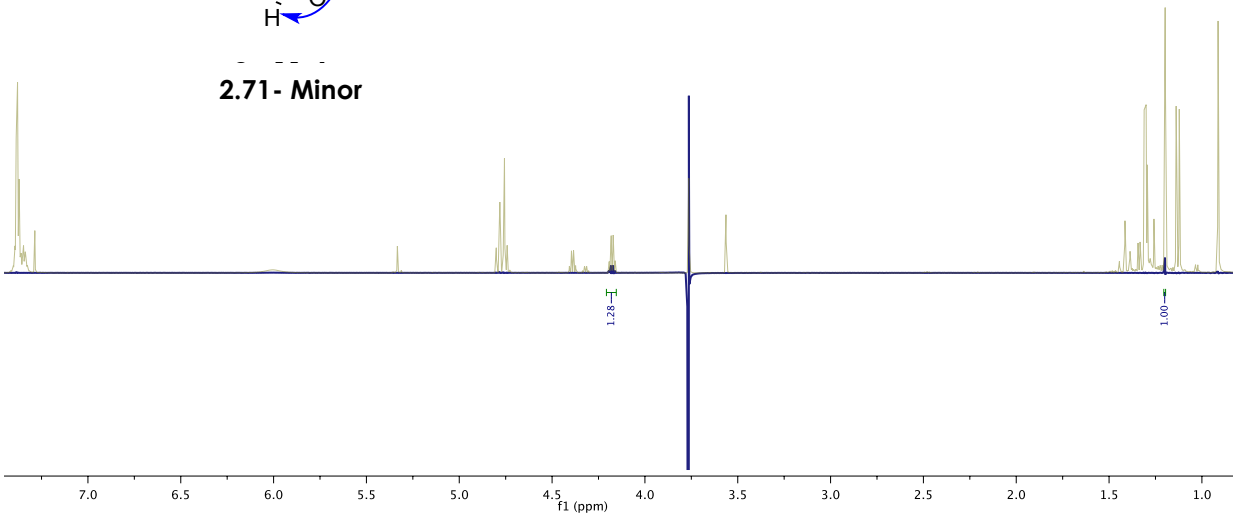

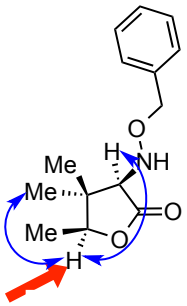

2.71 - Minor

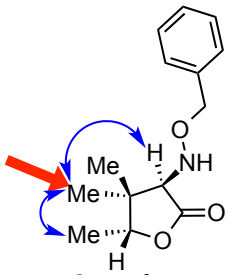

2.71 - Minor

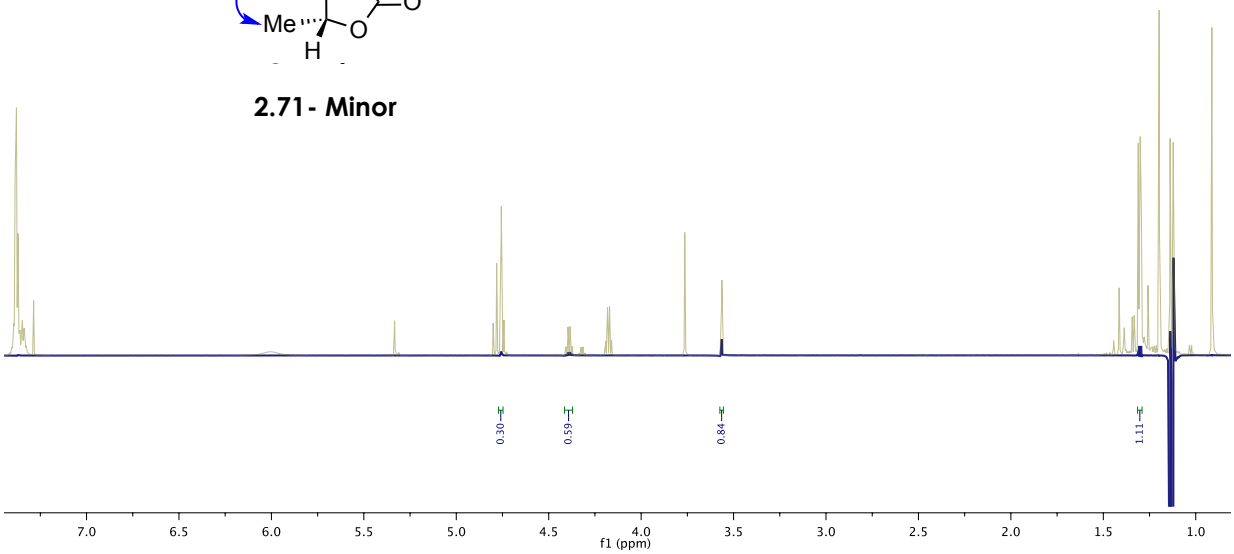

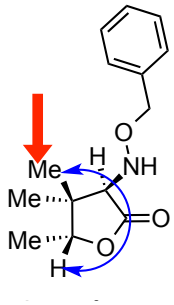

2.71 - Minor

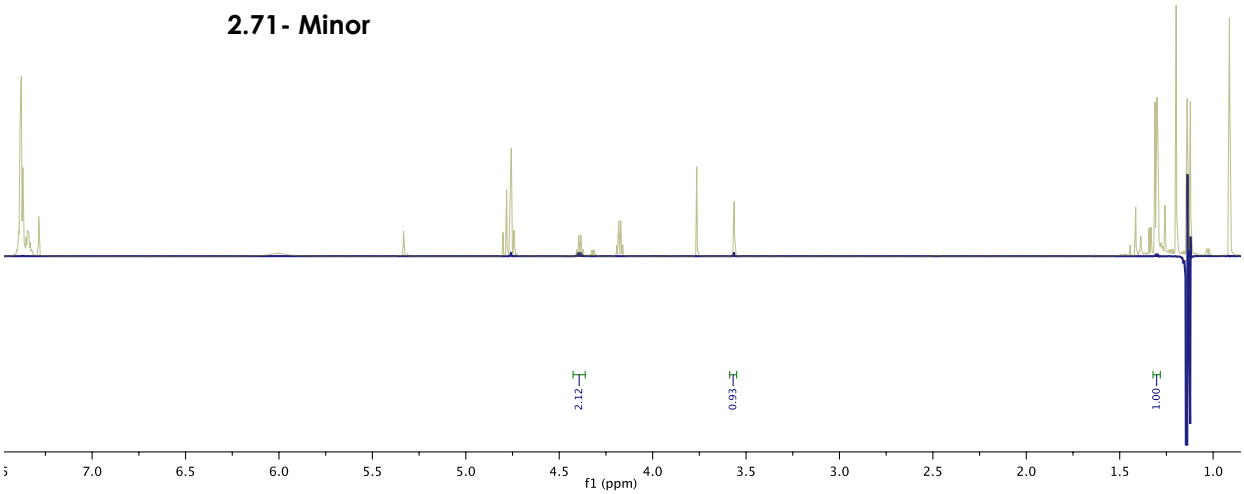

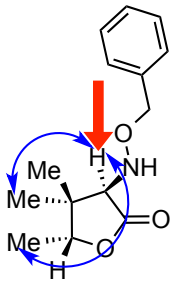

2.71 - Minor

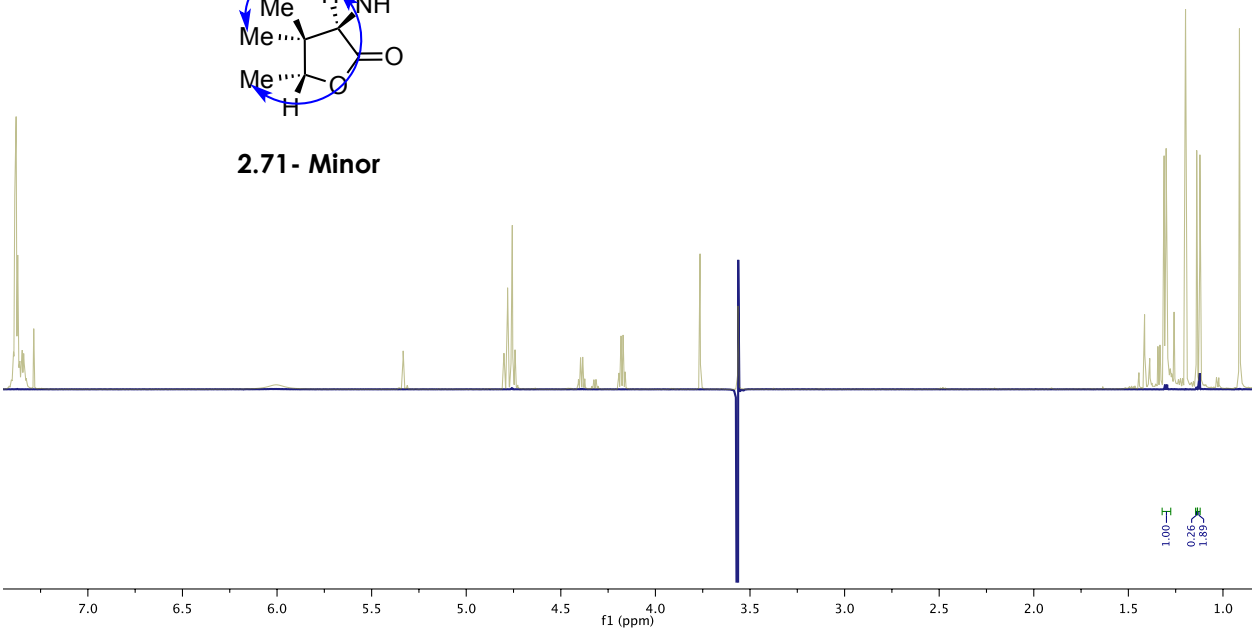

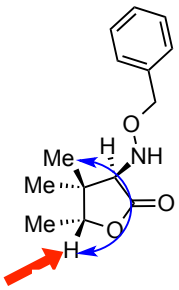

2.71 - Minor

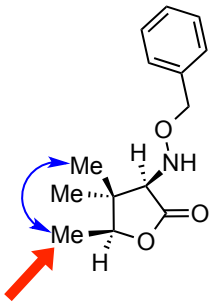

2.71- Major

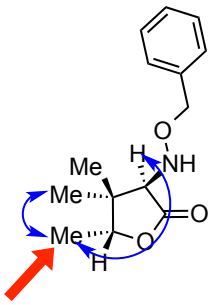

2.71- Minor

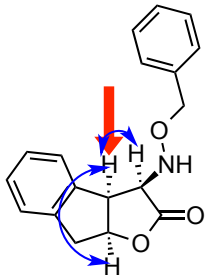

2.72- Major

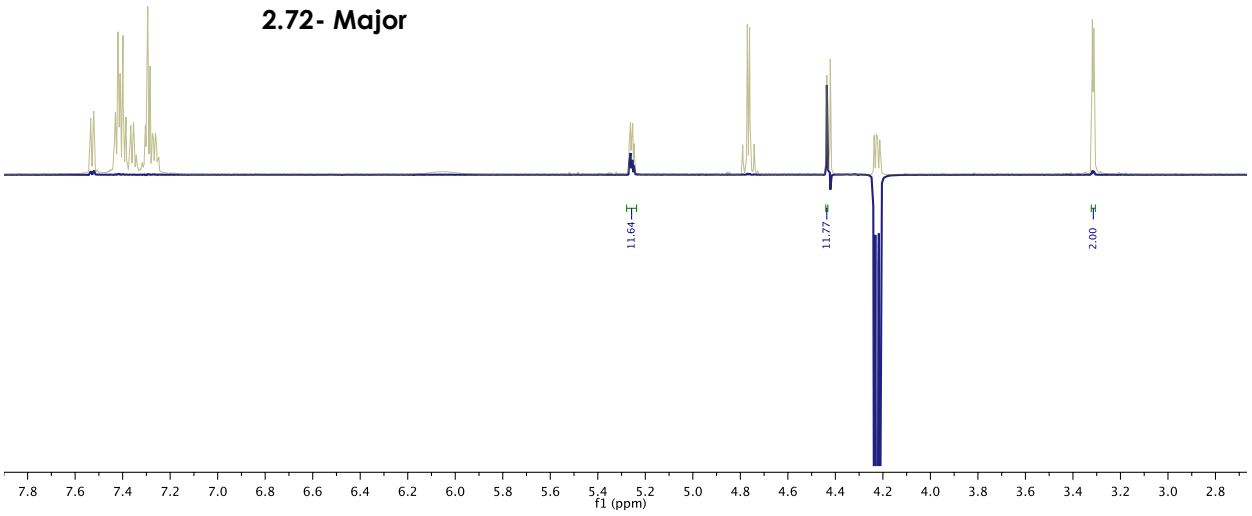

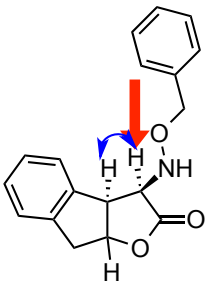

2.72- Major

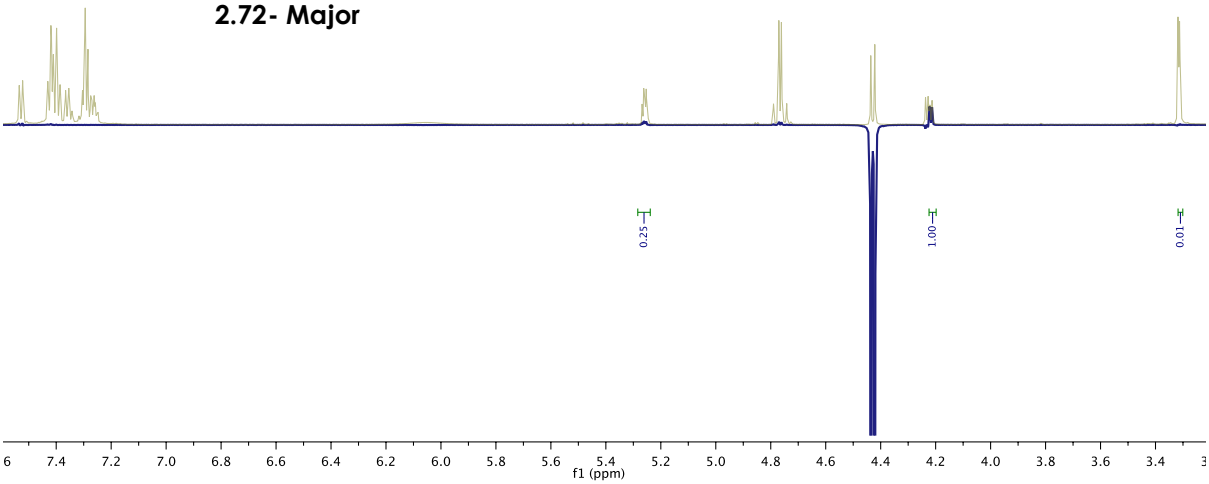

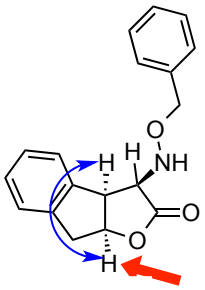

2.72- Major

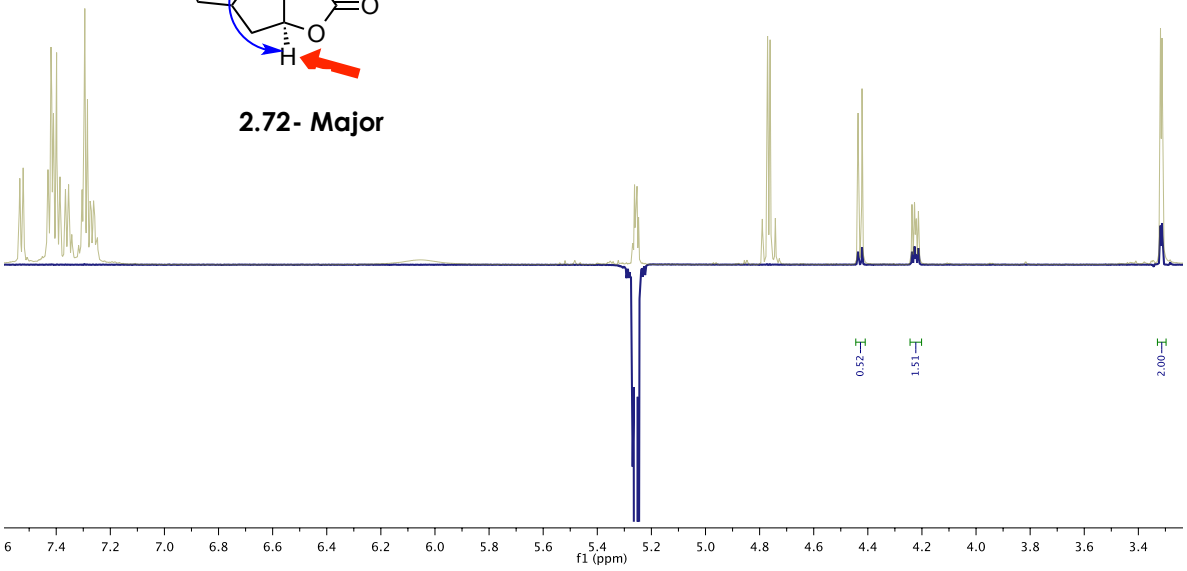

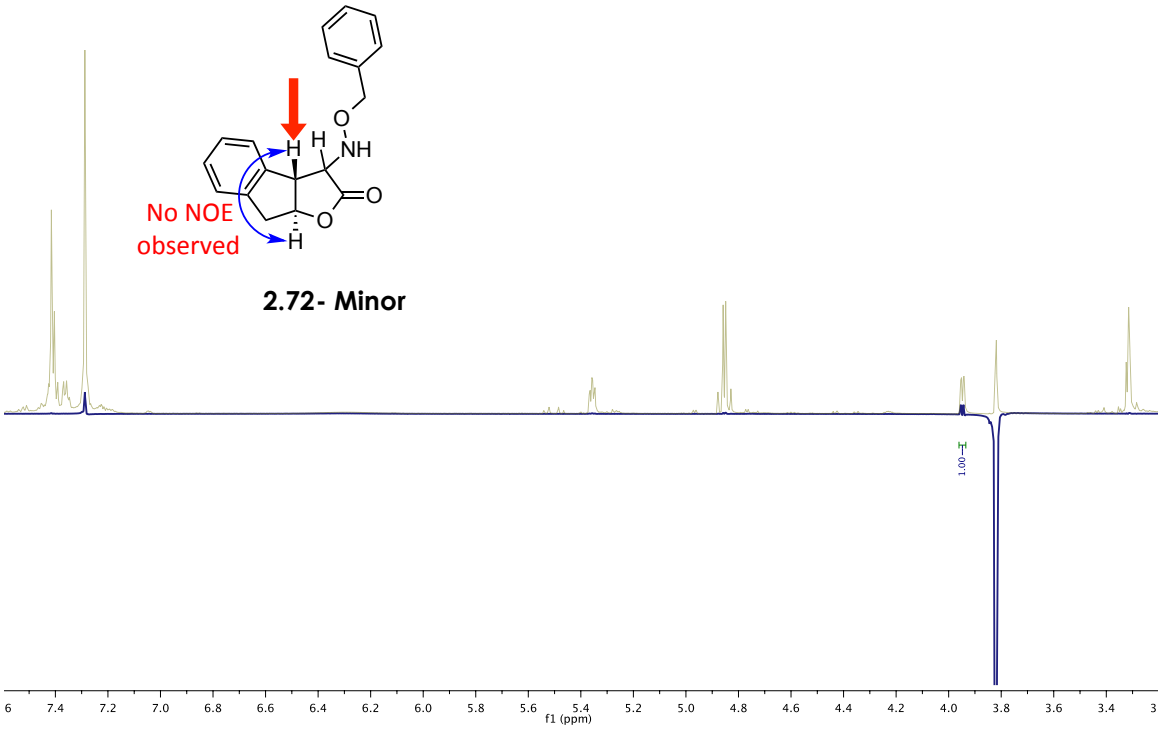
No NOE
observed
2.72- Minor
1.00
f1 (ppm)

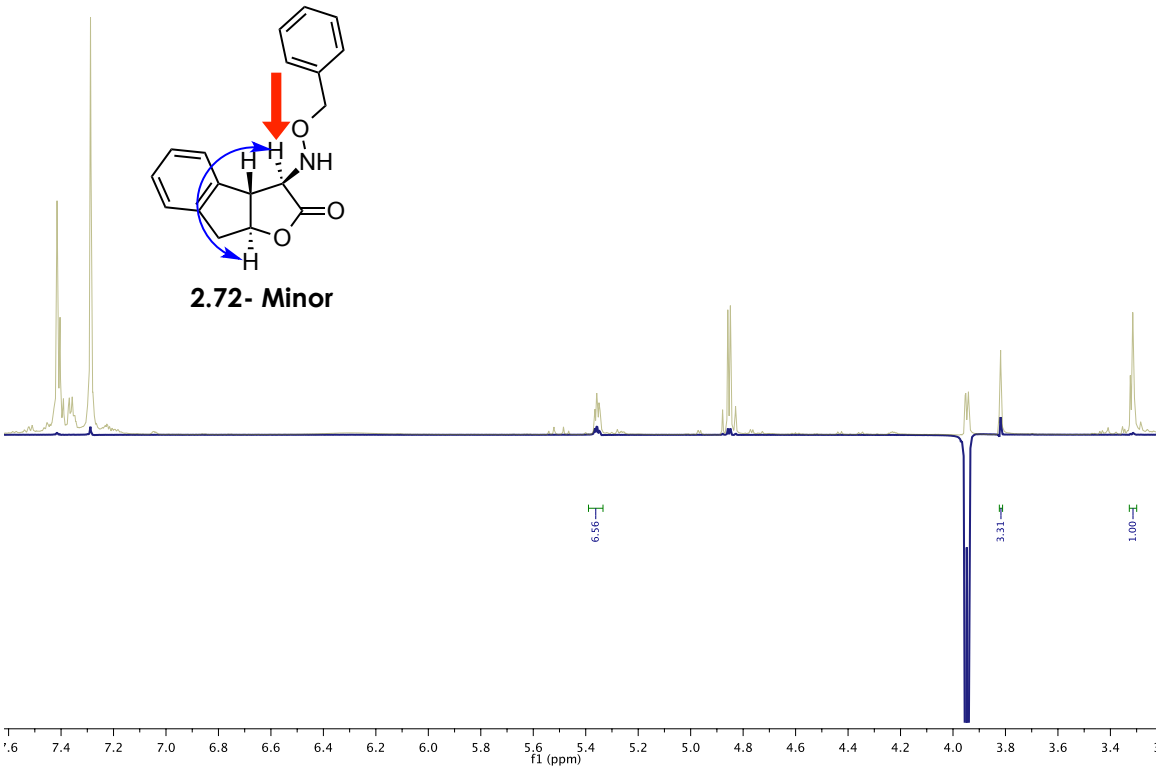
2.72- Minor
6.56
3.31
1.00
f1 (ppm)

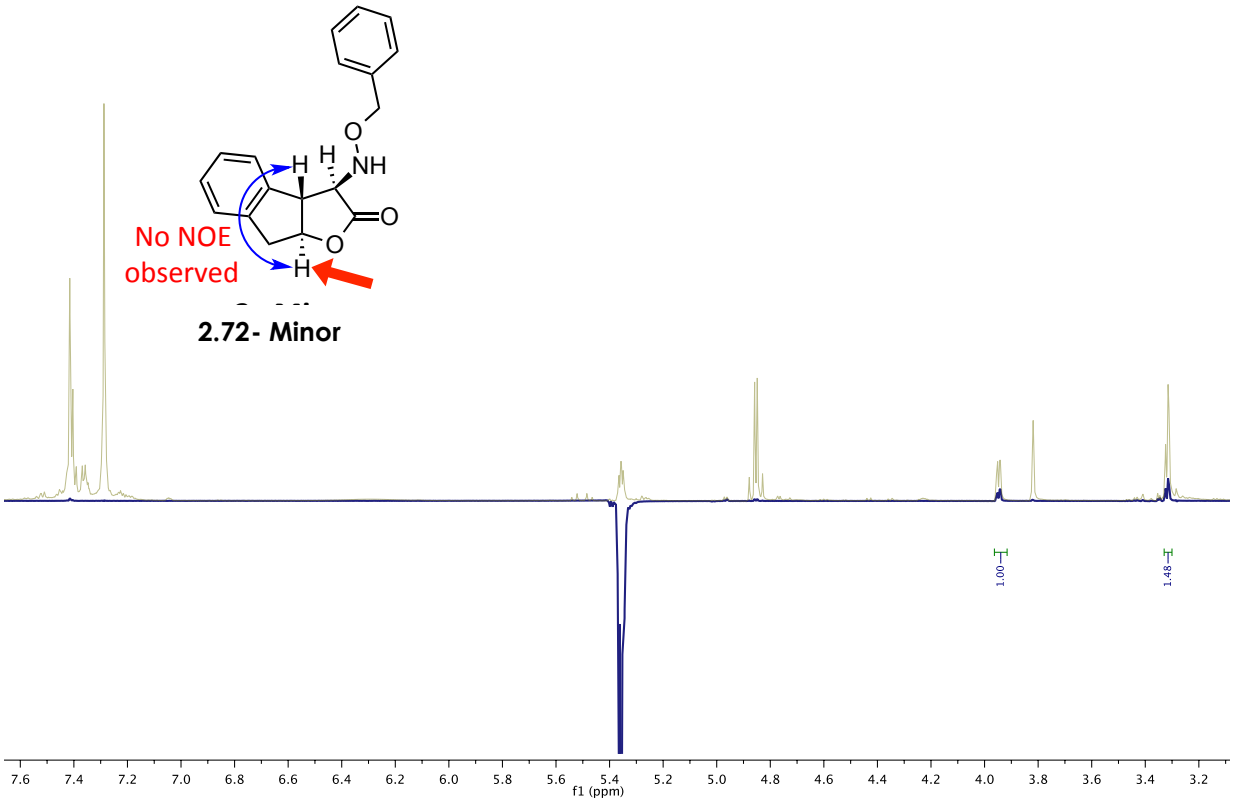
No NOE
observed
2.72- Minor
1.00
1.48
7.6 7.4 7.2 7.0 6.8 6.6 6.4 6.2 6.0 5.8 5.6 5.4 5.2 5.0 4.8 4.6 4.4 4.2 4.0 3.8 3.6 3.4 3.2
f1 (ppm)

REFERENCES

(1) Xie, X.; Stahl, S. S. *J. Am. Chem. Soc.* **2015**, *137* (11), 3767–3770.

(2) Ikan, R.; Weinstein, V.; Ravid, U. *Org. Prep. Proced. Int.* **1981**, *13*, 59–70.

(3) Fillman, J.; Albertson, N. *J. Am. Chem. Soc.* **1948**, *70*, 171–174.

(4) Ozinskas, A. J.; Rosenthal, G. A. *J. Org. Chem.* **1986**, *51*, 5047–5050.

(5) Ko, D.-H.; Kim, D. J.; Lyu, C. S.; Min, I. K.; Moon, H. *Tetrahedron Lett.* **1998**, *39*, 297–300.

(6) Venkataiah, M.; Reddipalli, G.; Jasti, L. S.; Fadnavis, N. W. *Tetrahedron Asymmetry* **2011**, *22*, 1855–1860.

(7) Ren, J.-L.; Zhang, X.-Y.; Yu, B.; Wang, X.-X.; Shao, K.-P.; Zhu, X.-G.; Liu, H.-M. *Eur. J. Med. Chem.* **2015**, *93*, 321–329.

(8) Mattmann, M. E.; Geske, G. D.; Worzalla, G. A.; Chandler, J. R.; Sappington, K. J.; Greenberg, E. P.; Blackwell, H. E. *Bioorg. Med. Chem. Lett.* **2008**, *18*, 3072–3075.

(9) Welch, M.; Dutton, J. M.; Glansdorp, F. G.; Thomas, G. L.; Smith, D. S.; Coulthurst, S. J.; Barnard, A. M. L.; Salmond, G. P. C.; Spring, D. R. *Bioorg. Med. Chem. Lett.* **2005**, *15*, 4235–4238.

(10) Lall, M. S.; Ramtohul, Y. K.; James, M. N. G.; Vederas, J. C. *J. Org. Chem.* **2002**, *67*, 1536–1547.

(11) Singh, S. P.; Michaelides, A.; Merrill, A. R.; Schwan, A. L. *J. Org. Chem.* **2011**, *76*, 6825–6831.

(12) Cooper, R. D. G.; Jose, F.; McShane, L.; Koppel, G. A. *Tetrahedron Lett.* **1978**, *19*, 2243–2246.

(13) Baldwin, J. E.; North, M.; Flinn, A. *Tetrahedron Lett.* **1987**, *28*, 3167–3168.

(14) Aslam, N. A.; Babu, S. A. *Tetrahedron* **2014**, *70*, 6402–6419.

(15) Simon, R. C.; Busto, E.; Schrittwieser, J. H.; Sattler, J. H.; Pietruszka, J.; Faber, K.; Kroutil, W. *Chem. Commun.* **2014**, *50*, 15669–15672.

(16) Ben-Ishai, D.; Moshenberg, R.; Altman, J. *Tetrahedron* **1977**, *33*, 1533–1542.

(17) Gasperi, T.; Loreto, M. A.; Tardella, P. A.; Veri, E. *Tetrahedron Lett.* **2003**, *44*, 4953–4956.

(18) Agami, C.; Couty, F.; Poursoulis, M. *Synlett* **1992**, *1992*, 847–848.

(19) Grandjean, J.-M. M.; Nicewicz, D. A. *Angew. Chem. Int. Ed.* **2013**, *52*, 3967–3971.

(20) Zeller, M. A.; Riener, M.; Nicewicz, D. A. *Org. Lett.* **2014**, *16*, 4810–4813.

(21) Nguyen, T. M.; Nicewicz, D. A. *J. Am. Chem. Soc.* **2013**, *135*, 9588–9591.

(22) Dénès, F.; Pichowicz, M.; Povie, G.; Renaud, P. T Chem. Rev., 2014, 114, 2587–2693

(23) Romero, N. A.; Nicewicz, D. A. *J. Am. Chem. Soc.* **2014**, *136*, 17024–17035.

(24) Gesmundo, N. J.; Grandjean, J.-M. M.; Nicewicz, D. A. *Org. Lett.* **2015**, *17*, 1316–1319.

(25) Clive, D. L. J.; Beaulieu, P. L. *J. Chem. Soc. Chem. Commun.* **1983**, 307–309.

(26) Clive, D. L. J.; Zhang, J. *Chem. Commun.* **1997**, 6, 549–550.

(27) Cavanaugh, C. L.; Nicewicz, D. A. Org. Lett., 2015, 17, 6082–6085.

(28) Torrente, S.; Alonso, R. *Org. Lett.* **2001**, *3*, 1985–1987.

(29) Roth, H. G.; Romero, N. A.; Nicewicz, D. A. *Synlett* **2016**, *27*, 714–723.

(30) Wilger, D. J.; Grandjean, J.-M. M.; Lammert, T. R.; Nicewicz, D. A. *Nat. Chem.* **2014**, *6*, 720–726.

(31) Al-Masum, M.; Alam, S. *Tetrahedron Lett.* **2009**, *50*, 5201–5204.

(32) Tomita, R.; Yasu, Y.; Koike, T.; Akita, M. *Angew. Chem. Int. Ed.* **2014**, *53*, 7144–7148.

(33) Kabalka, G. W.; Li, N.-S.; Tejedor, D.; Malladi, R. R.; Trotman, S. *J. Org. Chem.* **1999**, *64*, 3157–3161.

(34) Engler, T. A.; Combrink, K. D.; Ray, J. E. *J. Am. Chem. Soc.* **1988**, *110*, 7931–7933.

(35) Izawa, K.; Okuyama, T.; Fueno, T. *Bull. Chem. Soc. Jpn.* **1974**, *47*, 1480–1483.

(36) Cahiez, G.; Gager, O.; Lecomte, F. *Org. Lett.* **2008**, *10*, 5255–5256.

(37) Morimoto, T.; Hirano, M.; Echigoya, K.; Sato, T. *J. Chem. Soc. Perkin Trans.* **1986**, 2, 1205–1209.

(38) Byrne, P. A.; Rajendran, K. V.; Muldoon, J.; Gilheany, D. G. *Org. Biomol. Chem.* **2012**, *10*, 3531–3537.

(39) Yu, J.; Gaunt, M. J.; Spencer, J. B. *J. Org. Chem.* **2002**, *67*, 4627–4629.

(40) Lin, S.; Ischay, M. A.; Fry, C. G.; Yoon, T. P. *J. Am. Chem. Soc.* **2011**, *133*, 19350–19353.

(41) Herscheid, J. D. M.; Colstee, J. H.; Ottenheijm, H. C. J. *J. Org. Chem.* **1981**, *46*, 3346–3348.

CHAPTER THREE: REVERSING THE REGIOSELECTIVITY OF HALOFUNCTIONALIZATION REACTIONS THROUGH COOPERATIVE PHOTOREDOX AND COPPER CATALYSIS

3.1 Introduction

A 1,2-relationship between oxygen and halogen functionality has proven to be an invaluable feature in the synthesis of small, bioactive molecules and as a component in advanced synthetic routes. Whether existing in the halohydrin or halolactone form, this relationship is widely found in biologically active natural and unnatural products (Figure 3-1).

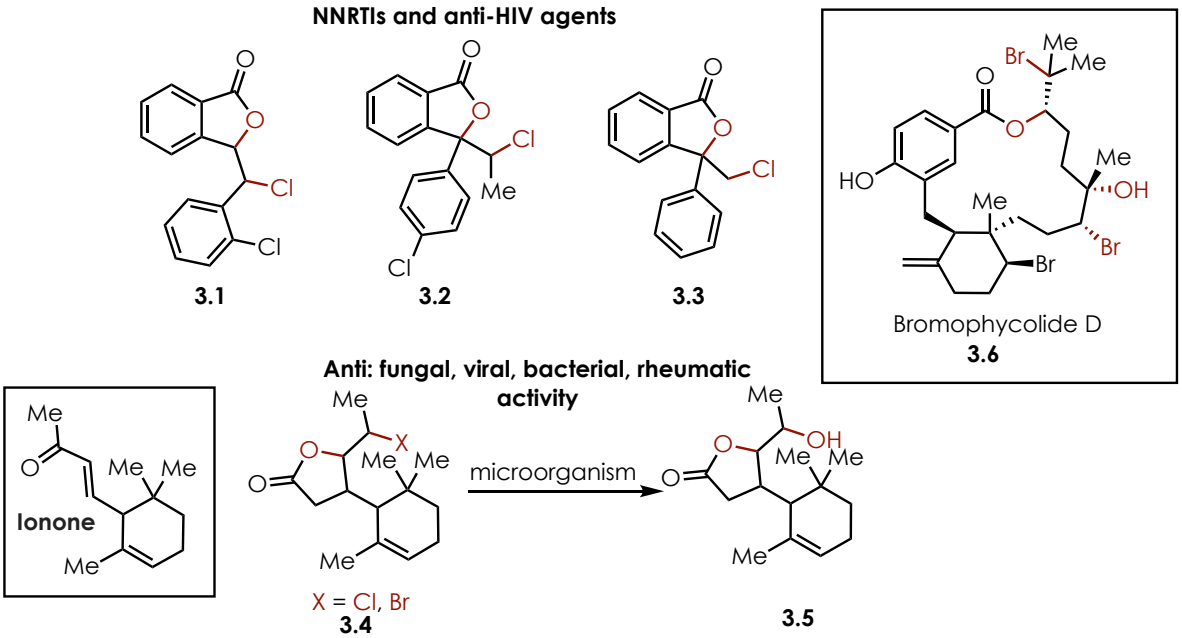

Figure 3-1. Biologically Active Natural and Unnatural Products Exhibiting a 1,2-Oxygen/Halogen Relationship

For example, halolactones 3.1-3.3 have been shown to express potent activity as non-nucleoside reverse transcriptase inhibitors (NNRTIs).[1] In order for HIV-1 to integrate its genetic information into its host's DNA, the reverse transcriptase (RT) enzyme must act to convert the virus' single-stranded viral RNA into the necessary double-stranded DNA form. Interrupting RT activity has proven to be an effective method for the treatment of HIV and consequently, NNRTI type drugs have been used in HIV combination therapy. As a result, the identification and synthesis of these inhibitors has been a key goal in the development of anti-HIV medication. In 2015, Zhou et al. reported this class of novel halolactone inhibitors and observed anti-HIV activity associated with them.

A common scaffold for the development of highly biologically active materials is the rose ketone, or ionone. It was been observed that analogues of this ketone are prevalent in nature, exhibiting a variety of biological properties in both plants and animals. Halolactones occur in molecules having cytotoxic, antifungal, antiviral, antibacterial, and anticancer activity. For example, chloro- and bromolactone derivatives 3.4 have been prepared by Anioł et al. in 2013 (Figure 3-1).[2] While potential bioactivity was recognized in the halolactone form, the value of these compounds was further demonstrated through the conversion to their hydroxylactone form (3.5). The latter class of lactones was studied for activity against bacteria, fungi, and yeast and was found to display activity against the growth of a variety of these microorganisms.

The natural product bromphycolide A (3.6) has both halolactone and halohydrin functionality that contribute to its interesting bioactivity. Since its initial isolation in 2015 from Fijian red algae (*Callophycus Serratus*), this macrolactone has been of interest due to its unique, molecular complexity as well as its antitumor and antimalarial activity. Additionally, bromphycolide derivatives have been shown to inhibit the growth of problematic bacterial strains such as MRSA

and VREF. Krauss and coworkers have presented a concise and impressive route to the asymmetric synthesis of the bromphycolide A and D skeleton, both displaying the highly valuable 1,2-relationship between oxygen and halogen functionality.[3]

Similarly, halohydrins are commonly incorporated into complex synthetic targets. Numerous syntheses have been directed toward the preparation of natural product exhibiting a 1,2-relationship between oxygen and chlorine/bromine atoms (Figure 3-2).[4] One of the most common arrangements in which this relationship exists is in the form of β-chloro/bromo cyclic ethers. This functionality has been observed in the core structure of a significant number of natural products (3.7-3.13), which have all been the target of impressive synthetic efforts.

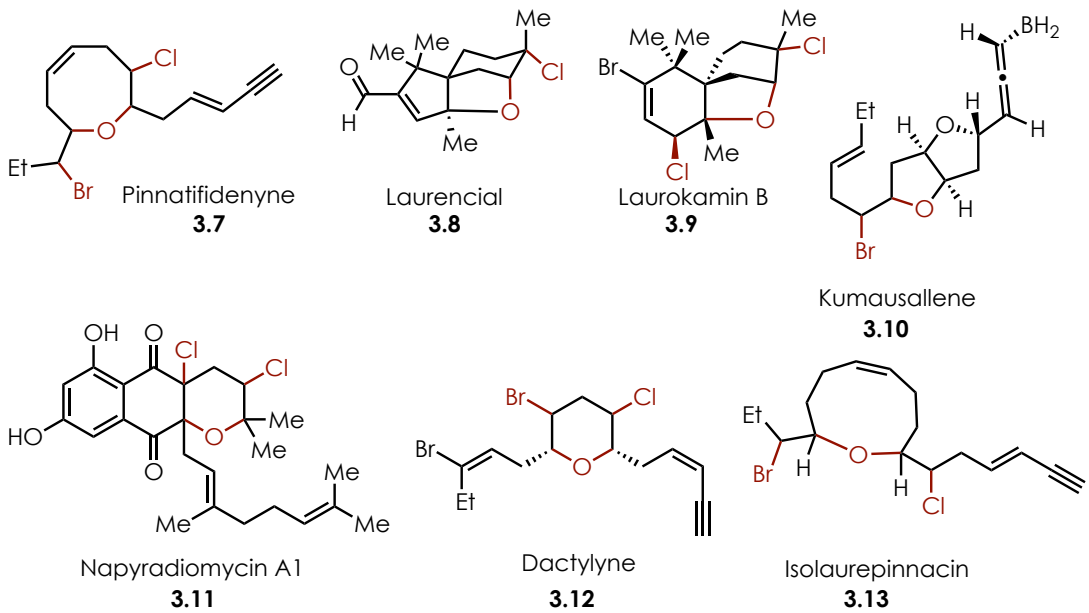

Figure 3-2. Biologically Active β-Halo-Cyclic Ethers

Accessing the desirable 1,2-oxygen-halogen relationship has long been a goal for organic chemists given their extensive presence in natural product structures and a diverse display of bioactivity. Given such interest, it is not surprising that halofunctionalization methods have been studied, developed, and applied extensively throughout the chemical literature.

3.2 Halofunctionalization of Alkenes

The halofunctionalization of alkenes is one of the oldest and most commonly employed reactions in the field of organic chemistry. In addition, it is also one of the introductory transformations has had a well-defined place within entry level textbooks since the 1930s.[5] The transformation is often introduced as a method of generating vicinal dihalides (Scheme 3-1).[6] Pi electrons of an olefin, acting as a nucleophile, are capable of attacking halogen molecules, including Br_2 and Cl_2, expelling a halide anion to form a positively charged, three-membered ring. The resulting halonium ion, possessing a halide atom with a complete octet, is particularly electrophilic given the positive charge and significant ring strain. Back-side, nucleophilic attack on the reactive species, by a halide anion, leads to efficient ring opening and stable, vicinal dihalide formation. By altering the nucleophilic, ring-opening reagent, it is possible to redirect the reactivity toward the formation of halohydrins rather than the dihalide adduct. The addition of a nucleophilic solvent, rather than using an inert solvent or neat reactions conditions, favors this alternative reaction pathway. Water efficiently opens halonium ions to generate chloro- or bromohydrins upon deprotonation.

Scheme 3-1. Halofunctionalization of Alkenes

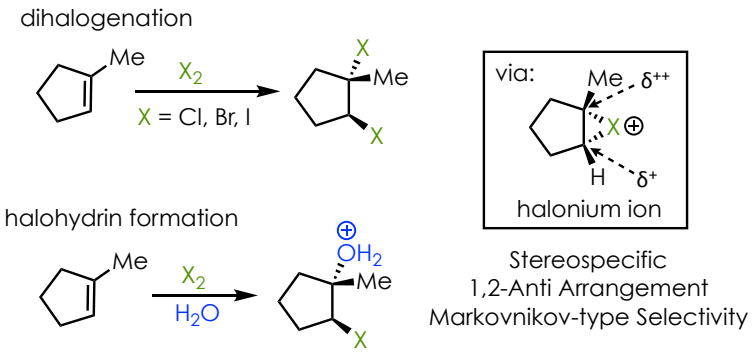

A significant advantage of this halofunctionalization method is the predictability of its reactivity. Due to halonium formation and the back-side nucleophilic addition, the overall reactions is a stereospecific anti addition. As a result, the diastereomer that forms exhibits a 1,2-*anti* arrangement between the electrophile and nucleophile. While the regioselectivity of ring opening is irrelevant in the case of dihalide generation, halohydrin product formation can be predicted using a modified version of Markovnikov's alkene addition rules. When asymmetric alkenes are used as halofunctionalization substrates, the resulting distorted, halonium exhibits a difference in partial positive charge between the more and less substituted carbons of the three-membered ring. Due to stabilizing effects, the more substituted carbon possesses a larger positive charge density and a weaker carbon-halogen bond than the less substituted carbon. The diastereo- and regioselective nature of this transformation makes it highly predictable and consequently a key asset in the organic chemistry toolbox for centuries.

Although useful, evidence suggests that the above analysis is overly simplistic. Recent work from Borhan et al. has demonstrated that olefins are often insufficient nucleophiles, reacting too slowly or not at all, for the purpose of alkene functionalization via halonium formation.[7,8] It has

been determined, in many cases, that the nucleophilic partner actually enhances the reactivity of the alkene through a form of electron donation known as nucleophile-assisted alkene activation (NAAN). Rather than relying on a general mechanism for halohydrin formation, Borhan suggests multiple mechanistic pathways, including a concerted process as well as stepwise routes that involve the formation of a distinct carbocation intermediate. In cases involving NAAN, electrophilic addition to the alkene is assisted by simultaneous nucleophilic attack, resulting in pre-polarization of the substrate (Scheme 3-2). The nucleophile's approach activates the olefin, through electron donation, allowing for more efficient attack on the electrophile rather than electronic repulsion, ultimately leading to increased reaction rates. However, evidence suggests that a classic mechanistic pathway dominates in systems with electron rich olefin substrates and sufficient halonium ion donor nucleofugality.

Scheme 3-2. Nucleophile-Assisted Alkene Activation in Olefin Halofunctionalization Reactions

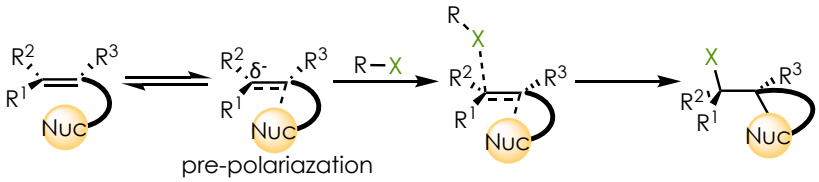

3.3 Synthesis of Halolactones

Over the past decades, several methods have been developed toward the synthesis of halolactones given the desirable 1,2-oxygen-halogen relationship and the biological activity they exhibit. Many groups have addressed the synthesis of these lactone products by developing catalytic, asymmetric lactonization methods, beginning from unsaturated acids. The first attempt to develop a reagent-controlled, asymmetric halolactonization was developed in 1992 (Scheme

3-3).[9] The method, utilizing stoichiometric quantities of a chiral titanium complex, was applied to the cyclization of a diallyl hydroxyacetic acid and an unsaturated diol affording the desired iodolactone products in a 67% and 65% ee, respectively.

Scheme 3-3. Enantioselective Iodolactonization Achieved Using a Chiral Titanium Complex

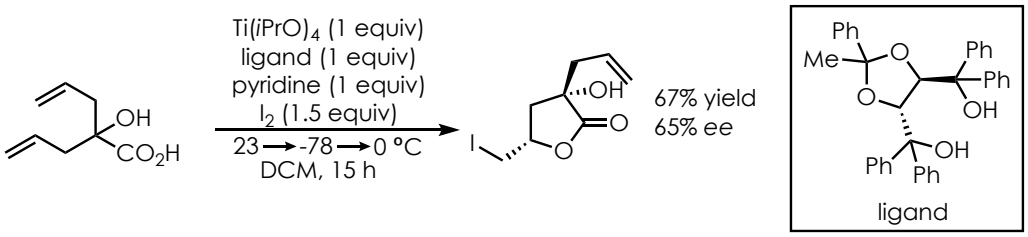

Inspired by this early work by Taguchi, the Borhan group, in 2010, sought to develop a organocatalytic, enantioselective method to generate chlorolactones from olefin substrates (Scheme 3-4).[10] By applying the chiral, hydroquinidine-derived catalyst $(DHQD)_2PHAL$, in the presence of DCDPH (1,3-dichloro-5,5-diphenylhydantoin), acting as a terminal chlorine source, the chlorolactonization of substituted 4-pentenoic acids was achieved. While other chlorinating agents were explored, including DCDMH (1,3-dichloro-5,5-dimethylhydantoin) and *N*-chlorosuccinimide. DCDPH was determined to be sufficiently reactive to allow for lower temperatures without being overly reactive, to the point where the nonselective, uncatalyzed, background reaction prevails.

Scheme 3-4. Enantioselective Chlorolactonization

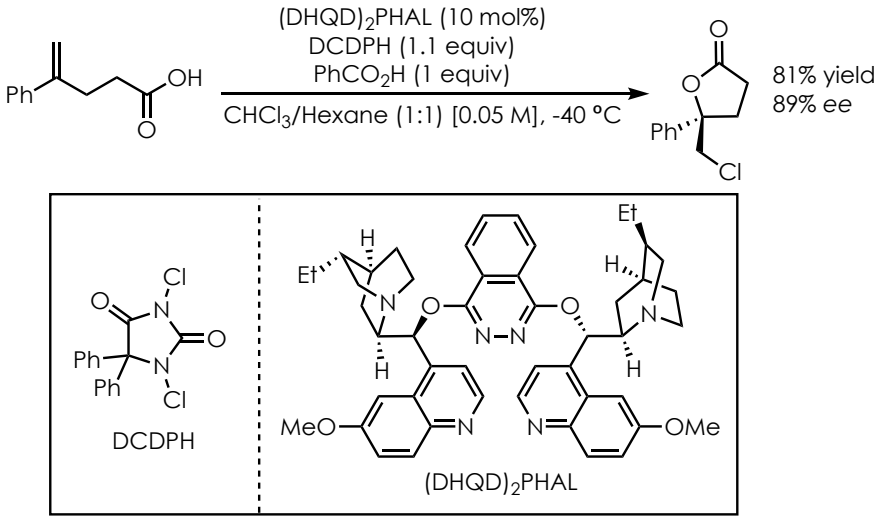

A catalyst–hydantoin complex was observed by ^{1}H NMR and was proposed as a key component in the asymmetric delivery of the halogen atom. Preliminary explorations of the system suggest that the interaction may exist in two possible forms, either as a hydrogen bond or ion pair mediated complex (Figure 3-3). Several chlorolactone products were produced in good yield with synthetically useful enantioselectivities.

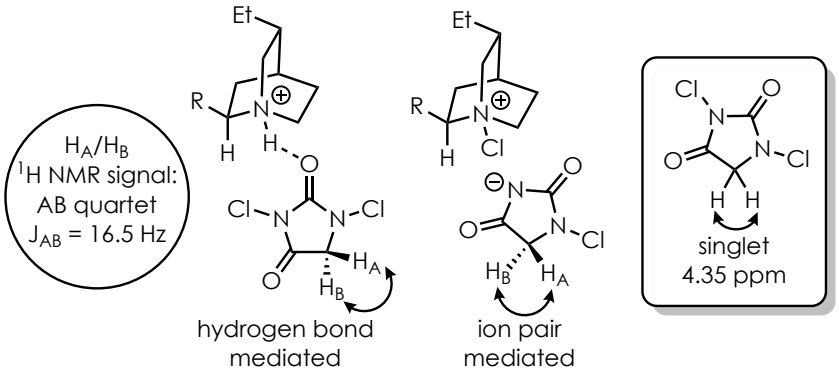

Figure 3-3. Proposed Catalyst–Hydantoin Complexes

In 2011, Yeung and coworkers developed an enantioselective synthesis of bromo-δ-lactones using a chiral amino-thiocarbamate catalyst and *N*-bromosuccinimide (NBS) as the bromine source (Scheme 3-5).[11] By applying this method to 1,2-disubstituted olefinic acids, it was possible to access δ-lactones moieties, rather than the typical γ-lactones that are obtained through the cyclization of 1,1-disubstituted unsaturated acids, as demonstrated in previous work.[12]

Scheme 3-5. Amino-Thiocarbamate Catalyzed Synthesis of Bromo-δ-Lactones

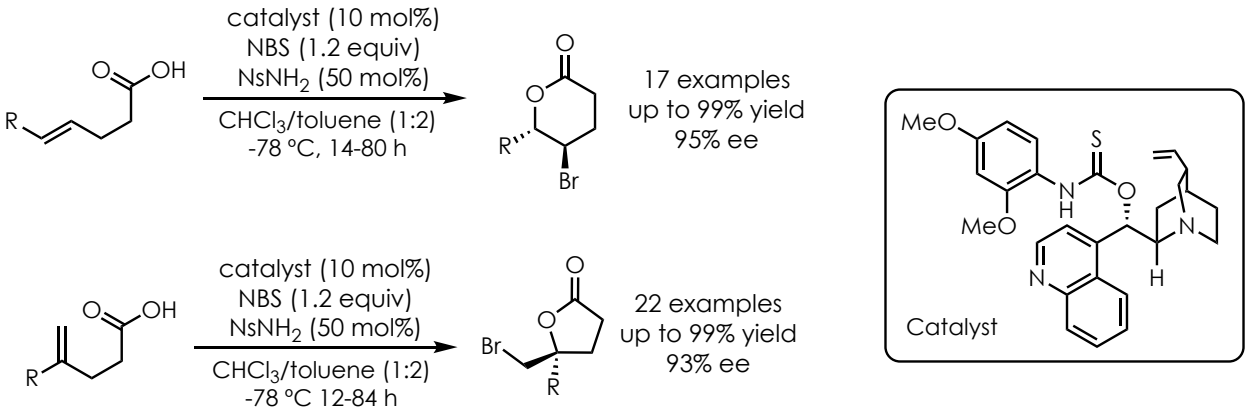

Optimized catalytic conditions led to the successful synthesis of over 15 bromolactones, favoring the 6-*endo*-cyclization pathway, in good enantioselectivity and yield (Figure 3-4). A stereochemical model was proposed to rationalize the formation of the major product enantiomer (Figure 3-5). In the favored pathway, bromine delivery occurs in a fashion that eliminates steric clashing with the backbone of the amino-thiocarbamate catalyst. The more sterically cumbersome approach exhibits several problematic interactions including those with the catalyst backbone and the *ortho*-methoxy substituent on the arene, which, when present, enhances the ee of the transformation by further destabilizing this approach. The authors do note a dependence on alkene geometry where the *Z*-isomer leads to lactone product formation in a lower yield and selectivity.

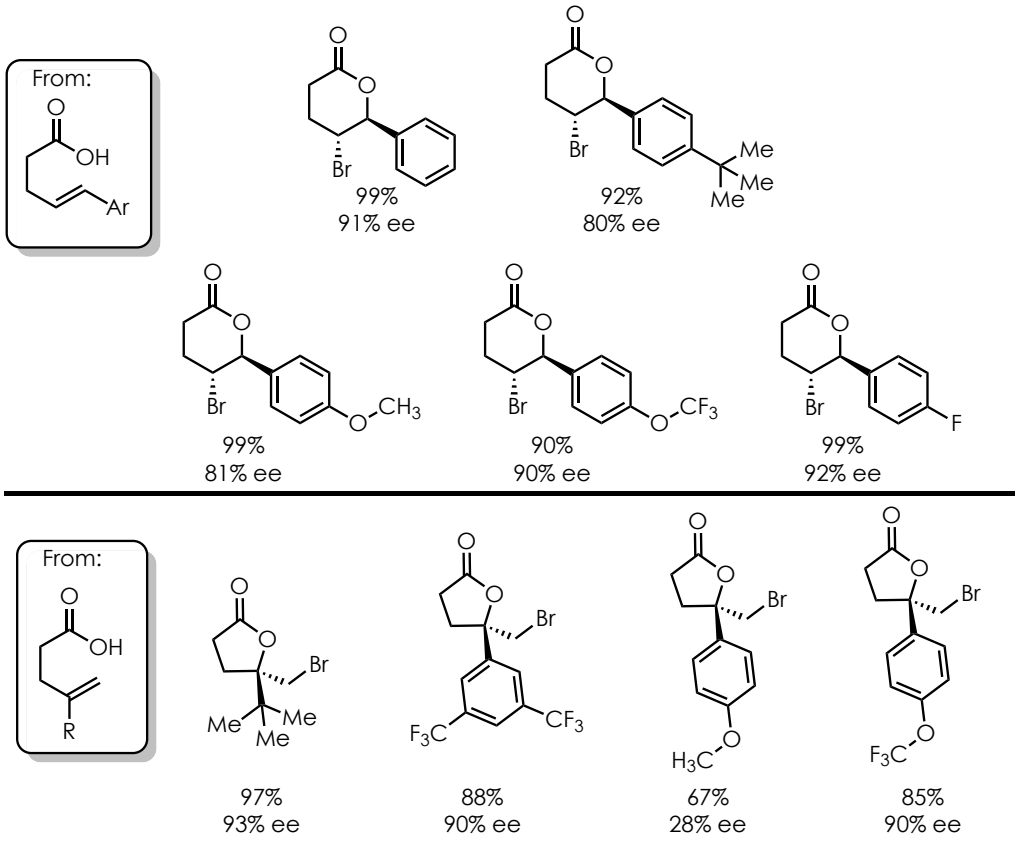

Figure 3-4. δ- and γ-Bromolactone Scope

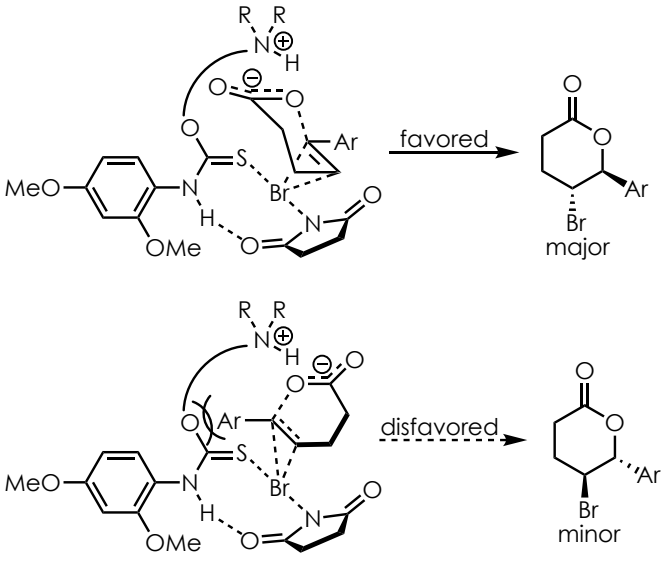

Figure 3-5. Stereochemical Model for Bromolactonization

The Johnston group also disclosed a method for the production of δ-lactones, this time using NIS as the halogen source.[13] This novel system relies on the relationship between a chiral Brønsted acid catalyst and an achiral counterion (Scheme 3-6). It has been proposed that the high enantioselectivity observed upon applying this system to the lactonization of substituted hexenoic acid derivatives is the result of acid activation of the iodine source and Brønsted base activation of the carboxylic acid substrate. Through a counterion screen, it was determined that more highly dissociative achiral counterions were critical in achieving high enantioselectivity as its identity may have a major effect on the catalyst's interaction with the substrate by influencing the size and shape of the binding pocket.

Scheme 3-6. Enantioselective Iodolatonization Achieved via Chiral Brønsted Acid Catalysis

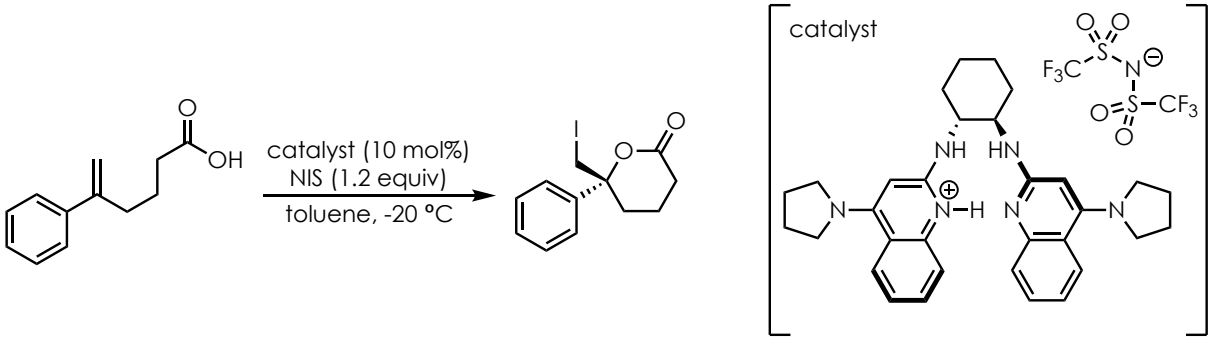

While iodolactonization methods have been thoroughly studied in the literature, chlorolactonization methods have been hard to come by, especially their enantioselective variants. Inspired by the work of Borhan[10] and motivated by a desire to overcome the limitations in the literature, Zhou et al. developed an efficient, asymmetric synthesis of chlorolactones.[14]

After developing a class of novel C_3-symmetric chiral cinchonine-squaramide (CSCS) organocatalysts,[15–18] Zhou hoped to apply their activity to the synthesis of valuable halolactones (Scheme 3-7). While the achiral lactone product could be achieved in good yield (95%) with the CSCS catalyst and DCDMH as a chlorine source, 4-nitrobenzenesulfonamide ($NsNH_2$) was necessary as a super-stoichiometric additive to access the product enantioselectively.

Scheme 3-7. Enatioselective Synthesis of Chlorolactones Using a Novel CSCS Organocatalyst

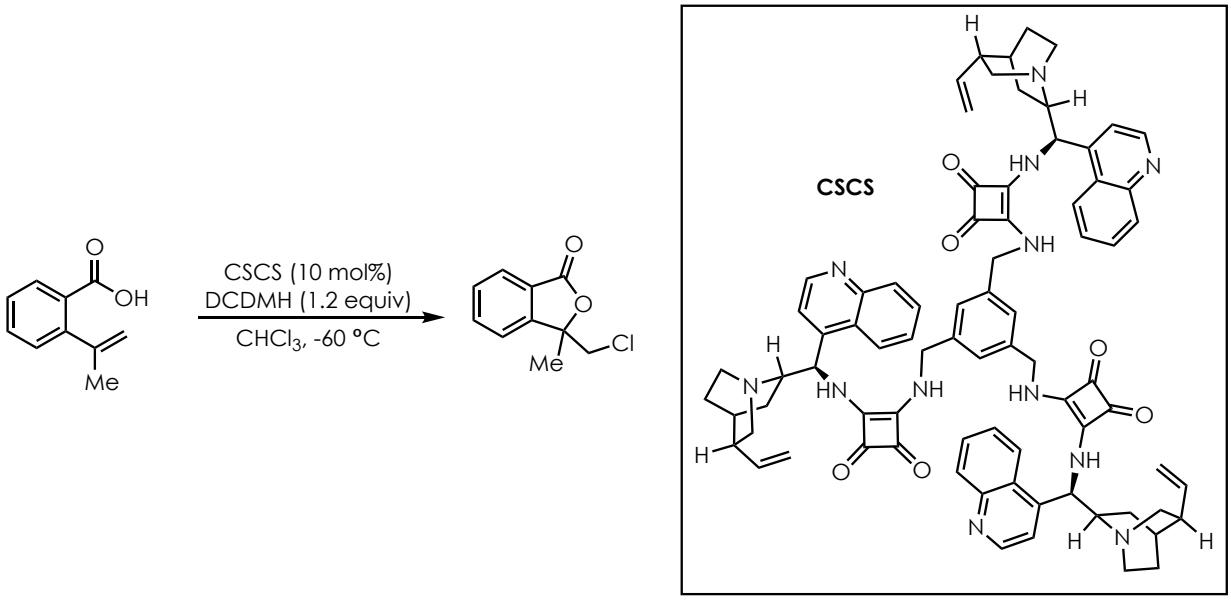

When exploring the scope of the transformation, it was observed that the substitution pattern of the substrate played a significant role in determining the regioselectivity of chloronium opening (Table 3-1). As expected, terminal alkenes gave the 5-*exo* products (Table 3-1, entries 1-3). When internal alkenes were utilized as substrates, the product distribution varied favoring the 6-*endo* cyclization pathway when electron withdrawing groups were present (Table 3-1, entries 4-6).

Table 3-1. Scope and Regioselectivity of CSCS Catalyzed Chlorolactonization

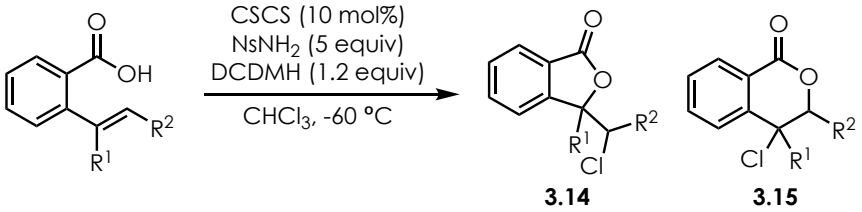

Entry	R^1	R^2	Yield (%)	3.14 : 3.15	ee (%)
1	Me	H	93	>99:1	83
2	H	H	95	99:1	67
3	Ph	H	92	99:1	57
4	4-BrC6H4	Me	92	1:3	99
5	4-FC6H4	Me	93	1:2	92
6	4-ClC6H4	Me	93	1:3	90

Additional studies were carried out to further demonstrate the value of this transformation. The CSCS class of squaramide catalysts was especially prized as it was observed that the species could be recovered and reused for six catalytic cycles without a significant erosion of yield or enantioselectivity (Table 3-2).

Table 3-2. Catalyst Recyclability

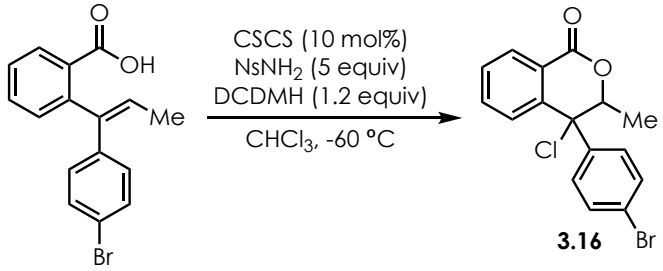

Cycle	Recovery (%)	Yield (%)	ee (%)
0	91	93	99
1	92	93	98
2	90	92	99
3	93	92	99
4	90	90	98
5	90	91	94

Two products obtained via this transformation were tested and found to be highly potent HIV-1 inhibitors (Figure 3-6).

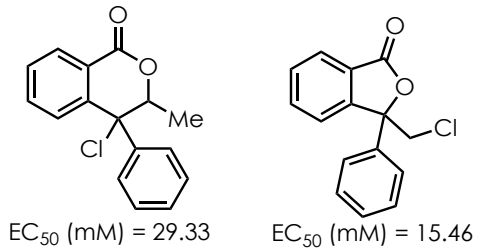

Figure 3-6. Demonstrated Potency Against HIV-1 in TZM-bl cells

Lastly, δ-lactone product 3.16 was further functionalized through an alkyne coupling to generate four enantiopure isochroman-1-ones possessing potential anti-bacterial and fungal activity (Scheme 3-8).

Scheme 3-8. Generation of Bioactive Products Through the Functionalization of Chlorolactone Products

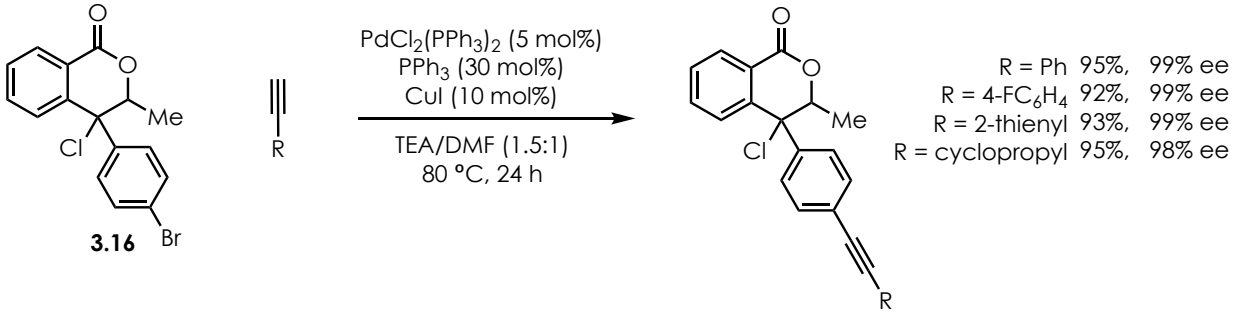

Given the apparent importance of halolactones as biologically-active, small molecules, their ability to be easily modified, and their versatility as organic building blocks,

halolactonizations have been considered to be highly valuable transformations. As a result, a significant amount of attention has been placed on developing methods of generating the halolactone scaffold. However, one major limitation of these current methods in the literature is the predetermined regioselectivity of the halonium opening/cyclization process, as governed by the substrate and the previously discussed, extended, Markovnikov rule. While this predictability can be an asset, we recognized the inherit significance in being able to reverse this classical selectivity when generating halolactones from unsaturated acid substrates.

3.4 Halofunctionalization Achieved Through Photoredox Catalysis

3.4.1 Background and Precedent

In seminal work by the Nicewicz lab from 2012, a novel, photoredox-mediated, anti-Markovnikov, hydroetherification method was applied to the cyclization of alkenol substrates.[19] Typically, the regioselectivity of electrophilic addition to alkenes is dictated by Markovnikov's rule. This longstanding rule, for olefin functionalization under acidic conditions, dates back to 1869 when Russian chemist Vladimir Markovnikov reported a defined regioselectivity for the addition of HBr to alkenes (Scheme 3-9). Upon protonation, the more stabilized cation intermediate forms, leading to nucleophilic attack by the bromide at this more substituted site resulting in the Markovnikov product. While this selectivity has be an undeniable advantage in synthesis, a significant amount of effort has been focused on the development of anti-Markovnikov, alkene functionalization methods to access products exhibiting the reverse selectivity. Though Hartwig[20,21] and Grubbs[22] have developed several methods for the anti-Markovnikov addition of amines and water to olefins, the methods rely on expensive transition metal catalysts and have only been successfully applied to the functionalization of terminal

styrene substrates. Methods developed by Gassman[23,24] and Arnold,[25] while impressive for their time, are limited in substrate scope, result in undesired side reactivity, and require large quantities of a single-electron photooxidant.

Scheme 3-9. Alkene Functionalization Demonstrating Markovnikov Selectivity

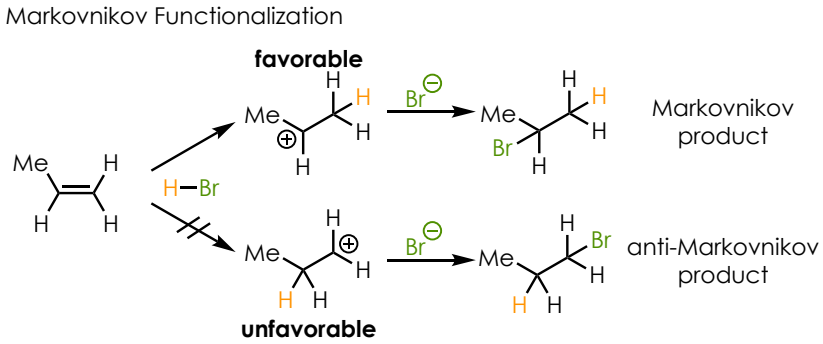

Seeking to overcome limitations in the literature and the precedent by Gassman and Arnold, our group developed a hydroetherification method utilizing the NMA photoredox catalyst to reverse the selectivity and favor anti-Markovnikov product formation. Hamilton and Nicewicz began by first determining favorable reaction conditions (Table 3-3). Alkenol 3.17 was used a model substrate to study reaction conditions, beginning with 5 mol% loading of NMA, in DCE, under irradiation by blue LEDs (450 nm) (Table 3-3, entry 1). To increase the yield from the initial hit of 36%, alternative photooxidants were then explored, including 9,10-dicyanoanthracene (Table 3-3, entry 2) and 1-cyanonaphthalene (Table 3-3, entry 3). Both led to diminished yields of the desired cyclic ether and increased byproduct formation. In order to render the transformation catalytic, the addition of a hydrogen atom donor cocatalyst was considered to complete the catalytic cycle. While screening potential cocatalysts, the BDE of each species was considered closely to ensure that HAT was an exothermic process. Those that

were screened possessed R-H BDE of <90 kcal/mol and included *N*-hydroxyphthalimide (BDE = 87 kcal/mol), 9-phenylfluorene (BDE = 74 kcal/mol), and 2-phenylmalononitrile (BDE = 77 kcal/mol) (Table 3-3, entries 4-5). While all three H-atom donors led to an increase in product formation, 2-phenylmalononitrile (PMN) proved to be the most efficient cocatalyst, regioselectively producing the ether, in 73% yield (Table 3-3, entry 6). Control reactions excluding photoredox catalyst (Table 3-3, entry 7) and light (Table 3-3, entry 8) demonstrated that both components were necessary to obtain the desirable reactivity. It was also determined that the commonly employed transition metal photooxidant $Ru(bpy)_3$ was incapable of oxidizing the alkene substrate and was ineffective at generating the expected product (Table 3-3, entry 9).

Table 3-3. Optimization of Photoredox Mediated Anti-Markovnikov Hydroetherification

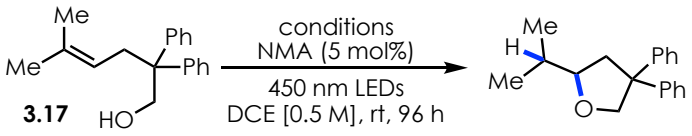

Entry	Conditions	Yield (%)
1	NMA (5 mol%)	36
2	9,10- dicyanoanthracene(20 mol%) light source: fluorescent bulbs >290 nm	5
3	1-cyanonaphthalene (50 mol%) light source: fluorescent bulbs >290 nm	15
4	*N*-hydroxyphthalimide (50 mol%)	41
5	9-phenylfluorene (50 mol%)	51
6	$PhCH(CN)_2$ (50 mol%)	73
7	No photooxidant	<5
8	No light	<5
9	$Ru(bpy)_3Cl_2$ (5 mol%)	<5

With the necessary reaction components identified, a mechanism was proposed for the transformation (Scheme 3-10). The catalytic cycle begins with the photoexcitation of NMA via blue LEDs to its excited state (NMA*). Irradiation and the resulting excited state catalyst allows

for single–electron oxidation of the unsaturated alcohol substrate (3.18) to occur, forming the reactive cation–radical species (3.19). This intermediate is then poised to undergo an intramolecular cyclization, exhibiting anti-Markovnikov regioselectivity, to generate 3.20. To furnish the final product, deprotonation and HAT steps must occur. Phenylmalononitrile (3.23), utilized in substoichiometric quantities, is capable of donating its hydrogen atom to the resulting trisubstituted radical species (3.21). This step affords the final product (3.22) and the corresponding phenylmalononitrile radical (3.24). To complete the cycle, the redox-active phenylmalononitrile radical then undergoes a single electron transfer with the acridine radical (NMA•) to turn over the photoredox catalyst and generated phenylmalononitrile anion (3.25). Protonation, via an equivalent of the substrate, regenerates the phenylmalononitrile that reenters the cycle to continue to function as a hydrogen atom donor.

Scheme 3-10. Proposed Mechanism For the Anti-Markovnikov Hydroetherification

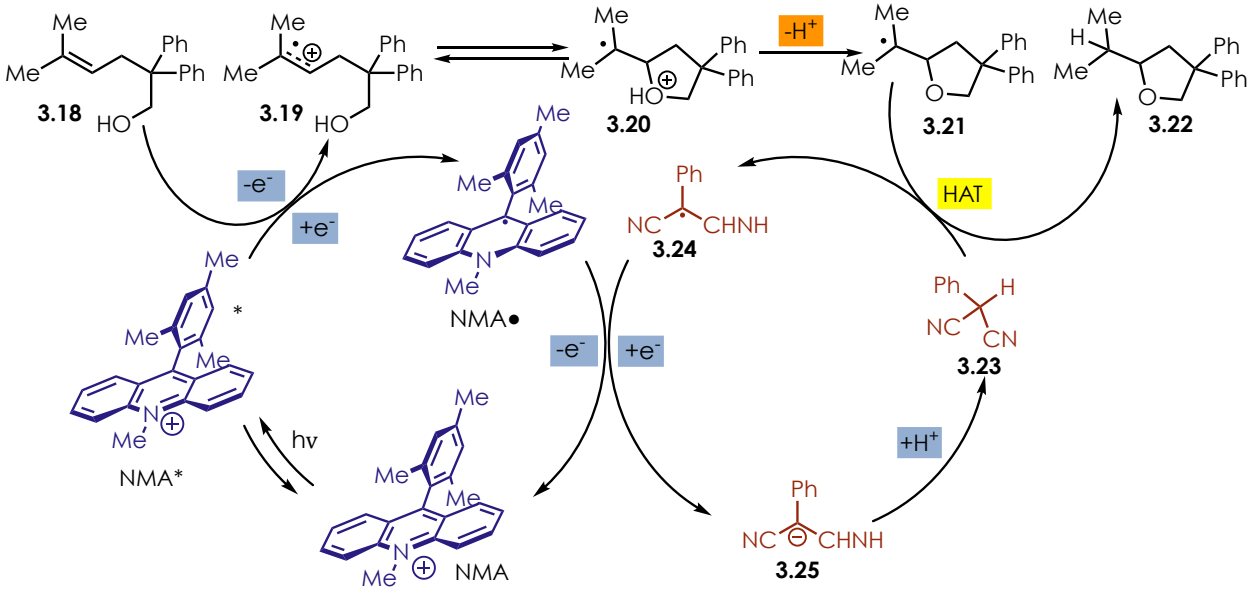

The alkenol scope of this photoredox-mediated hydroetherification method was explored to generate an electronically diverse substrate scope (Scheme 3-11). It was determined that more easily oxidized, electron-rich styrenes, results in the efficient generation of the hydroetherification product in 80% yield (3.26). The system was also tolerant of the more electron deficient 4-ClC_6H_4–substituted styrene, affording the corresponding product in 60% yield (3.27). While the desired 5-*exo* cyclization benefitted from gem-dialkyl substitution, it was not required as demonstrated by the highly selective formation of 3.28 from a substrate lacking the geminal dimethyl of diphenyl substitution pattern. Non-styreneyl, trisubstituted olefin substrates were also accessible through this methodology as alkenols 3.29 and 3.30 provided the ether product in good yield, with the latter exhibiting good diastereoselectivity as well. The mild nature of the transformation was highlighted with the successful cyclization of substrate 3.31, possessing a silyl-protected alcohol, which remains intact upon application of the reaction conditions.

Scheme 3-11. Substrate Scope for Photoredox Mediated Hydroetherification

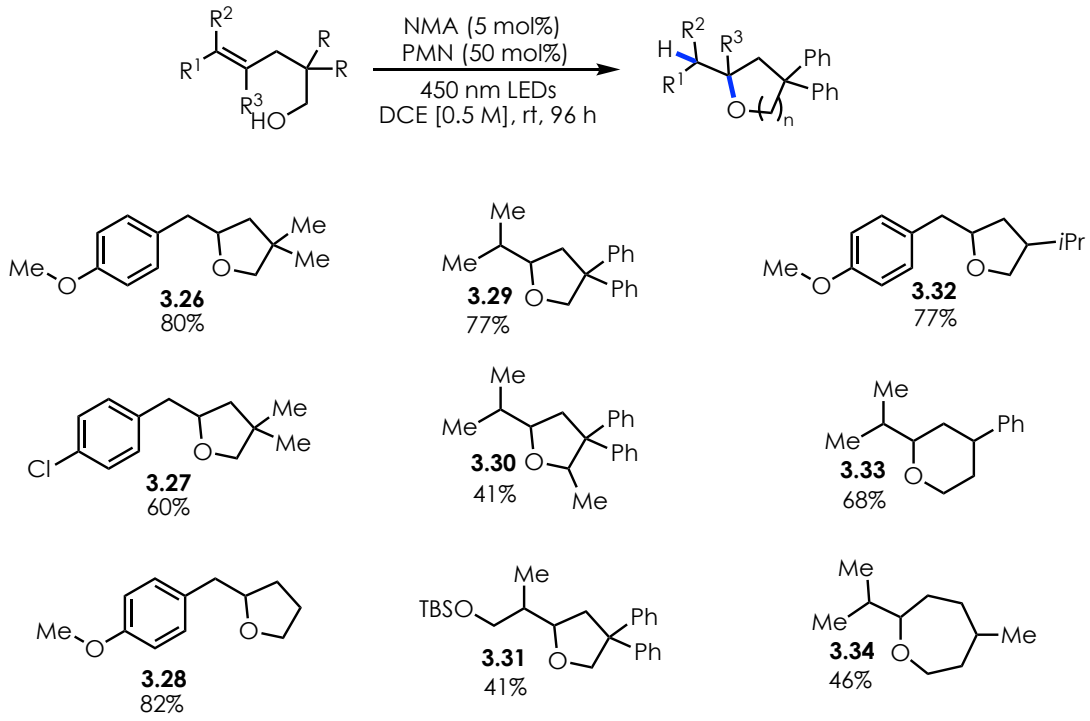

Because the regioselectivity of the transformation is dependent on the formation of the more stabilized carbon-centered radical upon cyclization, utilizing substrates with additional carbons between the alcohol and olefin functionality can alter the resulting ring size. This variation was modeled using substrates 3.32 through 3.34. Beginning with three carbons between the reactive functionality leads to 5-*exo* product formation (3.32). One and two additional carbons in the backbone allow for the 6- and 7-membered cyclic ethers to be generated, respectively, in good yield (3.33-3.34).

The efficiency of this regioselective transformation was further demonstrated through a set of comparative reactions (Scheme 3-12). Substrates 3.35 and 3.36 were allowed to react under

both Brønsted acid and photoredox-mediated conditions. Under acidic conditions, alkenol 3.35 forms the 6-*endo* Markovnikov product (3.37) while the photoredox methodology resulted in the formation of 5-membered cyclic ether 3.38. Substrate 3.36, while poised to undergo the kinetically favorable 5-*exo* cyclization, forms the 6-*endo* product in an impressive 77% yield when reacted under photoredox-mediated conditions (3.40). Alternatively, acidic conditions lead to the efficient formation of the Markovnikov product (3.39). This direct comparison between cyclization methods and product distribution excellently highlights the impressive selectivity of this novel transformation.

Scheme 3-12. Markovnikov vs. Anti-Markovnikov Regioselectivity of Hydroetherification Conditions

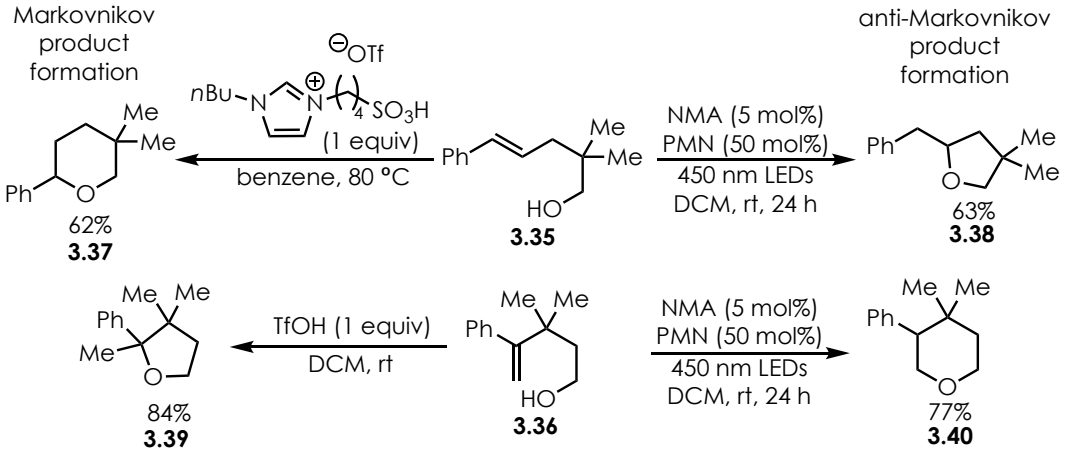

The identity of the oxygen-centered nucleophile was the final component of this transformation to be explored (Scheme 3-13). Beginning with anethole as a coupling partner, an intermolecular variant of the transformation was developed. The product was formed in an anti-Markovnikov fashion upon nucleophilic attack by methanol and the successive HAT step. Lastly,

an unsaturated acid was considered as a substrate to give completely regioselective access the anti-Markovnikov-type lactone adduct in a 72% yield.

Scheme 3-13. Intermolecular and Lactonization Variants of Hydrofunctionalization of Alkenes

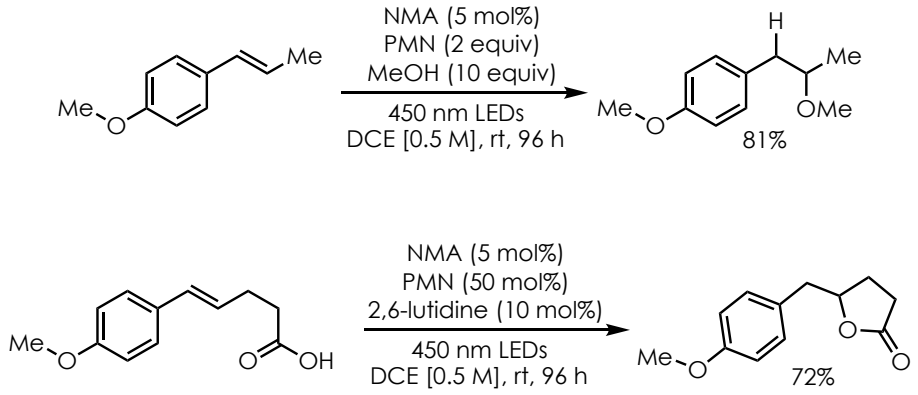

Overall, Hamilton and Nicewicz disclosed a method for the hydroetherification of alkenols substrates in a completely selective anti-Markovnikov fashion. A wide variety of substrates, with varying electronics, were cyclized to generate cyclic ether products in good to excellent yield. While this worked severed as an excellent model for the preparation oxygen heterocycles, including lactones, we wondered whether alternative radical traps, namely halogens, could be used to access desirable halolactone products.

3.4.2 Results and Discussion

The pervasive existence of halogens in organic molecules is impressive. As of 2016, it was reported that over 5,000 natural products containing at least one halogen atom have been discovered.[4] As a result methods for incorporating halogen functionality into molecules have been aggressively pursued. Having developed a wide variety of hydrofunctionalization methods

in our lab,[26–30] we decided to turn our attention towards the development of a photoredox-mediated, halofunctionalization system, which utilizes a halogen source as a radical trap rather than the previously explored hydrogen atom donor.

In a similar fashion to the previously reported hydrofunctionalization reactions, we hoped to develop a system, which is capable of outcompeting the Markovnikov-type regioselectivity exhibited by traditional halofunctionalization reactions (Scheme 3-14).[31] When we first set out to accomplish this goal, we recognized three potential pitfalls associated with generating halogenated products using photoredox catalysis:

1) In general, radical halogen sources are capable of reacting efficiently with olefins to directly form halonium ions. Consequently, the system requires that the catalytic pathway be much faster than this background reaction in order to outcompete it.
2) Halogen sources, with heteroatom-halogen bonds, are prone to homolysis. The potential to generate highly reactive, halogen-centered radicals could be problematic and lead to a variety of unwanted byproduct formation.
3) The halogenated products, obtained through this transformation, may be prone to further reactivity under the developed reaction conditions. This challenge is especially risky for cases in which the product possesses a benzylic halogen as they have been reported to undergo hydrolysis rapidly.

Scheme 3-14. Reversing Classical Regioselectivity of Alkene Halofunctionalization Reactions

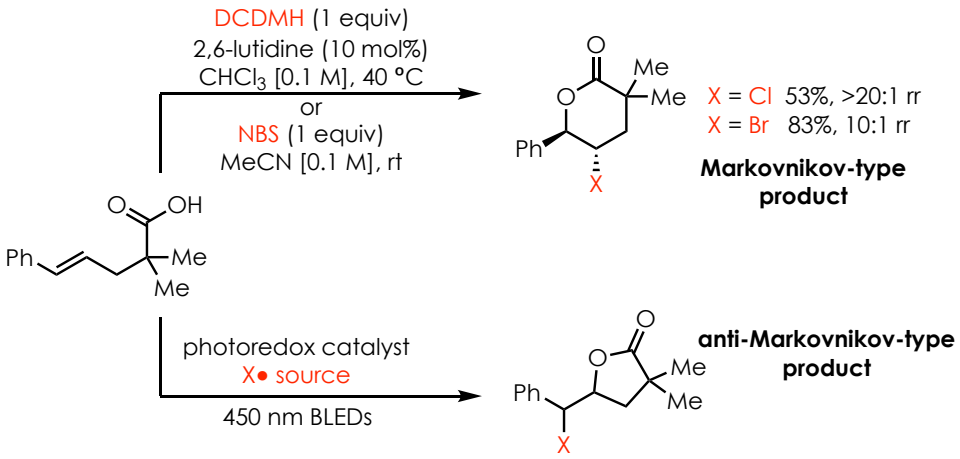

With these potential drawbacks in mind, we first began to develop a chlorolactonization system. Hamilton and Nicewicz's lactonization result served as inspiration for the initial application of this method. Optimization of these conditions, accomplished by Jeremy Griffin, started with the evaluation of several traditional chlorine radical sources, in combination with the NMA photoredox catalyst, to determine whether the simple addition of a halogen radical source would be sufficient to obtain the halofunctionalized product (Table 3-4). Tosyl chloride (TsCl) was first applied to the cyclization of aliphatic-substituted alkene-acid substrates and did, in fact, lead to the formation of the desired product though these conditions could not be successfully extended to the styrenyl-acid, model substrate (3.41) (Table 3-4, entry 1). Switching to other typical radical halogen sources, such as *N*-chlorosuccinimide (NCS) and *N*-chlorophthalimide (NCP), proved fruitless in generating the desired γ-lactone (3.42) but rather gave only small quantities of the undesired δ-lactone (3.43) regioisomer (Table 3-4, entries 2-3). Given the lack of desired product formation, this initial investigation illustrated inefficiencies in the halogen

transfer step of the current reaction conditions. At this point, it was determined that an additive would likely be required to aid in halogen radical transfer.

Table 3-4. Optimization of Chlorolactonization Conditions

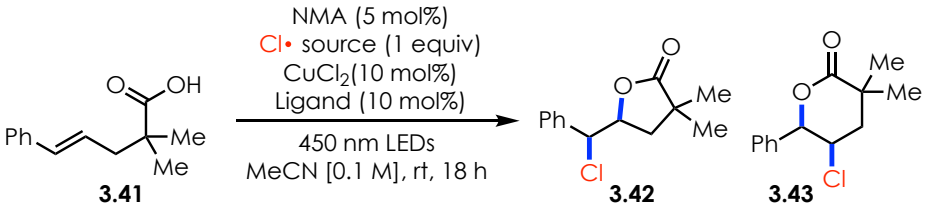

Entry	Cl Source	$CuCl_2$/Ligand	A (%)[a]	dr (A)	B (%)[a]
1	TsCl	---	---	---	---
2	NCS	---	---	---	50
3	NCP	---	---	---	30
4[b]	---	$CuCl_2$/bpy	62	1.5:1	---
5[c]	Lut^+Cl^-	$CuCl_2$/bpy	19	2.6:1	---
6	NCP	$CuCl_2$/bpy	90	2.3:1	---
7	NCP	CuCl/bpy	92	2.4:1	--
8	NCP	$CuCl_2$/phen	85	3.2:1	---
9[d]	NCP	$CuCl_2$/phen	25	2.2:1	12
10[e]	NCP	---	---	---	---
11[d]	NCP	---	---	---	---

Reactions were carried out in N_2-sparged MeCN [0.1m] under two LED lamps (l_{max}=450 nm) for 18 h. [a] Yield as determined by ^1H NMR spectroscopic analysis of the crude reaction mixture relative to the internal standard $(Me_3Si)_2O$. [b] The reaction was carried out with 1 equivalent of $CuCl_2$/bpy under air. [c] The reaction was carried out with $CuCl_2$/bpy (20 mol%) in the presence of O_2. [d] The reaction was carried out without NMA. [e] Reaction ran in dark

An exploration of the literature suggested that a copper (I) cocatalyst may be necessary in the system, to facilitate chlorine radical transfer, based on its reported efficiency in atom transfer radical polymerization (ATRP) (Scheme 3-15).[32] To achieve controlled polymerization conditions, it is necessary to regulate every component of several elementary reactions including the concentration and reactivity of each species involved. Consequently, halogen radical concentrations must be controlled and their transfer must only occur upon initiation of an

activation process. In this system, bromine-capped polymer (P_n-Br) and Cu(I)(bpy)$_2$ are the dominant structural forms and the equilibrium heavily favors a low radical concentration (k_{-1} ~10^7 $M^{-1}s^{-1}$). Due to its affinity for halogens, this copper (I) species is capable of abstracting the halogen atom, generating a radical polymer species (P_n•), which is able to react further with an equivalent of monomer (P_m), leading to the uniform elongation of the polymer chain (P_n-P_m). A second halogen transfer event, by the copper (II) species, leads to the regeneration of the copper (I) complex. This efficiency at abstracting and transferring halogen radicals led us to believe that a copper (I)/2,2'-bipyridine catalyst system could be effectively applied to our existing reaction conditions to support the problematic radical transfer step. Additionally, we were encouraged by evidence in the literature which suggests that copper(II) chloride is capable of undergoing irreversible chlorine-radical transfer with aryl cation radicals.[33]

Scheme 3-15. Copper Mediated Atom Transfer Radical Polymerization

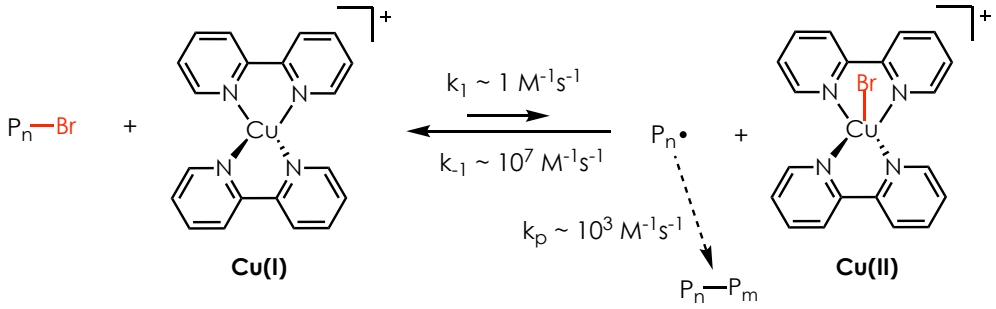

When $CuCl_2$ was simply added in combination with NMA in MeCN, upon irradiation, a small quantity of the desired product was obtained with O_2 acting as a terminal oxidant. With the

simple addition of 2,2'-bipyridine, as a copper ligand, the product could be obtained in a 62% yield (Table 3-4, entry 4). While pleased with this result, we were concerned about the use of stoichiometric copper and hoped to reduce its loading to catalytic quantities through the addition of a secondary chlorine source. Lutidinium chloride (Lut^+Cl^-) was first considered as chlorine source though this returned the product in only a limited quantity (19%) and resulted in significant byproduct formation (Table 3-4, entry 5). A significant increase in reaction efficiency was achieved with the addition of NCP in combination with just 10 mol% $CuCl_2$. The desired lactone was obtained, regioselectivity, in a 90% yield, with a dr of 2.3:1 (Table 3-4, entry 6). As a mechanistic probe, the CuCl/bpy complex was also tested under these conditions and provided the product in a comparable yield (Table 3-4, entry 7). This result suggests that the chlorinating agent, NCP, may be responsible for generating $CuCl_2$ in situ. Switching the bpy ligand out for 1,10-phenanthroline (phen) caused a minor drop in yield to 85% but displayed the added benefit of reducing the reaction time from 18 to just 2 hours and led to a boost in diastereoselectivity (3.2:1) (Table 3-4, entry 8).

As a control experiment, the reaction was run without the addition of NMA (Table 3-4, entry 9). After 18 hours of irradiation, under these reaction conditions, both regioisomers did form in a combined yield of 37%. However, it is important to note that when the reaction was stopped after 2 hours (reflective of the final conditions used in scope development), only unreacted starting material was observed. Running the reaction in the presence of NMA without irradiation results in returned starting material (Table 3-4, entry 10). When both the acridinium and copper catalysts were omitted, no reaction occurred (Table 3-4, entry 11).

The observed formation of undesired δ-lactone 3.43 with NMA and no copper (Table 3-4, entry 9) in combination with the lack of this product formation when NMA and copper were both

omitted (Table 3-4, entry 11) warrants a further explanation. We hypothesized that this background reactivity, in the presence of irradiated NMA, is the result of the in situ generation of a strong acid that is capable of activating the chlorine source, and leads to the observed formation of 3.43. We proposed that the strong acid (3.44) forms as a result of nucleophilic attack by the acid on the cation radical intermediate (Scheme 3-16). A second equivalent of the substrate is then able to undergo the background reaction to form an additional equivalent of strong acid (3.45), which can go on to propagate the reaction.

Scheme 3-16. Proposed Mechanism for In Situ Strong Acid Formation

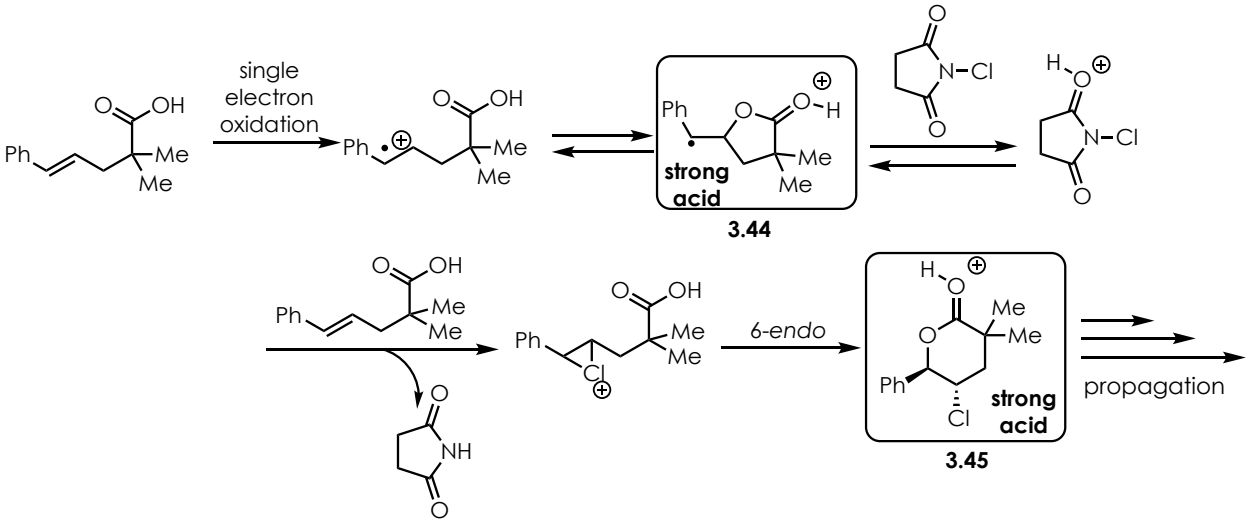

To test the likelihood of this proposed mechanism, the reaction was conducted without irradiation and NMA but in the presence of NCS and a catalytic quantity of acid. Initially, 5 mol% of trifluoroacetic acid (TFA, pKa = -0.25) was added to the reaction though no product

was obtained. When a significantly stronger acid was employed, i.e. triflic acid (CF_3SO_3H, pKa = -14), 66% of the undesired lactone was obtained (Scheme 3-17). From these results we concluded that the strong acid that forms in the presence of NMA and under irradiative conditions could be responsible for producing a more electrophilic chlorinating agent, existing in the form of either protonated NCS or Cl_2.

Scheme 3-17. Background Reactivity Initiated by Strong Acid Formation

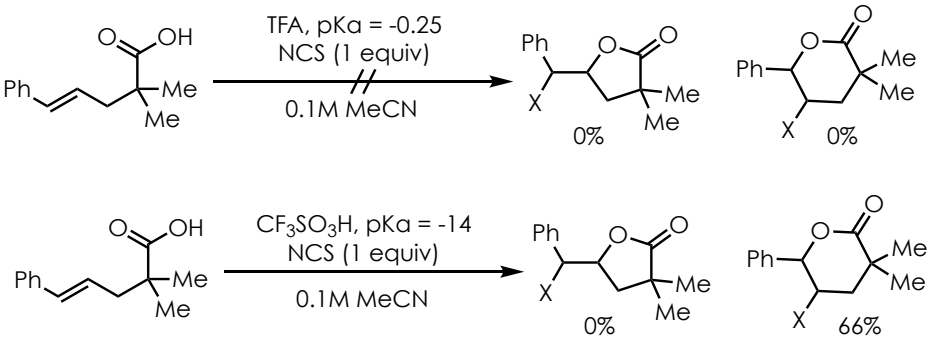

Concurrently, conditions were developed for the complementary bromolactonization system (Table 3-5). The development of chlorolactonization conditions provided a solid starting point for the development of bromination methodology though the conditions were not found to be directly transferable. Initially TsBr was found to be highly ineffective, leading to a 1:1 product regioisomer distribution (3.46:3.47) (Table 3-5, entry 1). While NCS and NCP were found to be competent halogen sources in the dual catalytic system, their bromine counterparts, NBS and NBP, were less efficient (Table 3-5, entries 2-4). Excellent mass balance was achieved, but while the desired 5-*exo*-type products were observed, the major product, in both cases, was the δ-lactone isomer.

Table 3-5. Optimization of Bromolactonization Conditions

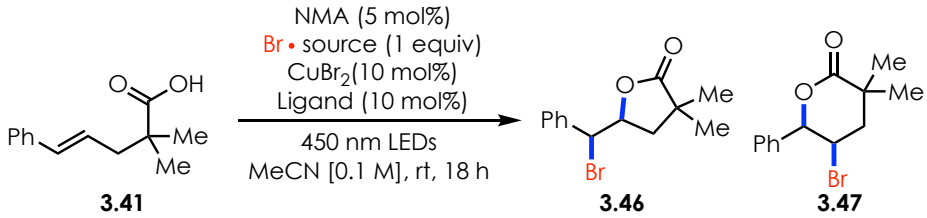

Entry	Br Source	$CuBr_2$/Ligand	3.46[a]	dr (3.46)	3.47[a]
1	TsBr	$CuBr_2$/bpy	1	n.d.	1
2	NBS	$CuBr_2$/bpy	1	>20:1	2.5
3	NBS	$CuBr_2$/phen	1	1.0:1	1.8
4	NBP	$CuBr_2$/bpy	39%	3.0:1	61%
5	DEBM	CuBr/bpy	79%	2.0:1	6%
6	DEBM	$CuBr_2$/phen	94%	2.0:1	6%
7	DEBM	$CuBr_2$/bpy	97%	2.4:1	3%
8[b]	DEBM	---	---	---	---
9	DEBM	$CuBr_2$/bpy	---	---	---
10	DEBM	---	---	---	---
11[c]	---	$CuBr_2$/bpy	35%	1.0:1	15%

Reactions were carried out in N_2-sparged MeCN [0.1m] under two LED lamps (l_{max}=450 nm) for 18 h. [a] Yield as determined by ^1H NMR spectroscopic analysis of the crude reaction mixture relative to the internal standard $(Me_3Si)_2O$.[b] The reaction was carried out without NMA. [c] Ran with 1 equiv $CuBr_2$/bpy

A literature search provided insight as to a potential alternative to the typical nitrogen-based bromine sources, as those proved to be too electrophilic to achieve strict regiocontrol. In their exploration of a triethylborane-induced bromine atom-transfer radical addition, Oshima et al. compiled a list of effective bromine radical sources. Diethyl bromomalonate (DEBM) was determined to be one of the most efficient bromine traps for carbon-centered radicals (Scheme 3-18).[34]

Scheme 3-18. Diethyl Bromomalonate as a Bromine Radical Source in Atom-Transfer Radical Addition Reactions

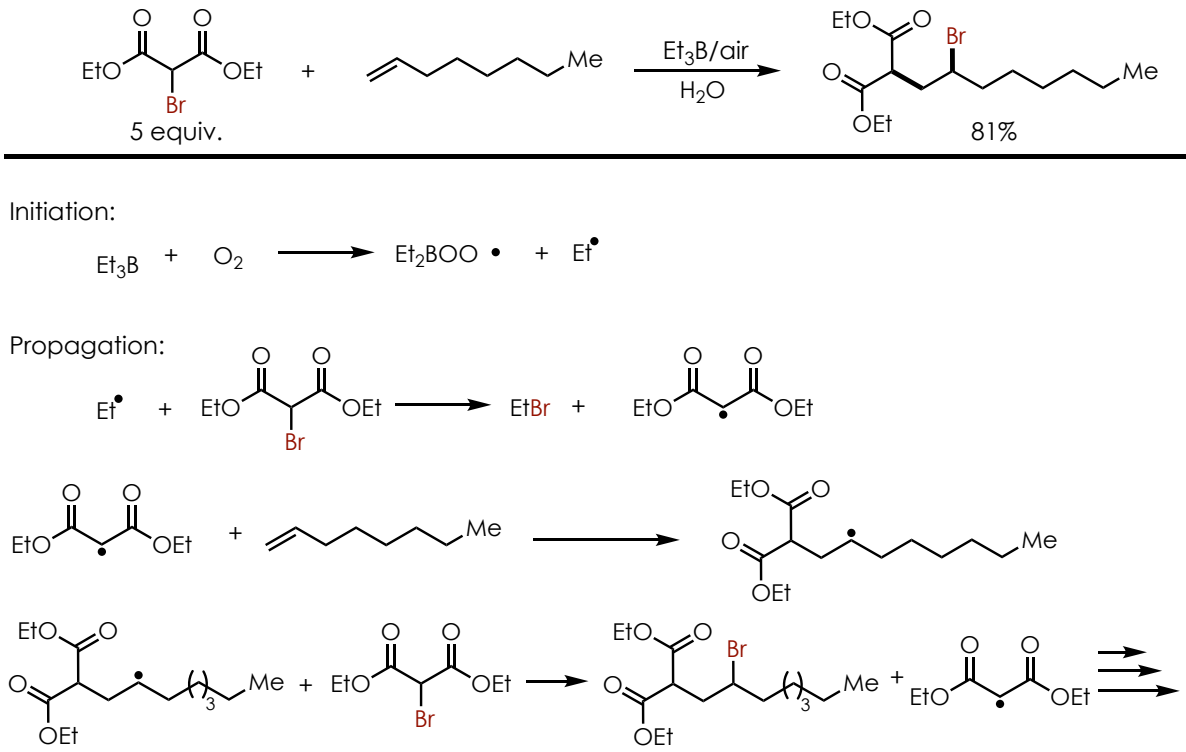

To our satisfaction, DEBM displayed the same proficiency as a halogen radical transfer agent in our lactonization conditions. Initially, a CuBr/bpy system provided the product in 79% yield (Table 3-5, entry 5) but the mass balance was improved by switching to a $CuBr_2$/phen catalyst system (Table 3-5, entry 6). Ultimately, the desired lactone regioisomer was obtained in 97% yield and a 2.4:1 dr when the phen ligand was exchanged for bpy (Table 3-5, entry 7).

Having optimized the bromolactonization reaction conditions, additional control experiments were conducted to further explore the transformation. When DEBM was the lone reagent included in the reaction vial with the unsaturated acid substrate (3.41), only returned starting material was observed (Table 3-5, entry 8). The same result was obtained upon

irradiation of the system also containing catalytic quantities of $CuBr_2$/bpy (Table 3-5, entry 9). Interestingly, no background or desired reactivity was observed when the system consisted of NMA and DEBM under irradiation by 450 nm LEDs (Table 3-5, entry 10). Based on the results of these control experiments, it seemed plausible that the copper had an additional role in the reaction, possibly activating the malonate towards more efficient halogen atom transfer (Scheme 3-19). When 1 equivalent of $CuBr_2$/bpy was used without the addition of DEBM both 3.46 and 3.47 were obtained in a 2.3:1 ratio (Table 3-5, entry 11).

Scheme 3-19. Proposed Copper Activation of Diethyl Bromomalonate

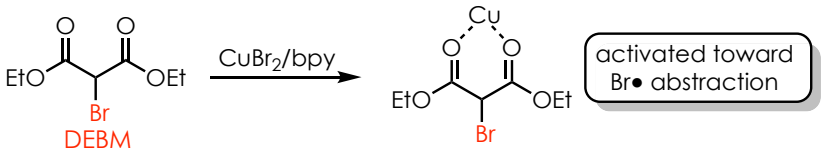

With both optimized chloro- and bromolactonization conditions in hand, we set out to explore the substrate scope of this novel methodology (Scheme 3-20). Styrene-derived acid substrates were first explored beginning with 1,2-disubstituted alkene 3.48. Both chlorination and bromination cyclization conditions were applied to the substrate successfully to give the products in comparable yields and diastereoselectivity (73%, 2.5:1 dr for 3.49, 74%, 2.3:1 dr for 3.50). Despite the potential for acceleration due to the Thorpe-Ingold effect, the addition of geminal dimethyl substitution to the carbon backbone did not have a significant influence on the yield of the chlorolactone (3.52), which was obtained in a 75% yield. Notably, a similar yield (66%) could be obtained when the reaction was conducted on a 1.3 gram scale. The bromolactonization of this substrate was very successful, affording the desired product in a 94%

yield (3.53). A trisubstituted olefin functioned effectively as a substrate under chlorolactonization conditions, albeit with a lack of diastereoselectivity (3.55). The bromolactonization conditions were successfully applied to this substrate as well, however the five-membered lactone was also the favored product regioisomer under classical halofunctionalization conditions. Products with varying substitution on the arene could also be obtained under both sets of conditions. Substrates bearing electron-withdrawing chorine (3.56) functionality were tolerant of chloro- and bromolactonization conditions (3.57 and 3.58). Moving to more electron-rich substrates, 3.59 and 3.61, provided the desired adducts in 64% and 72%, respectively. Bromination was successfully accomplished on moderately electron-rich substrates (3.61) but failed on the more electron-rich OMe-substituted styrene (3.59). The latter substrate was likely problematic due to the instability of the electron-rich, benzyl bromide product. Two additional γ-lactones were accessed from trisubstituted aliphatic olefin substrates. Highly substituted chlorolactone 3.65 was obtained in a 63% yield while the TBS-protected alcohol gave the corresponding lactone product in a slightly diminished, 46% yield (3.67).

Scheme 3-20. γ-Halolactone Scope

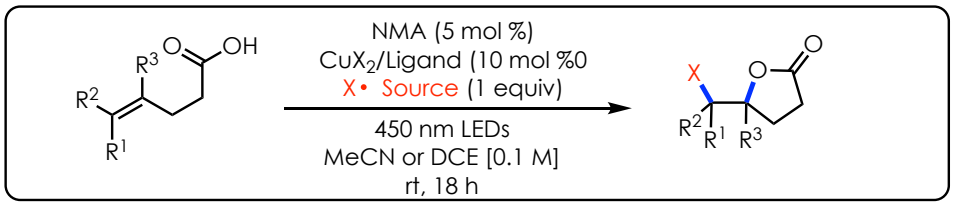

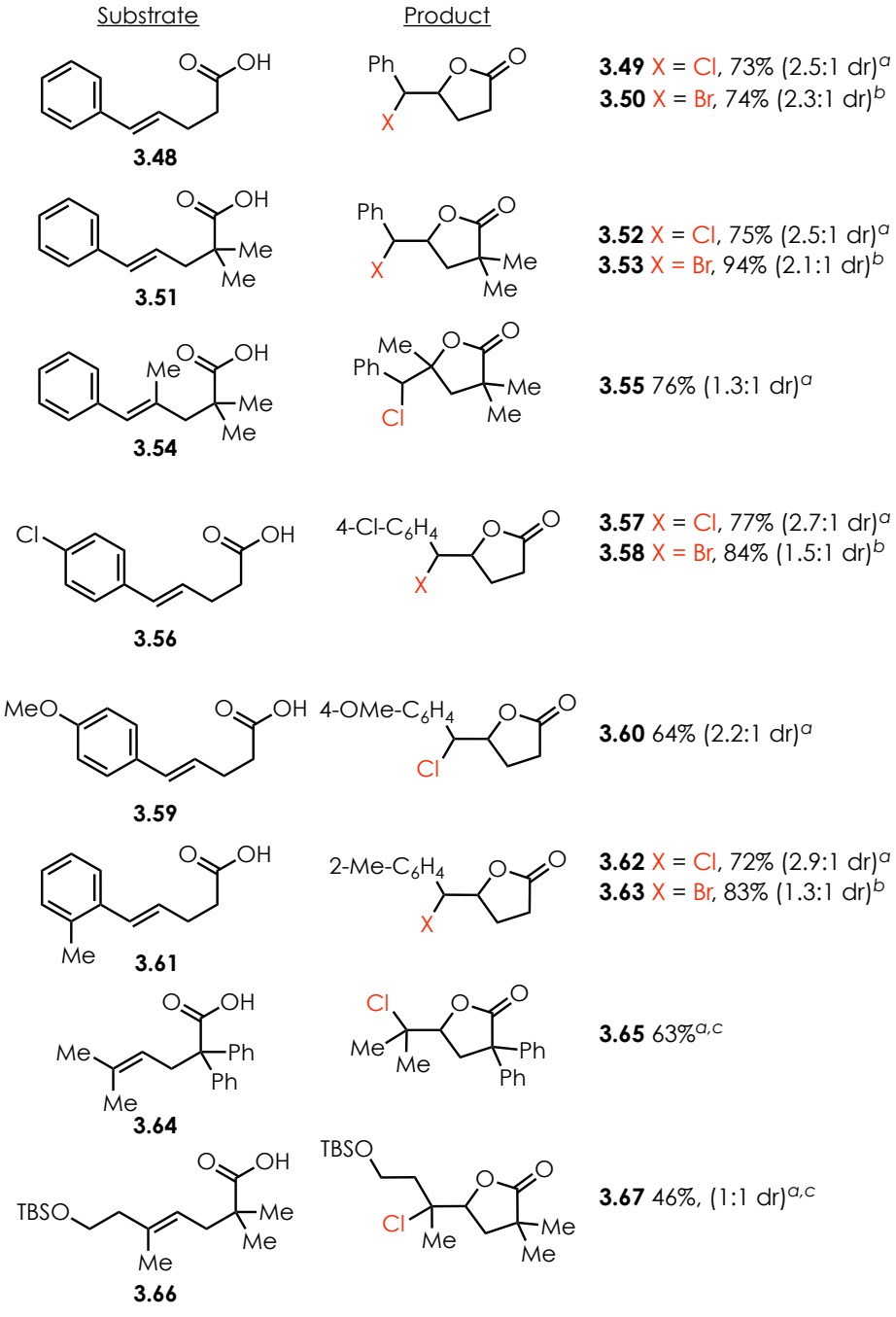

[a] $CuCl_2$/phen (10 mol%), NCP (1 equiv); [b] $CuBr_2$/bpy (10 mol%), DEBM (1 equiv); [c] with AcOH (5.0 equiv)

After thoroughly exploring internal olefin substrates, we turned our attention toward several 1,1-disubstituted-styrene substrates (Scheme 3-21). These terminally, unsaturated acids have been demonstrated as model substrates in classical halolactonization conditions and react in a Markovnikov fashion. Chloro-δ-lactones 3.68–3.72 were accessed in good yields from alkenes functionalized with electron-rich, -neutral, and -deficient arenes. The reactivity of the system shifted slightly upon the addition of geminal dimethyl groups to the α- and β-positions of the acid substrate. In the case of 3.74, a catalytic quantity of 2,6-lutidine base was required as an additive to aid in the cyclization under the bromination conditions. The regioselectivity of the chlorolactonization of substrate 3.74 and 3.77 proved mildly problematic. Lactone 3.75 was obtained in a 72% yield and 19:1 rr while 3.78 was accessed in a 66% yield but only with a selectivity of 4.4:1. This observed decrease in regioselectivity is likely a direct result of the Thorpe–Ingold effect accelerating the uncatalyzed background reaction. The final lactone product (3.80) was achieved by applying the chlorolactonization conditions to a benzoic acid substrate. The product was obtained in a good yield (64%) albeit with low regioselectivity (2.5:1).

Scheme 3-21. δ-Halolactone Scope

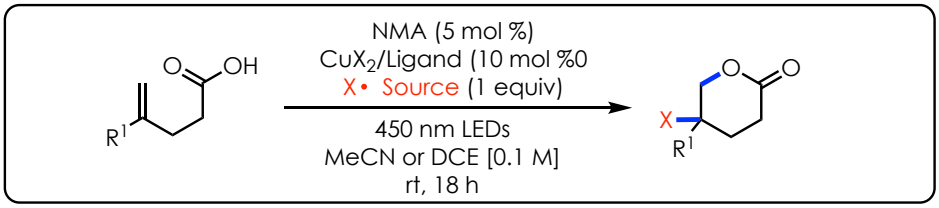

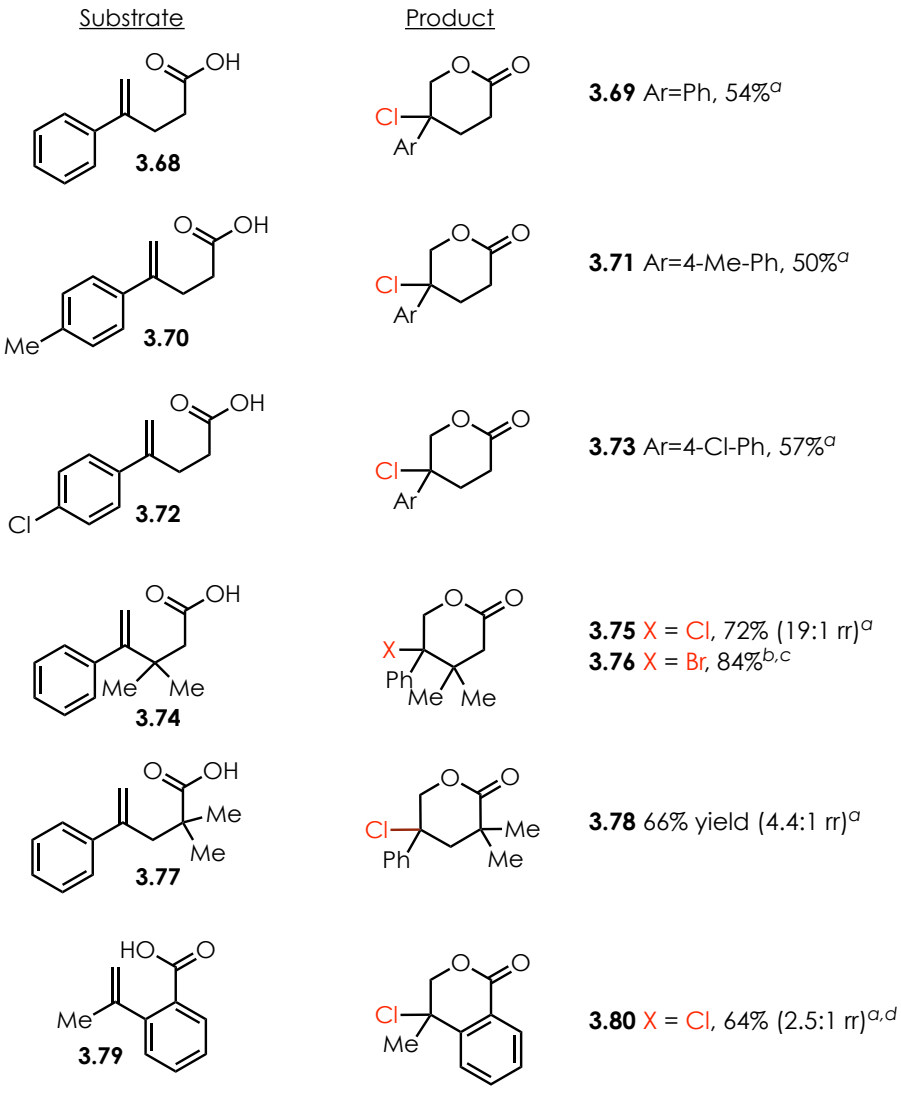

[a] CuCl2/phen (10 mol%), NCS (1 equiv); [b] CuBr2/bpy (10 mol%), DEBM (1 equiv);
[c] with 2,6-lutidine (10 mol%); [d] with AcOH (5.0 equiv);

While the generated products were directly compared to those previously reported in literature, for the purpose of identifying major diasterio- and regioisomers, additional steps were

taken to confirm that a trans relationship was indeed favored between the alcohol and halogen functionality. Model γ-lactone 3.52 was used to confirm this configuration using Borhan's conditions for reducing chlorolactones to the corresponding epoxy-alcohol (Scheme 3-22).[35] The major lactone diastereomer was subjected to the reaction conditions resulting in the formation of the epoxide (3.81). The products were isolated via column chromatography and were analyzed by ^{1}H NMR. A coupling constant of 2.1 Hz was observed between the protons of the epoxide. The small magnitude of this value is indicative of a *trans* relationship between the protons, arising from the epoxidation of a *trans* starting lactone. To emphasize this observation, the minor diastereomer was also subjected to these reduction conditions. In this case, the *cis* epoxide was obtained (3.82) and the coupling constant between the epoxide protons was determined to be 4.3 Hz. This larger coupling constant reinforced that a *cis* relationship existed between the protons of the minor diastereomer. From these observations, it was concluded that this transformation favors the production of a *trans* halogen-nucleophile relationship.

Scheme 3-22. Identification of Major/Minor Diastereomer Using Epoxidation Conditions

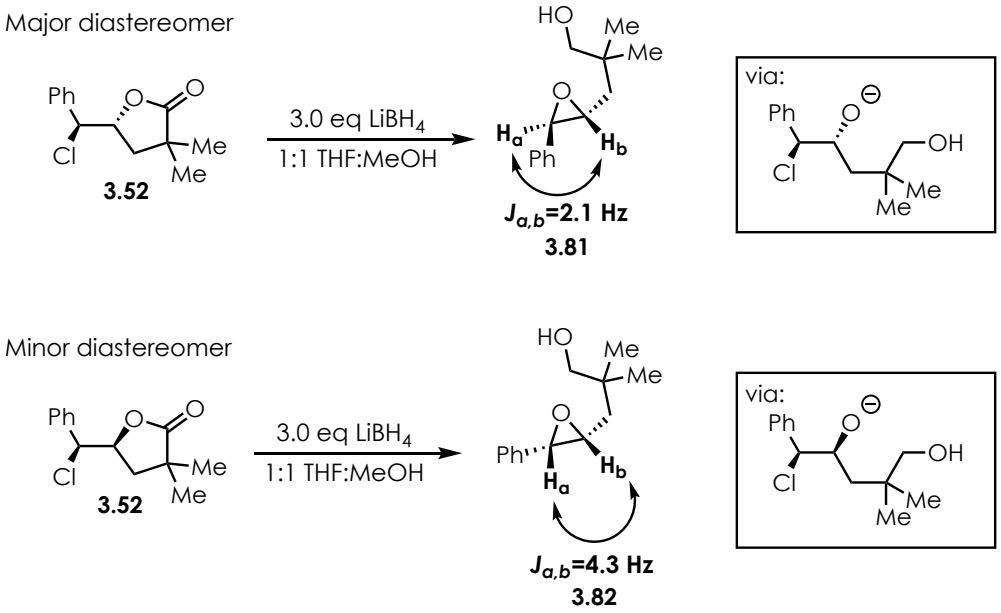

An additional effort was made to expand the substrate scope of the transformation by varying the identity of the nucleophile (Scheme 3-23). Further inspired by the work of Hamilton and Nicewicz,[19] we sought to demonstrate that our system could be applied to the synthesis of halogenated, cyclic ethers beginning from unsaturated alcohols. We were successfully able to generate 5- (3.84) and 6-membered (3.87) cyclic ethers under the chlorination conditions in good yields (61% and 57%, respectively). The 1,2-disubstituted alkene functioned successfully under our bromination conditions to form the 5-membered cyclic ether in a 71% yield (3.85). Inspired by other alkene hydrofunctionalization work from our lab, we successfully applied these halofunctionalization conditions with amine and acetate nucleophiles in intra- and intermolecular fashions. An unsaturated Boc-amine (3.88) could be cyclized to generate a chlorinated pyrrolidine adduct (3.89). Using β-methylstyrene (3.90) as an oxidizable olefin substrate, two intermolecular transformations were achieved. Though low yielding, these chloro-acetoxylation (3.91) and bromo-amination (3.92) reactions act as a proof of concept that this methodology can be extended to a variety of untethered nucleophiles.

Scheme 3-23. Alkene Halofunctionalization Scope

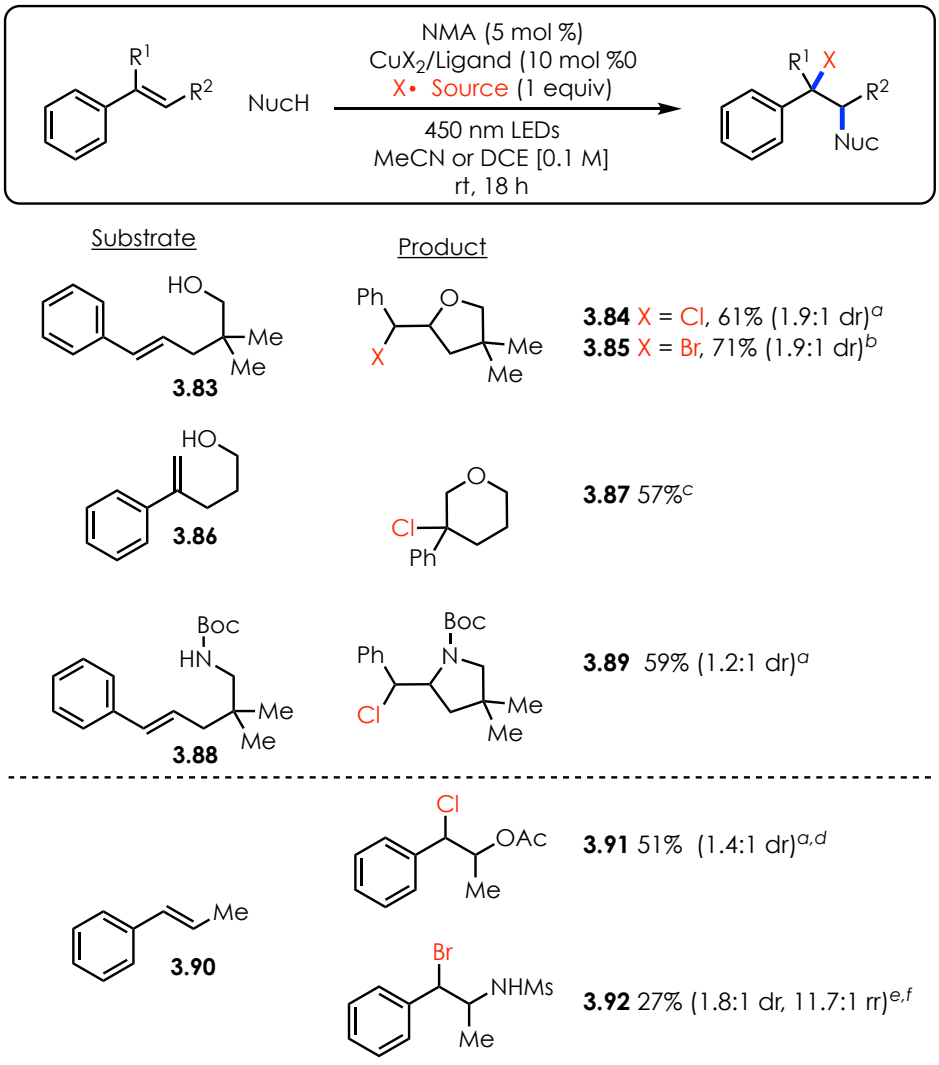

[a] $CuCl_2$/phen (10 mol%), NCP (1 equiv); [b] $CuBr_2$/bpy (10 mol%), DEBM (1 equiv); [c] $CuCl_2$/phen (10 mol%), NCS (1 equiv); [d] 15 equiv acetic acid [e] $CuBr_2$/phen (10 mol%), NBP (1 equiv); [f] 10 equiv methanesulfonamide

Overall, a widely developed substrate scope was achieved for this novel, halofunctionalization reaction. Though selective and high yielding when successful, the bromofunctionalization conditions proved to be less broadly applicable than the chlorination conditions. Substrates failed for various reasons including a lack of reactivity, returning only starting material, or a lack of regioselectivity resulting from highly competitive background

reactivity. To our dismay, in several cases, the uncatalyzed background reaction also resulted in the anti-Markovnikov-type product formation.

Based on insight obtained through control experiments and the mechanistic precedent from our lab's hydrolactonization work, we proposed a potential mechanism to accompany this novel halolactonization transformation (Scheme 3-24). Single electron oxidation of the olefin functionality (3.93), by the excited state NMA, affords the reactive cation radical (3.94). Reversible nucleophilic trapping of the polar component of 3.94 results in the more stabilized carbon-centered radical (3.95) upon deprotonation. The second component of this dual catalytic system begins with the copper-mediated transfer of the halogen atom. $CuCl_2$ is proposed to be the active chlorine transfer agent, trapping the carbon centered radical producing the final, desired product (3.96) and CuCl species. This atom radical trapping step may proceed through an outer-sphere direct atom-transfer or and inner-sphere Cu(III) pathway. The Cu(II) species, reflective in its catalytic use, can be regenerated from the resulting Cu(I) complex, which is reoxidized by the stoichiometric chlorine source, NCP. It is likely that NMA• could be successfully turned over by the nitrogen-centered radical (PhthN• or SucN•) or a copper(III) species to regenerate the ground state photoredox catalyst and reset the cycle. This proposed turnover step is supported by literature evidence that has demonstrated the ability of succinimide radical to undergo a very rapid and efficient single-electron oxidation event with $[Ru(bpy)_3]^{2+}$ ($k = 10^9$ $M^{-1}s^{-1}$).[36] In combination with the fact that SucN• has a sufficiently high reduction potential (+1.96 V vs. SCE)[36] to successfully oxidize NMA•, we have concluded that it is highly likely that the imidyl radicals would be capable of closing the catalytic cycle by regenerating the photoredox catalyst. This redox neutral process would include the formation of the reduced succinimide and phthalimide radicals ($PhthN^-$ or $SucN^-$). In further support of the proposed

mechanism, both succinimide (SucNH) and phthalimide (PhthNH) were observed, by ^{1}H NMR, as byproducts of these reaction conditions.

Scheme 3-24. Proposed Chlorolactonization Mechanism

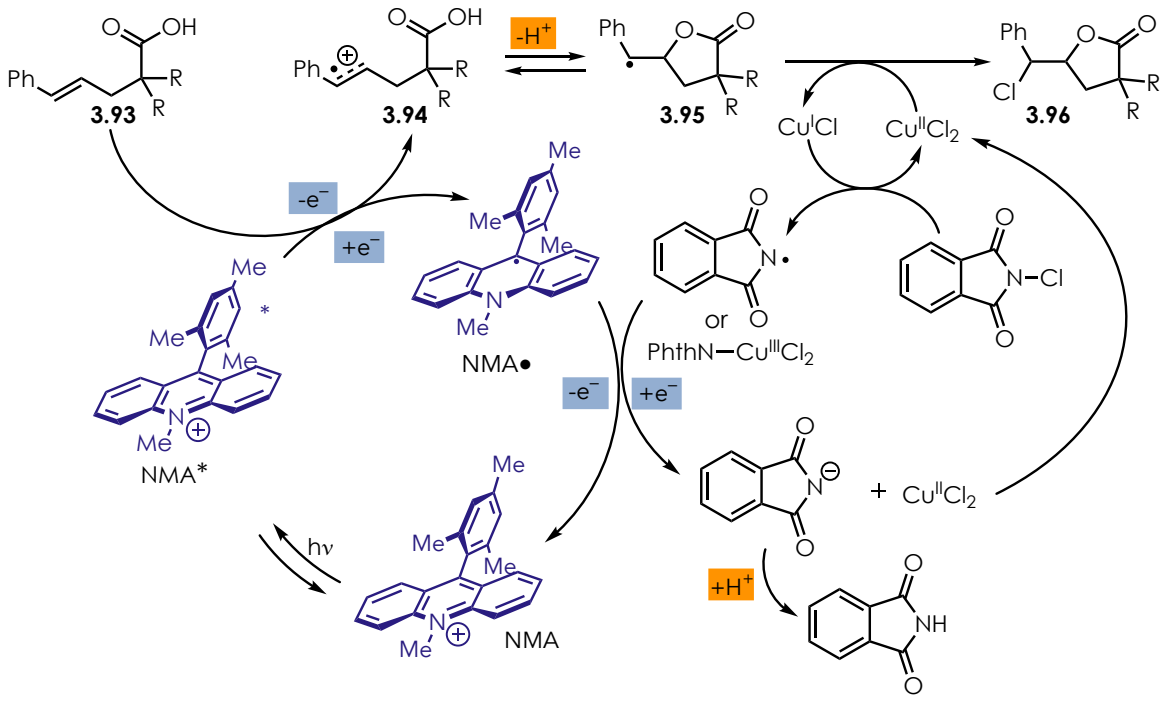

The bromolactonization method is proposed to undergo as comparable mechanism to that proposed for the chlorination conditions (Scheme 3-25). Under $CuBr_2$ catalyzed conditions, the carbon-centered radical is trapped in a similar fashion, either through an inner- or outer-sphere process. CuBr would then be reoxidized by DEBM to generate more of the Cu(II) active halogen transfer agent. The resulting malonate radical (DEM•) or copper(III)-malonate (Cu(III)-DEM) complex, is poised to undergo single electron transfer with the acridine radical, resetting the catalytic cycle and generating an equivalent of malonate anion (DEM^{-}). Protonation of this

species, by an equivalent of substrate, results in the generation of malonate (DEM), which was observed in the crude ^{1}H NMR and GC-MS. Given control experiment results, it is possible that bromine radical transfer may also occur from the activated DEBM-copper complex proposed in Scheme 3-19.

Scheme 3-25. Proposed Bromolactonization Mechanism

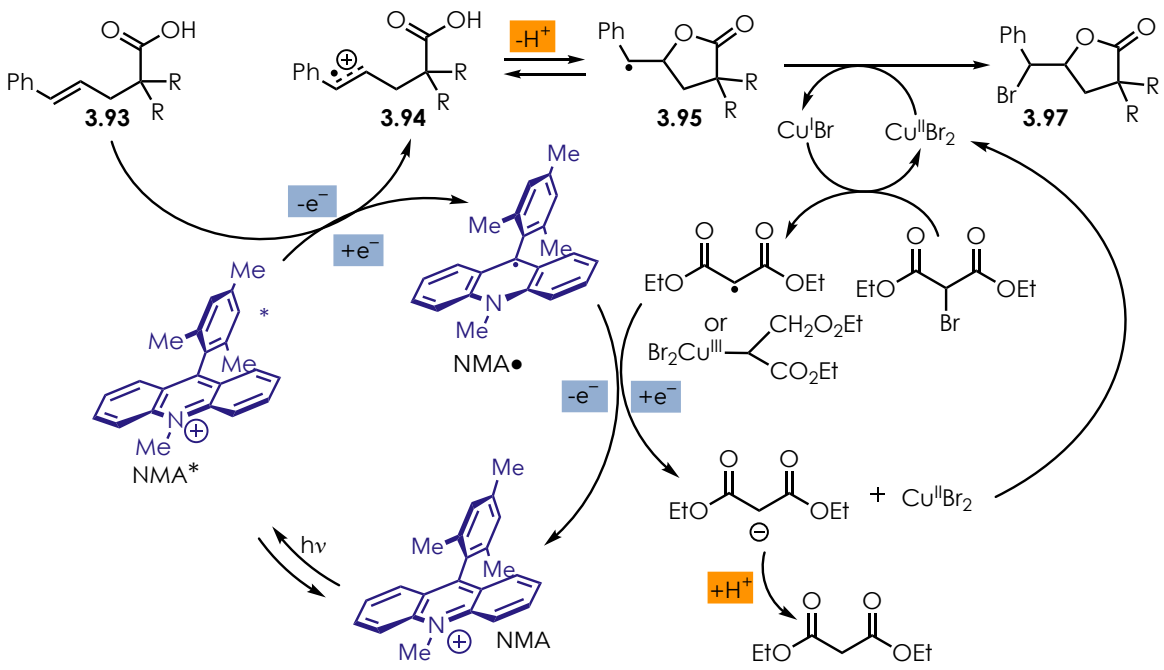

UV/Vis studies were conducted to further support the general proposed mechanism for this transformation. In particular, we looked to evaluate the likelihood of the copper-catalyst turnover step. Though the literature supported the formation of a copper (II) complex, from copper (I) in the presence of a stoichiometric halogen source, we sought to observe its formation by UV/Vis spectroscopy (See experimental section for spectra). Two initial samples, one containing a CuCl complex and the other containing $CuCl_2$, were prepared and analyzed to determine their characteristic absorbances. The Cu(I) species exhibited a λ_{max} of 439 nm. The

Cu(II) complex spectrum showed absorbances at and 388 and 714 nm. With these values in hand, a solution of NCP was added to the Cu(I) complex and a spectrum was obtained. The resulting spectrum match that of the lone Cu(II) complex, suggesting the immediate oxidation of Cu(I) in the presence of NCP.

This process was repeated for with CuBr, $CuBr_2$, and CuBr/DEBM (see experimental section for spectra). The characteristic peak for the Cu(I) complex at 424 nm immediately disappeared upon addition of DEBM and a peak, corresponding to the independently synthesized Cu(II) complex, formed. While these results do not eliminate the potential for other mechanistic pathways, they do support our proposal for the in situ generation of a copper (II) complex, turning over the copper catalytic cycle. Though the current proposed mechanism is supported by the literature, control experiments, and observations, we believe that additional mechanistic studies would only help to enhance our understanding of this novel dual catalytic system.

3.5 Conclusion

Ultimately, we have developed a novel method for the efficient generation of halolactones. This dual catalytic system, consisting of an acridinium photoredox catalyst and copper cocatalyst, was successfully applied to the synthesis of 19 halofunctionalized products, in good to excellent yields. The unique reactivity of the transformation made it possible to outcompete the regioselectivity of traditional halofunctionalization methods in favor of the anti-Markovnikov-type product formation in a completely selective fashion, excluding a few noted exceptions. Both chloro- and bromofunctionalization conditions were developed and applied to a variety of substrates. In addition to synthesizing both γ- and δ-lactone adducts from unsaturated acid substrates, we were able to extend this transformation to various nitrogen- and oxygen-centered nucleophiles in both an intra- and intermolecular fashion. While this innovative method

is highly valuable itself, the utility of the products enhance its appeal. The halofunctionalized products could potentially undergo functional group modifications, be used a synthetic building blocks, or function as biologically active small molecules. Additional efforts have been started towards developing an enantioselective variant of this methodology through the use of chiral copper ligands.

3.6 Experimental

General Methods

Proton, carbon, Heteronuclear Single Quantum Coherence, and Correlated Spectroscopy (**^{1}H NMR**, **^{13}C NMR**, **HSQC**, **COSY**, respectively) were recorded on a Bruker model DRX 400 or AVANCE III 600 CryoProbe spectrometer (^{1}H NMR at 400 MHz or 600 MHz, ^{13}C NMR at 100 MHz or 150 MHz respectively). Chemical shifts for proton NMR are reported in parts per million downfield from tetramethylsilane and are referenced to residual $CHCl_3$ in solution ($CHCl_3$ set to 7.26 ppm). Chemical shifts for ^{13}C NMR are reported in parts per million downfield from tetramethylsilane and are referenced to the carbon resonances of the solvent ($CDCl_3$ set to 77.00 ppm). NMR data are represented as follows: chemical shift, multiplicity (s = singlet, br s = broad singlet, d = doublet, dd = doublet of doublet, t = triplet, ddd = doublet of doublet of doublet, q = quartet, m = multiplet, etc.), coupling constants (Hz), and integration. High Resolution Mass Spectra (**HRMS**) were obtained using Thermo LTqFT mass spectrometer with electrospray ionization in positive mode. Low Resolution Mass Spectra (**LRMS**) were obtained using GC-MS (Agilent 6850 series GC equipped with Agilent 5973 network Electron Impact-MSD). Infrared (**IR**) spectra were obtained using a Jasco 260 Plus Fourier transform infrared spectrometer. Thin layer chromatography (TLC) was performed on SiliaPlate 250 μm thick silica gel plates purchased from Silicycle. Visualization was accomplished using fluorescence quenching, $KMnO_4$ stain, or ceric ammonium molybdate (CAM) stain followed by heating. Purification of the reaction products was carried out by chromatography using Siliaflash-P60 (40-63 μm) silica gel purchased from Silicycle. All reactions were carried out under an inert atmosphere of nitrogen in flame-dried glassware with magnetic stirring unless otherwise noted. Reactions were carried out in standard borosilicate glass vials purchased from

Fisher Scientific. Yield refers to isolated yield of analytically pure material unless otherwise noted. NMR yields were determined using hexamethyldisiloxane, $(Me_3Si)_2O$, as an internal standard.

Materials

Commercially available reagents were purchased from Sigma Aldrich, Acros, Alfa Aesar, Fisher Scientific, or TCI, and used as received unless otherwise noted. Diethyl ether (Et_2O), dichloromethane (DCM), tetrahydrofuran (THF), toluene (PhMe), and dimethylformamide (DMF) were dried by passing through activated alumina columns under nitrogen prior to use. 1,2-dichloroethane (DCE) was purchased from Fischer and sparged with N_2 before being stored over activated 4Å molecular sieves in a glovebox. Acetonitrile (MeCN) was dried by passing through activated alumina column under nitrogen. MeCN was commonly stored in a glovebox after sparging with N_2. Glacial acetic acid (AcOH) stored in the glovebox with 5% v/v acetic anhydride. Other common solvents such as chloroform ($CHCl_3$) were purified by standard published methods when necessary. Trans-β-methylstyrene was distilled over potassium hydroxide, sparged with N_2, and stored in a glovebox freezer.

Photoreactor Setup and Lamp Information

Reactions were irradiated using a photoreactor which consists of two Par38 Royal Blue Aquarium LED lamps (Model #6851) purchased from ecoxotic. A standard magnetic stir plate was used as the support. Reaction efficacy can be impacted by the type of LED used. A fan was added above to cool the reaction and keep the temperature below 30˚C.

Photoreactor setup used for halofunctionalization reactions. Reaction vials were placed about 5 cm from the face of both lamps. Above a simple fan was used to cool the reaction.

Preparation of Substrates

1,2 disubstituted styrene substrates were prepared according to the following Wittig olefination procedure:

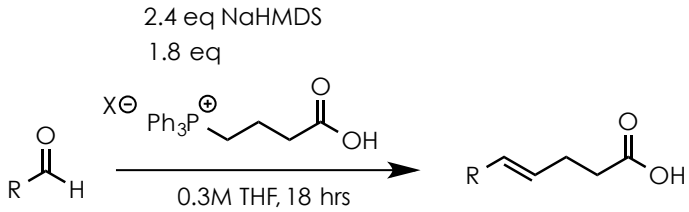

1.8 equiv (relative to the necessary aldehyde precursor) of 3-carboxypropyl)triphenylphosphonium bromide[37] or chloride was dispensed into a flame-dried round bottom flask equipped with a magnetic stir bar. The flask was flushed with N_2 and THF

was added to 0.3 M concentration. The solution was cooled to 0˚C before 2.4 equiv sodium hexamethyldisilazane (1.0 M in THF) was carefully added to the stirring solid. The contents were warmed to room temperature and stirred for 0.5 to 1 hour after which the solution was cooled to -78˚C and 1 equiv of the necessary aldehyde was added dropwise to the stirring ylide. The reaction stirred overnight while warming to room temperature. The reaction was quenched with H_2O, and diluted with equal amounts DI H_2O and diethyl ether, and the aqueous phase was acidified to pH of 1 before extracting 3 times with ethyl acetate. The organics were combined and dried over Na_2SO_4 and concentrated under reduced pressure. Purification was accomplished via column chromatography (gradient: 2:1 Et_2O:hexanes with 1% acetic acid by volume→1:1 Et_2O:hexanes with 1% acetic acid by volume).

(*E*)-5-Phenylpent-4-enoic acid:

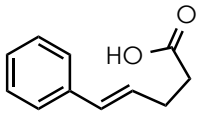

Obtained as the pure *E*-isomer in 65% isolated yield. Analytical data matched were in agreement with literature values.[11]

(*E*)-5-(4-Chlorophenyl)pent-4-enoic acid:

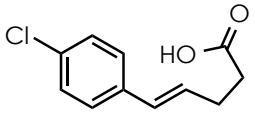

Obtained as a 6:1 mixture of *E:Z* isomers in an 89% isolated yield. Analytical data matched were in agreement with literature values.[11]

(*E*)-5-(4-Methoxyphenyl)pent-4-enoic acid:

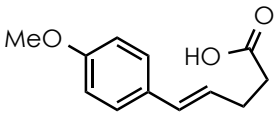

Obtained as a 8:1 mixture of *E:Z* isomers in an 84% isolated yield. Analytical data matched were in agreement with literature values.[11]

(*E*)-5-(*o*-Tolyl)pent-4-enoic acid:

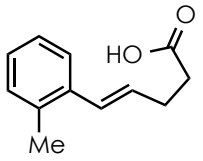

Obtained as a 1.9:1 mixture of *E:Z* isomers in an 93% isolated yield. Analytical data matched were in agreement with literature values.[11]

7-((*tert*-Butyldimethylsilyl)oxy)-2,2,5-trimethylhept-4-enoic acid

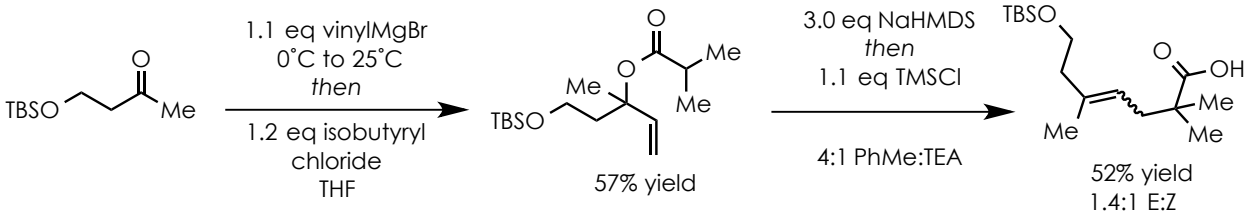

To a flame-dried 250 mL round bottom flask containing 3.9 g of 4-((*tert*-butyldimethylsilyl)oxy)butan-2-one[38] was flushed with N_2 before adding 100 mL dry THF. The solution was cooled to 0 ˚C before adding 21 mL of vinyl magnesiumbromide solution (1 M in THF) dropwise. This was allowed to stir for an additional hour while warming to room temperature, before 2.4 mL of isobutyryl chloride was added. The reaction was then stirred for 2 hours before the reaction was quenched with H_2O and then a saturated solution of ammonium chloride. The mixture was transferred to a separatory funnel where Et_2O was added. The phases

were separated, and the aqueous layer was back extracted twice with Et_2O. The combined organics were dried over $MgSO_4$ and the solution was concentrated. 5-((*tert*-butyldimethylsilyl)oxy)-3-methylpent-1-en-3-yl isobutyrate was obtained cleanly after column chromatography to give 3.3 g (57% yield) of a clear oil.

^{1}H NMR: (400 MHz, Chloroform-*d*) δ 5.97 (dd, *J* = 17.5, 11.0 Hz, 1H), 5.19 – 5.06 (m, 2H), 3.68 (t, *J* = 7.3 Hz, 2H), 2.48 (hept, *J* = 7.0 Hz, 1H), 2.07 (tdd, *J* = 20.5, 13.9, 7.3 Hz, 2H), 1.55 (s, 3H), 1.14 (d, *J* = 7.0 Hz, 6H), 0.88 (s, 9H), 0.04 (s, 6H).

To a flame-dried 250 mL round bottom flask was added 80 mL of dry toluene and 20 mL of freshly distilled triethylamine. Next, 3.3 g 5-((*tert*-butyldimethylsilyl)oxy)-3-methylpent-1-en-3-yl isobutyrate was added in a solution of toluene and the solution was cooled to -78˚C. Then a 33 mL of a solution of NaHMDS in THF (1M) was slowly added while stirring. This was stirred for 1 hour at -78 ˚C before 1.5 mL of TMSCl was added, and the solution was allowed to warm to room temperature while stirring overnight. The reaction was quenched by adding H_2O and 3M HCl solution. The reaction mixture was transferred to a separatory funnel and the aqueous layer was brought to a pH of 1 then extracted with Et_2O three times. The combined organics were washed with H_2O and brine, before drying with $MgSO_4$, filtered and concentrated to give a yellowish oil. The title compound was purified on column chromatography (15% EtOAc:hexanes, 150 mL dry silica gel) to obtain 1.7 g (52% yield) of 7-((*tert*-butyldimethylsilyl)oxy)-2,2,5-trimethylhept-4-enoic acid (1.4:1 *E:Z*, yellowish oil).

^{1}H NMR: Mixture of E:Z isomers (400 MHz, Chloroform-*d*) δ 5.17 (t, *J* = 6.7 Hz, 1H *E/Z*), 3.70 – 3.55 (m, 2H *E/Z*), 2.27 (t, *J* = 6.9 Hz, 2H, *E/Z*), 2.22 (t, *J* = 7.1 Hz, 1H, *E/Z*), 2.17 (d, *J* = 1.5 Hz, 1H, *E/Z*), 1.73 (s, 3H *Z*), 1.63 (s, 3H *E*), 1.19 (s, 6H *E/Z*), 0.89 (s, 3H *Z*), 0.88 (s, 3H *E*), 0.05 (d, *J* = 1.6 Hz, 6H *Z*), 0.04 (d, *J* = 1.6 Hz, 6H *E*).

^{13}C NMR: (151 MHz, $CDCl_3$) δ 183.58, 183.45, 135.37, 134.99, 121.81, 121.43, 62.39, 61.72, 53.41, 43.31, 42.58, 42.32, 38.23, 38.20, 35.60, 25.96, 25.94, 24.65, 24.49, 24.26, 18.36, 18.31, 16.61, -5.30.

IR (thin film cm^{-1}): 3447, 2956, 2930, 2858, 1701, 1473, 1256, 1095

HRMS: ***m/z*** **calculated** for $C_{16}H_{32}O_3Si[H]^+$: 301.2193; **found**: 301.2193

2-(Prop-1-en-2-yl)benzoic acid:

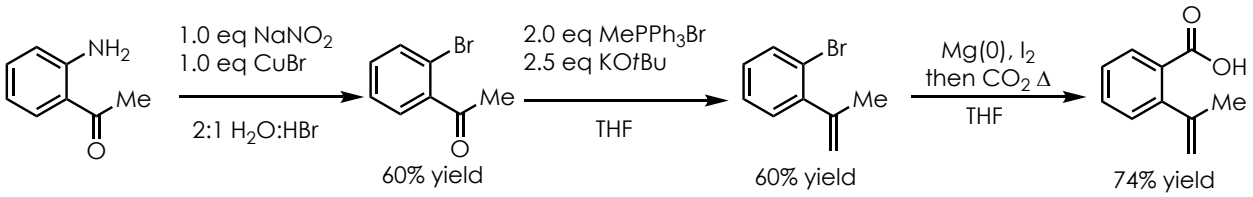

15 mL of 36% HBr and 35 mL of H_2O were added to a 250 mL round bottom flask, followed by 3 mL 1-(2-aminophenyl)ethan-1-one. The solution was cooled to 0˚C before adding 1.7 g of $NaNO_2$ dissolved in H_2O dropwise. This was allowed to stir about 20 minutes after all of the $NaNO_2$ had been added. 3.6 g of CuBr was added, with N_2 bubbles forming immediately. This was stirred overnight before quenching the reaction with a saturated solution of $NaHCO_3$. A precipitate formed which was filtered under vacuum. The mixture was then transferred to a separatory funnel and extracted 3 times with Et_2O. The organics were combined and dried over $MgSO_4$, and concentrated giving a brownish oil. This was passed through a plug of silica to give

3.0 g of 1-(2-bromophenyl)ethan-1-one as a yellow oil (60% yield). No further purification was necessary. Characterization matched previous reports.[39]

To a flame-dried 250 mL round bottom flask was added 10.8 g of methyltriphenylphosphonium bromide and 4.2 g of KO*t*Bu. The flask was then evacuated and refilled with N_2 before adding 150 mL of dry THF and stirring for 20 minutes. 3 g of 1-(2-bromophenyl)ethan-1-one was added and the solution was stirred overnight. The reaction was quenched with a saturated solution of ammonium chloride and the mixture was transferred to a separatory funnel. Et_2O was added and the two phases were separated. The aqueous layer was back extracted twice with Et_2O. The combined organics were dried with $MgSO_4$, filtered, and concentrated. The product was purified by dry loading the resulting material on celite and eluted from a short silica plug with hexanes. 1.8 g of 1-bromo-2-(prop-1-en-2-yl)benzene was obtained as a clear oil (60% yield). Characterization matched previous reports.[40]

To a flame-dried 100 mL round bottom flask was added 500 mg Mg° (2.0 equiv), and a small amount of I_2. The flask was purged with N_2 before adding 25 mL dry THF, resulting in an orange solution. 1.8 g of 1-bromo-2-(prop-1-en-2-yl)benzene was added. After about ten minutes the orange color subsided; the solution was allowed to stir an addition 30 minutes before the solution was sparged with a balloon of CO_2 for about 5 minutes. The flask was kept under a balloon of CO_2 while stirring overnight. The reaction was then quenched with H_2O and transferred to a separatory funnel where more H_2O and Et_2O were added. The organic layer was removed before bringing the aqueous layer to a pH of 1 forming a white precipitate. The aqueous layer was extracted three times with Et_2O and the combined organics were dried with $MgSO_4$, filtered, and

concentrated to give 1.1 g of 2-(prop-1-en-2-yl)benzoic acid (74% yield). No further purification was required. Characterization matched previous reports.[41]

***tert*-Butyl (*E*)-(2,2-dimethyl-5-phenylpent-4-en-1-yl)carbamate:**

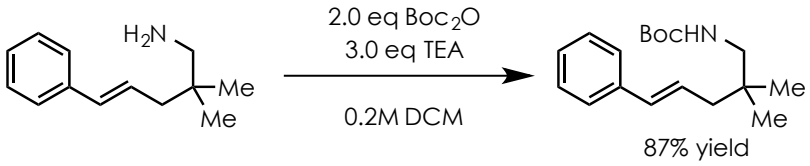

To a flame-dried 100 mL round bottom flask was added 1 gram of (*E*)-2,2-dimethyl-5-phenylpent-4-en-1-amine[42] and 2.3 grams of di-tert-butyl dicarbonate. The flask was flushed with N_2 before adding 25 mL of dry DCM and 2.2 mL of freshly distilled triethylamine. The reaction was allowed to stir overnight before removing DCM and most triethylamine under vacuum. The crude material was then purified on silica gel (20% EtOAc:hexanes) to give the product as a white solid 1.4 grams, 87% yield.

^{1}H NMR:(400 MHz,) δ 7.38 – 7.33 (m, 2H), 7.30 (dd, *J* = 8.5, 6.7 Hz, 2H), 7.23 – 7.17 (m, 1H), 6.39 (d, *J* = 15.7 Hz, 1H), 6.24 (dt, *J* = 15.4, 7.5 Hz, 1H), 4.59 (s, 1H), 3.01 (d, *J* = 6.5 Hz, 2H), 2.12 (dd, *J* = 7.5, 1.2 Hz, 2H), 1.45 (s, 9H), 0.92 (s, 6H).

^{13}C NMR: (151 MHz, $CDCl_3$) δ 156.19, 137.56, 132.54, 128.48, 127.01, 126.73, 126.04, 79.07, 50.49, 43.48, 35.46, 28.41, 24.84.

IR (thinfilm cm^{-1}): 3379, 2965, 2929, 1702, 1510, 1365, 1245, 1171, 967, 736

HRMS: ***m/z* calculated** for $C_{18}H_{27}NO_2[Na]^+$: 312.1934; **found**: 312.1932

(*E*)-2,2-Dimethyl-5-phenylpent-4-enoic acid:

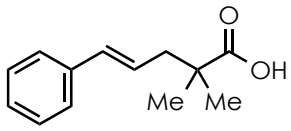

Prepared according to a previously reported literature procedure[19]

(*E*)-2,2,4-Trimethyl-5-phenylpent-4-enoic acid:

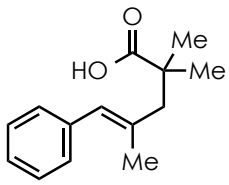

Prepared according to a previously reported literature procedure[19]

5-Methyl-2,2-diphenylhex-4-enoic acid:

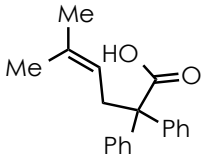

Prepared according to a previously reported literature procedure[19]

4-Phenylpent-4-enoic acid:

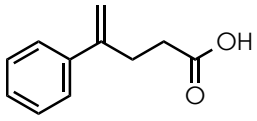

Prepared according to a previously reported literature procedure[21]

4-(*p*-Tolyl)pent-4-enoic acid:

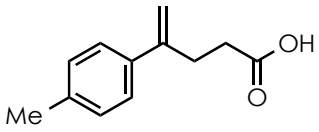

Prepared according to a previously reported literature procedure[43]

4-(4-Chlorophenyl)pent-4-enoic acid:

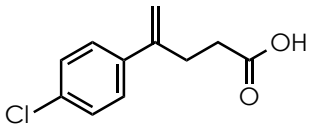

Prepared according to a previously reported literature procedure[43]

3,3-Bimethyl-4-phenylpent-4-enoic acid:

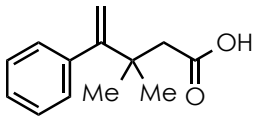

Prepared according to a previously reported literature procedure[19]

2,2-Dimethyl-4-phenylpent-4-enoic acid:

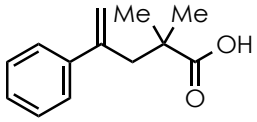

Prepared according to a previously reported literature procedure[44]

(*E*)-2,2-Dimethyl-5-phenylpent-4-en-1-ol

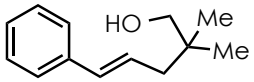

Prepared according to a previously reported literature procedure[19]

4-Phenylpent-4-en-1-ol:

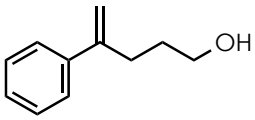

Prepared according to a previously reported literature procedure[45]

Halofunctionalization Procedures

General Procedure for Chlorofunctionalization:

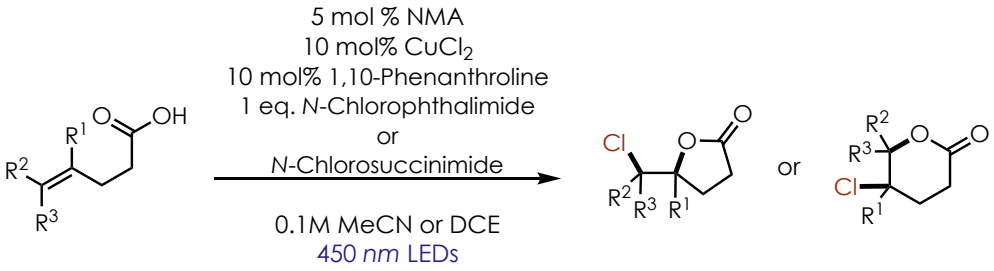

The carboxylic acid substrate, *N*-chlorophthalimide (**NCP,** 1.0 equiv**)** or *N*-chlorosuccinimide **(NCS,** 1.0 equiv**),** $CuCl_2$ (0.1 equiv), 1,10-phenanthroline, (0.1 equiv) and acridinium photoredox catalyst (0.05 equiv) were weighed and dispensed into a flame-dried vial (2-dram) equipped with a stir bar and Teflon-coated septum cap. The vial was moved to a nitrogen filled glovebox where solvent was dispensed by syringe (MeCN or DCE to 0.1 M). Where noted acetic acid was added to the vial as well. The vial was then sealed and removed from the glovebox and

the reaction vial was sealed with electrical tape. The reactions were irradiated (2x455 nm blue LED lamps) and stirred until completion. Reaction progress was monitored by GC/MS. Upon completion, the crude reactions were passed through a silica plug to remove $CuCl_2$ before NMR analysis.

General Procedure for Bromofunctionalization:

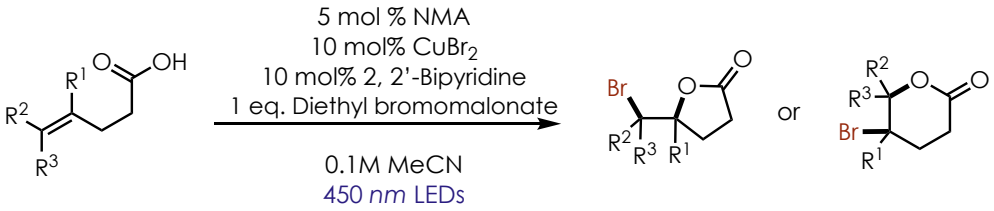

The carboxylic acid substrate (1.0 equiv), diethyl bromomalonate (1.0 equiv), $CuBr_2$ (0.1 equiv), 2,2'-bipyridine, (0.1 equiv) and acridinium photoredox catalyst (0.05 equiv) were weighed and dispensed into a flame-dried vial (2-dram) equipped with a stir bar and Teflon-coated septum cap. The vial was moved to a nitrogen filled glovebox where solvent was dispensed by syringe (MeCN to 0.1 M). When noted, 2,6-lutidine (0.1 equiv) was added to the vial as well. The vial was then sealed and removed from the glovebox and the reaction vial was sealed with electrical tape. The reactions were irradiated (2x455 nm blue LED lamps) and stirred until completion. Reaction progress was monitored by GC/MS. Upon completion, the crude reactions were concentrated then passed through a silica plug to remove $CuBr_2$ before NMR analysis.

Note: NCP and NCS were purchased from Sigma and stored in a desiccator away from light. This was found to be particularly important for avoiding background reactivity, most likely

through formation of Cl_2. Copper (II) sources as well as ligands were stored in the desiccator as well to avoid absorption of H_2O.

Note: Products 1m, 1n, and 1v were found to decompose upon standing. Characterization data for these compounds was collected after preparing fresh samples. It was also noted that compounds 1o, 1p, 1q, 1r, and 1s were slightly less prone to decomposition, but still experienced some degree of decomposition upon standing.

Note: Under the normal conditions products 1k and 1l were isolated with significant quantities of a new alkene product which was suspected to arise from chloride elimination. Using acetic acid as a buffer was found to alleviate this issue, and increased the yield of the desired chlorolactone.

5-(Chloro(phenyl)methyl)dihydrofuran-2(3*H*)-one (3.49)

The average yield for the title compound was 75% (2 trials) at the 0.5 mmol scale, generated using General Procedure for Chlorofunctionalization using 88 mg of the starting carboxylic acid (0.1M in MeCN), 90.8 mg NCP, 10 mg **NMA,** 6.7mg $CuCl_2$, 9 mg of 1,10-phenanthroline, and an irradiation time of 2 hours. The average diasteromeric ratio was 3.1:1. The products were isolated by column chromatography on silica gel (20 mL dry silica, 2 cm column, 15% EtOAc/hexanes) as a low melting white solid.

Analytical data for **1a**:

^{1}H NMR Major/minor diastereomers: ^{1}H NMR (600 MHz, Chloroform-*d*) δ 7.47 – 7.33 (m, 10H-5 major, 5 minor), 5.05 (d, *J* = 5.7 Hz, 1H-major), 4.98 (d, *J* = 5.1 Hz, 1H-minor), 4.92 – 4.88 (m, 1H-minor), 4.88 – 4.84 (m, 1H-major), 2.53 (m 3H-2 major, 1 minor), 2.47 – 2.39 (m, 1H-minor), 2.39 – 2.32 (m, 1H-major), 2.29 (dddd, *J* = 13.4, 12.5, 5.6, 3.9 Hz, 1H-major), 2.25 – 2.19 (m, 1H-minor), 2.15 – 2.07 (m, 1H-minor).

^{13}C NMR Major/minor diastereomers: (151 MHz, $CDCl_3$) δ 176.19 (minor), 176.16 (major), 136.28 (major), 136.04 (minor), 129.13 (minor), 129.04 (major), 128.82 (major), 128.80 (minor), 127.94 (minor), 127.70 (major), 81.93 (major), 81.90 (minor), 64.03 (major), 63.60 (minor), 28.27 (major), 28.05 (minor), 24.53 (minor), 24.18 (major).

IR (thin film, cm^{-1}): 1778, 1455, 1175, 1028, 919, 701

HRMS *m/z* **calculated** for $C_{11}H_{11}ClO_2$ $[H]^+$: 211.0520 and 213.0491; **found**: 211.0520 and 213.0491

5-(Bromo(phenyl)methyl)dihydrofuran-2(3*H*)-one (3.50)

The average yield for the title compound was 74% (2 trials) at the 0.5 mmol scale, generated using General Procedure for Bromofunctionalization using 88 mg of the starting carboxylic acid (0.1M in MeCN), 85 μL diethyl bromomalonate, 10 mg **NMA,** 11.2 mg $CuBr_2$, 7.8 mg 2,2'-bipyridine, and an irradiation time of 16 hours. The average diasteromeric ratio was 2.3:1. The products were isolated by silica gel (40 mL dry silica, 2.5 cm column, 10% EtOAc/hexanes then 30% EtOAc/hexanes) as a white solid.

Analytical data for **3.50**:

^{1}H NMR Major/minor diastereomers: (600 MHz, Chloroform-*d*) δ 7.45 (dd, *J* = 8.0, 1.4 Hz, 2H-minor), 7.44 – 7.40 (m, 2H-major), 7.39 – 7.30 (m, 6H-3 major, 3 minor), 5.01 (d, *J* = 6.9 Hz, 1H-major), 4.99 (d, *J* = 5.5 Hz, 1H-minor), 4.95 – 4.88 (m, 2H-1 major, 1 minor), 2.57 – 2.43 (m, 4H-3 major, 1 minor), 2.41 (dd, *J* = 10.0, 5.3 Hz, 1H-minor), 2.31 – 2.19 (m, 2H-1 major, 1 minor), 2.05 (dddd, *J* = 13.4, 10.1, 8.3, 6.8 Hz, 1H-minor).

^{13}C NMR Major/minor diastereomers: (151 MHz, Chloroform-*d*) δ 176.12 (major), 176.06 (minor) 137.08 (major), 136.87 (minor), 129.18 (minor), 129.12 (major), 128.93 (minor), 128.90 (major), 128.46 (minor), 128.30 (major), 82.03 (minor), 81.70 (major), 55.48 (major), 55.24 (minor), 28.63 (major), 28.40 (minor), 26.42 (major), 25.73 (minor).

IR (thin film, cm^{-1}): 1778, 1636, 1170, 1022, 911, 699

HRMS *m/z* **calculated** for $C_{11}H_{11}BrO_2$ $[H]^+$: 255.0015 and 256.9995; **found**: 255.0014 and 256.9994

5-(Chloro(phenyl)methyl)-3,3-dimethyldihydrofuran-2(3*H*)-one (3.52)

The average yield for the title compound was 75% (2 trials) at the 0.5 mmol scale, generated using General Procedure for Chlorofunctionalizations using 102 mg of the starting carboxylic acid (0.1M in MeCN), 90.8 mg NCP, 10 mg NMA, 6.7mg $CuCl_2$, 9mg of 1,10-phenanthroline,

and an irradiation time of 2 hours. The average diasteromeric ratio was 3.1:1. The products were isolated by column chromatography on silica gel (25 mL dry silica, 2 cm column, 10% EtOAc/hexanes) as a white solid.

The reaction was performed on 2.0 gram scale (8.38 mmol). 1.7 g of the starting carboxylic acid, 1.5 g of NCP (1.0 equiv), 167 mg of **NMA** (0.05 equiv)**,** 112.5 mg $CuCl_2$ (0.1 equiv), and 151 mg 1,10-phenanthroline (0.1 equiv) to a 100 mL round bottom flask (flame-dried) equipped with a Teflon stir bar. The flask was fitted with a septum and evacuated and then refilled with N_2 three times. 80 mL of dry MeCN (0.1M) was sparged with N_2 for 15 minutes and then transferred to the flask containing solid reagents via cannula. The flask was irradiated with two 455 nm blue LED lamps from either side, while cooling with a fan (see **S3**). After 3 hours TLC revealed the reaction had reached full conversion. Solvent was then removed in vacuo. The crude material was loaded onto celite and purified on column chromatography (4.5 cm column, 200 mL dry silica, gradient solvent system 3%→5%→7.5%→10% EtOAc in hexanes). Gradient column conditions were used in order to separate a small amount of undesired regioisomer as well the diastereomers. The combined yield of both diastereomers was 66%, 1.3 g, with 3.3:1 dr Diastereomers were only partially separated under these conditions. All fractions containing the minor disastereomer contained some of the major diastereomer.

Analytical data for **3.52**:

^{1}H NMR Major/minor diastereomers: (400 MHz, Chloroform-*d*) δ 7.39 (m, 10H-5major, 5 minor), 4.98 (d, *J* = 6.6 Hz, 1H-major), 4.87 (d, *J* = 6.4 Hz, 1H-minor), 4.84 – 4.78 (m, 1H-

minor), 4.75 (dt, *J* = 9.4, 6.4 Hz, 1H-major), 2.29 – 2.08 (m, 2H-major), 1.87 (qd, *J* = 13.0, 7.9 Hz, 2H-minor), 1.29 (s, 3H-major), 1.26 (s, 3H-major), 1.24 (s, 3H-minor), 1.19 (s, 3H-minor).

^{13}C NMR Major/minor diastereomers: (151 MHz, $CDCl_3$) δ 180.83 (major), 180.69 (minor), 136.75 (major), 136.41(minor), 129.16 (minor), 129.03 (major), 128.84 (minor), 128.75 (major), 127.91 (minor), 127.73 (major), 79.02 (minor), 78.49 (major), 63.87 (minor/major), 40.47 (minor), 40.39 (minor), 40.31 (major), 40.14 (major), 24.90 (major), 24.77 (minor), 24.71 (major), 24.66 (minor).

IR (thin film cm^{-1}) 2969, 2360, 1774, 1455, 1205, 1119, 1035, 915, 699, 667

HRMS *m/z* **calculated** for $C_{13}H_{15}ClO_2$ $[H]^+$: 239.0833 and 241.0804; **found**: 239.0833 and 241.0803

NMR Spectra (^{1}H, ^{13}C, HSQC, COSY): S51-S52

5-(Bromo(phenyl)methyl)-3,3-dimethyldihydrofuran-2(3*H*)-one (3.53)

The average yield for the title compound was 94% (2 trials) at the 0.5 mmol scale, generated using General Procedure for Bromofunctionalization using 102 mg of the starting carboxylic acid (0.1M in MeCN), 85 μL diethyl bromomalonate, 10 mg **NMA,** 11.2 mg $CuBr_2$, 7.8 mg 2,2'-bipyridine, and an irradiation time of 16 hours. The average diasteromeric ratio was 2.1:1. The products were isolated by silica gel (3 mL dry silica, 2 cm column, DCM) as a white solid.

Analytical data for **3.53**:

^{1}H NMR Major/minor diastereomers: (600 MHz, Chloroform-*d*) δ 7.47 – 7.40 (m, 4H-2 major, 2 minor), 7.40 – 7.30 (m, 6H-3 major, 3 minor), 4.94 (d, *J* = 7.7 Hz, 1H-major), 4.90 (d, *J* = 6.8 Hz, 1H-minor), 4.84 (dtd, *J* = 9.5, 7.9, 6.1 Hz, 2H-1 major, 1 minor), 2.41 (dd, *J* = 13.0, 6.1 Hz, 1H-major), 2.09 (dd, *J* = 13.0, 9.6 Hz, 1H-major), 1.95 (dd, *J* = 13.0, 6.2 Hz, 1H-minor), 1.81 (dd, *J* = 13.1, 9.7 Hz, 1H-minor), 1.29 (d, *J* = 4.9 Hz, 6H-major), 1.25 (s, 3H-minor), 1.22 (s, 3H-minor).

^{13}C NMR Major/minor diastereomers: (151 MHz, Chloroform-*d*) δ 180.83 (major), 180.49 (minor), 137.40 (major), 137.07 (minor), 129.12 (minor), 129.03 (major), 128.90 (minor), 128.78 (major), 128.24 (minor), 128.19 (major), 78.92 (minor), 78.15 (major), 55.52 (major), 55.02 (minor), 42.25 (major), 41.48 (minor), 40.66 (minor), 40.64 (major), 24.80 (major), 24.74 (minor), 24.68 (major/minor).

IR (thin film cm^{-1}): 2969, 2360, 1774, 1455, 1205, 1119, 1035, 915, 699, 667

HRMS ***m/z*** **calculated** for $C_{13}H_{15}BrO_2$ $[H]^+$: 283.0328 and 285.0308; **found**: 283.0327 and 285.0306

5-(Chloro(phenyl)methyl)-3,3,5-trimethyldihydrofuran-2(3*H*)-one (3.55):

The average yield for the title compound was 76% (2 trials) at the 0.5 mmol scale, generated using General Procedure for Chlorofunctionalizations using 109 mg of the starting carboxylic acid (0.1M in MeCN), 90.8 mg NCP, 10 mg **NMA,** 6.7mg $CuCl_2$, 9mg of 1,10-phenanthroline, and an irradiation time of 2 hours. The average diastereomeric ratio was 1.3:1. The products were isolated by column chromatography on silica gel (25 mL dry silica, 2 cm column, 10% EtOAc/hexanes) as a colorless oil.

Analytical data for **3.55**:

^{1}H NMR Major/minor diastereomers: (600 MHz, Chloroform-*d*) δ 7.51 – 7.30 (m, 10H, 5 major, 5 minor), 4.94 (s, 1H-minor), 4.84 (s, 1H-major), 2.60 (d, *J* = 13.4 Hz, 1H-minor), 2.51 (d, *J* = 13.5 Hz, 1H-major), 1.93 (t, *J* = 13.8 Hz, 2H-1 major, 1 minor), 1.47 (s, 3H-minor), 1.46 (s, 3H-major), 1.33 (s, 3H-minor), 1.32 (s, 3H-major), 1.15 (s, 3H-minor), 1.07 (s, 3H-major).

^{13}C NMR Major/minor diastereomers:(151 MHz, $CDCl_3$) δ 181.53, 181.30, 136.44, 136.22, 129.01, 128.96, 128.85, 128.70, 128.45, 128.27, 83.74, 83.34, 68.95, 68.91, 44.69, 44.16, 40.73, 40.41, 28.60, 28.29, 27.46, 26.29, 26.08, 25.64.

IR (thin film cm^{-1}): 2974, 1773, 1455, 1236, 1093, 962, 755, 701

HRMS ***m/z*** **calculated** for $C_{14}H_{17}ClO_2$ $[H]^+$: 253.0990 and 255.0960; **found**: 253.0988 and 255.0959

5-(Chloro(4-chlorophenyl)methyl)dihydrofuran-2(3*H*)-one (3.57):

The average yield for the title compound was 72% (2 trials) at the 0.5 mmol scale, generated using General Procedure for Chlorofunctionalizations using 105 mg of the starting carboxylic acid (0.1M in MeCN), 90.8 mg NCP, 10 mg **NMA,** 6.7mg $CuCl_2$, 9mg of 1,10-phenanthroline, and an irradiation time of 2 hours. The average diasteromeric ratio was 2.7:1. The products were isolated by column chromatography on silica gel (25 mL dry silica, 2 cm column, 10% EtOAc/hexanes) as a low melting white solid.

Analytical data for **3.57**:

^{1}H NMR Major/minor diastereomers:(600 MHz, Chloroform-*d*) δ 7.39 (m, 8H-4 major, 4 minor), 5.00-4.98 (m, 2H-1 major, 1 minor), 4.89 (ddd, *J* = 7.7, 6.2, 4.6 Hz, 1H-minor), 4.83 (td, *J* = 7.1, 6.2 Hz, 1H-major), 2.59 – 2.55 (m, 2H-major), 2.54 – 2.45 (m, 1H-minor), 2.45 – 2.40 (m, 1H-major), 2.40 – 2.35 (m, 1H-minor), 2.33 – 2.23 (m, 2H-1 major, 1 minor), 2.14 (dddd, *J* = 13.6, 10.2, 7.7, 6.2 Hz, 1H-minor).

^{13}C NMR Major/minor diastereomers:(151 MHz, $CDCl_3$) δ 175.99 (minor), 175.87 (major), 135.09 (minor), 135.00 (major), 134.96 (major), 134.73 (minor), 129.35 (minor), 129.09 (major), 129.02 (major), 128.97 (minor), 81.70 (major), 81.49 (minor), 63.14 (major), 62.91 (minor), 28.22 (major), 27.97 (minor), 24.52 (major), 24.45 (minor).

IR (thin film cm^{-1}): 2925, 1779, 1493, 1174, 1091, 1015, 916

HRMS *m/z* **calculated** for $C_{11}H_{10}Cl_2O_2$ $[H]^+$: 245.0131 and 247.0101; **found**: 245.0131 and 247.0101

5-(Bromo(4-chlorophenyl)methyl)dihydrofuran-2(3*H*)-one (3.58)

The average yield for the title compound was 84% (2 trials) at the 0.5 mmol scale, generated using General Procedure for Bromofunctionalization using 105 mg of the starting carboxylic acid (0.1M in MeCN), 85 μL diethyl bromomalonate, 10 mg **NMA,** 11.2 mg $CuBr_2$, 7.8 mg 2,2'-bipyridine, and an irradiation time of 16 hours. The average diasteromeric ratio was 1.5:1. The products were isolated by silica gel (40 mL dry silica, 2.5 cm column, 10% EtOAc/hexanes then 30% EtOAc/hexanes) as a clear oil.

Analytical data for **3.58**:

^{1}H NMR Major/minor diastereomers: (600 MHz, Chloroform-*d*) δ 7.43 – 7.38 (m, 2H-1 major, 1 minor), 7.38 – 7.30 (m, 6 H-3 major, 3 minor), (d, *J* = , 1H-minor), 4.93 (d, *J* = 7.4 Hz, 1H-major), 4.91 – 4.82 (m, 2H-1 major, 1 minor), 2.58 – 2.45 (m, 5H-3 major, 2 minor), 2.31 – 2.24 (m, 1H-minor), 2.24 – 2.16 (m, 1H-major), 2.05 (ddq, *J* = 8.5, 5.0, 1.8 Hz, 1H-minor).

^{13}C NMR Major/minor diastereomers: (151 MHz, Chloroform-*d*) δ 175.94 (minor), 175.92 (major), 135.80 (major), 135.66 (minor), 135.05(minor), 134.96 (major), 129.87 (major), 129.65

(minor), 129.09 (major/minor), 81.61 (minor), 81.50 (major), 54.48 (minor), 54.20 (major), 28.62 (major), 28.31 (minor), 26.63 (major), 25.76 (minor).

IR (thin film cm^{-1}): 1777, 1492, 1168, 1014, 915, 836

HRMS *m/z* **calculated** for $C_{11}H_{10}ClBrO_2$ $[H]^+$:288.9625 and 290.9605; **found**: 288.9625 and 290.9605

5-(Chloro(4-methoxyphenyl)methyl)dihydrofuran-2(3*H*)-one (3.60):

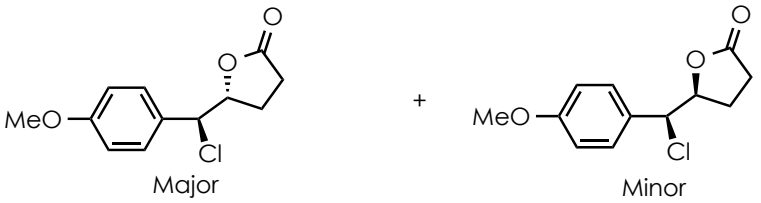

The average yield for the title compound was 64% (2 trials) at the 0.5 mmol scale, generated using General Procedure for Chlorofunctionalizations using 103 mg of the starting carboxylic acid (0.1M in DCE), 90.8 mg NCP, 10 mg **NMA,** 6.7mg $CuCl_2$, 9mg of 1,10-phenanthroline, and an irradiation time of 2 hours. The average diasteromeric ratio was 2.2:1. To separate from phthalimide, after the 2 hour reaction time the reaction was transferred to a separatory funnel and washed with a 10% NaOH solution and H_2O. The aqueous layer was back-extracted twice with DCM. The combined organics were dried and concentrated giving a dark brown oil. The products were isolated by column chromatography on silica gel (25 mL dry silica, 2 cm column, 20% EtOAc/hexanes) as a low melting white solid.

Analytical data for **3.60**:

^{1}H NMR Major/minor diastereomers: (600 MHz, Chloroform-*d*) δ 7.38 – 7.35 (m, 2H-minor), 7.35 – 7.32 (m, 2H-major), 6.93 – 6.87 (m, 4H-2 major, 2 minor), 5.00 (d, *J* = 5.8 Hz, 1H-

major), 4.94 (d, J = 5.2 Hz, 1H-minor), 4.87 (ddd, J = 7.6, 6.2, 5.2 Hz, 1H-minor), 4.84 (ddd, J = 7.3, 6.6, 5.8 Hz, 1H-major), 3.81 (s, 6H-3 major, 3 minor), 2.54 – 2.48 (m, 2H-major), 2.45 – 2.42 (m, 1H-minor), 2.42 – 2.34 (m, 1H-major), 2.32 – 2.25 (m, 2H-1 major, 1 minor), 2.24 – 2.16 (m, 1H-minor), 2.09 (dddd, J = 13.6, 10.2, 7.6, 6.2 Hz, 1H-minor).

^{13}C NMR Major/minor diastereomers:(151 MHz, $CDCl_3$) δ 176.27 (minor), 176.20 (major), 160.04 (minor), 159.98 (major), 129.21 (minor), 129.01 (major), 128.36 (major), 128.08 (minor), 114.13 (major), 114.10 (minor), 82.09 (minor), 82.04 (major), 63.86 (major), 63.43 (minor), 55.33 (major), 55.32 (minor), 28.28 (major), 28.08 (minor), 24.53 (minor), 24.42 (major).

IR (thin film cm^{-1}): 2936, 2839, 1778, 1611, 1514, 1252, 1177, 1029, 836

HRMS *m/z* **calculated** for $C_{12}H_{13}ClO_3$ $[H]^+$: 241.0626 and 243.0596; **found:** 241.0625 and 243.0596

5-(Chloro(*o*-tolyl)methyl)dihydrofuran-2(3*H*)-one (3.62):

The average yield for the title compound was 72% (2 trials) at the 0.5 mmol scale, generated using General Procedure for Chlorofunctionalizations using 95 mg of the starting carboxylic acid (0.1M in MeCN), 90.8 mg NCP, 10 mg **NMA,** 6.7mg $CuCl_2$, 9mg of 1,10-phenanthroline, and an irradiation time of 2 hours. The average diastereomeric ratio was 2.9:1. The products were isolated by column chromatography on silica gel (25 mL dry silica, 2 cm column, 10% EtOAc/hexanes) as a colorless oil.

Analytical data for **3.62**:

^{1}H NMR Major/minor diastereomers: (600 MHz, Chloroform-*d*) δ 7.61 – 7.54 (m, 1H-minor), 7.51 (dd, *J* = 7.3, 1.9 Hz, 1H-major), 7.31 – 7.22 (m, 4H-2 major, 2 minor), 7.20 – 7.17 (m, 2H-1 major, 1 minor), 5.32 (d, *J* = 6.2 Hz, 1H-major), 5.21 (d, *J* = 5.7 Hz, 1H-minor), 4.98 (ddd, *J* = 7.5, 6.9, 5.7 Hz, 1H-minor), 4.87 (td, *J* = 7.0, 6.2 Hz, 1H-major), 2.65 (ddd, *J* = 17.9, 9.8, 5.4 Hz, 1H-major), 2.57 (ddd, *J* = 18.1, 9.7, 8.9 Hz, 1H-major), 2.53 – 2.44 (m, 2H-minor), 2.44 – 2.35 (m, 8H-5 major, 3 minor), 2.30 – 2.21 (m, 1H-1 minor), 2.06 (dddd, *J* = 13.4, 9.8, 8.4, 6.7 Hz, 1H-1minor).

^{13}C NMR Major/minor diastereomers:(151 MHz, $CDCl_3$) δ 175.94 (major), 175.80 (minor), 135.51(major), 135.44 (minor), 134.62 (minor), 134.60 (major), 130.64 (minor), 130.55 (major), 128.75 (minor), 128.59 (major), 127.78 (minor), 127.05 (major), 126.56 (minor), 126.43 (major), 81.76 (minor), 80.80 (major), 60.17 (major), 59.79 (minor), 28.19 (major), 28.02 (minor), 25.06 (minor), 24.32 (major), 19.32 (minor), 19.12 (major).

IR (thin film cm^{-1}): 2919.7, 1784, 1460, 1169, 917, 734

HRMS *m/z* **calculated** for $C_{12}H_{13}ClO_2$ $[H]^+$: 225.0677 and 227.0647; **found:** 225.0676 and 227.0647

5-(Bromo(*o*-tolyl)methyl)dihydrofuran-2(3*H*)-one (3.63)

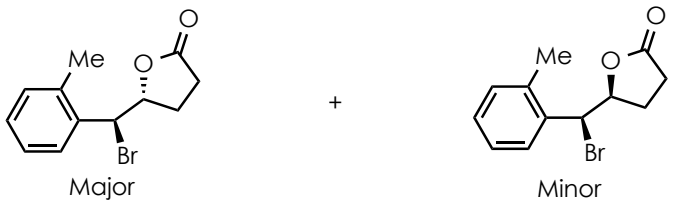

The average yield for the title compound was 83% (2 trials) at the 0.5 mmol scale, generated using General Procedure for Bromofunctionalization using 95 mg of the starting carboxylic acid

(0.1M in MeCN), 85 μL diethyl bromomalonate, 10 mg **NMA,** 11.2 mg $CuBr_2$, 7.8 mg 2,2'-bipyridine, and an irradiation time of 16 hours. The average diasteromeric ratio was 1.6:1. The products were isolated by silica gel (40 mL dry silica, 2.5 cm column, 10% EtOAc/hexanes then 30% EtOAc/hexanes) as a white solid.

Analytical data for **3.63**:

^{1}H NMR Major/minor diastereomers: (600 MHz, Chloroform-*d*) δ 7.59 – 7.53 (m, 1H-minor), 7.50 (dd, *J* = 7.4, 1.7 Hz, 1H-major), 7.26 – 7.19 (m, 4H-2 major, 2 minor), 7.19 – 7.14 (m, 2H-1 major, 1 minor), 5.26 (d, *J* = 7.7 Hz, 1H-major), 5.22 (d, *J* = 6.3 Hz, 1H-minor), 5.01 (dq, *J* = 16.4, 7.3 Hz, 2H-1 major, 1 minor), 2.68 – 2.51 (m, 5H- 3 major, 2 minor), 2.39 (d, *J* = 3.2 Hz, 6H-3 major, 3 minor), 2.36 – 2.23 (m, 2H-1 major, 1 minor), 1.94 (dtd, *J* = 13.3, 9.4, 7.4 Hz, 1H-minor).

^{13}C NMR Major/minor diastereomers: (151 MHz, Chloroform-*d*) δ 176.04 (major), 175.79 (minor), 135.92 (major), 135.62 (minor), 135.58 (minor), 135.50 (major), 130.88 (minor), 130.80 (major), 128.95 (minor), 128.83 (major), 128.22 (minor), 127.63 (major), 126.88 (minor), 126.67 (major), 82.00 (minor), 80.76 (major), 51.91 (major), 51.42 (minor), 28.68 (major), 28.51 (minor), 26.98 (major), 26.35 (minor), 19.44 (minor), 19.31 (major).

IR (thin film cm^{-1}): 1777, 1174, 1022, 916, 728, 657

HRMS *m/z* **calculated** for $C_{12}H_{13}BrO_2$ $[H]^+$:269.0172 and 271.0151; **found:** 269.0171 and 271.0150

5-(2-Chloropropan-2-yl)-3,3-diphenyldihydrofuran-2(3*H*)-one (3.65):

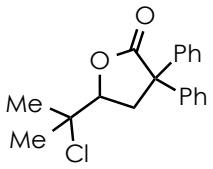

The average yield for the title compound was 63% (2 trials) at the 0.5 mmol scale, generated using General Procedure for Chlorofunctionalizations using 140 mg of the starting carboxylic acid (0.1M in DCE), 90.8 mg NCP, 10 mg **NMA,** 6.7mg $CuCl_2$, 9mg of 1,10-phenanthroline, 150μL of 95:5 Acetic acid:Acetic anhydride, and an irradiation time of 3 hours. The products were isolated by column chromatography on silica gel (25 mL dry silica, 2 cm column, 5% EtOAc/hexanes) as a white crystalline solid.

Analytical data for **3.65**:

^{1}H NMR (400 MHz, Chloroform-*d*) δ 7.59 – 7.12 (m, 10H), 4.30 (dd, *J* = 10.6, 5.2 Hz, 1H), 3.09 (dd, *J* = 13.2, 5.2 Hz, 1H), 2.96 (dd, *J* = 13.2, 10.6 Hz, 1H), 1.68 (s, 3H), 1.62 (s, 3H).

^{13}C NMR (151 MHz, $CDCl_3$) δ 176.41, 141.92, 139.17, 129.04, 128.44, 127.95, 127.71, 127.34, 127.32, 81.88, 68.18, 58.35, 39.38, 29.18, 27.88.

IR (thin film cm^{-1}): 3060, 2979, 1770, 1496, 1447, 1170, 698

HRMS *m/z* **calculated** for $C_{19}H_{19}ClO_2$ $[H]^+$: 315.1146 and 317.1117; **found:** 315.1145 and 317.1116

5-(4-((*tert*-Butyldimethylsilyl)oxy)-2-chlorobutan-2-yl)-3,3-dimethyldihydrofuran-2(3*H*)-one (3.67):

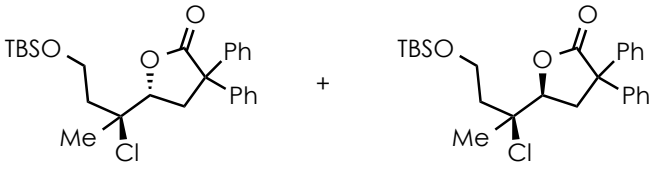

The average yield for the title compound was 47% (2 trials) at the 0.5 mmol scale, generated using General Procedure for Chlorofunctionalizations using 150 mg of the starting carboxylic acid as a mixture of alkene isomers (0.1M in DCE), 90.8 mg NCP, 10 mg **NMA,** 6.7mg $CuCl_2$, 9mg of 1,10-phenanthroline, 150μL of 95:5 Acetic acid:Acetic anhydride, and an irradiation time of 3 hours. The average diastereoisomeric ratio was 1.1:1. The products were isolated by column chromatography on silica gel (25 mL dry silica, 2 cm column, 5% EtOAc/hexanes), diastereomers could be separated on silica gel and thus were characterized separately. Both appeared as clear viscous oils.

Analytical data for **3.67-major**:

^{1}H NMR (600 MHz, Chloroform-*d*) δ 4.59 (t, *J* = 8.1 Hz, 1H), 3.84 (dd, *J* = 6.8, 5.7 Hz, 2H), 2.15 (d, *J* = 8.1 Hz, 2H), 2.01 (td, *J* = 6.3, 5.8, 4.7 Hz, 2H), 1.65 (s, 3H), 1.31 (s, 3H), 1.28 (s, 3H), 0.89 (s, 9H), 0.06 (d, *J* = 0.8 Hz, 6H).

^{13}C NMR (151 MHz, $CDCl_3$) δ 181.25, 80.94, 71.94, 59.22, 43.22, 40.33, 38.65, 25.88, 25.43, 25.42, 24.69, 18.19, -5.44, -5.47.

IR (thin film cm^{-1}):2956, 2930, 2857, 1780, 1463, 1255, 1122, 835, 778

HRMS *m/z* **calculated** for $C_{26}H_{35}ClO_3Si[H]^+$: 335.1804 and 337.1774; **found:** 335.1802 and 337.1772

Analytical data for **3.67-minor**:

^{1}H NMR (600 MHz, Chloroform-*d*) δ 4.54 (dd, *J* = 9.5, 6.7 Hz, 1H), 3.90 – 3.84 (m, 2H), 2.23 – 2.04 (m, 4H), 1.54 (s, 3H), 1.31 (s, 3H), 1.29 (s, 3H), 0.89 (s, 9H), 0.06 (d, *J* = 1.4 Hz, 6H).

^{13}C NMR (151 MHz, $CDCl_3$) δ 181.08, 81.15, 72.16, 59.52, 42.78, 40.33, 38.53, 25.87, 25.56, 25.33, 24.65, 18.18, -5.42, -5.45.

IR (thin film cm^{-1}): 2956, 2930, 2857, 1780, 1463, 1255, 1101, 835, 778

HRMS *m/z* **calculated** for $C_{26}H_{35}ClO_3Si[H]^+$: 335.1804 and 337.1774; **found:** 335.1802 and 337.1773

5-Chloro-5-phenyltetrahydro-2H-pyran-2-one (3.69):

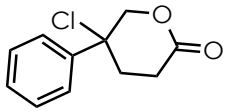

The average yield for the title compound was 54% (2 trials) at the 0.5 mmol scale, generated using General Procedure for Chlorofunctionalizations using 88.4 mg of the starting carboxylic acid (0.1M in DCE), 67 mg NCS, 10 mg **NMA,** 6.7mg $CuCl_2$, 9mg of 1,10-phenanthroline, and an irradiation time of 2 hours. After the reaction, the contents were transferred to a separatory funnel and diluted with DCM. The organic layer was washed with H_2O to remove succinimide. The aqueous layer was extracted twice more with DCM. All organics were combined and dried over Na_2SO_4. The organics were passed through a small plug of silica to remove any remaining Cu or acridinium impurities. After removing the solvent in vacuo the title compound was found to be clean by NMR.

Analytical data for **3.69**:

^{1}H NMR: (600 MHz, Chloroform-*d*) δ 7.58 – 7.54 (m, 2H), 7.46 – 7.42 (m, 2H), 7.41 – 7.37 (m, 1H), 4.68 (dd, *J* = 12.4, 2.6 Hz, 1H), 4.62 (dd, *J* = 12.3, 0.6 Hz, 1H), 3.08 – 2.98 (m, 1H), 2.76 – 2.67 (m, 2H), 2.66 – 2.59 (m, 1H).

^{13}C NMR: (151 MHz, $CDCl_3$) δ 168.32, 139.10, 129.19, 129.00, 125.79, 76.92, 66.05, 34.04, 27.58.

IR (thin film cm^{-1}): 2932, 1744, 1447, 1399, 1263, 1186, 1089, 753

HRMS *m/z* **calculated** for $C_{11}H_{11}ClO_2$ $[H]^+$:211.0520 and 213.0491; **found:** 211.0520 and 213.0491

5-Chloro-5-(*p*-tolyl)tetrahydro-2*H*-pyran-2-one (3.71):

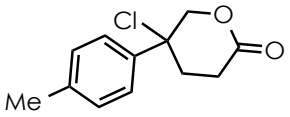

The average yield for the title compound was 50% (2 trials) at the 0.5 mmol scale, generated using General Procedure for Chlorofunctionalizations using 95 mg of the starting carboxylic acid (0.1M in DCE), 67 mg NCS, 10 mg **NMA,** 6.7mg $CuCl_2$, 9mg of 1,10-phenanthroline, and an irradiation time of 2 hours. After the reaction, the contents were transferred to a separatory funnel and diluted with DCM. The organic layer was washed with H_2O to remove succinimide. The aqueous layer was extracted twice more with DCM. All organics were combined and dried over Na_2SO_4. The organics were passed through a small plug of silica to remove any remaining

Cu or acridinium impurities. After removing the solvent in vacuo the title compound was found to be clean by NMR.

Analytical data for **3.71**:

^{1}H NMR: (600 MHz, Chloroform-*d*) δ 7.44 (d, *J* = 8.3 Hz, 2H), 7.24 (d, *J* = 8.1 Hz, 2H), 4.67 (dd, *J* = 12.3, 2.5 Hz, 1H), 4.60 (d, *J* = 12.4 Hz, 1H), 3.06 – 2.97 (m, 1H), 2.71 (dt, *J* = 7.1, 3.7 Hz, 1H), 2.68 (q, *J* = 7.4, 6.6 Hz, 1H), 2.65 – 2.59 (m, 1H), 2.37 (s, 3H).

^{13}C NMR: (151 MHz, $CDCl_3$) δ 168.32, 139.28, 136.21, 129.66, 125.69, 76.82, 66.05, 34.11, 27.64, 21.05.

IR (thin film cm^{-1}):1775, 1740, 1644, 1180, 818, 736

HRMS *m/z* **calculated** for $C_{12}H_{13}ClO_2$ $[H]^+$:225.0677 and 227.0647; **found:** 225.0677 and 227.0648

5-Chloro-5-(4-chlorophenyl)tetrahydro-2H-pyran-2-one (3.73):

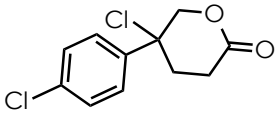

The average yield for the title compound was 57% (2 trials) at the 0.5 mmol scale, generated using General Procedure for Chlorofunctionalizations using 105 mg of the starting carboxylic acid (0.1M in DCE), 67 mg NCS, 10 mg **NMA,** 6.7mg $CuCl_2$, 9mg of 1,10-phenanthroline, and an irradiation time of 2 hours. After the reaction, the contents were transferred to a separatory funnel and diluted with DCM. The organic layer was washed with H_2O to remove succinimide.

The aqueous layer was extracted twice more with DCM. All organics were combined and dried over Na_2SO_4. The organics were passed through a small plug of silica to remove any remaining Cu or acridinium impurities. After removing the solvent in vacuo the title compound was found to be clean by NMR.

Analytical data for **3.73**:

^{1}H NMR: (600 MHz, Chloroform-*d*) δ 7.50 (d, *J* = 8.7 Hz, 2H), 7.41 (d, *J* = 8.7 Hz, 2H), 4.65 (dd, *J* = 12.4, 2.4 Hz, 1H), 4.60 (d, *J* = 12.3 Hz, 1H), 3.01 (ddd, *J* = 19.6, 9.5, 7.3 Hz, 1H), 2.72 – 2.64 (m, 2H), 2.61 (dtt, *J* = 13.8, 7.0, 3.4 Hz, 1H).

^{13}C NMR: (151 MHz, $CDCl_3$) δ 167.92, 137.75, 135.28, 129.21, 127.32, 76.63, 65.40, 34.27, 27.53.

IR (thin film cm^{-1}): 1745, 1495, 1401, 1186, 1086, 1013, 811, 578

HRMS *m/z* **calculated** for $C_{11}H_{10}Cl_2O_2$ $[H]^+$:245.0131 and 247.0101; **found:** 245.0131 and 247.0101

5-(Chloro(4-chlorophenyl)methyl)dihydrofuran-2(3*H*)-one (3.75):

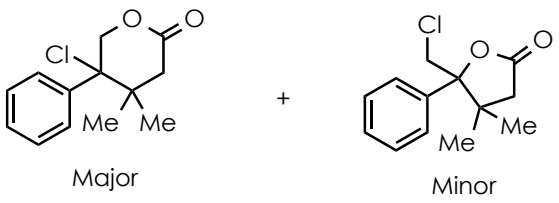

Major Minor

The average yield for the title compound was 72% (2 trials) at the 0.5 mmol scale, generated using General Procedure for Chlorofunctionalizations using 102 mg of the starting carboxylic acid (0.1M in DCE), 90.8 mg NCP, 10 mg **NMA,** 6.7mg $CuCl_2$, 9mg of 1,10-phenanthroline, and an irradiation time of 2 hours. The average regioisomeric ratio was 19:1. The products were isolated by column chromatography on silica gel (25 mL dry silica, 2 cm column, 10% EtOAc/hexanes) as a white solid.

Analytical data for **3.75**:

^{1}H NMR Major/minor regioisomers:(600 MHz, Chloroform-*d*) δ 7.73 – 7.49 (m, 4H-2 major, 2 minor), 7.49 – 7.35 (m, 6H-3 major, 3 minor), 5.24 (d, *J* = 12.5 Hz, 1H-major), 4.70 (d, *J* = 12.4 Hz, 1H-major), 4.10 (d, *J* = 12.4 Hz, 1H-minor), 3.97 (d, *J* = 12.4 Hz, 1H-minor), 3.01 (d, 1H-minor), 2.83 (d, *J* = 18.0 Hz, 1H-major), 2.38 (d, *J* = 18.1 Hz, 2H-1 major, 1 minor), 1.46 (s, 3H-minor), 1.19 (s, 3H-major), 1.06 (s, 3H-major), 0.70 (s, 3H-minor).

^{13}C NMR Major/minor regioisomers: (151 MHz, $CDCl_3$) δ 174.69 (minor), 169.08 (major), 137.66 (minor), 137.21 (major), 128.67 (major), 128.58 (minor), 128.41 (minor), 128.26 (minor), 128.05 (major), 127.96 (major), 124.49 (minor), 90.92 (minor), 75.46 (major), 74.48 (major), 49.26 (minor), 44.87 (minor), 42.57 (major), 39.40 (major), 28.11 (minor), 25.11 (major), 24.85 (major), 22.20 (minor).

IR (thin film cm^{-1}): 2977, 1744, 1445, 1251, 1213, 1068, 701, 641

HRMS *m/z* **calculated** for $C_{13}H_{15}ClO_2$ $[H]^+$:239.0833 and 241.0804; **found:** 239.0832 and 241.0803

5-Bromo-4,4-dimethyl-5-phenyltetrahydro-2*H*-pyran-2-one (3.76)

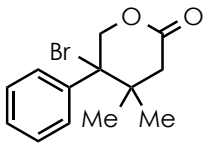

The average yield for the title compound was 84% (2 trials) at the 0.5 mmol scale, generated using General Procedure for Bromofunctionalization using 102 mg of the starting carboxylic acid (0.1M in MeCN), 85 μL diethyl bromomalonate, 10 mg **NMA,** 11.2 mg $CuBr_2$, 7.8 mg 2,2'-bipyridine, 6 μL 2,6-lutidine, and an irradiation time of 16 hours. The products were isolated by silica gel (40 mL dry silica, 2.5 cm column, 10% EtOAc/hexanes) as an off-white solid.

Analytical data for **3.76**:

^{1}H NMR : (600 MHz, Chloroform-*d*) δ 7.59 (dd, *J* = 8.0, 1.7 Hz, 2H), 7.40 – 7.31 (m, 3H), 5.23 (d, *J* = 12.5 Hz, 1H), 4.92 (d, *J* = 12.5 Hz, 1H), 2.73 (d, *J* = 18.0 Hz, 1H), 2.35 (d, *J* = 18.0 Hz, 1H), 1.34 (s, 3H), 1.09 (s, 3H).

^{13}C NMR: (151 MHz, Chloroform-*d*) δ 168.98, 138.41, 128.97, 128.72, 127.93, 75.08, 73.01, 42.98 , 39.78, 27.04, 24.63.

IR (thin film cm^{-1}): 2972, 1744, 1444, 1250, 1067, 701

HRMS *m/z* **calculated** for $C_{13}H_{15}BrO_2$ $[H]^+$:283.0328 and 285.0308; **found:** 283.0324 and 285.0307

5-Chloro-3,3-dimethyl-5-phenyltetrahydro-2*H*-pyran-2-one (3.78):

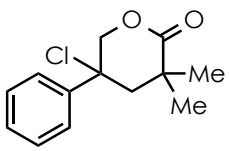

The average yield for the both regioisomers was 66% (2 trials) at the 0.5 mmol scale, generated using General Procedure for Chlorofunctionalizations using 102 mg of the starting carboxylic acid (0.1M in DCE), 67 mg NCS, 10 mg **NMA,** 6.7mg $CuCl_2$, 9mg of 1,10-phenanthroline, and an irradiation time of 2 hours. After the reaction, the contents were transferred to a separatory funnel and diluted with DCM. The organic layer was washed with H_2O to remove succinimide. The aqueous layer was extracted twice more with DCM. All organics were combined and dried over Na_2SO_4. The organics were passed through a small plug of silica to remove any remaining Cu or acridinium impurities. After removing the solvent in vacuo the title compounds were isolated as a mixture of regioisomers (4.4:1). The major regioisomer could be isolated by column chromatography on silica gel (15 mL dry silica, 2 cm column, 5% EtOAc/hexanes) as a white solid.

Analytical data for **3.78**:

^{1}H NMR Major regioisomer:(600 MHz, Chloroform-*d*) δ 7.59 – 7.50 (m, 2H), 7.42 (td, *J* = 7.3, 6.3, 1.4 Hz, 2H), 7.39 – 7.35 (m, 1H), 4.77 (d, *J* = 11.8 Hz, 1H), 4.69 (dd, *J* = 11.9, 1.9 Hz, 1H), 2.67 – 2.60 (m, 2H), 1.50 (s, 3H), 1.19 (s, 3H).

^{13}C NMR Major regioisomers: ^{13}C NMR (151 MHz, $CDCl_3$) δ 175.61, 139.57, 129.05, 128.93, 125.87, 75.05, 66.57, 50.43, 37.98, 30.16, 30.05.

IR (thin film cm^{-1}): 2977, 2359, 1739, 1447, 1389, 1134, 1064, 762, 697

HRMS *m/z* **calculated** for $C_{13}H_{15}ClO_2$ $[H]^+$:239.0833 and 241.0804; **found:** 239.0832 and 241.0803

5-Chloro-3,3-dimethyl-5-phenyltetrahydro-2*H*-pyran-2-one (3.80):

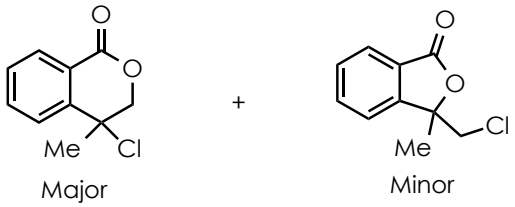

The average yield for the both regioisomers was 64% (2 trials) at the 0.5 mmol scale, generated using General Procedure for Chlorofunctionalizations using 81.1 mg of the starting carboxylic acid (0.1M in DCE), 67 mg NCS, 10 mg **NMA,** 6.7mg $CuCl_2$, 9mg of 1,10-phenanthroline, and 150μL of 95:5 Acetic acid:Acetic anhydride an irradiation time of 2 hours. After the reaction, the contents were transferred to a separatory funnel and diluted with DCM. The organic layer was washed with H_2O to remove succinimide. The aqueous layer was extracted twice more with DCM. All organics were combined and dried over Na_2SO_4. The average regioisomeric ratio was 2.5:1. Purified on column chromatography on silica gel (25 mL dry silica, 2 cm column, 10% EtOAc:Hexanes).

Analytical data for **3.80**:

^{1}H NMR Major/minor regioisomers (600 MHz, Chloroform-*d*) δ 8.13 (dd, *J* = 7.8, 1.4 Hz, 1H-major), 7.91 (dt, *J* = 7.7, 1.0 Hz, 1H-minor), 7.72 – 7.64 (m, 4H-2 major, 2 minor), 7.58 (td, *J* = 7.5, 1.0 Hz, 1H-minor), 7.51 (td, *J* = 7.5, 1.5 Hz, 1H-major), 4.62 (d, *J* = 11.7 Hz, 1H-major), 4.49 (d, *J* = 11.6 Hz, 1H-major), 3.91 – 3.75 (m, 2H-minor), 1.99 (s, 3H-major), 1.78 (s, 3H-minor).

^{13}C NMR Major/minor regioisomers (151 MHz, $CDCl_3$) δ 163.54 (major), 150.76 (minor), 143.22 (major/minor), 134.57 (major), 134.28 (minor), 130.78 (major), 129.80 (minor), 129.38 (major), 126.25 (minor), 125.93 (minor), 124.48 (major), 122.91 (major), 121.59 (minor), 85.16 (minor), 75.83 (major), 61.54 (major), 49.51 (minor), 27.64 (major), 23.51 (minor).

IR (thin film cm^{-1}):2926, 1768, 1735, 1604, 1464, 1281, 1247, 1102, 765

HRMS *m/z* **calculated** for $C_{10}H_9ClO_2$ $[H]^+$:197.0364 and 199.0334; **found:** 197.0363 and 199.0334

2-Chloro(phenyl)methyl)-4,4-dimethyltetrahydrofuran (3.84):

The average yield for the title compound was 61% (2 trials) at the 0.5 mmol scale, generated using General Procedure for Chlorofunctionalizations using 95.1 mg of the starting alcohol (0.1M in MeCN), 90.8 mg NCP, 10 mg **NMA,** 6.7mg $CuCl_2$, 9mg of 1,10-phenanthroline, and an irradiation time of 2 hours. The average diastereomeric ratio was 1.9:1. The products were isolated by column chromatography on silica gel (25 mL dry silica, 2 cm column, 5% EtOAc/hexanes) as a colorless oil.

Analytical data for **3.84**:

^{1}H NMR Major/minor diastereomers: (600 MHz, Chloroform-*d*) δ 7.45 – 7.39 (m, 4H-2 major, 2 minor), 7.38 – 7.34 (m, 4H-2 major, 2 minor), 7.34 – 7.29 (m, 2H-1 major, 1 minor), 4.86 (d, *J* =

7.0 Hz, 1H-major), 4.78 (d, *J* = 7.5 Hz-1H, minor), 4.55 – 4.40 (m, 2H-1 major, 1 minor), 3.60 – 3.54 (m, 3H-1 major, 2 minor), 3.51 (d, 1H, J = 8.3 Hz-major), 1.92 (dd, J = 12.6, 6.8 Hz, 1H-major), 1.83 (dd, *J* = 12.6, 9.0 Hz, 1H-major), 1.51 (dd, *J* = 12.6, 6.7 Hz, 1H-minor), 1.42 (dd, 12.6, 9.4 Hz, 1H-minor), 1.11 (s, 3H-major), 1.09 (s, 3H-major), 1.06 (s, 3H-minor), 1.04 (s, 3H-minor).

^{13}C NMR Major/minor diastereomers: (151 MHz, $CDCl_3$) δ 138.94 (major), 138.74 (minor), 128.57 (major), 128.53 (minor), 128.49 (major), 128.42 (minor), 127.80 (minor), 127.72 (major), 82.86 (minor), 82.46 (major), 80.79 (major), 80.54 (minor), 66.43 (minor), 65.88 (major), 44.50 (minor), 44.16 (major), 40.03 (minor), 39.81 (major), 26.30 (major), 26.23 (minor), 25.79 (minor), 25.55 (major).

IR (thin film cm^{-1}): 2959, 2869, 1726, 1496, 1453, 1368, 1062, 698

HRMS ***m/z*** **calculated** for $C_{13}H_{17}ClO$ $[H]^+$:225.1041, and 227.1011; **found:** 225.1040, and 227.1014

2-Bromo(phenyl)methyl)-4,4-dimethyltetrahydrofuran (3.85):

The average yield for the title compound was 71% (2 trials) at the 0.5 mmol scale, generated using General Procedure for Bromofunctionalization using 95.1 mg of the starting alcohol (0.1M in MeCN), 85 μL diethyl bromomalonate, 10 mg **NMA,** 11.2 mg $CuBr_2$, 7.8 mg 2,2'-bipyridine, and an irradiation time of 16 hours. The average diasteromeric ratio was 1.9:1. The products

were isolated by silica gel (40 mL dry silica, 2.5 cm column, 10% EtOAc/hexanes, 20% EtOAc/hexanes, then 30% EtOAc/hexanes) as a colorless oil.

Analytical data for **3.85**:

^{1}H NMR Major/minor diastereomers: (600 MHz, Chloroform-*d*) δ 7.43 (dd, *J* = 11.3, 7.5 Hz, 4H-2 major, 2 minor), 7.39 – 7.32 (m, 4H-2 major, 2 minor), 7.29 (q, *J* = 7.0, 6.1 Hz, 2H-1 major, 1 minor), 4.90 (d, *J* = 7.9 Hz, 1H-major), 4.87 (d, *J* = 7.8 Hz, 1H-minor), 4.59 (qd, *J* = 9.0, 6.8 Hz, 2H-1 major, 1 minor), 3.61 (d, *J* = 2.4 Hz, 2H-minor), 3.59 – 3.51 (m, 2H-major), 2.07 (dd, *J* = 12.6, 6.4 Hz, 1H-major), 1.79 (dd, *J* = 12.6, 8.9 Hz, 1H-major), 1.59 – 1.55 (m, 1H-minor), 1.39 (dd, *J* = 12.6, 9.2 Hz, 1H-minor), 1.11 (s, 6H-major), 1.08 (s, 3H-minor), 1.06 (s, 3H-minor).

^{13}C NMR Major/minor diastereomers: (151 MHz, Chloroform-*d*) δ 139.50 (major), 139.37 (minor), 128.66 (minor), 128.58 (major), 128.52 (minor), 128.45 (major), 128.16 (major), 128.08 (minor), 82.71 (minor), 82.01 (major), 80.87 (major), 80.47 (minor), 58.47 (minor), 58.06 (major), 46.08 (major), 45.30 (minor), 40.27 (minor), 39.95 (major), 26.32 (minor/major), 25.95 (minor), 25.59 (major).

IR (thin film cm^{-1}): 3031, 2959, 2868, 1496, 1454, 1368, 1059, 697, 664

HRMS *m/z* **calculated** for $C_{13}H_{17}BrO$ $[H]^+$:269.0536, and 271.0515; **found:**269.0535, and 271.0514

3-Chloro-3-phenyltetrahydro-2*H*-pyran (3.87):

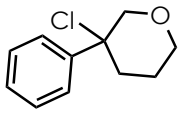

The average yield for the title compound was 57% (2 trials) at the 0.5 mmol scale, generated using General Procedure for Chlorofunctionalizations using 81 mg of the starting alcohol (0.1M in DCE), 67 mg NCS, 10 mg **NMA,** 6.7mg $CuCl_2$, 9mg of 1,10-phenanthroline, and an irradiation time of 2 hours. After the reaction, the contents were transferred to a separatory funnel and diluted with DCM. The organic layer was washed with H_2O to remove succinimide. The aqueous layer was extracted twice more with DCM. All organics were combined and dried over Na2SO_4. The organics were *p*assed through a small plug of silica to remove any remaining Cu or acridinium impurities. After removing the solvent in vacuo the title compound was obtained as a single regioisomer. The product was found to be volatile, therefore the use of high vacuum was avoided.

Analytical data for **3.87**:

^{1}H NMR (600 MHz, Chloroform-*d*) δ 7.61 – 7.56 (m, 2H), 7.39 (dd, *J* = 8.4, 6.9 Hz, 2H), 7.35 – 7.29 (m, 1H), 4.06 (dd, *J* = 12.2, 1.6 Hz, 1H), 3.99 (d, *J* = 12.3 Hz, 1H), 3.91 (dt, *J* = 11.5, 4.7 Hz, 1H), 3.62 (ddd, *J* = 11.7, 8.6, 3.3 Hz, 1H), 2.45 (dd, *J* = 9.2, 4.2 Hz, 1H), 2.41 (dddd, *J* = 13.8, 6.8, 3.0, 2.0 Hz, 1H), 2.09 (tq, *J* = 8.9, 4.4 Hz, 1H), 1.64 – 1.58 (m, 1H).

^{13}C NMR (151 MHz, $CDCl_3$) δ 142.02, 128.47, 128.16, 126.31, 76.16, 69.25, 67.99, 37.94, 23.20.

IR (thin film cm^{-1}): 2958, 2852, 1723, 1685, 1493, 1447, 1099, 1030, 755, 698, 587

LRMS *m/z* **calculated** for $C_{11}H_{13}ClO+$**:** 196.06 and 198.06, **found:** 196.10 and 198.05

***tert*-Butyl 2-(chloro(phenyl)methyl)-4,4-dimethylpyrrolidine-1-carboxylate (3.89)**

The average yield for the title compound was 59% (2 trials) at the 0.5 mmol scale, generated using General Procedure for Chlorofunctionalizations using 144.7 mg of the starting amine (0.1M in DCE), 90.8 mg NCP, 10 mg **NMA,** 6.7mg $CuCl_2$, 9mg of 1,10-phenanthroline, and an irradiation time of 3 hours. The average diastereomeric ratio was 1.2:1. The products were isolated by column chromatography on silica gel (40 mL dry silica, 2.5 cm column, 10% EtOAc/hexanes) as a colorless oil.

Analytical data for **3.89**:

^{1}H NMR Major/minor diastereomers: (600 MHz, Chloroform-*d*) δ 7.44 (d, *J* = 7.3 Hz, 2H-1 major, 1 minor), 7.36 – 7.26 (m, 8H-4 major, 4 minor), 6.04 (d, *J* = 3.0 Hz, 1H-major), 5.75 (d, *J* = 3.1 Hz, 1H-minor), 4.21 (ddd, *J* = 9.9, 7.3, 3.0 Hz, 1H-major), 4.17 – 4.08 (m, 1H-minor), 3.52 (dd, *J* = 10.5, 1.9 Hz, 1H-minor), 3.35 (dd, *J* = 10.5, 1.8 Hz, 1H-major), 3.08 (dd, *J* = 12.7, 10.5 Hz, 2H- 1 major, 1 minor), 2.03 (ddd, *J* = 22.0, 12.6, 9.3 Hz, 2H-1 major, 1 minor), 1.56 (s, 9H-minor), 1.50 (s, 9H-major), 1.36 – 1.29 (m, 2H-1 major, 1 minor), 1.10 (d, *J* = 8.3 Hz, 6H-minor), 0.90 (s, 6H-major).

^{13}C NMR Major/minor diastereomers: (151 MHz, Chloroform-*d*) δ 155.09 (major), 154.42 (minor), 138.59 (major), 138.53 (minor), 128.43 (minor), 128.27 (major), 128.03 (minor), 127.85 (major), 127.24 (major), 127.01 (minor), 80.00 (minor), 79.63 (major), 65.63 (minor), 64.57 (major), 63.01 (minor), 62.94 (major), 60.45 (major), 59.52 (minor), 39.61 (minor), 38.72 (major), 36.91 (major), 36.68 (minor), 28.62 (minor), 28.56 (major), 26.50 (major), 26.48 (minor), 25.48 (major), 25.43 (minor).

IR (thin film cm^{-1}): 2960, 2871, 1690, 1452, 1401, 1366, 1253, 1164, 1104, 950, 699

HRMS *m/z* **calculated** for $C_{18}H_{26}ClNO_2$ $[H]^+$:324.1725, and 326.1695; **found:** 324.1724 and 326.1694

Procedure for photoredox/copper mediated intermolecular chloroacetoxylation

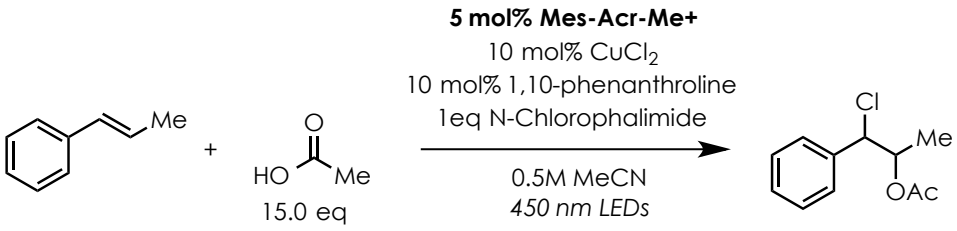

91 mg of *N*-chlorophthalimide (**NCP,** 1.0 equiv), 7 mg $CuCl_2$ (0.1 equiv), 9 mg 1,10-phenanthroline (0.1 equiv), 10 mg **NMA** (0.05 equiv), were weighed and dispensed into a flame-dried vial (1-dram) equipped with a stir bar and Teflon-coated septum cap. The vial was moved to a nitrogen filled glovebox where 65 μL β-methylstyrene, 429 μL glacial acetic acid (AcOH, 15.0 equiv) with 5% v/v acetic anhydride, and solvent (MeCN 0.5 M) were dispensed by syringe. The vial was then sealed and removed from the glovebox and the reaction vial was sealed with electrical tape. The reactions were irradiated (2x455 nm blue LED lamps) and stirred for 2 hours. Upon completion, the crude reactions were passed through a silica plug to remove $CuCl_2$ before NMR analysis.

1-Chloro-1-phenylpropan-2-yl acetate (3.91)

The average yield for the title compound was 51% (2 trials) at the 0.5 mmol scale. The average diastereomeric ratio was 1.4:1. The products were isolated by column chromatography on silica gel (10 mL dry silica, 1.0 cm column, 5% EtOAc/hexanes) as a colorless oil.

Analytical data for **3.91**:

^{1}H NMR (400 MHz, Chloroform-*d*) δ 7.44 – 7.29 (m, 10H- 5 major, 5 minor), 5.38 – 5.24 (m, 2H-1 major, 1 minor), 4.98 (d, *J* = 5.7 Hz, 1H-major), 4.84 (d, *J* = 7.5 Hz, 1H-minor), 2.10 (s, 2H-minor), 1.97 (s, 3H-major), 1.32 (d, *J* = 6.3 Hz, 3H-major), 1.14 (d, *J* = 6.4 Hz, 3H-minor).

^{13}C NMR (151 MHz, Chloroform-*d*) δ 170.19 (minor), 170.02 (major), 137.87 (minor), 137.61 (major), 128.79 (minor), 128.65 (major), 128.47 (minor), 128.38 (major), 127.82 (major/minor), 73.19 (minor), 73.05 (major), 65.25 (minor), 64.89 (major), 21.09 (minor), 20.97 (major), 17.55 (minor), 16.01 (major)

IR (thin film cm^{-1}): 3033, 2989, 2938, 1742, 1495, 1454, 1372, 1238, 1059, 959, 699, 603

HRMS *m/z* **calculated** for $C_{11}H_{13}ClO_2$ $[H]^+$:213.0677, and 215.0647; **found:** 213.0679 and 215.0649

Procedure for photoredox/copper mediated intermolecular bromoamination

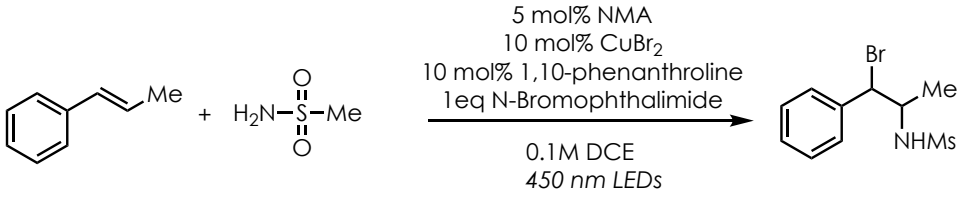

48 mg methanesulfonamide, 113 mg *N*-bromophthalimide (**NBP,** 1.0 equiv), 11 mg $CuBr_2$ (0.1 equiv), 9. mg 1,10-phenanthroline (0.1 equiv), 10 mg **NMA** (0.05 equiv), were weighed and dispensed into a flame-dried vial (2-dram) equipped with a stir bar and Teflon-coated septum cap. The vial was moved to a nitrogen filled glovebox where 65 μL β-methylstyrene and solvent (DCE 0.1 M) were dispensed by syringe. The vial was then sealed and removed from the glovebox and the reaction vial was sealed with electrical tape. The reactions were irradiated (2x455 nm blue LED lamps) and stirred for 3 hours. Upon completion, the crude reactions were passed through a silica plug to remove $CuBr_2$ before NMR analysis.

***N*-(1-Bromo-1-phenylpropan-2-yl)methanesulfonamide (3.92)**

The average yield for the title compound was 27% (2 trials) at the 0.5 mmol scale. The average diastereomeric ratio was 1.8:1. The average regioisomeric ratio was 11.7:1. The products were

isolated by column chromatography on silica gel (60 mL dry silica, 2.5 cm column, 10% EtOAc/hexanes then 30% EtOAc/hexanes) as a colorless oil.

Analytical data for **3.92**:

^{1}H NMR Major/minor diastereomers (minor regioisomer noted for observable peaks): (600 MHz, Chloroform-*d*) δ 7.44 (ddd, *J* = 7.6, 3.2, 1.9 Hz, 4H- 2 major, 2 minor), 7.39 – 7.34 (m, 4H- 2 major, 2 minor), 7.34 – 7.28 (m, 2H- 1 major, 1 minor), 5.39 (d, *J* = 8.8 Hz, 1H-minor regioisomer), 5.13 (d, *J* = 5.0 Hz, 1H-major), 4.99 (d, *J* = 5.5 Hz, 1H-minor), 4.65 (dd, *J* = 8.8, 4.4 Hz, 1H-minor regioisomer), 4.60 (d, *J* = 9.0 Hz, 1H-minor), 4.56 (d, *J* = 9.2 Hz, 1H-major), 3.94 – 3.83 (m, 2H- 1 mjor, 1 minor), 2.82 (s, 3H-major), 2.71 (s, 3H-minor), 2.67 (s, 3H- minor regioisomer), 1.58 (d, *J* = 6.9 Hz, 3H- minor regioisomer), 1.35 (dd, *J* = 8.7, 6.6 Hz, 6H-3 major, 3 minor).

^{13}C NMR Major/minor diastereomers:(151 MHz, Chloroform-*d*) δ 138.07 (minor), 137.90 (major), 128.84 (minor), 128.69 (major), 128.66 (minor), 128.64 (major), 128.49 (major), 128.39 (minor), 60.64 (major), 59.59 (minor), 56.27 (minor), 55.86 (major), 42.08 (major), 41.49 (minor), 21.48 (minor), 19.06 (major).

IR (thin film cm^{-1}): 3281, 2927, 1452, 1319, 1149, 993, 755, 700

HRMS *m/z* **calculated** for $C_{10}H_{14}BrNO_2S$ [K+]: 329.9560 and 331.9540; **found:** 329.9560 and 331.9540

General Procedure for Polar Chlorofunctionalization:

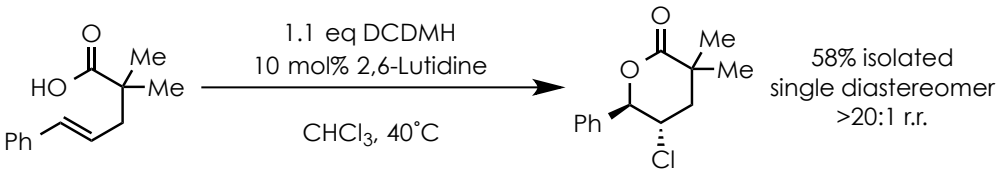

The carboxylic acid substrate (1.0 equiv, 102 mg) and Dichlorodimethyl hydantoin (DCDMH, 1.1 equiv, 108 mg) were weighed and dispensed into a flame-dried vial (2-dram) equipped with a stir bar and Teflon-coated septum cap. The vial was moved to a nitrogen filled glovebox where solvent was dispensed by syringe ($CHCl_3$ to 0.1 M), and 6 μL of 2,6-Lutidine was added via syringe. The vial was then sealed and removed from the glovebox and the reaction vial was sealed with electrical tape. The reaction was then heated at 40˚C with a heating block for 24 hrs. $CHCl_3$ was then removed in vacuo and NMR analysis revealed the reaction had reached full conversion. The compound could be partially purified on column chromatography (10% EtOAc:Hex) however the product coeluted with monochlorodimethyl hydantoin. This impurity could be removed by bringing the sample up in DCM and washing with 10% sodium hydroxide solution. The isolated yield for the sole trial was 58%, however the purification was not optimized.

5-Chloro-3,3-dimethyl-6-phenyltetrahydro-2H-pyran-2-one :

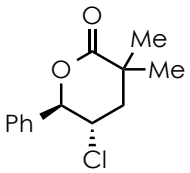

Analytical data for **5-chloro-3,3-dimethyl-6-phenyltetrahydro-2H-pyran-2-one**:

^{1}H NMR (400 MHz, Chloroform-*d*) ^{1}H NMR 7.64 – 7.33 (m, 5H), 5.19 (d, *J* = 9.8 Hz, 1H), 4.28 (ddd, *J* = 11.1, 9.8, 4.8 Hz, 1H), 2.49 – 2.21 (m, 2H), 1.46 (s, 3H), 1.43 (s, 3H).

^{13}C NMR (151 MHz, $CDCl_3$) δ 175.10, 136.45, 129.27, 128.52, 127.19, 86.41, 54.34, 44.76, 39.70, 28.19, 27.70.

IR (thin film cm^{-1}):3035, 2982, 2931, 2872, 1731, 1459, 1388, 1236, 1129, 1000, 842, 716, 642

HRMS ***m/z*** **calculated** for $C_{13}H_{15}ClO_2$ $[H]^+$: 239.0833 and 241.0804; **found**: 239.0832 and 241.0803

General Procedure for Polar Bromofunctionalization:

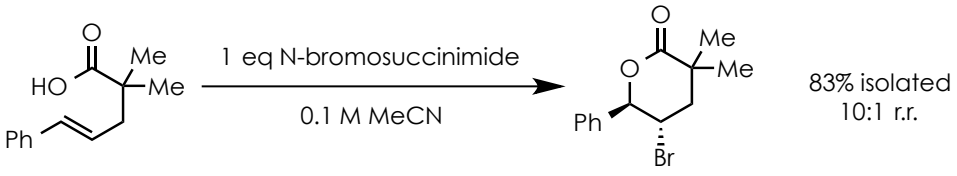

The carboxylic acid substrate (1.0 equiv, 102 mg) and *N*-bromosuccinimide (1.0 equiv, 89 mg) were weighed and dispensed into a flame-dried vial (2-dram) equipped with a stir bar and Teflon-coated septum cap. The vial was moved to a nitrogen filled glovebox where solvent was dispensed by syringe (MeCN to 0.1 M). The vial was then sealed and removed from the

glovebox and the reaction vial was sealed with electrical tape. The reaction was stirred in the dark overnight. The product was isolated via column chromatography (40 mL dry silica, 2.5 cm column, 10% EtOAc/hexanes) as white solid. The regioisomers were inseparable and resulted in a single isolated yield of 83% 10:1 rr

5-Bromo-3,3-dimethyl-6-phenyltetrahydro-2*H*-pyran-2-one

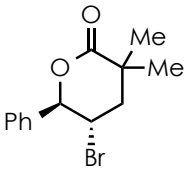

Analytical data for **5-bromo-3,3-dimethyl-6-phenyltetrahydro-2*H*-pyran-2-**:

^{1}H NMR Major/minor regioisomers: (600 MHz, Chloroform-*d*) δ 7.44 – 7.36 (m, 10H-5 major, 5 minor), 5.30 (d, *J* = 10.4 Hz, 1H-major), 4.94 (d, *J* = 7.7 Hz, 1H-minor), 4.87 – 4.77 (m, 1H-minor), 4.37 (td, *J* = 10.2, 6.3 Hz, 1H-major), 2.45 – 2.38 (m, 3H-2 major, 1 minor), 2.09 (dd, *J* = 13.0, 9.7 Hz, 1H-minor), 1.47 (s, 3H-major), 1.42 (s, 3H-major), 1.29 (d, *J* = 5.1 Hz, 6H-minor).

^{13}C NMR Major/minor regioisomers: (151 MHz, Chloroform-*d*) δ 180.83 (minor), 175.11 (major), 137.42 (minor), 136.75 (major), 129.35 (major), 129.05 (minor) 128.80 (minor), 128.51 (major), 128.20 (minor), 127.34 (major), 86.83 (major), 78.17 (minor), 55.53 (minor), 45.83 (major), 45.18 (major), 42.30 (minor) 40.71 (major), 40.66 (minor), 27.99 (major), 27.50 (major), 24.81(minor), 24.70 (minor).

IR (thin film cm^{-1}): 1725, 1459, 1387, 1210, 1130, 984, 706

HRMS ***m/z*** **calculated** for $C_{13}H_{15}BrO_2$ $[H]^+$: 283.0328 and 285.0308; **found**: 283.0327 and 285.0306

General Procedure for Polar Bromoetherification:

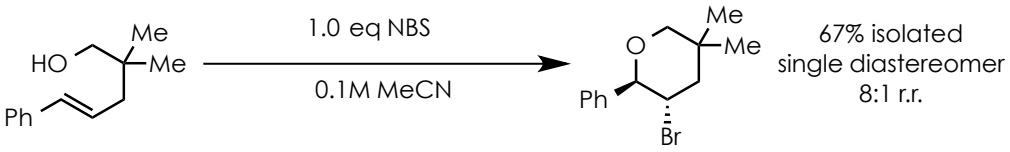

The alcohol substrate (1.0 eqiv, 95 mg) and *N*-bromosuccinimide (**NBS**, 1.0 eqiv, 89 mg**)** were weighed and dispensed into a flame-dried vial (2-dram) equipped with a stir bar and Teflon-coated septum cap. The vial was moved to a nitrogen filled glovebox where solvent was dispensed by syringe (MeCN to 0.1 M). The vial was then sealed and removed from the glovebox and the reaction vial was sealed with electrical tape. The reaction was stirred in the dark overnight. The product was isolated via column chromatography (40 mL dry silica, 2.5 cm column, 10% EtOAc) colorless oil. The regioisomers were inseparable and resulted in a single isolated yield of 67% 8:1 rr

3-Bromo-5,5-dimethyl-2-phenyltetrahydro-2*H*-pyran

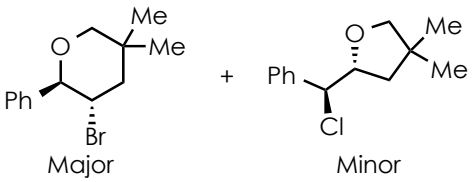

Analytical data for **3-bromo-5,5-dimethyl-2-phenyltetrahydro-2*H*-pyran**:

^{1}H NMR Major/minor regioisomers: (600 MHz, Chloroform-*d*) 7.50 – 7.43 (m, 4H-2 major, 2 minor), 7.43 – 7.34 (m, 6H-3 major, 3 minor), 4.94 (d, J = 7.9 Hz, 1H-minor), 4.64 (ddd, J = 8.9, 7.9, 6.4 Hz, 1H-minor), 4.33 – 4.21 (m, 2H-major), 3.69 (dd, J = 11.3, 2.6 Hz, 1H-major), 3.62 –

3.56 (m, 2H-minor), 3.45 (d, J = 11.2 Hz, 1H-major), 2.40 – 2.28 (m, 1H-major), 2.10 (ddd, J = 12.6, 6.4, 0.9 Hz, 1H-minor), 2.06 – 1.96 (m, 1H-major), 1.83 (dd, J = 12.6, 8.9 Hz, 1H-minor), 1.26 (s, 3H-major), 1.15 (d, J = 1.9 Hz, 6H-minor), 0.97 (s, 3H-major).

^{13}C NMR Major/minor regioisomers: (151 MHz, Chloroform-*d*) δ 139.32 (minor), 139.25 (major), 128.48 (minor), 128.41 (major), 128.36 (minor), 128.14 (major), 128.10 (minor), 127.45 (major), 85.47 (major), 81.93 (minor), 80.75 (minor), 78.26 (major), 58.00 (minor), 50.61 (major), 49.08 (major), 45.99 (minor), 39.75 (minor), 34.99 (major), 26.43 (major), 26.26 (minor), 25.52 (minor), 23.56 (major).

IR (thin film cm^{-1}): 2956, 2866, 1646, 1455, 1368, 1277, 1078, 791, 756, 698

HRMS ***m/z*** **calculated** for $C_{13}H_{17}BrO$ [H^+]: 269.0536 and 271.0515; **found** 269.0536 and 271.0515

General Procedure for Polar Chloroacetoxylation:

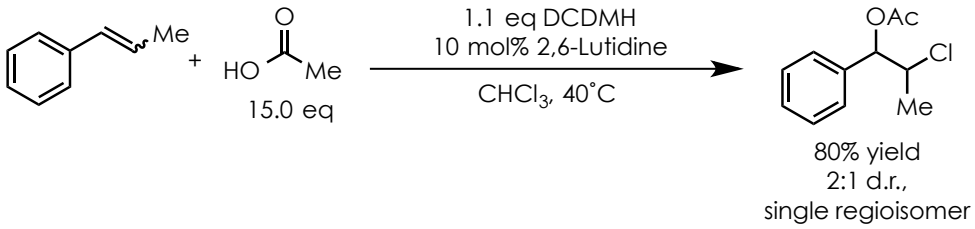

Dichlorodimethyl hydantoin (DCDMH, 1.1 equiv, 108 mg) was weighed and dispensed into a flame-dried vial (1-dram) equipped with a stir bar and Teflon-coated septum cap. The vial was moved to a nitrogen filled glovebox where solvent was dispensed by syringe ($CHCl_3$ to 0.5 M). This was followed by the addition of 430 μL (15 equiv) of acetic acid, and 6 μL of 2,6-lutidine (0.1 equiv). Finally, 65 μL of *trans*-betamethyl styrene was added (single alkene isomer). The

vial was then sealed and removed from the glovebox and the reaction vial was sealed with electrical tape. The reaction was then heated at 40˚C with a heating block for 24 hrs. $CHCl_3$ and acetic acid were then removed in vacuo and NMR analysis revealed the reaction had reached full conversion. The product was isolated on silica gel (20 mL dry silica, 2cm column, 10% EtOAc:Hexanes) as a mixture of diastereomers (80% yield, 2:1 dr).

2-Chloro-1-phenylpropyl acetate:

Analytical data for **2-chloro-1-phenylpropyl acetate**:

^{1}H NMR (600 MHz, Chloroform-*d*) δ 7.39 – 7.31 (m, 10H-5 major, 5 minor), 5.91 (d, *J* = 5.2 Hz, 1H-major), 5.79 (d, *J* = 7.6 Hz, 1H-minor), 4.33 – 4.24 (m, 2H-1 major, 1 minor), 2.15 (s, 3H-major), 2.13 (s, 3H-minor), 1.47 (d, *J* = 6.7 Hz, 3H-major), 1.35 (d, *J* = 6.7 Hz, 3H-minor).

^{13}C NMR (151 MHz, $CDCl_3$) δ 169.76 (minor), 169.73 (major), 137.01 (minor), 136.71 (major), 128.73 (minor), 128.55 (major), 128.48 (minor), 128.30 (major), 127.29 (minor), 127.19 (major), 79.11 (minor), 78.12 (major), 58.87 (major), 58.53 (minor), 21.33 (minor), 20.99 (major/minor), 19.99 (major).

IR (thin film cm^{-1}): 2983, 1746, 1454, 1372, 1228, 1029, 758, 703, 623

HRMS ***m/z*** **calculated** for $C_{11}H_{13}ClO_2$ $[H]^+$: 213.0677 and 215.0647; **found**: 213.0677

Product identification: distinguishing regio- and diasteroisomers

Distinguishing Regioisomers:

Regioisomers of chlorofunctionalization could generally be distinguished by analysis of the ^1H NMR. The 6-endo product was generated via reaction of the corresponding alkene with dichlorodimethylhydantoin. Comparing the two regioisomers shows H_a in the 6-endo product is further downfield than H_a in the 5-exo product. H_b in the 6-endo product is further upfield than H_b in the 5-exo product. The shifts of both H_a and H_b in each product match with the expected relative shifts.

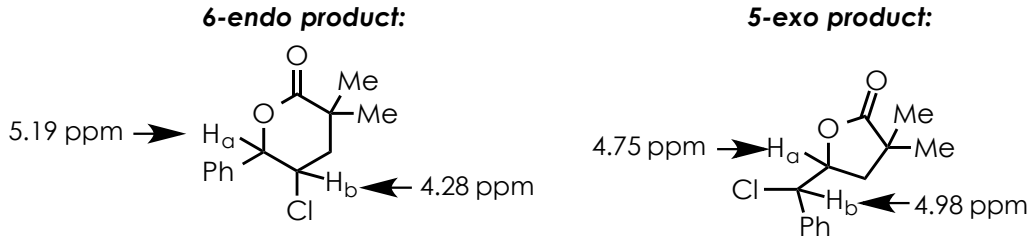

HSQC data could be used as further evidence of the regioselectivity of the reaction. Via HSQC correlation C_a and C_b could be assigned for each product. As expected C_a is further downfield in the 6-endo product, while C_b is further upfield.

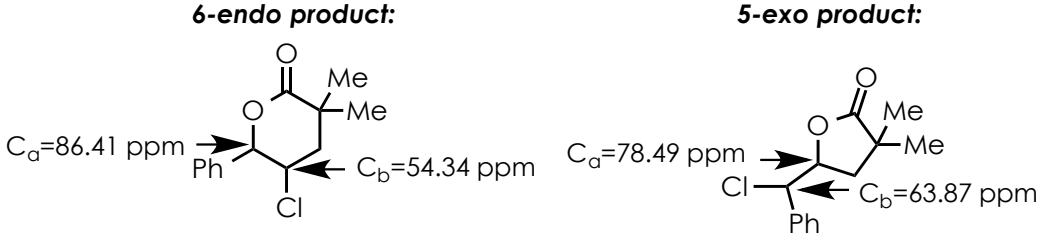

These analyses could be extrapolated to products 3.49-3.63 and 3.91. Analysis of HSQC data alone was sufficient for determining the regioisomer for products 3.65, 3.67, 3.84, and 3.85 (the relevant carbon shifts were more consistent with being adjacent to oxygen rather than a halogen).

^{1}H and ^{13}C spectra of products 3.87,[10] 3.80[18] and 3.87[7] were compared to reported literature values of the corresponding regioisomers. These shifts were inconsistent with the reported values herein. This analysis could be further extrapolated to products 3.71-3.78.

UV/vis Spectroscopy:

UV/vis spectra were taken on a Hewlett-Packard 8453 Chemstation absorption spectrometer.

$[CuCl/Phen]_2$: A solution of $[CuCl/Phen]_2$ was prepared by weighing equimolar amounts of CuCl and 1,10-phenanthroline into a vial (0.05 mmol). In a glovebox, 10 mL MeCN (N_2 sparged) was added to give a 5 x 10^{-3} M solution of the complex. 350µL of this solution was transferred to a 2-dram vial and then diluted to 3.5 mL total volume, giving a 5 x 10^{-4} M solution of $[CuCl/Phen]_2$. 3mL of this solution was transferred to a quartz cuvette and a UV/vis spectrum was obtained.

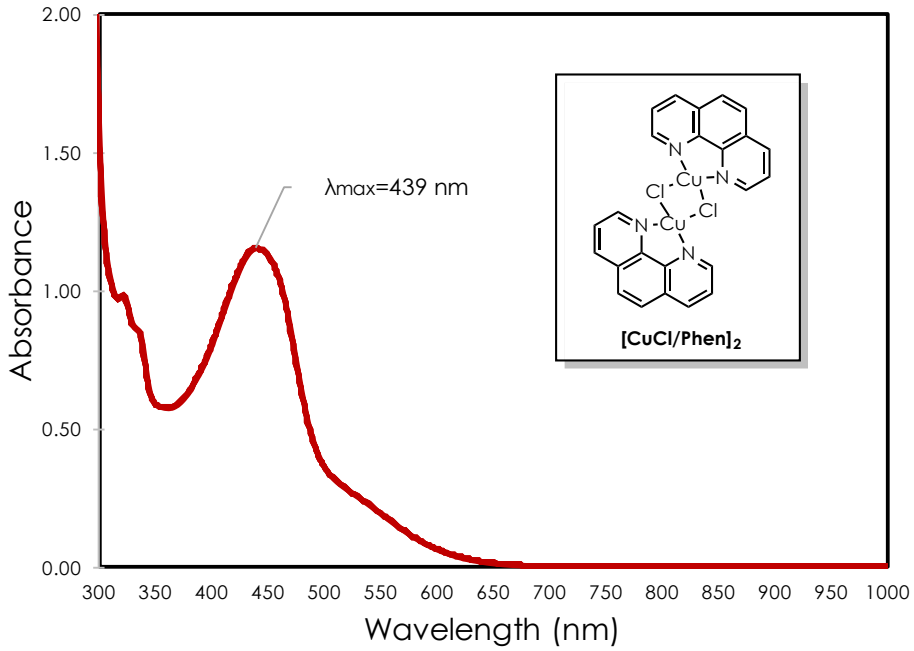

$CuCl_2$/Phen: A saturated solution of $CuCl_2$/Phen was prepared by weighing equimolar amounts of $CuCl_2$ and 1,10-phenanthroline into a vial (0.05 mmol). In a glovebox 10 mL MeCN (N_2 sparged) was added to give a saturated solution of unknown concentration of $CuCl_2$/Phen (due to the low solubility of $CuCl_2$/Phen). 350µL of this solution was transferred to a 2-dram vial and then diluted to 3.5 mL total solution volume of $CuCl_2$/Phen. 3mL of this solution was transferred to a quartz cuvette and a UV/Vis spectrum was obtained.

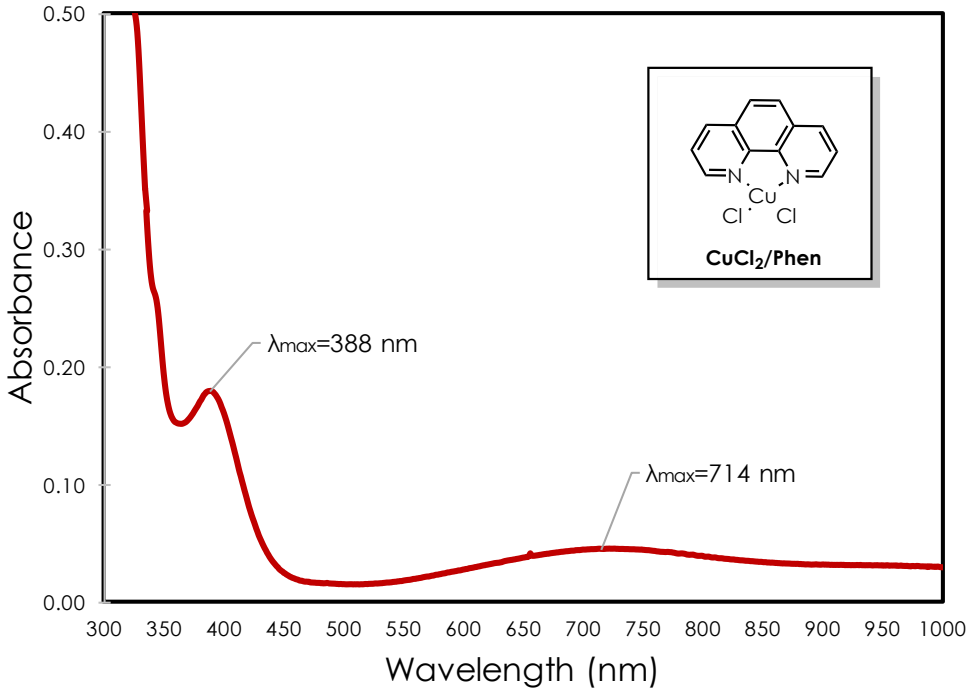

[CuCl/Phen]$_2$ + NCP: To the cuvette containing [CuCl/Phen]$_2$ discussed above, was added 1 mL of 7.5 x 10^{-3} M solution of NCP in MeCN (5 equiv relative to Cu^+). The solution immediately lost its orange color and became a light blue solution. Adjusted concentrations of Cu^+ and NCP were 3.75 x 10^{-4} M and 1.875 x 10^{-3} M respectively. A UV/vis spectrum was recorded immediately after mixing the solution.

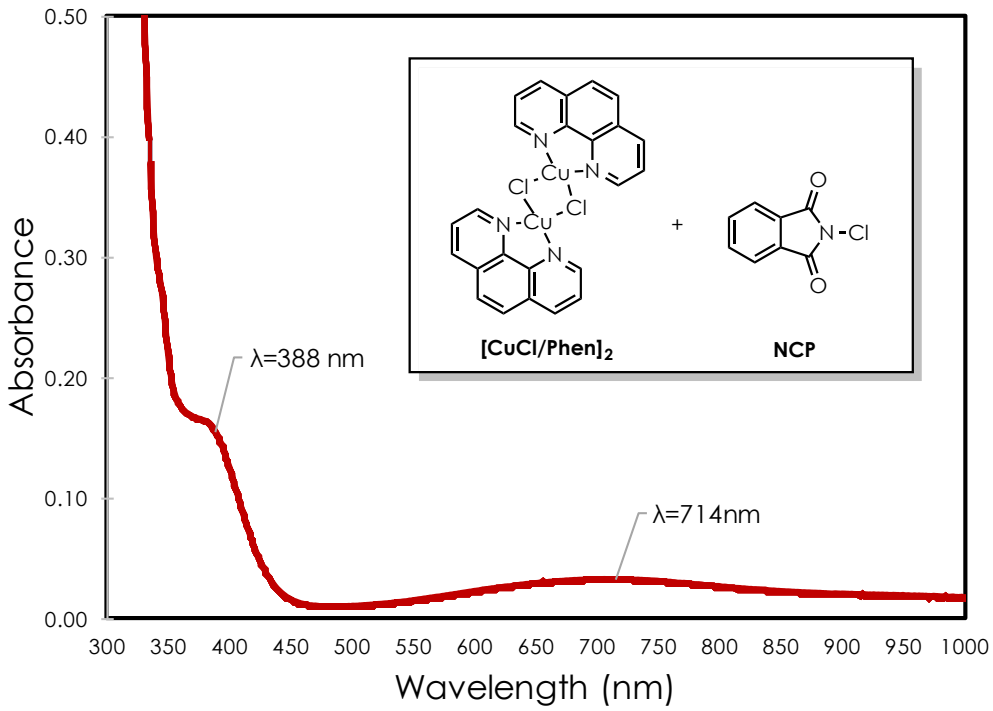

Solutions of $[CuBr/Bpy]_2$, $CuBr_2$/Bpy, and DEBM were made analogously to their counterparts as described above.

UV/vis spectra were taken on a Hewlett-Packard 8453 Chemstation absorption spectrometer.

$[CuBr/Bpy]_2$: A solution of $[CuBr/Bpy]_2$ was prepared by weighing equimolar amounts of CuBr and 2,2′-bipyridine into a vial (0.05 mmol). In a glovebox, 10 mL MeCN (N_2 sparged) was added to give a 5 x 10^{-3} M solution of the complex. 350μL of this solution was transferred to a 2-dram vial and then diluted to 3.5 mL total volume, giving a 5 x 10^{-4} M solution of $[CuBr/Bpy]_2$. 3mL of this solution was transferred to a quartz cuvette and a UV/vis spectrum was obtained.

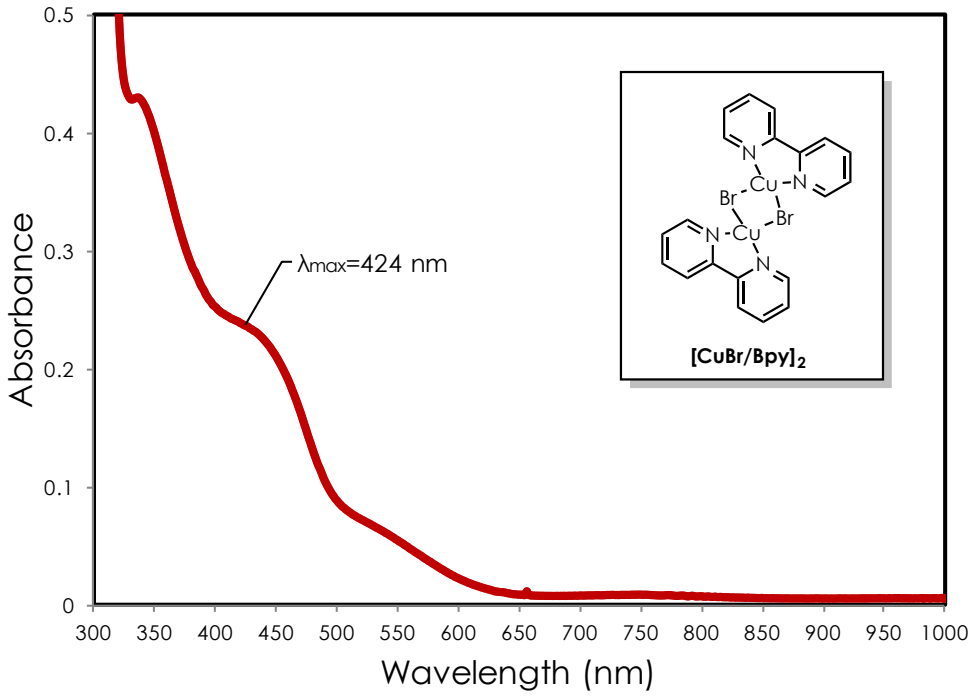

$CuBr_2$/Bpy: A saturated solution of $CuBr_2$/Bpy was prepared by weighing equimolar amounts of $CuBr_2$ and 2,2′-bipyridine into a vial (0.05 mmol). In a glovebox 10 mL MeCN (N_2 sparged) was added to give a saturated solution of unknown concentration of $CuBr_2$/Bpy (due to the low solubility of $CuBr_2$/Bpy). 350µL of this solution was transferred to a 2-dram vial and then diluted to 3.5 mL total solution volume of $CuBr_2$/Bpy. 3mL of this solution was transferred to a quartz cuvette and a UV/vis spectrum was obtained.

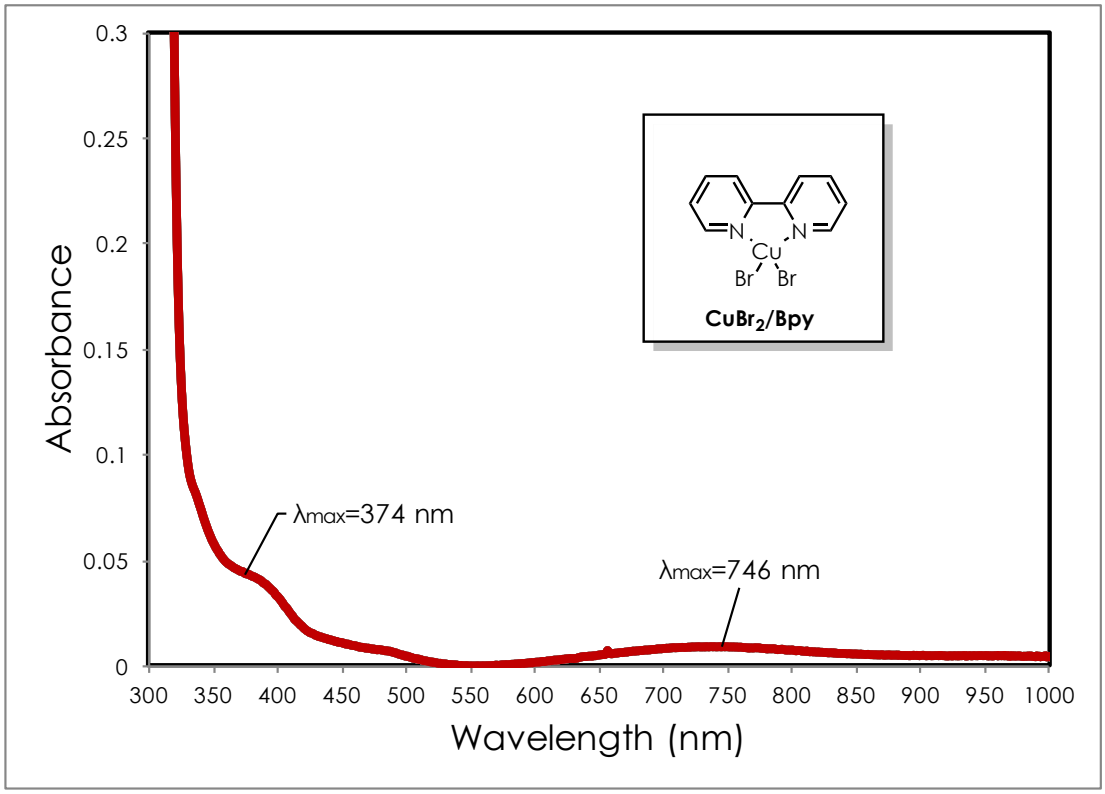

[CuBr/Bpy]$_2$ + DEBM: To the cuvette containing [CuBr/Bpy]$_2$ discussed above, was added 1 mL of 7.5 x 10^{-3} M solution of DEBM in MeCN (5 equiv relative to Cu^+). The solution immediately lost its orange color and became a light blue solution. Adjusted concentrations of Cu^+ and DEBM were 3.75 x 10^{-4} M and 1.875 x 10^{-3} M respectively. A UV/Vis spectrum was recorded immediately after mixing the solution.

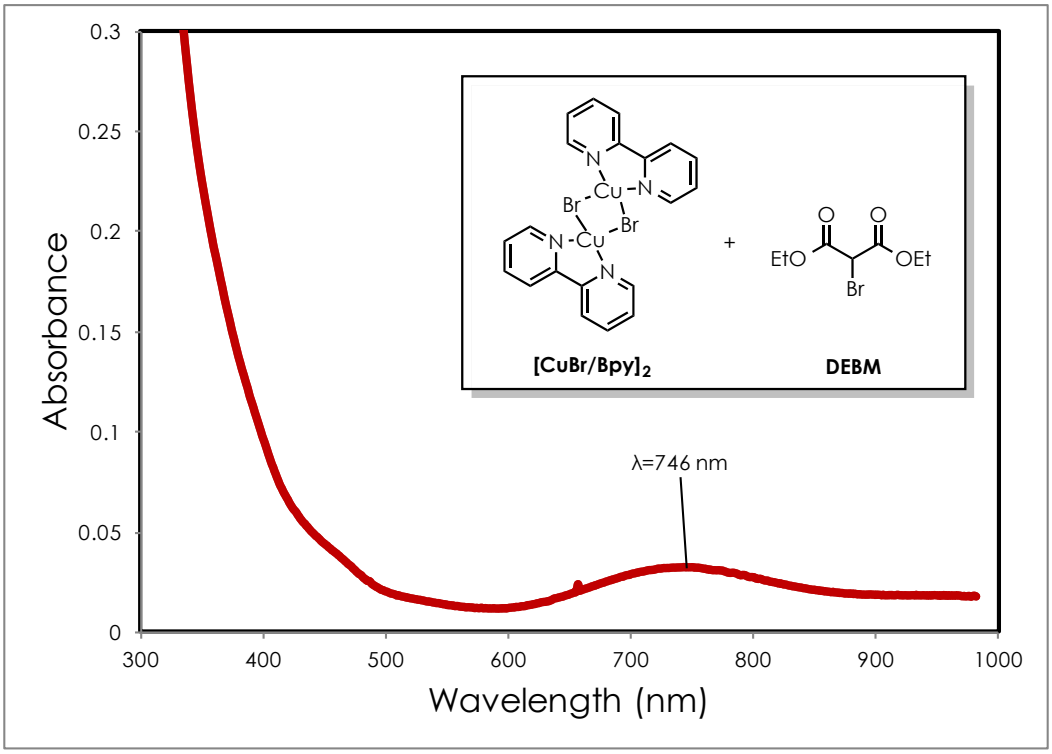

Upon the addition of the respective halogenating reagents to each Cu^{+} complex, the characteristic absorbance (439 nm for $[CuCl/Phen]_2$ and 424 nm for $[CuBr/Bpy]_2$) immediately disappeared. In both cases new features were observed which closely correspond with those observed in the UV/vis spectrum of the independently synthesized Cu^{2+} complexes. This is sufficient evidence to support the oxidation of the Cu^{+} metal center. Unfortunately, due to the very low solubility of both Cu^{2+} complexes quantitative data could not be recorded and the present data cannot be used to determine whether $CuCl_2$/Phen or $CuBr_2$/Bpy are the sole products of the oxidation. While at least some amount of Cu^{2+} does seem to be forming, it is still feasible that a Cu(III) intermediate could be formed under these conditions as well.

REFERENCES

(1) Han, X.; Wu, H.; Dong, C.; Tien, P.; Xie, W.; Wu, S.; Zhou, H.-B. *RSC Adv.* **2015**, *5*, 10005–10013.

(2) Grabarczyk, M.; Mączka, W.; Wińska, K.; Żarowska, B.; Anioł, M. *J. Mol. Catal. B Enzym.* **2014**, *102*, 195–203.

(3) Lin, H.; Pochapsky, S. S.; Krauss, I. J. *Org. Lett.* **2011**, *13*, 1222–1225.

(4) Chung, W.; Vanderwal, C. D. *Angew. Chem. Int. Ed.* **2016**, *55*, 4396–4434.

(5) Denmark, S. E.; Kuester, W. E.; Burk, M. T. *Angew. Chem. Int. Ed.* **2012**, *51*, 10938–10953.

(6) Wade, L. G. *Organic Chemistry*, 7th ed.; Pearson Prentice Hall: Upper Saddle River, NJ, 2010.

(7) Ashtekar, K. D.; Vetticatt, M.; Yousefi, R.; Jackson, J. E.; Borhan, B. *J. Am. Chem. Soc.* **2016**, *138*, 8114–8119.

(8) Ashtekar, K. D.; Marzijarani, N. S.; Jaganathan, A.; Holmes, D.; Jackson, J. E.; Borhan, B. *J. Am. Chem. Soc.* **2014**, *136*, 13355–13362.

(9) Kitagawa, O.; Hanano, T.; Tanabe, K.; Shiro, M.; Taguchi, T. *J. Chem. Soc. Chem. Commun.* **1992**, *0*, 1005–1007.

(10) Whitehead, D. C.; Yousefi, R.; Jaganathan, A.; Borhan, B. *J. Am. Chem. Soc.* **2010**, *132*, 3298–3300.

(11) Tan, C. K.; Zhou, L.; Yeung, Y.-Y. *Org. Lett.* **2011**, *13*, 2738–2741.

(12) Zhou, L.; Tan, C. K.; Jiang, X.; Chen, F.; Yeung, Y.-Y. *J. Am. Chem. Soc.* **2010**, *132*, 15474–15476.

(13) Dobish, M. C.; Johnston, J. N. *J. Am. Chem. Soc.* **2012**, *134*, 6068–6071.

(14) Han, X.; Dong, C.; Zhou, H. B. *Adv. Synth. Catal.* **2014**, *356*, 1275–1280.

(15) Dong, Z.; Qiu, G.; Zhou, H. B.; Dong, C. *Tetrahedron Asymmetry* **2012**, *23*, 1550–1556.

(16) Han, X.; Wu, X.; Min, C.; Zhou, H.-B.; Dong, C. *RSC Adv.* **2012**, *2*, 7501–7505.

(17) Han, X.; Liu, B.; Zhou, H.-B.; Dong, C. *Tetrahedron Asymmetry* **2012**, *23*, 1332–1337.

(18) Min, C.; Han, X.; Liao, Z.; Wu, X.; Zhou, H.-B.; Dong, C. *Adv. Synth. Catal.* **2011**, *353*, 2715–2720.

(19) Hamilton, D. S.; Nicewicz, D. A. *J. Am. Chem. Soc.* **2012**, *134*, 18577–18580.

(20) Utsunomiya, M.; Hartwig, J. F. *J. Am. Chem. Soc.* **2004**, *126*, 2702–2703.

(21) Utsunomiya, M.; Kuwano, R.; Kawatsura, M.; Hartwig, J. F. *J. Am. Chem. Soc.* **2003**, *125*, 5608–5609.

(22) Chatterjee, A. K.; Choi, T.-L.; Sanders, D. P.; Grubbs, R. H. *J. Am. Chem. Soc.* **2003**, *125*, 11360–11370.

(23) Gassman, P. G.; Bottorff, K. J. *Tetrahedron Lett.* **1987**, *28*, 5449–5452.

(24) Gassman, P. G.; Bottorff, K. J. *J. Am. Chem. Soc.* **1987**, *109*, 7547–7548.

(25) Neunteufel, R. A.; Arnold, D. R. *J. Am. Chem. Soc.* **1973**, *95*, 4080–4081.

(26) Wilger, D. J.; Gesmundo, N. J.; Nicewicz, D. A. *Chem. Sci.* **2013**, *4*, 3160–3165.

(27) Wilger, D. J.; Grandjean, J.-M. M.; Lammert, T. R.; Nicewicz, D. A. *Nat. Chem.* **2014**, *6*, 720–726.

(28) Nguyen, T. M.; Nicewicz, D. A. *J. Am. Chem. Soc.* **2013**, *135*, 9588–9591.

(29) Nguyen, T. M.; Manohar, N.; Nicewicz, D. A. *Angew. Chem. Int. Ed.* **2014**, *53*, 6198–6201.

(30) Perkowski, A. J.; Nicewicz, D. A. *J. Am. Chem. Soc.* **2013**, *135*, 10334–10337.

(31) Griffin, J. D.; Cavanaugh, C. L.; Nicewicz, D. A. *Angew. Chem. Int. Ed.* **2017**, *56*, 2097–2100.

(32) K. Matyjaszewski, J. Xia, Chem. Rev. 2001, 101, 2921 – 2990.

(33) Ledwith, A.; Russell, P. J. *J. Chem. Soc. Chem. Commun.* **1974**, *0*, 291–292.

(34) Yorimitsu, H.; Shinokubo, H.; Matsubara, S.; Oshima, K.; Omoto, K.; Fujimoto, H. *J. Org. Chem.* **2001**, *66*, 7776–7785.

(35) Yousefi, R.; Ashtekar, K. D.; Whitehead, D. C.; Jackson, J. E.; Borhan, B. *J. Am. Chem. Soc.* **2013**, *135*, 14524–14527.

(36) Lind, J.; Jonsson, M.; Eriksen, T. E.; Merenyi, G.; Eberson, L. *J. Phys. Chem.* **1993**, *97*, 1610–1614.

(37) Wube, A. A.; Hüfner, A.; Thomaschitz, C.; Blunder, M.; Kollroser, M.; Bauer, R.; Bucar, F. Design, *Bioorg. Med. Chem.* **2011**, *19*, 567–579.

(38) Khrizman, A.; Cheng, H. Y.; Moyna, G. *J. Label. Compd. Radiopharm.* **2011**, *54*, 401–407.

(39) Cabrero-Antonino, J. R.; Leyva-Pérez, A.; Corma, A. *Chem. – Eur. J.* **2012**, *18*, 11107–11114.

(40) Maity, S.; Zheng, N. A. *Angew. Chem. Int. Ed.* **2012**, *51*, 9562–9566.

(41) Hemric, B. N.; Shen, K.; Wang, Q. *J. Am. Chem. Soc.* **2016**, *138*, 5813–5816.

(42) Gribkov, D. V.; Hultzsch, K. C.; Hampel, F. *J. Am. Chem. Soc.* **2006**, *128*, 3748–3759.

(43) Geary, G. C.; Hope, E. G.; Stuart, A. M. *Angew. Chem. Int. Ed.* **2015**, *54*, 14911–14914.

(44) Gorin, C. F.; Beh, E. S.; Bui, Q. M.; Dick, G. R.; Kanan, M. W. *J. Am. Chem. Soc.* **2013**, *135*, 11257–11265.

(45) Takemiya, A.; Hartwig, J. F. *J. Am. Chem. Soc.* **2006**, *128*, 6042–6043.